Sterol Regulatory Element Binding Proteins:

Their role in the hypoxic response of cancer cells

and

their regulation by the Akt/mTORC1 pathway

Caroline Amy Lewis

A thesis submitted to University College London

for the degree of Doctor of Philosophy

September 2011

University College London

and

Cancer Research UK London Research Institute

PhD Supervisor: Dr. Almut Schulze

Declaration

I Caroline Amy Lewis confirm that the work presented in this thesis is my own. Where information has been derived from other sources, I confirm that this has been indicated in the thesis.

Abstract

Sterol regulatory element binding proteins (SREBPs) are transcription factors that regulate the expression of genes involved in fatty acid and cholesterol biosynthesis. It has been established that SREBPs are regulated downstream of the PI3-Kinase/Akt/mTORC1 signalling axis, a pathway that is frequently hyper-activated in cancer. SREBP target genes are upregulated in some forms of human cancer and a role for lipid metabolism in tumourigenesis has been suggested.

Glioblastoma multiforme (GBM) is a cancer type that is associated with hyperactivation of the PI3-kinase/Akt signalling pathway and frequently displays poorly oxygenated (hypoxic) regions. SREBP1 has been implicated in the tumourigenic potential of this cancer type. However, the exact role of SREBPs in tumourigenesis is not known. In oder to investigate the SREBP-transcriptional response in cancer cells, a gene expression microarry analysis was carried out. It was found that SREBPs regulate genes involved in a variety of cellular processes including lipid metabolism, cell cycle regulation, redox regulation and cellular stress response. In addition, the role of SREBPs in lipid metabolism in hypoxia was investigated. It was found that hypoxia leads to distinct changes in the expression of different SREBP isoforms and their target genes and is associated with a decrease in pyruvate-dependent lipid synthesis and increased lipid storage.

SREBPs are regulated downstream of the Akt/mTORC1 pathway, although the exact mechanism of this regulation remains to be elucidated. Possible mechanisms by which Akt and mTORC1 regulate SREBPs were investigated. It was found that inhibition of mTORC1 differentially affects the expression of individual SREBP isoforms. The results described in this thesis also show that mTORC1 modulates the transcriptional activity of mature SREBP and may regulate its stability in a GSK3-independent manner.

Acknowledgements

I am indebted to my supervisor, Dr. Almut Schulze, for all of her help, advice and support over the last four years. I also need to thank Beatrice Griffiths, for her technical help and advice, and for reading this thesis. Thanks also to the other members of the GEA lab, past and present: Claudio Santos, Emma Ferber, Franzi Baenke, Susana Ros, Heike Miess and Barrie Peck. I couldn't have done this without you! Thank you all, not just for being such great lab colleagues, but also for the wonderful friendships.

I thank my thesis committee, Dr. Julian Downward and Dr. Barry Thompson for their helpful comments and discussions. I would also like to thank members of the STL and TCT labs for their advice and support.

I need to thank many other colleagues at the LRI for their technical and bioinformatics skills. Thank you to the staff of the equipment park, especially Graham Clark, Vicky Dearing and David Phillips for their patience and extensive QPCR knowledge. Thanks to Mike Howell (LRI HTS) for helping me quantify lipid droplets. Thanks to members of the Light Microscopy service for letting me loose on the confocal. And thanks also to Phil East and Probir Chakravarty (LRI BABS) who analysed the microarray data in this thesis and helped with the subsequent pathway analysis.

I now say a huge thank you to Sophie, Anna and Vanni. Thanks for all the fun times and for picking up the pieces towards the end. I'll miss you guys. Thanks also to those who continued to answer the phone well into the night and listened patiently to the sobs, in particular the lovely Miss Chewitt and Bov.

Last, but by no means least, thank you to my wonderful family for always believing in me and supporting me throughout.

Robyn, this thesis is for you.

Table of Contents

Table of figures

List of tables

Abbreviations

4-OHT	4-hydroxytamoxifen
4E-BP	eIF4E-binding protein
ACC	acetyl-coA carboxylase
ACLY	ATP-citrate lyase
ACSS2	acetyl-coA synthetase 2
Akt/PBK	protein kinase B
AMP	adenosine mono-phosphate
AMPK	AMP-activated protein kinase
ATF6a	activating transcription factor 6
ATP	adenosine tri-phosphate
bHLH-Zip	basic helix-loop-helix-leucine zipper
BSA	bovine serum albumin
CA9	carbonic anhydrase
ChIP	chromatin immunoprecipitation
ChoRE	carbohydrate response elements
CIH	chronic intermittent hypoxia
CoA	coenzyme A
COPII	coat protein complex II
CPT1	carnitine palmitoyltransferase 1
DMEM	Dullbecco's modified eagle medium
EGF	epidermal growth factor
EGFR	EGF receptor
eIF4E	eukaryotic initiation factor 4E
ER	endoplasmic reticulum
ER	oestrogen receptor
EtOH	ethanol
FA	fatty acid
FABP	fatty acid binding protein
FASN	fatty acid synthase
FCS	foetal calf serum

FFA	free fatty acids
FIH	factor inhibiting hypoxia
flSREBP	full-length SREBP
FOXO	forkhead box other transcription factor
G6PD	glucose-6-phosphate dehydrogenase
GAP	GTPase activating protein
GBM	glioblastoma multiforme
GPAT	glycerol-3-phosphate acyltransferase
GPD1	glycerol-3-phosphate dehydrogenase 1
GSK3	glycogen synthase kinase 3
HDAC1	histone deacetylase complex 1
HIF1	hypoxia inducible factor 1
HIG2	hypoxia inducible gene 2
HMG-CoA	3-hydroxy-3-methylglutaryl-CoA
HMGCR	HMG-coA reductase
HMGCS	HMG-coA synthase
HNF-4a	hepatic nuclear factor 4a
HRE	hypoxia response element
HRP	horseradish peroxidase
IGF1	insulin like growth factor
INSIG	insulin induced gene
IR	insulin receptor
IRE	insulin response element
IRS	insulin receptor substrate
KGF	keratincoyte growth factor
LD	lipid droplet
LDH	lactate dehydrogenase
LDLR	low-density lipoprotein receptor
LPDS	lipoprotein deficient serum
LXR	liver x receptor
MAGL	monoacylglycerol lipase
MAPK	mitogen activated protein kinase
MCT	monocarboxylate transporter

ME	malic enzyme
mSREBP	mature SREBP
mTOR	mammalian target of rapamycin
mTORC1/2	mTOR complex 1/2
MUFA	monounsaturated fatty acid
OSA	obstructive sleep apnea
OXPHOS	oxidative phosphorylation
PDGF	platelet derived growth factor
PDK1	3-phosphoinositide-dependent kinase 1
PDK1	pyruvate dehydrogenase kinase 1
PDK4	pyruvate dehydrogenase kinase 4
PH	plektrsin homology
PHD	prolyl hydroxylase
PI3K	phosphatidylinositol 3-kinase
PIP2	phosphatidylinositol-4,5-bisphosphate
PIP3	phosphatidylinositol-3,4,5-triphosphate
PLAP	placental alkaline phosphatase
PPAR	peroxisome proliferator-activated receptor
PPP	pentose phosphate pathway
PRAS40	proline rich Akt substrate of 40kDA
pSREBP2	processed (C-terminal) SREBP2
PTEN	tensin homologue deleted on chromosome 10
PUFA	polyunsaturated fatty acid
Rapa	rapamycin
Rheb	Ras homologue enriched in brain
RIP	regulated intramembrane proteolysis
RNAi	RNA interference
RPE	retinal pigment epithelial
RTK	receptor tyrosine kinase
S1P	site-1 protease
S2P	site-2 protease
S6	ribosomal protein S6

S6K	ribosomal protein S6 kinase
SCAP	SREBP cleavage activating protein
SCD	stearoyl-coA desaturase
SFA	saturated fatty acid
SH2	Src-homology 2
shRNA	short-hairpin RNA
siRNA	small interfering RNA
SIRT1	sirtuin 1
SRE	sterol regulatory element
SREBP	sterol regulatory element binding protein
SSD	sterol sensing domain
SUMO	small ubiquitin-related modifier-1
TAG	triaclyglyceride
TCA cycle	tricarboxylic acid cycle
TOS	TOR signalling motif
TSC1	tuberous sclerosis protein 1
TSC2	tuberous sclerosis protein 2
VEGFA	vascular endothelial growth factor A
VHL	von Hippel Lindau

Chapter 1. Introduction

1.1 Cellular metabolism and cancer

At a very basic level, cancer can be described as uncontrolled cellular proliferation. In order to sustain increased proliferation rates, cells require energy in the form of ATP and must synthesise macromolecules in the form of nucleotides, proteins, fatty acids and membrane lipids. Synthesis of these molecules occurs through several key metabolic pathways, including glycolysis (conversion of glucose to pyruvate and lactate), the tricarboxylic acid cycle (TCA cycle: generation of metabolic precursors and electrons in the form of NADH and $FADH_2$), oxidative phosphorylation (OXPHOS: generation of ATP), the pentose phosphate pathway (PPP: oxidative and non-oxidative for the generation of NADPH and riboses for nucleotide synthesis), lipid synthesis (synthesis of fatty acids and sterols) and fatty acid β-oxidation (generation of ATP by the breakdown of fatty acids). It stands to reason, therefore, that cellular metabolism and proliferation are intimately linked and that cancer cells require rapid nutrient uptake and energy production in order to sustain high rates of proliferation.

The observation that cancer cells exhibit an altered metabolism from non-transformed cells was made decades ago by the German biochemist Otto Warburg. In his pivotal paper published in 1956 he described the discovery that cancer cells preferentially utilise the glycolytic pathway to generate energy, even in the presence of an ample supply of oxygen (Warburg, 1956). The conversion of glucose to lactate in the presence of oxygen has been termed aerobic glycolysis. Aerobic glycolysis is therefore accompanied by increased glucose uptake and lactate secretion. This shift to aerobic glycolysis is a paradox, as glycolysis is a much less efficient pathway for producing cellular energy in the form of ATP than oxidative phosphorylation. This phenomenon has since been termed the “Warburg effect”. It is now also clear that alterations in cancer cell metabolism are required in order to facilitate the survival of cancer cells in less than favourable tumour microenvironments. Altered tumour metabolism is now considered an emerging hallmark of cancer and is included in the “revised” edition of the seminal Hallmarks of Cancer paper (Hanahan and Weinberg, 2000; Hanahan and Weinberg, 2011).

1.2 Lipid metabolism

Fatty acids (FA) consist of a long hydrocarbon chain and a terminal carboxylate group. Fatty acids play a major role in the function of the cell. They are the building blocks for phospholipids, the main component of membranes. In addition, many proteins are covalently modified by FA, resulting in the targeting of these proteins to the membrane. FA are also used as energy stores in the form of triacylglycerols (TAGs). Finally, FA derivatives are precursors for steroid hormone synthesis and lipid second messengers. The synthesis and degradation of fatty acids therefore represent key cellular processes that must be tightly regulated.

Cellular lipids are either acquired from the diet or from carbohydrate-derived fatty acids resulting from *de novo* synthesis. In most adult tissues *de novo* lipid synthesis and expression of enzymes required for lipid synthesis is low, as most tissues receive the majority of their fatty acids from the circulation (Swinnen et al., 2006). Cells store excess fatty acids for subsequent breakdown and energy release (a process known as lipolysis) as neutral lipids, predominantly in the form of triacylglycerides (TAGs) and cholesterol-esters. These neutral lipids are stored in ubiquitous organelles called lipid droplets (LDs), which consist of a neutral lipid core surrounded by a phospholipid monolayer (Farese and Walther, 2009). Although the mechanism of LD biogenesis, catabolism and function are not fully understood, it is thought that sequestration of excess FA in these organelles protects cells from the toxic effects of excess amounts of lipids (Farese and Walther, 2009; Listenberger et al., 2003).

FA degradation is essentially the reverse of lipid synthesis. Lipid synthesis takes place in the cytosol, whilst FA β-oxidation occurs in the mitochondria. Interestingly, the expression of many genes encoding enzymes required for FA and cholesterol biosynthesis are regulated by a small family of transcription factors, the sterol regulatory element binding proteins (SREBPs, discussed in section 1.3) (Figure 1.1) (Horton, 2002).

FA are produced from the repeated condensation of 2-carbon units via a multistep process. The acetyl groups for this reaction are provided by cytoplasmic acetyl-

Coenzyme A (acetyl-CoA). The TCA cycle intermediate citrate is the main source of cytoplasmic acetyl-CoA. Citrate is exported from the mitochondria by citrate transporters and hydrolysed to acetyl-CoA and oxaloacetate, a reaction catalysed by the enzyme ATP-citrate lyase (ACLY). Acetyl-CoA is then used for biosynthetic processes, whilst oxaloacetate can re-enter the TCA cycle. Since the mitochondrial membrane is impermeable to oxaloacetate it is first converted into malate via malate dehydrogenase 1 (MDH1) before being decarboxylated to pyruvate by malic enzyme (ME). This reaction produces the reducing power required for lipid synthesis in the form of NADPH. Acetyl-CoA can also be synthesised from cytosolic acetate by the enzyme ACSS2 (Yoshii et al., 2009).

The activation of acetyl-CoA by carboxylation to form malanoyl-CoA is the first and committed step in FA synthesis. This reaction is catalysed by the enzyme acetyl-CoA carboxylase (ACC) and the activity of ACC is highly regulated. Two isoforms of ACC (ACACA and ACACAB) have been described and are thought to differ in their ability to be activated by citrate (Locke et al., 2008). In addition, it is thought that ACACA and ACACB play distinct roles in FA synthesis and degradation, respectively (Munday, 2002). Malanoyl-CoA is then converted through a series of condensation reactions catalysed by the enzyme fatty acid synthase (FASN) to the 16 carbon saturated FA (SFA) palmitate. In higher order eukaryotes, FASN is a multi-component enzyme complex joined in a single polypeptide chain. FASN is expressed at low levels in most adult tissues in keeping with low rates of *de novo* lipid synthesis.

Desaturation of FA to yield monounsaturated FA (MUFA) significantly alters the physical properties of long-chain FA and is an important determinant of membrane fluidity. The balance between SFA and MUFA is tightly regulated. Key enzymes involved in the regulation of the SFA:MUFA ratio are the stearoyl-CoA desaturases (SCD). Two isoforms of this enzyme have been reported in humans: SCD1 and SCD5 (Wang et al., 2005; Zhang et al., 1999). SCD1 (simply referred to as SCD) is the best-characterised (Ntambi and Miyazaki, 2004). SCD is an endoplasmic reticulum (ER) resident enzyme and is a delta 9 desaturase, catalysing the formation of a double bond at the ninth position (C-9) from the carboxyl end of the FA. This reaction generates

palmitoleoyl-CoA from palmityl-CoA and oleoyl-CoA from stearoyl-CoA. In humans, SCD is ubiquitously expressed but the brain, liver, heart and lungs exhibit elevated SCD expression levels (Zhang et al., 1999). Interestingly, mammals lack enzymes capable of introducing double bonds beyond the C-9 in the FA chain. Therefore FA with double bonds at C-12 or C-15, such as linoleate and linolenate, respectively, are termed essential FA and must be supplied in the diet.

Acetyl-CoA can also be used to synthesise cholesterol. Cholesterol is an important component of biological membranes and is used as a precursor for the synthesis of steroid hormones. Acetyl-CoA is condensed with acetoacetyl-CoA to form 3-hydroxy-3-methylglutaryl-CoA (HMG-CoA), a reaction catalysed by the enzyme HMG-CoA synthase 1 (HMGCS1). HMG-CoA is the substrate for HMG-CoA reductase (HMGCR), the enzyme that catalyses the production of mevalonate. This reaction is the rate-limiting step for cholesterol synthesis and the activity of HMGCR is highly regulated. HMGCR is a transmembrane protein and is anchored to the ER membrane. It contains a sterol-sensing domain (SSD) and is targeted for degradation by the proteasome pathway following accumulation of certain sterols (Goldstein et al., 2006a).

It can be concluded that lipid synthesis therefore represents a coordinated series of reactions relying on intermediates and energy produced by more than one cellular metabolic pathway. Lipid synthesis requires the metabolites of the TCA cycle and the reducing power of the pentose phosphate pathway (PPP), as well as ATP supplied by glycolysis and oxidative phosphorylation (OXPHOS) (see Figure 1.1).

As previously mentioned, the process of FA degradation for the release of energy in the form of ATP is known as FA β-oxidation. The first step in FA β-oxidation is the transport of FA across the mitochondrial membrane. Free FA (FFA) are first activated in the cytoplasm by coupling to CoA. However, the mitochondrial membrane is impermeable to this large molecule. In order to facilitate transport into the mitochondrial matrix, the acyl chain must first be transferred to carnitine by carnitine palmitoyltransferase 1 (CPT1). The activity of this enzyme is inhibited by the FA synthesis intermediate malonyl-CoA, thereby ensuring that FA β-oxidation and lipid

synthesis are mutually exclusive reactions. As previously mentioned, the synthesis of malonyl-CoA is catalysed by ACC and ACACB is considered to be the main isoform regulating FA β-oxidation (Munday, 2002). Following entry into the mitochondria, acyl-chains are coupled to CoA and degraded by oxidation and hydration, thereby releasing acetyl-CoA and producing energy in the form of NADPH and $FADH_2$. The expression of a large number of genes encoding enzymes required for FA β-oxidation, including CPT1, is regulated by the peroxisome proliferator-activated receptor α (PPARα) transcription factor (Mandard et al., 2004).

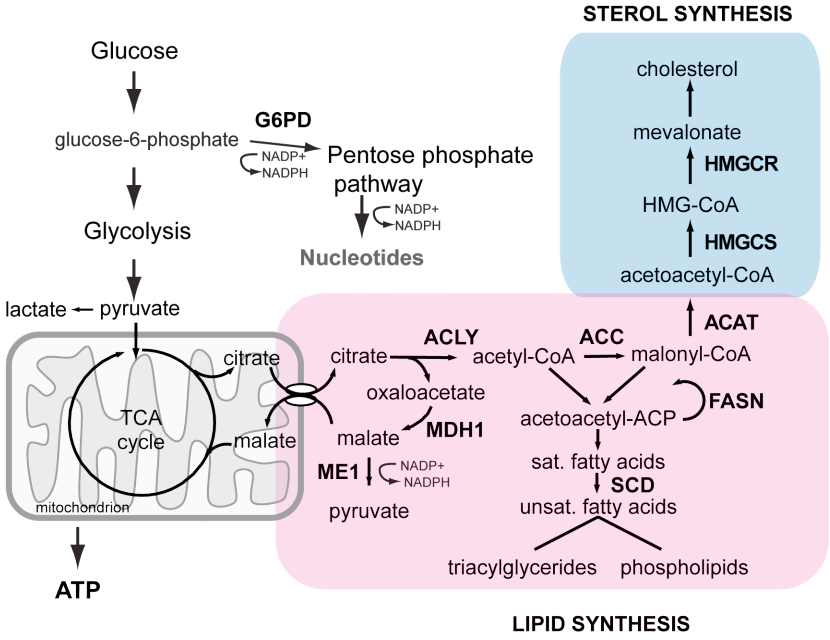

Figure 1-1: SREBPs regulate genes involved in lipid synthesis
Carbohydrate-derived lipid synthesis is regulated by the family of SREBP transcription factors. Glucose is converted into pyruvate which enters the TCA cycle. Mitochondrial citrate is exported into the cytoplasm where it is converted into acetyl-CoA by ACLY. The conversion of acetyl-CoA into malonyl-CoA is catalysed by ACC and is the rate-limiting step in fatty acid biosynthesis. Malonyl-CoA can also directed into the cholesterol biosynthesis pathway, where the rate-limiting step is the conversion of HMGCoA into mevalonate, regulated by HMGCR. Lipid synthesis requires the metabolites of the TCA cycle and the reducing power of the pentose phosphate pathway, as well as ATP supplied by glycolysis and oxidative phosphorylation. All of the enzymes shown are regulated at the transcriptional level by SREBPs.

1.2.1 Lipid metabolism and cancer

Glucose-derived *de novo* lipid synthesis is mainly restricted to the liver and adipose tissue in adults, but appears to be reactivated in many tumours despite availability of external lipids (Baron et al., 2004; Menendez and Lupu, 2007; Swinnen et al., 2006). The reason for this remains unclear, although it has been postulated that lipid synthesis may act as a carbon sink for the conversion of excess pyruvate that results from increased glycolytic flux (Hatzivassiliou et al., 2005). Furthermore, increased rates of lipid synthesis provide the cell with the phospholipids required for membrane biogenesis and synthesis of cholesterol and phospholipids is coordinated with the cell cycle (Igal, 2010).

There is substantial evidence for increased rates of *de novo* lipid synthesis in cancer cells, most notably reflected by the increased expression of FASN. Indeed, FASN was originally identified as a molecule associated with poor prognosis in breast cancer patients (Kuhajda et al., 1994). Furthermore, upregulation of FASN has been observed in a large variety of other human cancers, including colorectal, prostate, bladder, ovary, oesophagus, stomach, and lung (Menendez and Lupu, 2007). In addition, coordinated overexpression of FASN, ACC and ACLY has been observed in hepatocellular carcinoma (Yahagi et al., 2005). The increased expression of ACLY also correlates with decreased survival rates in patients with glioma (Beckner et al., 2009) and inhibition of ACLY can decrease tumour growth and prevent tumour cell differentiation in a variety of human cancer cell lines (Bauer et al., 2005; Hatzivassiliou et al., 2005). Upregulation of ACC has also been demonstrated in breast, (Yoon et al., 2007) as well as liver (see above) and prostate cancer cells (Swinnen et al., 2000b).

A comprehensive lipidomics study in breast cancer patients found that products of *de novo* FA synthesis incorporated into membrane phospholipids were increased in tumours and that this increase associated with poor patient survival (Hilvo et al., 2011). In addition, silencing of several genes involved in lipid synthesis (including FASN, SCD and ACACA) resulted in changes to membrane phospholipid composition as well as decreased cell viability in breast cancer cell lines compared with non-malignant cells (Hilvo et al., 2011). Another report using a mass-spectrometry phospholipid approach

found that increased FASN expression in tumours correlated with increased amounts of SFA and MUFA in membrane lipids, whilst levels of polyunsaturated FA (PUFA) were reduced (Rysman et al., 2010). This again supports the idea that tumour cells increase *de novo* lipogenesis, whilst decreasing lipid uptake. Interestingly, it was also found that increased generation of SFAs and MUFAs through increased lipid *de novo* lipid synthesis reduced levels of peroxidated lipid species in tumour cells, and that increased levels of PUFAs rendered the cancer cells susceptible to oxidative-stress induced cell death. Therefore, the lipogenic phenotype in cancer cells may also protect them from the damaging effects of lipid peroxidation (Rysman et al., 2010).

Additionally, other components of the lipid metabolic pathways have also been implicated in cancer. In keeping with the increased lipid synthesis observed in cancer cells in comparison to non-transformed cells, SCD is also upregulated in a number of cancer types, including breast, lung, renal, prostate, colon, bladder and leukaemia (Igal, 2010). However, a study in prostate cancer cells suggests that SCD expression is lost in this cancer type (Moore et al., 2005). In addition, there is evidence for increased amounts of MUFA in cancer cells and cohort studies show that an imbalance of the SFA:MUFA ratio correlates with cancer incidence (Igal, 2010). Interestingly, inhibition of SCD in breast cancer cells resulted in the activation of AMP-kinase (AMPK) and subsequent inactivation of ACC and a decrease in lipid synthesis (Scaglia et al., 2009). It is proposed that overexpression of SCD in cancer represents a mechanism to prevent inhibition of ACC by removal of SFAs, inhibitors of ACC activity (Igal, 2010). Increased conversion of SFAs to MUFAs by overexpression of SCD may also protect cancer cells from lipotoxicity as a result of increased lipid synthesis (Listenberger et al., 2003). Furthermore, increased levels of lipid droplets have been reported in cancer cells (Accioly et al., 2008; Bozza and Viola, 2010). Although their functional significance in cancer remains unclear, increased lipid droplet formation in cancer is in keeping with the idea of protecting cells from lipotoxcity. In addition, it was found that monoacylglycerol lipase (MAGL), the enzyme responsible for FA mobilisation from lipid stores, is overexpressed in aggressive human cancer cells and primary tumours (Nomura et al., 2010). This implicates lipolysis in tumour progression. In addition, the oxidative arm of the PPP has been linked to cancer progression. The tumour suppressor

p53 binds the rate-limiting enzyme of the PPP, glucose-6-phosphate dehydrogenase (G6PD) (Jiang et al., 2011). Active p53 therefore prevents G6PD activity, subsequently reducing glucose consumption, NADPH production and lipid biosynthesis. Mutations in p53 prevent its suppression of G6PD, resulting in enhanced glucose flux through the PPP (Jiang et al., 2011).

The coordinated regulation of biosynthetic pathways in cancer cells is regulated by a number of signalling networks. Mutations in various oncogenes and tumour suppressors within these regulatory networks contribute to the ability of cancer cells to increase aerobic glycolysis and lipid biosynthesis (Deberardinis et al., 2008). One of the major signalling pathways that regulates glycolysis and lipid metabolism is the PI3K/Akt/mTORC1 pathway. Indeed, Akt is considered to be the major integrator of signals that control lipid metabolism, cell proliferation, survival and oncogenic transformation (Deberardinis et al., 2008). This signalling pathway and its contribution to cancer is discussed in more detail in section 1.4.

1.3 Sterol regulatory element binding proteins

Sterol regulatory element binding proteins (SREBPs) belong to the family of basic helix-loop-helix-leucine zipper (bHLH-Zip) transcription factors (Bengoecheaalonso and Ericsson, 2007). Three SREBP isoforms were originally identified by cDNA cloning: SREBP1a, SREBP1c and SREBP2 (Hua et al., 1993; Yokoyama et al., 1993). The SREBF1 gene, which is located on chromosome 17, encodes for both SREBP1a and SREBP1c (Hua et al., 1995). The rat SREBP1c homologue is occasionally referred to as adipocyte determination and differentiation factor-1 (ADD1) (Eberle et al., 2004). Alternative transcription start sites result in the production of the two major SREBP1 isoforms, which differ only in their first exons (see Figure 1.2) (Bengoecheaalonso and Ericsson, 2007). Additional splice variants have also been reported, although it is likely that they represent only minor forms ((Nohturfft and Zhang, 2009) and references therein). The SREBF2 gene encodes for SREBP2 and is located on chromosome 22 (Hua et al., 1995). All three proteins share a common domain structure: an N-terminal transactivation domain, a DNA-binding domain, two transmembrane domains and a C-

terminal regulatory domain (Bengoecheaalonso and Ericsson, 2007; Sato et al., 1994) (see Figure 1.2). SREBPs are highly conserved throughout evolution, with homologues being identified in *Schizosaccharomyces pombe*, *Cryptococcus neoformans*, *Drosophila melanogaster*, and *Caenorhabditis elegans* (Nohturfft and Zhang, 2009). Furthermore, SREBP homologues have been predicted across all eukarya (Osborne and Espenshade, 2009).

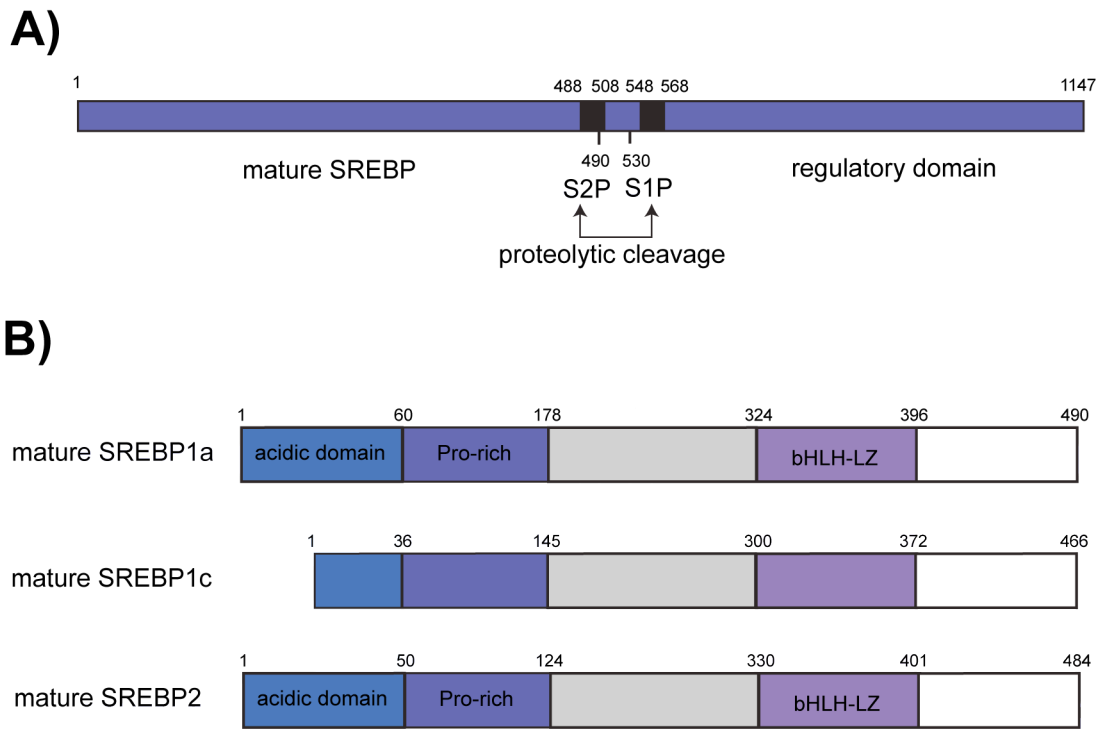

Figure 1-2 Domain structure of SREBP proteins.
Domain structure of full-length SREBP proteins showing the N-terminal mature SREBP and the C-terminal regulatory region. The two transmembrane segments are coloured black. The proteolytic cleavage sites for S1P and S2P are indicated. Numbers refer to amino acids within SREBP1a. (B) Domain structure of the mature SREBPs (mSREBPs). SREBP1a and SREBP1c are transcribed from alternative start-sites, resulting in the shorter acidic transactivation domain in SREBP1c. This domain binds transcriptional coactivators and regulators. The proline rich domain and the basic helix-loop-helix leucine zipper (bHLH-LZ) domains are also indicated. Adapted from Advances in Enzyme Regulation, (Lewis et al., 2011), copyright © 2011, with permission from Elsevier.

1.3.1 SREBP isoforms and the function of their target genes

As previously mentioned, most SREBP target genes encode for enzymes required for FA and cholesterol biosynthesis as well as the production of NADPH. Indeed, SREBPs were first identified through the search for regulators of the low-density lipoprotein receptor (LDLR) gene (Yokoyama et al., 1993), as well as the soluble form of HMGCS, HMGCS1 (Wang et al., 1994) and HMGCR (Hua et al., 1993). Other SREBP target genes identified early on include FASN (Bennett et al., 1995), as well as ACACA (Magana et al., 1997) and ACLY (Sato et al., 2000).

SREBPs differ from other bHLH transcription factors in that they have a tyrosine in place of the arginine residue found in their DNA binding domain (Kim et al., 1995). This allows the dual binding specificity of SREBPs to both E-boxes and the sterol regulatory element (SRE). The SRE was originally identified in the promoter of LDLR gene and consists of 10 nucleic acids (5'-ATCACCCCAC-3') containing a direct CAC repeat (Briggs et al., 1993). In the LDLR gene promoter, this SRE site is embedded in a 16 base pair sequence (repeat 2) that is directly followed by a 16 base pair sequence containing a binding site for the transcription factor SP1 (repeat 3) (Briggs et al., 1993). Other cholesterogenic genes contain SREs as well as binding sites for the transcription factor nuclear factor Y (NF-Y) (Amemiya-Kudo et al., 2002). It has also been shown in several studies that the co-regulatory factors SP1 and/or NF-Y are required for maximal transcriptional activity of SREBPs at the promoters of their target genes (Cagen et al., 2005; Murphy et al., 2006; Oh, 2003; Teran-Garcia et al., 2007). In addition, the promoters of genes encoding for lipogenic enzymes contain E-box-like and SRE-like motifs as well as carbohydrate response (ChoRE) elements (Amemiya-Kudo et al., 2002).

Studies in transgenic mice have yielded a large list of direct SREBP target genes (Horton et al., 2002). Although the SREBP isoforms have been shown to share many common transcriptional targets, the three SREBP isoforms have also been shown to function differentially *in vivo*. SREBP1c mainly activates genes involved in FA biosynthesis (Shimano et al., 1997a), whereas SREBP2 activates genes required for

cholesterol synthesis (Horton et al., 2003; Horton et al., 1998). SREBP1a appears to regulate genes involved in both biosynthetic pathways (Horton et al., 2003).

Over the last few years a number of studies using gene expression microarray analysis, chromatin immunoprecipitation (ChIP) and promoter occupancy methods as well as RNA interference (RNAi) screens have identified novel SREBP target genes that are involved in FA and cholesterol biosynthesis, as well as those involved in cellular processes other than lipid metabolism. Targeted RNAi screening identified novel SREBP targets, including the transmembrane protein 97 (TMEM97), which localises to endosomal/lysosomal compartments and binds the cholesterol transport-regulating protein Niemann-Pick C1 (NPC1) (Bartz et al., 2009). DNA microarray analysis of transgenic mouse livers expressing SREBP1a revealed that the cyclin-dependent kinase inhibitor p21 (CDKN1A) is a direct SREBP1a target gene (Inoue et al., 2005). A ChIP-chip study in HepG2 cells following treatment with insulin and glucose identified further novel SREBP1 target genes, including genes involved in lipid metabolism, the insulin signalling pathway and cell cycle control (Reed et al., 2008). DNA microarray analysis in human skeletal muscle cells overexpressing mSREBP1a or mSREBP1c showed that SREBPs play a role in functional pathways other than lipid metabolism, including mitochondrial respiration and redox, immune response and inflammation, regulation of cell cycle, proliferation and apoptosis (Rome et al., 2008). In addition, binding sites for SREBP1 have been found in the cell cycle regulator host cell factor C1 (HCFC1) and filamin A (FLNA), further suggesting a role for SREBPs in processes other than lipid metabolism (Motallebipour et al., 2009). Moreover, a recent study using ChIP-seq (ChIP-deep sequencing) for SREBP2 targets revealed that SREBP2 plays a role in autophagy and apoptosis (Seo et al., 2011). Furthermore, this study also showed that SREBP2 is required for autophagosome formation, and that SREBP2 deficiency decreases colocalisation of LDs with autophagosomes and triglyceride mobilisation in response to serum starvation (Seo et al., 2011).

In addition, a gene expression microarray study in human foreskin fibroblasts (AG01518 cells) infected with an adenovirus encoding mSREBP1c revealed that SREBP1c activates expression of the PI3K regulatory subunit p55γ (PI3KR3) and haem

oxygenase 1 (HMOX1), as well as other genes involved in the cellular stress response (Kallin et al., 2007). Furthermore, luciferase reporter analysis in HepG2 cells showed that the expression of HMOX1 is sensitive to both SREBP1a and SREBP1c expression, but not SREBP2, indicating that regulation of HMOX1 is SREBP1-specific in human hepatocarcinoma cells (Kallin et al., 2007). Interestingly, this is not the only evidence for SREBP-dependent regulation of the PI3K pathway. The insulin receptor substrate 2 (IRS2) is an adapter protein required for insulin-dependent PI3K activation. SREBP1c inhibits transcription of the insulin receptor substrate 2 (IRS2) in mouse livers (Ide et al., 2004). Interestingly, this is through direct binding of SREBP1c to an SRE that overlaps the insulin response element (IRE) in the IRS2 promoter. Furthermore, SREBP1c directly competes with FOXO1 for binging to the IRS2 promoter, resulting in reciprocal regulation of IRS2 expression between FOXO1 and SREBP1c (Ide et al., 2004). Regulation of PI3KR2 by SREBP could therefore represent another negative feedback loop in the insulin-signalling pathway.

Other SREBP target genes whose function has not previously been connected to lipid metabolism include two members of the human caspase family. Caspase 2 (CASP2) and caspase 7 (CASP7) have both been shown to contain SREs within their promoters. In addition, these genes are regulated by SREBP1 and SREBP2 in HepG2 cells (Gibot et al., 2009; Logette et al., 2005). However, no regulation of these genes has been observed *in vivo* in mouse livers, although the authors argue that this is due to the substantial difference between the human and murine promoters (Logette et al., 2005). It is unclear what role CASP2 and CASP7 play in the regulation lipid metabolism. No positive effect on cholesterol levels was observed following SREBP-dependent CASP7 activation (Gibot et al., 2009). In contrast, CASP2 silencing reduced cellular lipid levels and is believed to provide an amplification loop to restore normal lipid levels in response to lipid depletion (Logette et al., 2005).

Studies in livers of transgenic mice over-expressing the individual SREBP isoforms, as well as knockout mice lacking individual components of the SREBP activation pathway (see section 1.3.2.1) have confirmed SREBPs as essential genes (Horton et al., 2002). Mice lacking all SREBP isoforms die early on during embryonic development (Yang et

al., 2001). Interestingly, mice lacking the SREBF2 gene are embryonic lethal, although lethality occurs at a later stage when compared with mice lacking all SREBP isoforms (Horton et al., 2002). Mice lacking the SREBF1 gene, and therefore both SREBP1a and SREBP1c isoforms, display only partial embryonic lethality. SREBP2 mRNA expression is increased in these animals, suggesting that SREBP2 can compensate for loss of both SREBP1 isoforms (Shimano et al., 1997b). Mice harbouring an SREBP1c-specific deletion are viable (Liang, 2002), indicating that the partial embryonic lethality observed in SREBF1$^{-/-}$ mice is due to the loss of the SREBP1a isoform (Horton et al., 2002). This is consistent with observations that SREBP1a is a stronger transcriptional activator than SREBP1c due to its larger transactivation domain (Shimano et al., 1997a) and that SREBP1c is not stably recruited to promoters of SREBP target genes in intact cells (Bennett, 2004). However, SREBF1c$^{-/-}$ mice exhibit significantly higher liver cholesterol content than their wt counterparts, as well as decreased levels of plasma cholesterol and plasma TAGs and mRNA levels of FA synthesis genes are significantly reduced (Liang, 2002).

In addition, tissue-specific distribution of the three isoforms differs. SREBP1c is considered to be the dominant SREBP1 isoform *in vivo*, with particularly high expression in the liver (Shimomura et al., 1997). In addition, SREBP1c expression is higher than that of SREBP1a in mouse and human adrenal gland, white adipose tissue and brain (Shimomura et al., 1997). In cultured cells, however, SREBP1a is the predominant isoform (Shimomura et al., 1997). SREBP2 is expressed in all human tissues as well as cultured cells (Hua et al., 1993).

1.3.2 Regulation of SREBP activity

Regulation of SREBP transcriptional activity is governed by a number of processes, including proteolytic cleavage, post-translational modification and transcriptional regulation. This results in the tightly controlled activity of SREBPs as master regulators of lipid homeostasis (Eberle et al., 2004).

1.3.2.1 Regulated intramembrane proteolysis (RIP)

Seminal papers from the laboratories of Goldstein and Brown over the last 20 years have identified a complex mechanism by which the SREBPs are regulated in response to cellular sterol levels; so-called regulated intramembrane processing (RIP) (Brown and Goldstein, 1997; Sakai et al., 1996). This process results in the release of the active transcription factor from its precursor form. An overview of the RIP process is shown in Figure 1.3.

SREBPs are synthesised as inactive, 125 kDa precursors. The full-length proteins are inserted into the ER membrane, where the C-terminal regulatory domain of SREBP interacts with the C-terminus of the SREBP cleavage activating protein (SCAP) (Sakai et al., 1997). SCAP was originally identified from mutant Chinese hamster ovary (CHO) cells that fail to suppress cleavage of SREBPs in the presence of sterols (Hua et al., 1996). It is a membrane-bound protein with two distinct domains: an N-terminal region that contains eight membrane-spanning regions and a hydrophilic C-terminal domain containing four WD repeats (Brown and Goldstein, 1997; Nakajima et al., 1999). The N-terminal half of the protein also contains the sterol-sensing domain (SSD), which is required for the sterol-regulated cleavage of SREBPs (Hua et al., 1996). Under conditions of sterol depletion, the SCAP/SREBP complex is clustered into coat protein complex II (COPII)- coated vesicles which then translocate from the ER to the Golgi (Sun, 2005), where SREBP undergoes a two-step proteolytic cleavage event. Association of SCAP to components of the COPII protein complex facilitates this ER-Golgi translocation. More specifically, sterol depletion results in the binding of SCAP via its MELADL amino acid sequence to the Sec24 COPII protein (Sun, 2005). Sterol saturated conditions within the ER membrane induce a conformational change in SCAP which results in its interaction with the insulin induced genes (INISG1 or INSIG2) (Brown et al., 2002; Yang et al., 2002). This conformational change sequesters the MELADL sequence away from Sec24 (Sun et al., 2007), preventing the incorporation of the SCAP/SREBP complex into the COPII-coated vesicles and thereby retaining the SCAP/SREBP complex in the ER. The sterol sensing mechanism involves both binding of cholesterol to SCAP and the binding of oxysterols to INSIG, both of which result in conformational changes in SCAP described above (Radhakrishnan et al., 2007; Sun et

al., 2007). SCAP is considered indispensible for mammalian SREBP sterol-dependent regulation. However, in *Drosophila melanogaster*, it has been shown that larvae lacking dSCAP still process dSREBP in certain tissues, suggesting an alternative mechanism of regulation in this organism (Matthews et al., 2010). In addition, processing of dSREBP is regulated by phosphatidylcholine rather than sterols in flies (Dobrosotskaya, 2002).

Cellular levels of INSIGs are also controlled by the proteasome pathway. Following dissociation from SCAP, INSIG1 is targeted by the membrane bound E3 ubiquitin ligase GRP78 resulting in its proteasomal degradation (Lee et al., 2006). In addition, INSIG1 (but not INSIG2) is an SREBP target gene (Horton et al., 2003). Thus, the retention of the SCAP/SREBP complex in the ER is dependent on the SREBP-dependent re-synthesis of INSIG1, creating a convergent mechanism for feedback control of SREBPs (Gong et al., 2006). The intricate details of the INSIG/SCAP/SREBP interactions along with the sterol sensing mechanisms are reviewed extensively in (Goldstein et al., 2006b).

Following transport from the ER to the Golgi, SREBPs are proteolytically cleaved to release the active transcription factor for nuclear translocation. This sequential cleavage requires the Golgi resident membrane proteins site-1 and site-2 proteases (S1P and S2P) (Goldstein et al., 2002). S1P cleaves the N-terminal luminal loop of SREBP in a sterol-regulated manner, resulting in two halves of the protein, which initially remain tethered to the membrane (Brown and Goldstein, 1999). This partially cleaved form has been designated the intermediate fragment of SREBP (Sakai et al., 1996). The second cleavage occurs independently of sterol concentrations and is performed by S2P at a site just within the membrane-spanning domain of SREBP (Brown and Goldstein, 1999). This second cleavage event results in the release of the N-terminal active transcription factor, termed mature SREBP (mSREBP) (Goldstein et al., 2002). The sterol-dependency of S1P cleavage is presumably as a result of the SCAP/SREBP translocation from the ER to the Golgi, whereas S2P cleavage is dependent upon the initial cleavage by S1P (Brown and Goldstein, 1999).

Following cleavage by S1P and S2P proteases, the N-terminal mature protein translocates to the nucleus where it binds promoters of its target genes as a homodimer (Parraga et al., 1998). There is only limited literature surrounding the exact mechanisms by which SREBPs enter the nucleus. However, it has been shown that SREBP2 interacts with the nuclear import protein Importin-β via its bHLH domain (Lee et al., 2003; Nagoshi et al., 1999). Furthermore, this interaction is dependent on the dimeric form of mSREBP2, as monomeric mSREBP2 cannot enter the nucleus and is not recognised by Importin-β (Nagoshi and Yoneda, 2001). These studies put forward the idea the bHLH domain serves as a nuclear localisation signal for SREBPs. Given the homology between all SREBP isoforms, it is entirely plausible that this is also true for mSREBP1a and mSREBP1c.

It should be noted that sterol-sensitive regulation does not necessarily apply to all three SREBP isoforms, at least not *in vivo*. Studies performed *in vivo* show that liver SREBP1 is not regulated in response to sterol, while SREBP2 is only processed in sterol-depleted cells (Sheng et al., 1995). Furthermore, SREBP1c in mouse liver is processed in response to insulin treatment, in a sterol-independent manner (Hegarty et al., 2005). In addition, studies performed in HEK293 cells show that in certain metabolic conditions, the addition of cholesterol blocks processing of SREBP1 but not SREBP2 (Hannah et al., 2001). This is interesting as it suggests that the SREBP isoforms may be differentially regulated in response to different stimuli.

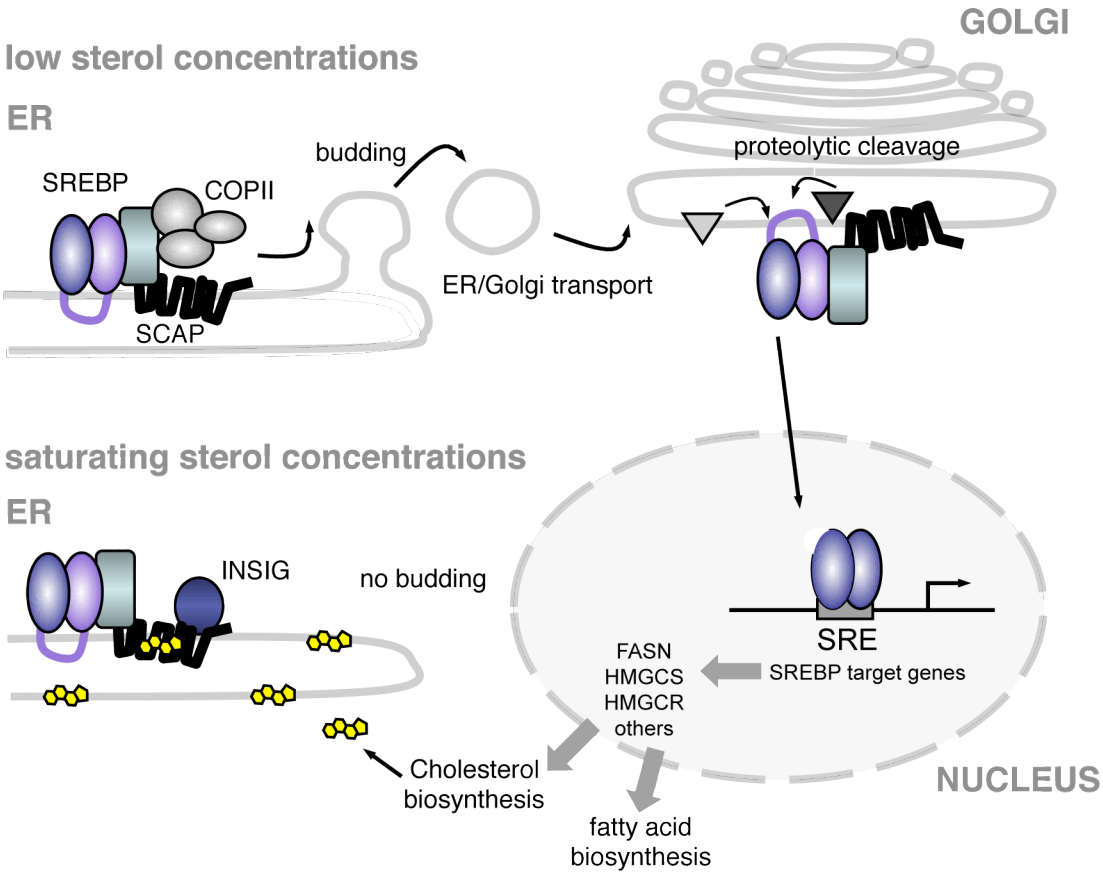

Figure 1-3: SREBPs are activated by regulated intramembrane processing (RIP)
SREBPs are synthesised as inactive precursors inserted into the ER membrane. Under low sterol concentrations, the SREBP-SCAP complex binds COPII vesicles, resulting in translocation to the Golgi. SREBP undergoes a two-step proteolytic cleavage by S1P and S2P. Once cleaved, the N-terminus (mature of SREBP) translocates to the nucleus where it binds to the SRE in promoters of target genes as a homodimer. When sterol conditions are saturating, SCAP undergoes a conformational change, resulting in the binding of INSIG which anchors the SREBP-SCAP complex in the ER. Adapted from an article originally published in Biochemical Society Transactions, (Porstmann et al., 2009), © the Biochemical Society.

1.3.2.2 Transcriptional regulation

Transcriptional activity of SREBPs is also regulated at the transcriptional level. Interestingly, although changes in mRNA expression levels have been reported for all three isoforms in response to various stimuli, much of the evidence of transcriptional regulation concerns SREBF1c (Eberle et al., 2004).

SREBF1c mRNA expression is regulated in response to nutritional changes in the liver (Horton et al., 2002) and insulin is known to induce expression of SREBF1c in both adipocytes (Kim et al., 1998) and hepatocytes (Azzout-Marniche et al., 2000). The effects of insulin on SREBF1c expression have been shown to be mediated downstream of the PI3K pathway (Fleischmann and Iynedjian, 2000) and Akt activation in human retinal pigment epithelial (RPE) cells induces the expression of both SREBF1c and SREBF1a, but not that of SREBF2 (Porstmann et al., 2005). The regulation of SREBP activation downstream of this pathway is described in more detail in section 1.4.3. Activation of SREBP has also been observed downstream of other mitogenic stimuli, including platelet derived growth factor (PDGF) (Demoulin, 2004), keratinocyte growth factor (KGF) (Chang et al., 2005) and epidermal growth factor (EGF) (Guo et al., 2009b; Swinnen et al., 2000a). In addition, transcription of SREBF1c is induced by binding of the pancreatic-duodenal homeobox-1 (PDX-1) and hepatic nuclear factor-4α (HNF-4α) transcription factors to elements within its promoter (Tarling et al., 2004).

SREBF1c expression is also controlled by the liver X receptor-alpha (LXRα). LXRα is a nuclear hormone receptor that is expressed at high levels in the liver and is activated by oxysterols (Baranowski, 2008). It is considered to be a cholesterol sensor, explaining how SREBF1c is upregulated in a sterol-sensitive manner (Eberle et al., 2004). LXRα regulates the transcription of SREBF1c through the RXR/LXR response elements (LXREs) within the SREBF1c promoter. PPARα is also a member of this superfamily of nuclear hormone receptors. In addition to LXRs and SREBPs, PPARs also play a major role in lipid metabolism and FA β-oxidation. A recent study identified PPARα as a novel regulatory factor in SREBF1c expression and demonstrated that PPARα agonists act in cooperation with insulin and LXR to induce lipid synthesis (Fernandez-Alvarez et al., 2011).

Other regulatory factors of SREBF1c expression include the family of forkhead box-"other" (FOXO) transcription factors. These transcription factors are regulated downstream of Akt and play a major role in key cellular processes, including metabolism and the response to cellular stress (Greer and Brunet, 2005). In the absence

of activated Akt, FOXOs are localised to the nucleus, where they regulate the transcription of their target genes. Upon activation of Akt in response to growth factors, FOXOs are phosphorylated, resulting in their exclusion from the nucleus and the inhibition of their target gene transcription. It has been shown that in transgenic mouse livers, FOXO1 negatively regulates the expression of genes involved in glycolysis, the PPP and lipid synthesis, including SREBF1c (Zhang et al., 2006b). Furthermore, in skeletal muscle of transgenic mice, FOXO1 abrogates the RXRα/LXRα-dependent expression of SREBF1c (Kamei et al., 2008). A study in HepG2 cells revealed that this FOXO1-dependent reduction in SREBF1c expression required the LXRE motif in the SREBF1c promoter, and that FOXO1 inhibits binding of LXRα to the SREBF1c promoter (Liu et al., 2010).

SREBF1c and SREBF2 contain SREs within their promoters (Amemiya-Kudo, 2000; Sato et al., 1996), resulting in feed-forward transcriptional regulation. Furthermore, over-expression of SREBPs in transgenic mice results in the induction of SREBF1c mRNA (Horton et al., 2003). In addition, the promoters of all three SREBF isoforms contain binding sites for the transcription factor SP1, and SREBF1c and SREBF2 promoters also contain NF-Y binding sites (Amemiya-Kudo, 2000; Sato et al., 1996; Zhang et al., 2005). Transcriptional regulation of SREBF1a is induced at low levels compared to SREBF1c in response to sterol depletion, although this is only true for cultured cells and not in mouse livers (Shimomura et al., 1997). The promoter region for SREBF1a is contained within a very small promoter-proximal region, containing two SP1 binding sites (Zhang et al., 2005). This may explain why SREBF1a expression is low and constant in most tissues. A recent study into the effects of glutamine on SREBP transcriptional activity in HepG2 cells has revealed that glutamine increases SREBF1a expression through increased binding of SP1 to its promoter (Inoue et al., 2011). In addition, glutamine increases processing of SREBP1a and SREBP2, which in turn leads to the increased expression of SREBF2 via the feed-forward mechanism described above (Inoue et al., 2011).

Transcriptional activity of SREBPs is also subject to negative feedback via unsaturated FA. The MUFA oleate (C18:1), has been shown to potentiate the effect of sterols on

reducing nuclear levels of both SREBP1 and SREBP2 (Thewke et al., 1998). In addition, the effects of MUFA and PUFA on SRE-dependent gene expression are independent and additive to the effects of exogenous sterol (Worgall et al., 1998). Interestingly, in HEK293 cells, both SREBP1a and SREBP1c are subjected to negative regulation in response to both MUFA and PUFA, whereas SREBP2 remains unaffected (Hannah et al., 2001). It has been shown that in rat hepatoma cells, unsaturated fatty acids down-regulate levels of SREBF1c in liver at least in part through antagonising the actions of LXRα (Ou et al., 2001). A more recent study by Takeuchi and colleagues using *in vivo* reporter assays demonstrated that PUFA selectively regulate expression of SREBP1c in the livers of mice (Takeuchi et al., 2010). However, they showed that this regulation was independent of the LXRα and that the decreased expression of SREBP1c in response to PUFA was actually mediated through autoloop regulation of SREBP1c itself. PUFA specifically prevented SREBP1 cleavage activation (but not SREBP2), thereby reducing nuclear levels of the mature transcription factor resulting in decreased transcription of SREBF1c itself (Takeuchi et al., 2010).

1.3.2.3 Post-translational modification

The stability of mature SREBPs represents a major mechanism of regulation of their transcriptional activity. A number of different post-translational modifications have been reported, which generally affect either the stability of the SREBP proteins, their transcriptional activity, or both. Phosphorylation appears to be the major post-translational modification regulating SREBP activity. Most reports describe the phosphorylation of mSREBP1a, although sequences within both SREBP1 isoforms and SREBP2 are conserved and it is likely that SREBP2 is regulated in a similar manner (Sundqvist et al., 2005).

Perhaps the best characterised of these phosphorylation events are those carried out by the glycogen synthase kinase 3β (GSK3β) isoenzyme. It was initially shown that mature SREBPs are targeted for degradation by the proteasome (Hirano et al., 2001), and that this is dependent on the transcriptional activity of the transcription factor (Sundqvist and Ericsson, 2003). This latter study demonstrated that mutations within the transactivation or DNA binding domain of SREBP1a inhibit the transcriptional activity

of the protein, leading to stabilisation of the protein (Sundqvist and Ericsson, 2003). Transcriptionally active mSREBP1a is targeted for degradation by the ubiquitin-proteasome pathway (Sundqvist and Ericsson, 2003). It was later shown that this proteasomal degradation depends on the phosphorylation of mSREBP1a by GSK3β (Sundqvist et al., 2005). Initially, two phosphorylation sites within the C-terminus of mSREBP1a were identified: Threonine 426 and Serine 430 (T426/S430). Phosphorylation of these sites by GSK3β is recognised by the ubiquitin ligase SCF^{Fbw7} complex and results in ubiquitination and subsequent proteasomal degradation of the phosphorylated protein (Sundqvist et al., 2005). More recently, a third phosphorylation site has been identified several residues downstream of the existing sites (S434) (Bengoechea-Alonso and Ericsson, 2009). Phosphorylation of this "priming" site by GSK3β results in the subsequent phosphorylation of T426 and S430. GSK3-dependent phosphorylation is enhanced upon binding of mSREBP to DNA (Punga, 2006), further confirming that transcriptional activity of mSREBPs and their stability are intricately linked.

In addition to GSK3β, other kinases have been reported to phosphorylate SREBPs. It has been shown that hyperphosphorylation of mSREBP1a and mSREBP1c leads to the increased stability of the proteins in mitotic cells (Bengoechea-Alonso et al., 2005). This hyperphosphorylation was later shown to be dependent on the Cdk1/ cyclin B complex. Indeed, mSREBP1 interacts with this complex and is phosphorylated on residue S439 during mitosis (Bengoechea-Alonso and Ericsson, 2006).

Since SREBPs are regulated downstream of PI3K/ Akt/ mTORC1 signalling (see section 1.4.3), it seems likely that one or more of the kinases within this pathway may be directly interacting with, and phosphorylating, SREBPs. To date, there is no evidence to support a direct interaction of SREBP with mTORC1, although a putative Tor signalling (TOS) motif has been identified within the C-terminus of SREBP1a (Almut Schulze, personal communication). It has been reported that both flSREBP1c and mSREBP1c (but not SREBP2) are phosphorylated by Akt in primary rat hepatocytes (Yellaturu et al., 2009). However, the exact residues that are phosphorylated have not been identified. This phosphorylation reportedly results in the

increased association of the SREBP/SCAP complex with COPII vesicles and therefore increased ER to Golgi transport (Yellaturu et al., 2009). Interestingly, it has been demonstrated that Akt directly phosphorylates Sec24 *in vitro* (Sharpe et al., 2010). Sec24 is a component of COPII complex required for ER-Golgi translocation of the SCAP-SREBP complex. This Akt-dependent phosphorylation of Sec24 results in the increased binding affinity of Sec24 for its interaction partner Sec23, another component of the COPII complex (Sharpe et al., 2010). However, the exact residue that is targeted by Akt phosphorylation is unknown, and it remains to be shown whether this phosphorylation event increases ER-Golgi translocation of the SCAP-SREBP complex.

In addition, mature forms of SREBP1a, SREBP1c and SREBP2 have been shown to be phosphorylated in response to insulin signalling downstream of the mitogen activated protein kinase (MAPK) pathway (Kotzka et al., 2000). Insulin treatment induces the phosphorylation of S117 on SREBP1a by Erk1/2 *in vitro* and mutation of this residue to alanine abolished ERK1/2 related transcriptional activation of SREBP *in vivo* (Roth et al., 2000). SREBP2 is phosphorylated by ERK1/2 on S432 and S455 *in vivo* and this phosphorylation does not affect the DNA binding of mSREBP2 but increases its transcriptional activity (Kotzka et al., 2004). It has also been shown that SREBPs are phosphorylated by the cAMP-dependent kinase PKA (Lu, 2006). Both mSREBP1a and mSREBP1c are phosphorylated by PKA *in vitro* and in HepG2 cells, resulting in decreased DNA binding and transactivation (Lu, 2006).

The AMP-activated protein kinase (AMPK) is involved in cellular energy homeostasis and antagonises pathways stimulated by insulin (Kahn et al., 2005). Recently, it was found that AMPK is able to phosphorylate serine residues in the bHLH domain of SREBP1c and SREBP2 in diabetic rat livers (Li et al., 2011). These phosphorylation events prevent cleavage and subsequent nuclear translocation of the transcription factors in response to polyphenols and metformin treatment (Li et al., 2011).

SREBPs are also regulated by acetylation. Lysine residues in both SREBP1a and SREBP2 are acetylated by the intrinsic acetylase activity of the co-activator protein p300 and CBP (Giandomenico et al., 2003). The acetylation of K324 and K333 within

the DNA-binding domain of mSREBP1a confers stability of the protein (Giandomenico et al., 2003). Since K333 is also targeted by ubiquitination, acetylation of mSREBP1a may increase stability by preventing ubiquitination and proteasome-dependent degradation (Giandomenico et al., 2003). In keeping with this hypothesis, it was recently shown that sirtuin 1 (SIRT1) deacetylates mSREBP1c and that this leads to degradation of the protein and subsequent decrease in SREBP target gene expression (Ponugoti et al., 2010; Wang et al., 2009). In addition, the activating transcription factor-6 (ATF6) can form a complex with DNA-bound mSREBP2 in glucose-deprived cells, resulting in the recruitment of histone deacetylase complex-1 (HDAC1) and attenuated transcriptional activity of mSREBP2 (Zeng et al., 2004).

In addition, SREBPs are also modified by the small ubiquitin-related modifier-1 (SUMO1). Two residues within mSREBP1a and a single site within SREBP2 have been shown to be SUMOylated (Hirano et al., 2003). In contrast to most of the post-translational modifications described so far, SUMOylation inhibits the transactivation capacity of mSREBPs (Hirano et al., 2003). Moreover, ERK-dependent phosphorylation of mSREBP2 in response to insulin like growth factor 1 (IFG1) inhibits SUMOylation of mSREBP2, thereby increasing its transcriptional activity (Arito et al., 2008).

Although a great deal of evidence exists for the regulation of stability of the mature SREBPs, little is known about whether the full length precursor proteins are also targeted for degradation. Interestingly, overexpression of the translocation in renal carcinoma on chromosome 8/ RING finger protein 139 (TRC8/RNF139) ubiquitin ligase results in the increased degradation of flSREBP in response to long-term sterol depletion (Lee et al., 2010). This suggests that the stability of the mature proteins, as well as that of the flSREBPs are regulated, further complicating the regulation of SREBP activity.

1.3.3 SREBPs and cancer

Despite SREBPs playing a central role in the expression of lipid synthesis genes and the clear association of altered lipid metabolism with various cancer types, there is little evidence for a direct role of SREBPs in cancer. Most evidence comes from the dysregulation of SREBP target genes (see section 1.2.1). However, a study by Swinnen and colleagues demonstrated that the upregulation of FASN expression in response to epidermal growth factor (EGF) signalling in the human prostate cancer cell line LnCap is mediated through SREBP1 (Swinnen et al., 2000a). Furthermore, SREBP1 was shown to participate in the upregulation of FASN in colorectal neoplasia (Li et al., 2000). Increased FASN expression in a panel of breast cancer cell lines was also shown to be dependent on SREBP1c (Yang et al., 2003), clearly implicating SREBP in the increased lipogenic phenotype of cancer cells. In addition, studies from glioblastoma patients treated with the EGF receptor (EGFR) inhibitor lapatinib showed that EGFR induces the cleavage and activation of SREBP in this cancer type (Guo et al., 2009b). Moreover, increased phosphorylated Akt correlated with increased nuclear mSREBP1 as well as increased levels of FASN and ACC expression in tumours from primary GBMs. Tumours formed from U87 or U87-EGFRvIII cells in mice were smaller when treated with the FASN inhibitor C75. Inhibition of lipid synthesis resulted in increased apoptosis in U87-EGFRvIII cells *in vitro* and *in vivo*, showing that a persistently active EGFR allele sensitises GBMs to apoptotic cells death in response to inhibition of lipogenesis (Guo et al., 2009b). These data demonstrate a role for SREBP in this EGFR-mediated prosurvival pathway in glioblastoma.

1.4 The PI3K/Akt/mTORC1 signalling pathway:

1.4.1 Akt/PKB

The Akt/ PKB (protein kinase B) is a serine/ threonine kinase that plays a vital role in many cellular processes including metabolism, proliferation, cell survival and growth control (Figure 1.4) (Manning and Cantley, 2007). Three closely related homologues of Akt have been identified in humans (Bellacosa et al., 1991; Coffer and Woodgett, 1991; Jones et al., 1991). Although double knockout mouse models indicate a significant overlap in isoform function *in vivo*, the phenotypes of loss-of-function mouse models have established non-redundant functions for the three individual isoforms: Akt1 plays a major role in embryonic development and postnatal survival; Akt2 functions in glucose homeostasis and Akt3 is important for brain development (Dummler and Hemmings, 2007).

Akt is activated downstream of the lipid kinase phosphatidylinositol 3-kinase (PI3K) in response to growth factors and insulin signalling (Figure 1.4). Class I_A PI3Ks are heterodimers that consist of a regulatory subunit (p85) and a catalytic subunit (p110) (reviewed in (Engelman, 2009)). Ligand binding to growth factor receptors results in autophosphorylation of the cytoplasmic domain of receptor tyrosine kinases (RTKs). The p85 regulatory subunit of PI3K binds via its Src-homology2 (SH2) domain to phosphotyrosine residues on activated RTKs. In case of the insulin receptor (IR), p85 binds to an adaptor molecule (IR substrate: IRS). The binding of the p85 subunit serves to recruit the p85-p110 heterodimer to the membrane and to relieve basal inhibition of p110 (Yu et al., 1998). Once at the membrane, PI3K phosphorylates its substrate phosphatidylinositol-4,5-bisphosphate (PIP_2) to generate the second messenger phosphatidylinositol-3,4,5-triphosphate (PIP_3). Akt binds PIP_3 via its plekstrin-homology (PH) domain. The interaction of Akt and PIP_3 serves to recruit Akt to the plasma membrane (Andjelkovic et al., 1997; Bellacosa et al., 1998), where it is phosphorylated by 3-phosphoinositide-dependent kinase (PDK1) on T308 (Akt1) within the protein kinase T-loop (Alessi et al., 1997). Phosphorylation of Akt on T308 results in a conformational change that facilitates ATP and substrate binding (Stephens et al.,

1998). However, full activation of Akt occurs only upon an additional phosphorylation on S473 (Akt1), located within a hydrophobic motif proximal to the C-terminus. This phosphorylation is carried out by the mammalian target of rapamycin complex 2 (mTORC2) (Hresko and Mueckler, 2005; Sarbassov et al., 2005), although other kinases have been reported to phosphorylate Akt on this residue (Woodgett, 2005). While both phosphorylation events are required for complete activation of Akt, they can occur independently (Jacinto et al., 2006; Williams et al., 2000). Phosphorylation of Akt on S473 enables its translocation to the nucleus, meaning that subcellular compartmentalisation may infer substrate specificity (Jacinto et al., 2006).

Many direct substrates of Akt have been identified, and these substrates reflect the role of Akt in regulating metabolism, protein synthesis, survival and proliferation. Indeed, one of the first Akt substrates to be identified was the glycogen synthase kinase-3α and -3β (GSK3α/β). Akt-mediated phosphorylation of GSK3α/β inhibits their activity (Cross et al., 1995). GSK3 phosphorylates and inhibits glycogen synthase (GS), resulting in the inhibition of glycogen synthesis from glucose-6-phosphate. Activated Akt stimulates the association of hexokinase with the mitochondrial membrane which is important for the conversion of glucose to glucose-6-phosphate (Robey and Hay, 2006). Glucose uptake is also stimulated by Akt-dependent translocation of the glucose transporter GLUT4 to the membrane (Kohn et al., 1998). Akt also increases the expression of several glycolytic enzymes via activation of HIF1α (Manning and Cantley, 2007). Glucose metabolism is further regulated by Akt-dependent phosphorylation of FOXO1, resulting in decreased expression of gluconeogenesis genes (Manning and Cantley, 2007). Akt also plays a major role in lipid metabolism by positively regulating carbohydrate-derived lipid synthesis. Aside from regulating SREBPs (see section 1.4.3), Akt directly phosphorylates ACLY, possibly increasing its activity (Berwick et al., 2002). Akt phosphorylates and inhibits the hepatic transcriptional coactivator PGC1α (Li et al., 2007). PGC1α regulates the expression of genes required for FA β-oxidation, as well as gluconeogenesis (Puigserver, 2005). In addition, Akt phosphorylates and inhibits the transcription factor FOXA2, thereby suppressing expression of genes encoding enzymes involved in β-oxidation (Wolfrum et al., 2004). Akt, therefore, is a key player in carbohydrate-derived lipid metabolism by

co-ordinately upregulating glycolysis and lipid synthesis whilst decreasing gluconeogenesis and FA β-oxidation.

Aberrant activation of the PI3K/Akt/mTORC1 signalling pathway, for example, via the constitutive activation of oncogenic Ras or the loss of the phosphatase and tensin homolog deleted on chromosome 10 (PTEN) tumour suppressor protein is found in many cancers (Altomare and Testa, 2005). Amplification of Akt itself has been found in a number of human cancers and a somatic mutation in the PH-domain of Akt1 has been observed in breast, colorectal and ovarian cancers (Carpten et al., 2007). This mutation results in membrane recruitment in a PI3K-independent manner and constitutive activation of Akt (Carpten et al., 2007). Activating mutations in the PI3K p110α subunit are found in a variety of human cancers, including ovarian, cervical and lung cancers (Ma et al., 2000; Massion et al., 2002; Shayesteh et al., 1999). Moreover, mutations and amplifications of upstream receptor tyrosine kinases (RTKs) are also frequently found in human cancers. For example, copy numbers of epidermal growth factor receptor (EGFR) are vastly increased in malignant gliomas (Sauter et al., 1996). In addition, the deletion of exons 2-7 in EGFRvIII mutations confers constitutive kinase activity in glioblastomas (Narita et al., 2002). HER2, another EGFR family member, is overexpressed in 25-30% of invasive breast and ovarian cancers and is associated with poor prognosis (Moasser, 2007). Loss of the tumour suppressor protein PTEN represents the most common mechanism of activation of the PI3K/Akt pathway (Shaw and Cantley, 2006). PTEN is the second most mutated tumour suppressor in human cancers after p53, and PTEN mutations have been found in a wide range of human malignancies (Shaw and Cantley, 2006; Yuan and Cantley, 2008).

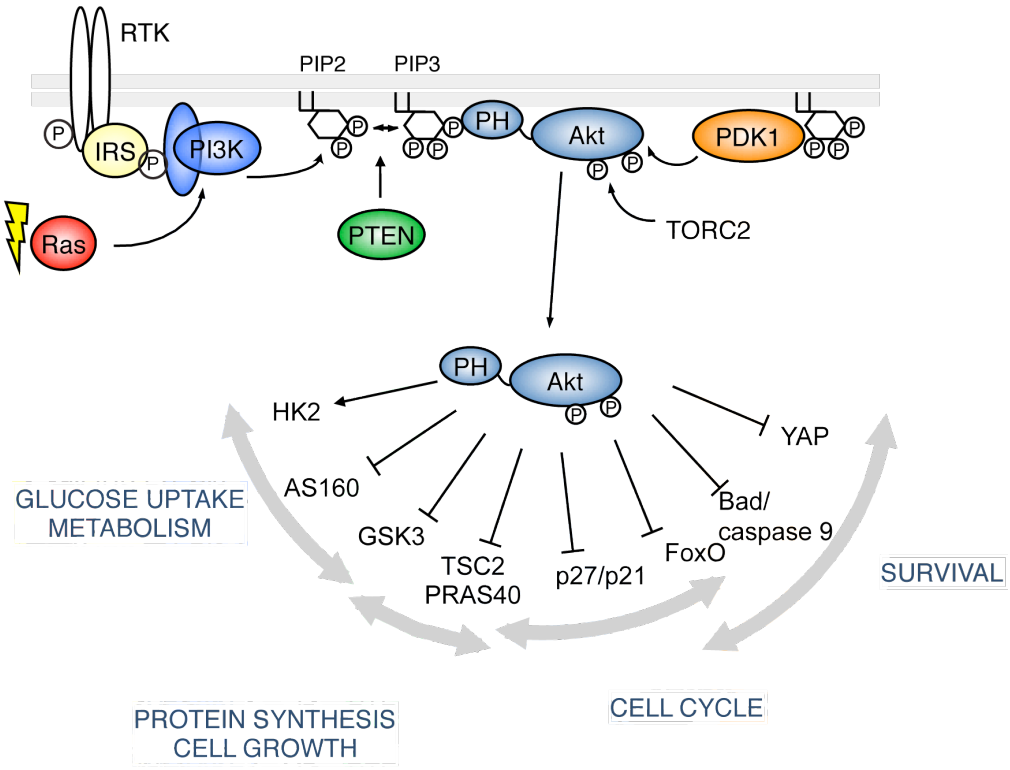

Figure 1-4: The PI3K/Akt signalling pathway
Class I_A PI3K are activated in response to ligand binding to the receptor (RTK). Activation either occurs through direct binding of the p85 subunit to the phosphorylated receptor or via adaptor proteins such as IRS1. Activation of PI3K results in the recruitment of Akt to the plasma membrane via its PH domain where it is phosphorylated and activated by PDK1 and mTORC2. Both phosphorylation events are required for full Akt kinase activity. Akt targets are involved in cellular processes including metabolism, proliferation, cell survival and growth control. The PI3K/Akt pathway is upregulated in many cancers through the oncogenic activation of Ras or loss of the tumour suppressor protein PTEN. Figure adapted from T.Porstmann.

1.4.2 Mammalian target of rapamycin complex 1 (mTORC1)

mTORC1 functions in many crucial cellular processes, including metabolism, protein synthesis, autophagy, cell survival and apoptosis and mTORC1 has emerged as a vital downstream target of Akt in growth control (Guertin and Sabatini, 2007). mTOR is a conserved serine/ threonine kinase that is found in two distinct complexes that are functionally different: mTOR complex 1 (mTORC1) and mTOR complex 2 (mTORC2) (Guertin and Sabatini, 2007). In addition, the two mTORCs are differentially regulated and have different sensitivities to the compound rapamycin (Howell and Manning, 2011).

Besides the mTOR kinase, other components of mTORC1 include Raptor and mLST8 (Wullschleger et al., 2006). The activity of mTORC1 is regulated by a number of upstream signalling inputs and can be blocked by the mTORC1-specific inhibitor rapamycin (Figure 1.5). Upstream signals lead to regulation of mTORC1 activity via two mechanisms: 1) the direct modification of mTORC1 components or 2) the regulation of Rheb (Sengupta et al., 2010). Rheb is a small GTPase that directly interacts with mTORC1 when bound to GTP, leading to mTORC1 activation (Long et al., 2005). Akt modulates mTORC1 activation via both mechanisms and Akt-dependent regulation of mTORC1 represents growth factor sensing by mTORC1. Akt phosphorylates the proline rich Akt substrate of 40kDA (PRAS40), a negative regulator of mTORC1, (Haar et al., 2007; Sancak et al., 2007; Wang et al., 2007). Phosphorylation of PRAS40 results in its dissociation from the mTORC1 complex, thereby activating mTORC1. In addition, Akt phosphorylates and inhibits the tuberous sclerosis protein 2, TSC2, a component of a heterodimeric complex that acts as a GTPase activating protein (GAP) for Rheb (Potter et al., 2002). Active TSC2 promotes the conversion of Rheb-GTP to Rheb–GDP, thereby preventing mTORC1 activation (Inoki et al., 2003; Tee et al., 2003). Phosphorylation of TSC2 by Akt relieves inhibition of mTORC1 via the build-up of active Rheb-GTP (Manning and Cantley, 2007).

Besides responding to growth factor signalling, mTORC1 activity is sensitive to cellular nutrient and energy levels, as well as oxygen supply. Low glucose levels and glycolytic

flux result in an increase in the AMP:ATP ratio and lead to the activation of the AMPK. Under low energy conditions, the tumour repressor LKB1 activates AMPK, which can directly phosphorylate and activate TSC2, resulting in the inhibition of mTORC1 (Shaw et al., 2004). In addition, mTORC1 senses amino acid levels. Withdrawal of amino acids leads to decreased mTORC1 activity in a wide variety of organisms (Sengupta et al., 2010). It has been shown that amino acids induce the recruitment of mTORC1 to the lysosomal membranes, where the Ragulator complex resides (Sancak et al., 2010). Ragulator is thought to serve as a scaffold for a heterodimer of Rag-GTPases. Amino acid stimulation results in the activation of the Rag heterodimer, which interacts with mTORC1 through raptor, therefore enabling the recruitment of mTORC1 to the lysosomal membrane (Sancak et al., 2010; Sancak et al., 2008). Here, mTORC1 is proposed to interact with a lysosomal pool of Rheb-GTPase, resulting in its activation.

Activity of mTORC1 is also sensitive to oxygen levels. Exposure to hypoxia blocks activation of mTORC1 in a HIF1α-independent manner (Arsham et al., 2003). Hypoxia-induced inhibition of mTORC1 signalling via activation of TSC1/TCS2 is also downstream of the transcriptional regulation of REDD1/DDIT 4 (DNA-damage inducible transcript 4) (Brugarolas et al., 2004; Reiling and Hafen, 2004). However, this transcriptional regulation does not account for the rapid reduction in mTORC1 signalling observed by Arsham and colleagues (Arsham et al., 2003) and AMPK-mediated activation of the TSC1/2 complex in response to hypoxia has also been reported (Liu et al., 2006).

Activation of mTORC1 by Akt results in the direct phosphorylation of downstream targets that include the ribosomal protein S6 kinases (S6K1 and S6K2) and the eukaryotic initiation factor 4E (eIF4E)-binding proteins (4E-BP1 and 4E-BP2) (Manning and Cantley, 2007). Phosphorylation of these proteins by mTORC1 results in increased mRNA translation and ribosome biogenesis. Interestingly, the mTORC1-dependent phosphorylation of 4EBP has been found to be rapamycin resistant whilst phosphorylation of S6K1 is rapamycin-sensitive (Guertin and Sabatini, 2009). In addition, long-term rapamycin treatment may also prevent mTORC2 activity, at least in some cell types (Sarbassov et al., 2006). S6K1 participates in an mTORC1-dependent

feedback mechanism by phosphorylating and inhibiting IRS1 (Shah and Hunter, 2006; Shah et al., 2004; Tremblay et al., 2007). Additional feedback mechanisms include the direct phosphorylation of IRS1 by mTORC1 (Shah and Hunter, 2006; Tzatsos and Kandror, 2006), as well as the phosphorylation of rictor by S6K1 leading to the subsequent inhibition of mTORC2 (Dibble et al., 2009; Treins et al., 2009).

By activation of upstream signalling processes, mTORC1 activity is upregulated in a vast number of human cancers. Germline mutations in TSC1 or TSC2 lead to the tuberous sclerosis complex, a hamartoma syndrome that is linked to malignant predisposition (Huang and Manning, 2008). Mutations in the tumour suppressor LKB1 are found in the familial cancer disorder Peutz-Jeghers syndrome, as well as in a wide variety of sporadic human cancers (van Veelen et al., 2011). In addition, activating mutations in mTOR were initially identified in yeast and similar mutations have since been found in human cancer (Hardt et al., 2011; Urano et al., 2007). The link between hyperactivation of mTORC1 and cancer has prompted major efforts in developing mTOR inhibitors for use in the clinic, and substantial progress has been made in recent years (Garcia-Echeverria, 2011). Rapamycin analogues (rapalogues) have been used in several clinical trials with anti-tumour activity in different tumour types, including breast cancer and non-small cell lung cancer (Chan, 2004; Chan et al., 2005). However, mTORC1 inhibitors may only provide clinical benefit in a subset of patients and tumour types and further work is required to find combinations of therapies that target individual nodes of the PI3K/Akt/mTORC1 pathway (Garcia-Echeverria, 2011).

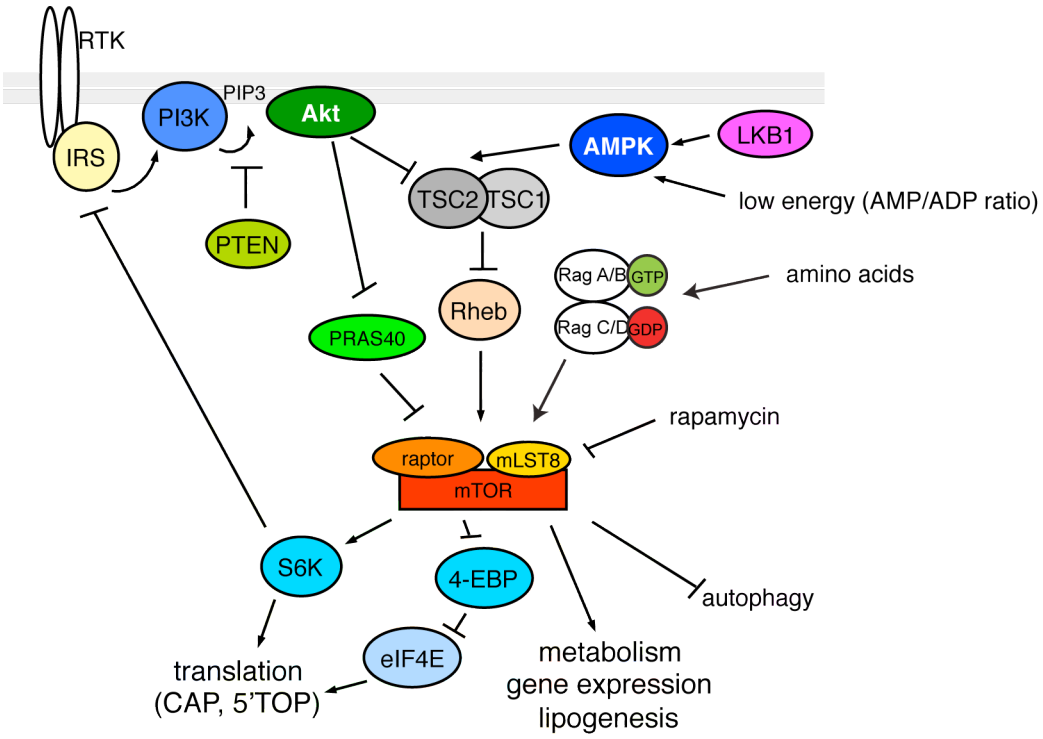

Figure 1-5: Regulation of mTORC1 signalling
mTORC1 comprises raptor, mLST8 and mTOR. mTORC1 is activated by the PI3K/Akt pathway and amino acid stimulation. The mTORC1 specific inhibitor rapamycin blocks mTORC1 signalling. Low cellular energy status results in AMPK activation and mTORC1 inhibition. In addition, S6K participates in negative feedback loops by phosphorylating the IRS, as well as raptor in mTORC2, resulting in attenuation of Akt signalling. mTORC1 regulates translation and ribosome biogenesis, as well as regulating transcription factors involved in cellular metabolism, including SREBP.

1.4.3 Regulation of SREBPs by the Akt-mTORC1 Pathway:

A number of studies have linked SREBP1 with the PI3K/ Akt pathway via insulin signalling (Azzout-Marniche et al., 2000; Fleischmann and Iynedjian, 2000; Shimomura et al., 1999). In addition, it has been shown that mTORC1 is required for *de novo* lipogenesis in rat livers and cultured hepatocytes (Brown et al., 2007; Li et al., 2010). The GEA lab have previously shown that Akt regulates the expression of genes involved in lipogenesis through SREBP1 activation (Porstmann et al., 2005), and that mTORC1 is required for Akt-dependent lipogenesis (Porstmann et al., 2008). Furthermore, it was demonstrated that nuclear accumulation of mSREBP1 as well as the expression of the SREBP1 target genes FASN and ACLY is blocked by rapamycin.

Silencing of the mTORC1-specific component Raptor resulted in attenuated expression of FASN and ACLY in response to Akt activation as well as a reduction in Akt-dependent *de novo* lipogenesis (Porstmann et al., 2008). However, silencing of Rictor (the mTORC2-specific component) did not have this effect, indicating that regulation of SREBP1 is mediated by mTORC1 and not mTORC2 (Porstmann et al., 2008). Others have shown that rapamycin decreases the expression of SREBF1 mRNA in human BJAB B-lymphoma cells and murine CTLL-2 T lymphocytes (Peng et al., 2002) and it has been reported that the insulin-induced increase in SREBF1c mRNA levels in rat livers and cultured hepatocytes requires mTORC1 (Li et al., 2010). However, inhibition of mTORC1 by rapamycin did not affect accumulation of mSREBP1 protein in HepG2 cells (where the predominant isoform is SREBP1c) (Bengoechea-Alonso and Ericsson, 2009), possibly indicating that mTORC1-dependent regulation of SREBP processing is isoform-specific.

In another study, it was shown that low-density lipoprotein receptor (LDLR) -mediated cholesterol ester accumulation in HepG2 cells in the presence of inflammatory cytokines was inhibited by rapamycin (Ma et al., 2007). Furthermore, rapamycin decreased mRNA levels of both SREBF2 and SCAP, as well as preventing SCAP/SREBP ER to Golgi translocation under these conditions (Ma et al., 2007). Rapamycin also downregulates LDLR expression, although in an SREBP2-independent manner (Sharpe and Brown, 2008).

A number of studies have investigated the expression of SREBP target genes in response to modulation of the mTORC1 effectors S6K and 4E-BP. Expression of SCD1 has been shown to be regulated downstream of S6K1 in the breast cancer cell line MCF7, although it was not investigated whether this was dependent on SREBP activity (Heinonen et al., 2008). In contrast, another study reported that the inhibition of SCD1 expression by rapamycin in MCF7 and MDA-MB-468 cells lies downstream of eIF4E and SREBP (Luyimbazi et al., 2010). Furthermore, silencing of S6K1 did not affect SREBP1 or SCD1 expression, indicating that SCD1 expression may be regulated by the mTORC1/ 4E-BP1 axis (Luyimbazi et al., 2010).

It was reported by Düvel and colleagues that S6K1 is required for SREBP1 processing and induction of its target genes in mouse embryonic fibroblasts (MEFs) (Düvel et al., 2010). This group used an experimental model that exploits the differences between mTOR signalling in wild type, $TSC1^{-/-}$ and $TSC2^{-/-}$ MEFs. Cells lacking TSC1 or TSC2 exhibit growth factor-independent activation of mTORC1, thereby isolating mTORC1 signalling from that of Akt. They used several approaches to demonstrate the requirement for SREBP1 and SREBP2 in mTORC1-induced expression of genes involved in fatty acid and sterol biosynthesis. Furthermore, they showed that ablation of S6K1 by RNAi in TSC deficient cells resulted in a decrease in nuclear accumulation of mSREBP suggesting that S6K1 is required for activation of SREBP by mTORC1 (Düvel et al., 2010).

1.5 Hypoxia

Rapidly proliferating tumours often outgrow their blood vasculature, resulting in poor oxygen supply. This reduction in the partial pressure of oxygen is termed hypoxia and often results in cell death if the lack of oxygen is severe or prolonged. Cancer cells often undergo genetic changes and metabolic adaptations that allow them to survive and even proliferate in the hypoxic tumour microenvironment. Indeed, hypoxia is considered a common feature of solid tumours and low oxygen tension in tumours is associated with increased metastasis, poor survival and resistance to radiotherapy (Favaro et al., 2011; Harris, 2002).

1.5.1 Hypoxia inducible factor (HIF)

The cellular adaptive response to hypoxia is driven mainly by the hypoxia inducible factor (HIF). HIF is a heterodimeric transcription factor that consists of two subunits: the labile α subunit and the stable β subunit (also called ARNT). Three isoforms of the α subunit exist in mammals: HIF1α, HIF2α and HIF3α with HIF1α and HIF2α being the most characterised (Majmundar et al., 2010). Whilst HIF1α is ubiquitously expressed, expression of HIF2α appears to be tissue specific (Bertout et al., 2008). HIF1α and HIF2α regulate the expression of partially overlapping sets of genes (Warnecke et al., 2008).

HIFα subunits are sensitive to cellular oxygen levels due to regulation of their stability by a family of prolyl hydroxylases (PHDs) (Figure 1.6). In normoxic conditions (4-6% O_2), PHDs hydroxylate HIFα on two serine residues resulting in the binding of the von Hippel Lindau (VHL) tumour suppressor protein. VHL acts as an E3 ubiquitin ligase and targets HIFα for degradation by the proteasome. The hydroxylation reaction requires molecular oxygen. Therefore, in conditions of insufficient oxygen, PHD activity and subsequent binding of VHL to HIFα is inhibited. This prevents the degradation of HIFα and promotes its stabilisation. HIFα subunits are also targeted by another oxygen-sensing enzyme: Factor inhibiting HIF1α (FIH). Under normoxic conditions, HIFα is hydroxylated by FIH. This disrupts the interaction of HIFα with its coactivator p300/CREB and inhibits its transcriptional activity (Majmundar et al., 2010). In addition, the stability of HIF1α, but not that of HIF2α, is regulated independently of oxygen and VHL by the hypoxia associated factor (HAF) (Koh et al., 2008). Once stabilised, HIFα translocates to the nucleus where the HIFα/HIF1β heterodimers bind HIF response elements (HRE: 5′-ACGTG-3′) in the promoters of their target genes. Transcriptional activity is achieved via the recruitment of coactivator proteins such as p300/CREB. Regulation of HIF1α transcriptional activity is also regulated by SIRT1. SIRT1 binds to, and deacetylates HIF1α preventing its interaction with p300/CREB (Lim et al., 2010). In hypoxic conditions, SIRT1 expression and activity is decreased due to decreased levels of NAD^+, contributing to the activation of HIF1α (Lim et al., 2010).

Most studies concerning hypoxia and cancer development have focussed on HIF1α. In addition, HIF1α appears to be the predominant isoform regulating the hypoxic transcriptional response (Sowter et al., 2003). Therefore the following text is concerned with HIF1α activity in hypoxia.

Activation of the HIF1α transcriptional programme in hypoxia promotes glycolysis but inhibits oxidative phosphorylation (Denko, 2008). For example, increased expression of the glucose transporters GLUT1 and GLUT3 by HIF1α results in increased glucose uptake and flux through the glycolytic pathway (Chen et al., 2001; Maxwell et al., 1997). HIF1α also induces the expression of the gene encoding pyruvate dehydrogenase

kinase 1 (PDK1) (Kim et al., 2006; Papandreou et al., 2006), as well as PDK3 (Lu et al., 2008). Expression of PDK1 results in the phosphorylation and inhibition of pyruvate dehydrogenase (PDH), the mitochondrial enzyme that mediates pyruvate entry into the TCA cycle. HIF1α activation therefore inhibits pyruvate oxidation by the TCA cycle, resulting in increased lactate production via lactate dehydrogenase A (LDHA). Lactate is exported from the cell via the activity of the monocarboxylate transporters (MCT). Expression of LDHA and MCT4 is induced by HIF1α (Semenza et al., 1996; Ullah et al., 2006). In addition, HIF1α induces expression of carbonic anhydrase 9 (CA9) (Wykoff et al., 2000). CA9 is localised to the membrane where it catalyses the reversible hydration of carbon dioxide. The increased export of lactate, together with the activity of CA9, results in increased cellular pH levels and acidification of the extracellular space (Parks et al., 2011). It has been suggested that these could be important factors in promoting tumour invasion and lactate secreted by hypoxic cancer cells may fuel oxidative metabolism in oxygenated parts of the tumour (Sonveaux et al., 2008). In addition, HIF1α transcriptionally regulates vascular endothelial growth factor (VEGFA) and the induction of angiogenesis (Forsythe et al., 1996; Maxwell et al., 1997), a process that is crucial to tumour expansion and metastasis formation.

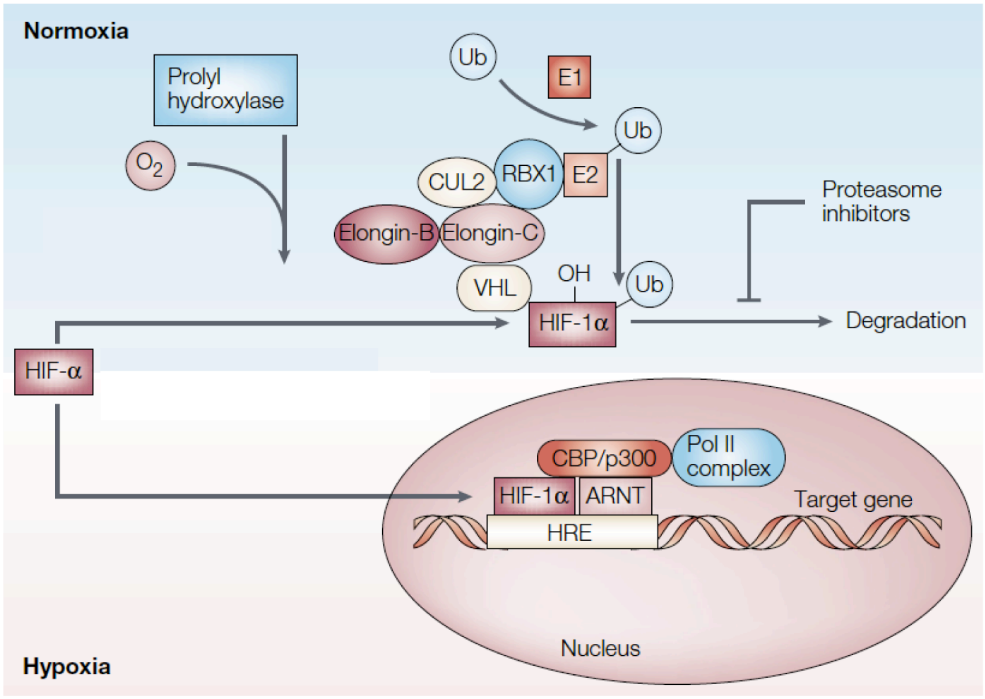

Figure 1-6: The HIF1 pathway
The cellular hypoxic response is regulated by the HIF1α transcription factor. In the presence of oxygen, HIF1α is hydroxylated by prolyl hydroxylases (PDHs), leading to the binding of the tumour suppressor protein VHL. VHL is part of a larger complex that includes Elongin-B, Elongin-C, CUL2 and RBX1, as well as the ubiquitin conjugating enzyme E2. Together with the ubiquitin activating enzyme E2, this complex leads to the ubquitination of HIF1α, resulting in its degradation by the proteasome pathway. Since the activity of the PHDs requires molecular oxygen, hypoxia inhibits the activity of PHDs resulting in the stabilisation and nuclear translocation of HIF1α. HIF1α binds the promoters of target genes containing hypoxia response elements (HRE) together with ARNT (HIF1β) as a heterodimer. Additional cofactors such as CBP/p300 act together with HIF1α/ARNT to regulate gene expression. Figure adapted by permission from Macmillan Publishers Ltd: Nature Reviews Cancer (Harris, 2002), copyright © 2002.

1.5.2 Lipid metabolism and hypoxia

Given the intimate connection between glycolysis, mitochondrial function and lipid metabolism, it is no surprise that hypoxia also alters lipid metabolism. However, the exact nature of the changes in lipid metabolism in hypoxia remains unclear.

It has been recognised for some time that changes in lipid metabolism occur after exposure to hypoxia. A study in cultured cells showed that hypoxia causes the

reversible accumulation of free fatty acids that are subsequently stored as TAGs in structures characteristic of lipid droplets (Gordon et al., 1977). Furthermore, ischemia results in decreased FA β-oxidation and an increase in intracellular lipid accumulation in rat hearts (Whitmer et al., 1978). An interesting study by Hull and colleagues in 1975 revealed that increased mitochondrial NADH:NAD ratios generated in the absence of oxygen result in the accumulation of fatty acids as a consequence of decreased β-oxidation (Hull et al., 1975). Hypoxia is also known to convert macrophages into lipid loaded foam cells (Bostrom et al., 2006).

In recent years, a direct role for HIF1α in the alterations of cellular lipid metabolism and mitochondrial function has been demonstrated. In a model of renal cell carcinoma with constitutive HIF1α expression, HIF1α inhibits mitochondrial biogenesis and cellular respiration by inhibiting c-myc activity and reducing PGC1β expression (Zhang et al., 2007). In addition, HIF1α results in increased neutral lipid accumulation in cardiomyocytes via inhibition of the positive regulator of β-oxidation, PPARα (Belanger et al., 2007). HIF1α reduces expression of CPT1, the rate-limiting enzyme for β-oxidation, and this is likely to occur through inhibiting the DNA binding ability of PPARα (Belanger et al., 2007). Reduction in FA utilisation and the accompanying increase in lipid storage capacity is a continuing theme. Gimm and colleagues identified a novel lipid droplet associated protein (hypoxia inducible protein 2: HIG2) that is a direct transcriptional target for HIF1α (Gimm et al., 2010). Interestingly, overexpression of HIG2 in normoxic conditions was sufficient to increase cellular lipid deposition, indicating that proteins required for lipid droplet formation may be connected to the signalling pathways that regulate lipid metabolism. Furthermore, in a mouse model of HIF-dependent liver steatosis it was found that the increase in cellular lipid accumulation was the result of HIF2α-dependent inhibition of β-oxidation (Rankin et al., 2009). Notably, this model also showed that expression of enzymes critical for lipid synthesis was downregulated. These included genes encoding SREBP1, LDLR, HMGCS, FASN, ACC and SCAP (Rankin et al., 2009). The authors suggest that in the liver, HIF2α is the predominant isoform regulating lipid metabolism. It has also been shown that cholesterol synthesis is perturbed in hypoxic conditions, again resulting in increased lipid accumulation (Mukodani et al., 1990). In both human and mouse

cardiomyocytes, HIF1α directly induces transcription of PPARγ, resulting in an increase in the expression of genes encoding enzymes required for glycerolipid synthesis, including glycerol-3-phosphate dehydrogenase 1 (GPD1) and glycerol-3-phosphate acyltransferase (GPAT) (Krishnan et al., 2009). Activation of the HIF1α/ PPARγ signalling axis in this context also increased intracellular TAG accumulation (Krishnan et al., 2009). Furthermore, the authors observed a decrease in expression of both PPARα and PPARβ/δ; transcription factors regulating lipid catabolic genes.

There is also evidence that hypoxia upregulates expression of genes required for lipid synthesis. In a model for obstructive sleep apnea (OSA), in which chronic intermittent hypoxia (CIH) occurs, it was found that CIH induces genes controlling both fatty acid and cholesterol biosynthesis, including SREBF1 (Li et al., 2005a). In addition, CIH resulted in elevation of cellular lipid content in the liver, but cholesterol levels remained unaffected (Li et al., 2005a). In another study by the same group, it was found that intermittent hypoxia increased fasting serum levels of total cholesterol, high-density lipoprotein (HDL) cholesterol, phospholipids, and TAGs, and enhanced liver TAG content in lean mice when compared to obese mice (Li et al., 2005b). This indicates that low baseline levels of lipid accumulation augment the effects of hypoxia on lipid metabolism. Furthermore, Li and colleagues went on to show that the effects of intermittent hypoxia on lipid accumulation in the mouse liver were HIF1α-dependent and that $HIF1^{+/-}$ mice exhibited perturbed SREBP1 mRNA and protein levels, as well as decreased expression of SCAP and SCD (Li et al., 2006). In addition, a study in *Caenorhabditis elegans* demonstrated that hypoxia-induced fat accumulation was dependent on activation of SBP1 (the homologue of SREBP1 in worms) (Taghibiglou et al., 2009).

Furuta and colleagues (2008) also observed a role for SREBP1 in increased lipid synthesis in response to hypoxia. They demonstrated that hypoxia induces activation of Akt, increased SREBP1 nuclear accumulation and increased expression of FASN in breast cancer cells (Furuta et al., 2008). Furthermore, FASN expression was induced by reactive oxygen species (ROS), indicating that upregulation of FASN expression in response to hypoxia was due to the hypoxia-dependent generation of ROS and increased

SREBP1 expression was dependent on HIF1α (Furuta et al., 2008), suggesting that both Akt activation and HIF1α activity are required for the regulation of SREBP1 in hypoxia. The enzyme acetyl-CoA synthetase short-chain family member 2 (ACSS2) converts cytosolic acetate to acetyl-CoA for lipid synthesis and is regulated at the transcriptional level by all three isoforms of SREBP (Howard et al., 1974; Luong et al., 2000; Sone et al., 2002). Tumour cells incorporate increased amounts of ^{14}C-acetate compared to non-transformed cells, and this correlates with increased proliferation rates (Yoshimoto et al., 2001). Increased expression of ACSS2 has been observed in mouse tumour cells in hypoxia when compared to normoxia (Yoshii et al., 2009). Here, the authors of this study showed that increased ACSS2 expression correlated with increased acetate excretion from the cell, leading them to propose that in hypoxic tumour cells ACSS2 is able to catalyse the reverse reaction of acetyl-CoA to acetate. Therefore ACSS2 may play a buffering role in acetyl-CoA/acetate metabolism in cancer cells (Yoshii et al., 2009).

It is clear that lipid metabolism is altered in response to hypoxia. However, the exact role of the HIFα isoforms is not fully understood. It is also not clear whether lipid accumulation in response to hypoxia is the consequence of inhibited β-oxidation, increased lipid synthesis or a combination of both. In addition, increased fatty acid uptake may be involved (Krishnan et al., 2009). Furthermore, the transcriptional programmes induced by HIFα isoforms may well be cell-type specific (Warnecke et al., 2008).

1.6 Aims of this thesis

SREBPs are transcription factors regulating the expression of genes involved in fatty acid and cholesterol biosynthesis. A common feature of cancer cells is increased flux through the glycolytic pathway and an increase in lipid synthesis. SREBPs are at the centre of the regulation of lipid synthesis. However, little is known about the role of these transcription factors in cancer. One of the aims of this thesis was to examine the transcriptional signatures of SREBPs in a cancer cell line using gene expression microarray analysis.

Solid tumours often have areas of low oxygenation as a result of poorly developed tumour vasculature. Hypoxia induces changes in lipid metabolism in tissues such as heart, muscle and liver yet little is known about the effects of hypoxia on lipid metabolism in cancer cells. An additional aim of this thesis was to investigate the regulation of lipid metabolism in hypoxia in human glioblastoma cells, and furthermore to study the role of SREBPs in the regulation of lipid metabolism in these cells.

SREBPs are regulated downstream of the Akt/mTORC1 pathway. This pathway is often upregulated in human cancers. Although it has been established that both Akt and mTORC1 regulate SREBPs, the exact mechanism of regulation by this important signalling pathway remains to be elucidated. Chapter 5 of this thesis examines potential mechanisms by which SREBP is regulated by Akt and mTORC1.

Chapter 2. Materials and Methods

2.1 Molecular Biology

2.1.1 DNA Restriction Digests

Confirmation that plasmids contained the expected insert was achieved by restriction digestion (as well as sequencing, section 2.1.6). DNA (2.5-10 µg per reaction) was mixed with 2µL 10x restriction enzyme buffer (New England Biolabs, NEB), 1 µL 10x bovine serum albumin (BSA, NEB) and 1µL of restriction enzyme (typically 10-20 units) in a final volume of 20 µL (made up with distilled water, dH_2O) and incubated for 1 hour at 37°C. Reaction products were analysed by agarose gel electrophoresis (see 2.1.2).

2.1.2 Agarose gel electrophoresis

Agarose gel electrophoresis was used to separate linear DNA samples at 80 volts for 1 hour. Typically, midi-gel apparatus (Biorad) were used. Gels were made by dissolving 0.8-2% (w/v) agarose in TAE buffer (Tris-acetate: 40 mM Tris Acetate, 2 mM EDTA, diluted with dH_2O). Ethidium bromide was added to the gel to a final concentration of 5 µL/ 100 mL gel in order to detect DNA by UV light. As an alternative to ethidium bromide, SafeView® (NBS Biologicals) was sometimes used and added to the gel and buffer to a final concentration of 0.1µL/mL. Prior to loading, DNA samples were mixed with 6x Orange G DNA loading dye (for 25 mL stock: 0.125g Orange G (Sigma), 5g Ficoll, 20 mM EDTA were dissolved in dH_2O). Sizes of the DNA fragments were estimated using the 100bp DNA ladder (NEB).

2.1.3 *E. coli* transformation by "heat shock"

Competent *E. coli* (DH5α strain, Invitrogen) in 50 µL aliquots were thawed on ice. DNA to be transformed was added directly to the *E. coli* in 1.5 mL microcentrifuge tubes. Typically, 10-100 ng of maxi prep DNA was used. The DNA and *E. coli* were mixed by flicking the tubes several times and the tubes were incubated on ice for 20

minutes. The *E. coli*/ DNA mix was incubated at 42°C for 45 seconds and then immediately placed on ice for 5 minutes. 500 µL of LB-Broth (pre-warmed to 37°C) was added and the cells were incubated at 37°C with gentle agitation for 10-30 minutes. 50 µL (10%) of transformed bacteria were plated onto LB agar plates containing the appropriate antibiotic for selection (ampicillin: 50 µg/mL or kanamycin: 30 µg/mL) and incubated overnight at 37°C.

2.1.4 DNA maxi preps from bacterial cultures

Overnight cultures of bacterial cells transformed as in section 2.1.3 with the relevant plasmid were harvested by centrifugation at 3,000 x g (Rotor: Beckman JA-10) and plasmid purification was achieved using the Qiagen Plasmid Maxi Kit according to the manufacturer's instructions. A slight modification was made. Following DNA precipitation using isopropanol, DNA pellets were washed once in 70% ethanol and then transferred to a 1.5 mL microcentrifuge tube in 1 mL 70% ethanol. DNA pellets were centrifuged at 16,000 x g for 10 minutes before the ethanol was carefully removed and pellets were allowed to air-dry. DNA was dissolved in TE buffer pH 8.0 (10 mM Tris; 1 mM EDTA) and stored at -20°C. Stock dilutions (typically 0.1 mg/mL if being used for transfection) were stored at 4°C. DNA purity and concentration was analysed by spectrophotometry ($Abs_{260/280}$).

2.1.5 DNA constructs used in this thesis

Table 2.1 describes DNA constructs that were used in this thesis:

Construct:	Vector:	Description:	Source:	Reference:
pBabe-puro3	pBabe-puro3	Retroviral expression vector	H. Land	(Morgenstern and Land, 1990)
pBabe-puro ER™-mSREBP1a	pBabe-puro ER™	ER™ fused to 19bp linker then N-term (mature) SREBP1a (2-460)	Thomas Porstmann, GEA	N/A
pBabe-puro ER™-mSREBP2	pBabe-puro ER™	ER™ fused to 19 bp linker then N-term (mature) SREBP2 (2-468)	Thomas Porstmann, GEA	N/A
pWZL-neo-EcoR	pWZL-neo-EcoR	Retroviral expression vector coding for the ecotropic receptor	Signal Transduction Lab, CRUK	N/A
pSRE-luc	pGL2-basic	Contains 3 tandem copies of repeats 2 and 3 (SRE) of the human LDL receptor prmoter (-68/-37) fused to luciferase gene	ATCC	(Yokoyama et al., 1993)
FASN-luc	pGL2-basic	Contains FASN promoter (-150/-43) wt fused to luciferase gene	Timothy Osborne	(Shimano et al., 1997a)
pRL-SV40	N/A	contains the SV40 enhancer and early promoter elements to provide high-level expression of *Renilla* luciferase	Promega	N/A
pCMV-SCAP	pRc/CMV7SB	Contains SCAP (hamster)	ATCC	(Hua et al., 1996)

pCMV-PLAP-SREBP2(513-1141)	pCMV/SEAP	Contains PLAP(2-501) C-term SREBP2 (513-1141) fusion separated by a single Y residue	Axel Nohturfft	(Sakai et al., 1998)
pCDNA3-myc-mSREBP1a wt	pCDNA3	Contains N-term myc-tagged mature SREBP1a (1-490) wt	Johann Ericsson	(Sundqvist et al., 2005)
pCDNA3-myc-mSREBP1a T246A/S430A	pCDNA3	Contains N-term myc-tagged mature SREBP1a T426A/S430A mutant	Johann Ericsson	(Sundqvist et al., 2005)

Table 2-1 DNA constructs used in this thesis

2.1.6 DNA sequencing

Fluorescent cycle sequencing was performed using gene specific primers (Table 2.3) and the BigDye Terminator v3.1 Kit (Applied Biosystems, ABI). Reactions were carried out using 8 µL BigDye Terminator (BDT) mix, 200-500 ng plasmid DNA, and 5 pmol primer. The final volume was adjusted to 20 µL using Nuclease free water (Ambion). The cycling parameters are shown in Table 2.2:

Step	Conditions:	No. of cycles
Denaturation	96°C 0:10	
Annealing	55°C 0:05	25
Extension	60°C 4:00	

Table 2-2 Cycling parameters used in DNA sequencing reactions

In order to remove any unincorporated dye, samples were purified using the DyeEx 2.0 Spin Kit (Qiagen) according to the manufacturer's instructions. Sequencing itself was carried out by staff of the CRUK LRI Equipment Park. Sequences were then analysed using DNA Strider 1.4f1 (CEA, France) or SeqMan Pro 8.1.5 (3) (Lasergene 8, DNAStar).

Primer Name (including bp number and direction):	Sequence (5'-3'):
SREBP1a 74-93R	GTCTTCGATGTCGGTCAGCA
SREBP1a 207-226F	AGGCAGCTTGTCTCCACCTC
SREBP1a 466-485F	CAGTTCAGCTCCACCCCTGT
SREBP1a 466-485R	ACAGGGGTGGAGCTGAACTG
SREBP1a 978-997F	AGCCCACAACGCCATTGAGA
SREBP1a 978-997R	TCTCAATGGCGTTGTGGGCT
SREBP1a 1481-1500F	TCTTCCTCTGCCTGTCCTGC
SREBP1a 1481-1500R	GCAGGACAGGCAGAGGAAGA
SREBP1a 1968-1987F	TGCTCTGCGAGTGGATGCTA
SREBP1a 1968-1987R	TAGCATCCACTCGCAGAGCA
SREBP1a 2515-2534F	TACCTGCAGCTGCTGAACAG
SREBP1a 2515-2534R	CTGTTCAGCAGCTGCAGGTA
SREBP1a 2921-2940F	GTGACCTGCTTCTTGTGGTG
SREBP1a 2921-2940R	CACCACAAGAAGCAGGTCAC
SREBP1a 3380-3399F	TGCTGCACGACTGTCAGCAG
SREBP2 463-482F	ACATTCAGCACCACTCCGCA
SREBP2 463-382R	TGCGGAGTGGTGCTGAATGT
SREBP2 1021-1040F	CGATATCGCTCCTCCATCAA
SREBP2 1021-1040R	TTGATGGAGGAGCGATATCG
pBpER 898-917F	AGCTCCACTTCAGCACATTC
pBp MCS 1448-1467R	TTGCATACTTCTGCCTGCTG

Table 2-3 Sequencing primers used in this thesis

2.1.7 Extraction of RNA

Total RNA from cells was isolated using the RNeasy Kit (Qiagen) according to the manufacturer's instructions. Typically, $3x10^6$ (U87) or $2.5\ x10^6$ (RPE) cells were seeded in 60 mm dishes. Following experimental culture, medium was removed from the cells and 350 µL Buffer RLT was added directly to the dish. Cells were scraped into Qiagen Shredders in order to homogenise the sample. RNA was bound to the RNeasy spin

columns and DNA was digested using the RNase-free-DNase set (Qiagen). RNA was then eluted in 30 µL RNase-free water (Qiagen). The quality and purity of the isolated RNA was measured by NanoDrop spectrophotometry ($Abs_{260/280}$).

Alternatively, RNA that was subsequently used for Illumina Array analysis (section 2.1.10) was extracted using RNA Bee (Amsbio) according to the manufacturer's instructions. Briefly, RNA Bee uses a phenol-chloroform phase-separation and subsequent isopropanol precipitation to extract the RNA. Cells were washed in PBS and 1 mL RNA Bee was added directly to the cells. Cells were scraped into a 1.5 mL RNase free tube, placed on ice and 200 µL chloroform was added. The mixture was vortexed for 15- 20 seconds and phase separation was achieved by centrifugation at 12,000 x g for 15 minutes at 4°C. The aqueous phase was transferred to a fresh 1.5 mL microcentrifuge tube (RNase-free) and RNA was precipitated by adding 1x volume of isopropanol and incubating the mixture for 1 hour at -80°C. Following centrifugation at 12,000 x g for 10 minutes at 4°C, the resulting RNA pellet was washed once in 70% ethanol (-20°C) and dissolved in 50 µL RNase-free water. Purity and quantity of the extracted RNA was measured as described above.

2.1.8 Complementary DNA (cDNA) synthesis

cDNA was synthesised from total RNA using the SuperScript II enzyme (Invitrogen) according to the manufacturer's instructions using oligo dT_{12-18} primers (Invitrogen). Typically, 50-400 ng RNA was used per reaction depending on the total amount of RNA isolated in each experiment and the reaction volume adjusted to 20 µL.

2.1.9 Quantitative reverse-transcription real-time PCR (RT-QPCR)

For a typical reaction, 100 ng cDNA from section 2.1.8 was used as a template for semi-quantitative PCR (RT-QPCR) analysis. For this analysis, the increase in fluorescence of SYBR Green was monitored in real time on the ABI 7800HT detector system. Relative transcript levels of target genes were normalised to β-2-microglobulin (B2M) or β actin (depending on the cell line). For most reactions, the Quantitect system

(Qiagen) of gene specific primers (table 2.5) was used in combination with Platinum SYBR green (Invitrogen). Quantitect primer pairs have been optimised to all have the same efficiency of amplification so that the ΔΔCT method of data analysis may be used. Total reaction volumes were adjusted to 25 µL containing 12.5 µL 2X SYBR green, 2.5 µL 10X primer solution and 10 µL cDNA template (10 ng/µL: 100 ng final conc.). A dissociation curve was generated at the end of each reaction in order to control for primer specificity. Cycling parameters recommended by Invitrogen are shown in Table 2.4 below:

Stage	**Condition**	**No. of cycles**
Hot start	95°C 10:00	1
Denaturation Annealing/ Extension	95°C 00:15 60°C 1:00	40

Table 2-4 Cycling conditions used in SREBP isoform specific QPCRs

Gene (Gene Symbol):	**Quantitect Cat. No:**
ACACA	QT01670053
ACACB	QT00996352
ACLY	QT00062286
ACSS2	QT00089271
ACTB (beta Actin)	QT01680476
B2M	QT00088935
DDIT3 (CHOP	QT00082278
FABP3	QT00018809
FABP7	QT00007322
FASN	QT00014588
HIF1A	QT00083664
HMGCR	QT00004081
HMGCS1	QT00055531
INSIG1	QT00090314
INSIG2	QT01674337

PDK1	QT00069636
PDK4	QT00003325
SCAP	QT00197764
SCD	QT01669521
SREBF1 (SREBF1a)	QT00036897
SREBF2	QT0005205
VEGFA	QT01682072

Table 2-5 Quantitect QPCR primers used in this thesis

When SREBF1c isoform-specific QPCR was performed, isoform-specific primers for SREBF1c (Porstmann et al., 2005) were purchased from Sigma (see table 2.6 for sequences) and used at a final concentration of 300 nM in a total reaction volume of 25 μL. In addition, PCR products were checked on an agarose gel to ensure primer specificity. The SREBF1c primers have different amplification efficiencies from the SREBF1a and SREBF2 primers as well as the loading controls (Quantitect), meaning the ΔΔCT method of data analysis cannot be used. Instead, a relative standard curve was generated for each gene every time an RT-QPCR analysis was performed. Equal volumes of cDNA from each sample within individual experiments were mixed together and serially diluted 1:4 or 1:2 (depending on the quantity and quality of the starting RNA) to form the standards. The CT values were then converted into "relative" quantities by the SDS software (ABI) using the known quantities of the standards.

Primer	**Sequence (5'-3')**
SREBF1c Forward	GGAGGGGTAGGGCCAACGGCCT
SREBF1c Reverse	CATGTCTTCGAAAGTGCAATCC

Table 2-6 Sequences of QPCR primers targeting SREBF1c

For both methods, data were first normalised to the loading control and then within each experiment to the internal experimental control. All reactions were performed in duplicate.

2.1.10 Gene expression microarray analysis using the Illumina platform

Cells from the three cell lines described in the previous sections were seeded in 100 mm dishes at a density of $3x10^6$. 24 hours later, cells were treated with 100 nM 4-OHT to induce SREBP activation for 6 or 24 hours. In addition, cells were treated with solvent (EtOH) as a control. Total RNA was extracted as described in section 2.1.7 and used for transcriptome analysis on HumanRef-8 v2 Expression BeadChip arrays (Illumina, performed by Dr. Charles Mein's laboratory, Bart's and the London Medical School). Data analysis was performed in collaboration with Philip East and Probir Chakravarty (LRI BABS). Data represent three independent replicate experiments.

2.1.10.1 Analysis of expression data generated by the Illumina microarray (Philip East)

The Illumina bead level intensity data was processed using Bead Studio from Illumina. To correct for intensity dependent variance effects and give the data a normal distribution suitable for subsequent statistical analysis the data were VST transformed (variance stabilisation transformation: equivalent to log transformation) (Lin et al., 2008). To correct for systematic effects such as variations in RNA concentration between samples a quantile normalisation was applied to the data. This corrects for differences in intensity across chips making the distribution of intensity values across the samples the same. This technique employs the assumption that the expression of the majority of genes on the chip does not change. To remove non-expressed transcripts from further analysis probes with a detection p-value greater than 0.01 in all samples were removed. Differential probes were selected using a 0.05 FDR (False Discovery Rate). To create the FDR, standard errors were corrected using an empirical Bayes shrinkage method and multiple testing was accounted for by applying a Benjamini & Hochberg correction. To identify time dependent changes specific to the SREBP1a and SREBP2 cell types and independent of vector effects, interactions between time and cell type factors were tested for. Differential probes were identified using the same 0.05 FDR as above. Analysis was carried out in Bioconductor (Gentleman et al., 2004). The Lumi package was used for annotation and data processing. The statistical analysis was carried out using Limma.

2.1.10.2 Generation of a heat map using probe expression data (Probir Chakravarty)

Samples were clustered using a 1-Pearson correlation distance matrix and average linkage clustering. Probes were clustered using a Euclidean distance matrix and average linkage clustering. Clustering was carried out using the software package Gene Cluster (Java TreeView; (Eisen et al., 1998)). Expression of each probe at a given time point relative to its control was displayed using Java TreeView (controls not shown).

2.1.10.3 Pathway, process and transcription factor enrichment analysis (in collaboration with Probir Chakravarty)

Gene sets for enrichment analysis were identified using Venn diagrams generated using Venny software (http://bioinfogp.cnb.csic.es/tools/venny/index.html). Gene sets were imported into Metachore (GeneGo Inc, St. Joseph, MI) and pathways, processes and transcription factors within the Metacore pathway tool were analysed for enrichment. The analysis employs a hypergeometric distribution to determine the most enriched gene set.

2.2 Cell Biology

2.2.1 Cell lines and maintenance

Primary mouse embryonic fibroblasts (MEFs) (wt and S6K1/2$^{-/-}$) were from Mario Pende (Université Paris Descartes, Paris) (Pende et al., 2004). Immortalised MEFs were obtained from Esther Castellano (LRI, STL). Human glioma U87 cells were from A. Harris (CRUK, WIMM, Oxford). Human osteosarcoma U2OS cells were obtained from ATCC. Human retinal pigment epithelial cells transformed with the human telomerase (RPE-hTERT) were purchased from BD Biosciences. RPE-myrAkt-ER and U2OS-myrAkt-ER cells were originally developed by Dr. S. Basu (CRUK, Bart's Hospital). Human embryonic kidney (HEK) 293-TLA cells were purchased from Open Biosystems. Phoenix packaging cells were from ATCC. U87-pBabePuro (U87-EV), U87-ER.mSREBP1a and U87-ER.mSREBP2 cells were generated using retroviral

transduction (see section 2.2.6). U87-pLKO-TetOn-SREBP1 and U87-pLKO-TetOn-Scrambled cell lines were produced using lentiviral transduction (see section 2.2.7).

Immortalised MEFs and primary MEFs, all U87 based cell lines, U2OS, U2OS-myrAkt-ER, HEK-293-TLA and Phoenix were cultured in Dulbecco's Modified Eagle medium (DMEM, Gibco) supplemented with 10% foetal calf serum (FCS, Gibco), 100U/ mL penicllin/ streptomycin (Gibco) and 4 mM L-glutamine (CRUK Cell Services). RPE-hTERT and RPE-myr-Akt-ER cell lines were maintained in DMEM/ Ham's F12 (1:1) medium with low glucose (5 mM) (CRUK Cell Services) supplemented with 10% FCS, 2 mM L-glutamine and 0.384 % sodium bicarbonate (CRUK Cell Services). All cells were grown in incubators at 37°C in 5% CO_2.

2.2.2 Culturing of cells in hypoxic conditions

Cells cultured in hypoxia were incubated in an Invivo$_2$ Hypoxia Workstation (Ruskinn) in 0.1-0.5% O_2 and 5% CO_2 at 37°C and 77% humidity. Dishes and plates containing cells were wrapped in aluminium foil to prevent evaporation of the media and to protect the cells from light. For cells cultured in hypoxia and subjected to RNA and protein extracts the initial stages of the extractions were performed in hypoxia. Cells were washed once and lysis buffer was added before the cells were removed from hypoxia.

2.2.3 Cryopreservation and thawing of cultured cells

Cells were suspended in 1 mL complete medium according to the cell line (see section 2.2.1) supplemented with 10% DMSO and 10% FCS (total 20% FCS). Aliquots were stored in freezing tubs containing isopropanol at -80°C for 48 hours before being permanently stored in liquid nitrogen.

To thaw cells, aliquots were thawed in a 37°C water bath and then added to 10 mL of pre-warmed complete medium in a 15 mL falcon tube. Cells were centrifuged at 200 x g for 5 minutes to remove the DMSO. Cells were resuspended in 10 mL pre-warmed complete medium and plated into 100 mm culture dishes and incubated over night.

2.2.4 Passaging of RPE, U2OS and U87 cells and their derivatives

Cultured cells were passaged when they reached approximately 80% confluency, typically every three to four days depending on the cell line. Cells were washed once using sterile phosphate buffered saline (PBS) and treated with 1 mL Trypsin (0.05%)/ Versene (0.016%) (CRUK, Cell Services) per 100 mm culture dish for 2-10 minutes (depending on the cell line) at 37°C. Cells were detached from the plate using gentle tapping and resuspended in 11 mL complete culture medium. Typically, cells for maintenance were re-seeded into new culture dishes at a dilution of 1:4. For experiments, cells were counted on a haemocytometer or the ViCell (Beckman Coulter) and seeded at appropriate densities.

2.2.5 Passaging of HEK-293-TLA and Phoenix cells

Cells were cultured as above (2.2.4) with the following modification: Cells were re-seeded into new culture dishes at a dilution of 1:10. For experiments, cells were counted on a haemocytometer and seeded at appropriate densities.

2.2.6 Generation of U87-EV, U87-ER.mSREBP1a and U87-ER.mSREBP2 by retroviral transduction

U87 cells expressing the ecotropic receptor (EcoR) were established. Phoenix amphotropic packaging cells were transfected with 5µg pWZL-neo-EcoR construct. 24 hours prior to transfection the cells were seeded at a density of 2.5 x10^6 cells per 10 cm dish. Cells were then transfected using Lipofectamine™ PLUS™ reagent (Invitrogen) according to the manufacturer's instructions (see section 2.2.8). 48 hours post-transfection the virus was harvested, filtered through a 0.45 µm sterile filter (Millipore) and hexadimethrine bromide (Polybrene, Sigma) was added to a final concentration of 1 µg/mL. The virus was then used to immediately infect U87 cells that had been seeded the day before at a density of 7.5 x10^5 cells per 100 mm dish. Infection was carried out for 72 hours before the virus was removed and cells were cultured in complete medium supplemented with geneticin ((G148) 0.4 mg/mL, Invitrogen).

U87-EcoR cells were then infected with ecotropic retroviruses carrying the pBabe-puro3 (EV), pBabe-puro-ER.mSREBP1a and pBabe-puro-ER.mSREBP2 constructs. PhoenixEcoR cells were transfected with 5 μg of the above constructs using Lipofectamine™ PLUS™ reagent according to the manufacturer's instructions (2.2.8). 48 hours post-transfection the virus was harvested (as described above) and used immediately to infect U87-EcoR cells. 72 hours post-infection, cells were cultured in complete medium supplemented with puromycin (Sigma, 1μg/mL). Selection was complete after 48 hours. U87-EV, U87-mSREBP1a.ER or U87-mSREBP2.ER cells that survived selection were then maintained in complete medium without puromycin.

2.2.7 Generation of U87-pLKO-TetOn-SREBF1 and U87-pLKO-TetOn-scrambled using lentiviral transduction

U87 cells stably expressing inducible short hairpin RNAs (shRNAs) targeting SREBF1 and a non-targeting control (scrambled) were generated using the pLKO-TetON system. shRNA sequences (Mission, Sigma: see table 2.5) were cloned into the Tet-pLKO-puro lentiviral vector (Addgene)(Wee et al., 2008; Wiederschain et al., 2009) by Susana Ros (GEA lab). HEK-293-TLA cells were seeded in 100 mm culture dishes so that they were confluent on the day of transfection. Lentiviruses were generated by co-transfecting the cells with 10 μg shRNA plasmid and 7.5 μg pCMVΔR8.91 (gag-pol) and 2.5 μg pMD.G (VSV-G glycoprotein) packaging plasmids (Zufferey et al., 1997) using Lipofectamine™ 2000, according to the manufacturer's instructions (2.2.8). After 24 hours, 5 mL complete medium containing heat inactivated FCS (10%) was added to the cells. 48 hours post-transfection supernatant containing the virus was filtered through a 0.45 μm filter (Millipore). 5 mL fresh virus containing 16 μg/mL polybrene was used to infect 1x 100 mm dish of U87 cells seeded the day before at a density of 3x 10^6 cells/ dish. Cells were incubated with the virus overnight and 5 mL fresh DMEM containing heat inactivated FCS (10%) was added after 16 hours. 24 hours later, the virus was removed and the cells were incubated in selective medium (containing 1 μg/mL puromycin) for 48 hours. Once selection was complete, the cells were maintained without puromycin. Doxycycline (1 μg/mL) was used to induce expression of the shRNAs. As the half-life of doxycycline in cell culture is between 24 and 48

hours, fresh doxycycline was added every 48 hours to prevent fluctuation in shRNA expression.

Oligonucletotide:	Sequence (5'-3')
shSREBF1 forward	CCGGCCAGAAACTCAAGCAGGAGAACTCGAGTTCTCCTGCTTGAGTTTCTGGTTTTT
shSREBF1 reverse	AATTAAAAACCAGAAACTCAAGCAGGAGAACTCGAGTTCTCCTGCTTGAGTTTCTGG
shScrambled forward	CCGGCCTAAGGTTAAGTCGCCCTCGCTCGAGCGAGGGCGACTTAACCTTAGG
shScrambled reverse	AATTCCTAAGGTTAAGTCGCCCTCGCTCGAGCGAGGGCGACTTAACCTTAGG

Table 2-7 Oligonucleotides used to generate shRNAs used in this thesis

2.2.8 Transient transfection of cells with cDNA

Cell lines were transiently transfected with cDNA using the transfection reagents shown in table 2.8 according to the manufacturer's protocol. Amounts of DNA plasmids transfected are stated in the individual experimental protocols described in this chapter.

Cell Line:	Format:	No. of cells:	Reagent:	Amount (µL):	Manufacturer:
Phoenix	100 mm dish	2.5 x10^6	Lipofectamine™ Plus™ reagent	Lipo: 25 µL Plus: 17.5 µL	Invitrogen
HEK-293-TLA	100 mm dish	2.5 x10^6	Lipofectamine™ 2000	60 µL	Invitrogen
RPE	6 well plate	2.5 x10^5	FuGENE	3:1 FuGENE (µL): DNA (µg) ratio	Roche
U2OS	6 well plate	1.5 x10^5	Effectene	10 µL	Qiagen
U87	6 well plate	3 x10^5	Lipofectamine™ 2000	1.25 µL	Invitrogen

Table 2-8 Transfection reagents used for transient transfection of cDNA in this thesis

2.2.9 Transient transfection of cells with siRNA

2.2.9.1 Transient transfection of RPE cells using Dharmafect1 (Dharmacon)

Transient transfection of RPE cells with siRNA duplexes was performed using a reverse transfection protocol with Dharmafect1 (Dharmacon) according to the manufacturer's instructions. Final siRNA concentration (50 nM) was calculated for a final volume of 1.5 mL for cells transfected in 6-well plate format. Briefly, siRNA duplexes were diluted in opti-MEM (Gibco). Dharmafect1 (2 μL) was diluted in opti-MEM and incubated at room temperature for 5 minutes. Diluted siRNA duplexes were mixed with diluted Dharmafect1 and incubated at room temperature for 20 minutes. During this time cells were trypsinised and resuspended at a density of 2.5 $x10^5$ in a total of 1.2 mL complete medium. siRNA duplexes (300 μL total volume) were added to the wells and cells were added on top. The following day, cells were media changed to complete medium. 96 hours later cells were assayed for gene knockdown.

2.2.9.2 Transient transfection of U87 cells using Lipofectamine™ 2000

Transient transfection of U87 cells was performed using a reverse transfection protocol using Lipofectamine™ 2000 (Invitrogen) according to the manufacturer's instructions. Final siRNA concentration was calculated for a final volume of 1.5 mL for cells transfected in 6-well plate format. Briefly, siRNA duplexes were diluted in opti-MEM (Gibco). Lipofectamine™ 2000 (5 μL) was diluted in opti-MEM and incubated at room temperature for 5 minutes. Diluted siRNA duplexes were mixed with diluted Lipofectamine™ 2000 and incubated at room temperature for 20 minutes. During this time cells were trypsinised and resuspended at a density of 3.0 $x10^5$ in a total of 1 mL complete medium. siRNA duplexes (500 μL total volume) were added to the wells and cells were added on top. The following day, cells were media changed to complete medium. 96 hours later cells were assayed for gene knockdown.

Table 2.8 describes the siRNA oligos (Dharmacon) used in this thesis.

Gene:	Cat. No:	Sequence:
Non-targeting control oligo no. 3	D-001210-03	Unknown
SREBF1	D-006891-01	UGACUUCCCUGGCCUAUUU
	D-006891-02	ACAUUGAGCUCCUCUCUUG
	D-006891-03	GCGCACUGCUGUCCACAAA
	D-006891-04	ACACAGACGUGCUCAUGGA
SREBF2	D-009549-01	GAGCGGAGCUGGUCUGUGA
	D-009549-02	GAAGAGAGCUGUGAAUUCU
	D-009549-03	GCACAAGUCUGGCGUUCUG
	D-009549-04	AAACUCAGCUGCAACAACA
HIF1A	D-004018-01	GGACACAGAUUUAGACUUG
	D-004018-03	GAUGGAAGCACUAGACAAA
	D-004018-05	CGUGUUAUCUGUCGCUUUG
	D-004018-27	GAUGAAAGAAUUACCGAAU
FRAP1 (mTOR)	D-003008-05	GAGAAGAAAUGGAAGAAAU
	D-003008-06	CCAAAGUGCUGCAGUACUA
	D-003008-08	GGUCUGAACUGAAUGAAGA
	D-003008-23	AUAAAGUUCUGGUGCGACA
EIF4EBP1 (4EBP1)	D-003005-06	CGCAAUAGCCCAGAAGAUA
	D-003005-07	GAGAUGGACAUUUAAAGCA
	D-003005-09	AGUUUGAGAUGGACAUUUA
	D-003005-10	CAUCUAUGACCGGAAAUUC
RPS6KB1 (S6K1)	D-003616-09	CCAAGGUCAUGUGAAACUA
	D-003616-10	CAUGGAACAUUGUGAGAAA
	D-003616-11	GACAAAAUCCUCAAAUGUA
	D-003616-12	GCAGGAGUGUUUGACAUAG
RPS6KB2 (S6K2)	D-004671-01	GCAAGGAGUCUAUCCAUGA
	D-004671-02	GACGUGAGCCAGUUUGAUA
	D-004671-03	GGAAGAAAACCAUGGAUAA
	D-004671-04	GGAACAUUCUAGAGUCAGU

Table 2-9 Dharmacon siRNA oligos used in this thesis

2.2.10 Chemicals used in cell biology experiments

Table 2.9 describes chemicals used in cell biology experiments in this thesis

Name:	Function:	Stock Dilution:	Final Conc.:	Source:
Lipoprotein deficient serum (LPDS)	Limits availability of exogenous lipids	100%	1%	Intracell
Normal goat serum (NGS)	Used as a blocking reagent in IF	100%	0.3%	Jackson Immuno Research
4-hydroxy tamoxifen (4-OHT)	Artificial ligand for the oestrogen receptor (ER)	1 mM in EtOH	100 nM	Sigma
Rapamycin (Rapa)	Selective mTORC1 inhibitor: binds FKBP12 forming inhibitory complex	200 μM in DMSO	50 nM	Calbiochem
MEM amino acid solution	Essential amino acids (without L-glutamine)	50 x	1 x	Gibco
Insulin	Hormone that regulates carbohydrate and fat metabolism	10 mg/mL	10 μg/mL	Sigma
Thapsigargin (TG)	ER stress inducer: blocks transient increase in intracellular Ca^{2+} levels	1 mM in DMSO	50 nM	Merk
Tunicamycin (TM)	ER stress inducer: inhibits GPT and N-linked glycoprotein synthesis	5 mg/mL	5 μg/mL	Sigma
FA free bovine serum albumin (BSA)	Starves cells of growth factors and exogenous lipids	20% in PBS	0.5%	Sigma
SB-216763	Selective ATP-competitive GSK3α/β inhibitor	7.5 mM in DMSO	5 μM	Calbiochem

Table 2-10 List of chemicals used in cell biology experiments in this thesis

2.2.11 Immunofluoresence microscopy

Cells were seeded directly onto coverslips (13mm, Thermo Scientific Nunc) in 12-well plates at a density of 1.5 x10^5 cells/ well. Following culture, cells were washed twice in PBS and fixed in 3.7% formaldehyde/ PBS (Stock: 37% formaldehyde, histological grade, Sigma) for 30 minutes at room temperature. Following two washes in PBS, cells were permeabilised in 0.1% Triton-X 100/ 0.3% normal goat serum (NGS) for 15 minutes at room temperature. Primary antibodies were diluted in 0.1% Triton-X 100/ 0.3% NGS (see table 2.11) and incubated overnight at 4°C in a humidified chamber. Coverslips were washed three times in PBS and incubated in the secondary antibody solution (see table 2.11) containing DAPI (1 µg/ mL) for 1 hour at room temperature. Following three washes in PBS, coverslips were dipped once in dH_2O and once in methanol to remove residual salt and mounted on a microscope slide (Thermo Scientific) with Mowiol (Calbiochem). Images were obtained using a LSM 710 Upright Confocal Microscope (Carl Zeiss) with a 63x Plan-APOCHROMAT 1.4 Oil immersion objective (Carl Zeiss) at room temperature. Image capture was performed using the Zen 2009 (Carl Zeiss) software. Channels were separated using Image J software (National Institute of Health) and brightness and contrast were adjusted using Photoshop CS4 (Adobe). All images from the same experiments were adjusted using identical parameters according to LRI image processing guidelines.

		Stock Conc.	**Working Dilution:**	**Source:**
Primary Antibody	Anti-SREBP1 (K10)	200 µg/ mL	1:50	Santa Cruz Biotechnology, Inc.
Secondary Antibody	Alexa Fluor® 546 goat anti-mouse	2mg/mL	1:500	Molecular Probes

Table 2-11 Antibodies used in immunofluorescence microscopy

2.2.12 Analysis of Lipid Droplets

2.2.12.1 Visualisation of lipid droplets using confocal microscopy

Cells that were to be analysed for lipid droplet formation by confocal microscopy were seeded in the same way as in section 2.2.11. Following fixation for 30 minutes with 3.7% formaldehyde/ PBS, cells were stained in 0.1 μg/mL Nile Red (Molecular Probes) and 1 μg/mL DAPI (Roche) in 150 mM NaCl for 10 minutes at room temperature. Cells were washed twice in PBS, and once in dH_2O and mounted onto microscope slides (Thermo Scientific) using Mowiol (Calbiochem). Cells were imaged using a LSM 710 Upright Confocal Microscope (Carl Zeiss) as described in section 2.2.11. Nile Red was scanned using the FITC filter.

2.2.12.2 Lipid droplet quantification using Array Scan VTi

For lipid droplet quantification, cells were grown in 96-well plates (black with clear bottom 96-well Microtest™ Optilux™ plates, BD Falcon™) at a density of 4,000-8,000 cells per well, depending on the nature of the experiment. Cells were fixed and stained as described above (2.2.12.1). Following the final wash in PBS, a final volume of 100 μL PBS was added to the cells. The plates were sealed with foil (Brandel) and scanned on the ArrayScanVTi (Cellomics) using the DAPI filter (nuclei) and the FITC filter (Nile Red) (Mike Howell, LRI HTS). The scanning protocol was set up such that 15 images per well were captured. The nuclei were then defined using the DAPI channel and a mask was drawn around the nucleus defining a single cell (valid object). A ring around each nucleus (region of interest: ROI) was then defined using a distance of -3 pixels (inner threshold) to 22 pixels (outer threshold). Spots within this ROI were further defined using local pixel intensity and the Compartmental Analysis V4 algorithm (Cellomics Bioapplication) (see figure 2.1). The "mean ring spot total intensity" was then plotted. This is a measurement of the sum of all the pixel intensities within all spot regions per single object (cell). Taking the mean of this measurement ensures that data is normalised to cell number.

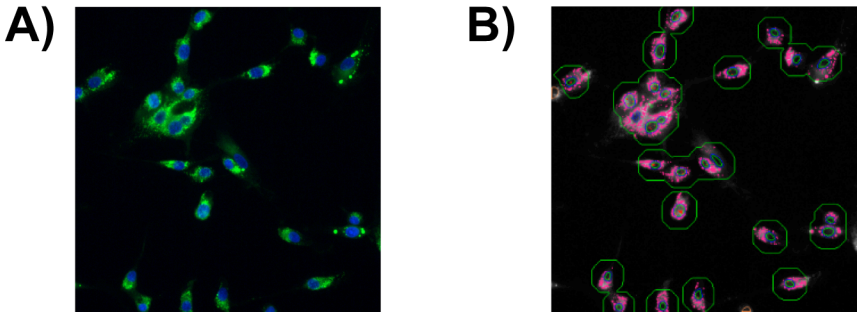

Figure 2-1: Quantification of lipid droplet staining using Array Scan VTi (Cellomics). Representative images taken by the Array Scan VTi. (A) Composite image showing staining of nuclei (DAPI: blue) and lipid droplets (Nile Red: green). (B) Image A showing the masks used to define the following: Valid objects (single cells: blue ring); ROI (green ring); and ring spots (lipid droplets: pink spots).

2.2.13 Sulforhodomine B Assay (Cell Mass)

Total protein content (cell mass) was measured as an indicator of cell viability/ cell number and was measured using the Invitro Toxicology Assay Kit (Sulforhodomine B based, Sigma) according to the manufacturer's instructions. The Sulforhodomine B assay is based on the ability of the dye to bind basic amino acid residues on trichloroacetic acid (TCA) fixed cells and the results are linear with cell number (Voigt, 2005). Cells were fixed by adding ¼ of the culture volume of cold 50% TCA to the growth medium and incubated for 1 hour at 4°C. Cells were then washed twice with dH_2O and allowed to air-dry before incubation at room temperature for one hour with 0.5x culture volume of 0.4% sulforhodamine B in 1% acetic acid. The stain was removed and cells were washed twice with 1% acetic acid and allowed to air-dry overnight. The dye was re-solublised by adding 1x culture volume 10 mM Tris and placing the culture vessel on a rotator for 10 minutes to evenly distribute the dye. 100 µL/ sample was transferred to a well of a 96 well plate and read at 492 nm using a SpectraMax 190 plate reader (Molecular Devices) and analysed using SoftMax® Pro software (Molecular Devices).

2.3 Protein Biochemistry and Biochemical Techniques

2.3.1 Preparation of cell lysates

For the detection of SREBP mature proteins, all cells were treated with ALLN (25 μg/mL, Calbiochem) or MG-132 (25 μM, Calbiochem) for 1.5 hours before lysis, or as indicated in the text.

Cell monolayers were washed once with ice cold PBS and 200 μL TNET Buffer (1% Triton-X-100, 50 mM Tris pH 7.5, 300 mM NaCl, 1 mM EGTA, 1 mM DTT, Protease Inhibitor Cocktail (Roche) and PhosStop Phosphatase Inihibitor Cocktail (Roche)) was added directly to the cells. Cells were lysed on ice for 15 minutes with gentle rocking. Cell lysates were scraped into 1.5 mL microcentrifuge tubes and the lysates were cleared by centrifugation at 16,000 x g for 10 minutes at 4°C. Cleared lysates were transferred to a fresh microcentrifuge tube, snap frozen on dry ice and stored at -80°C.

2.3.2 Nuclear fractionation of cells

The following protocol is based on that originally described by Wang and colleagues for the nuclear fractionation of mature SREBP proteins (Wang et al., 1994) and has been adapted to ensure optimal enrichment of nuclear proteins from RPE cells (Porstmann et al., 2008).

RPE cells from two 15 cm dishes (U87 cells: 2x 100 mm dishes) were washed once in ice cold PBS, scraped into 1 mL ice cold PBS containing Protease Inhibitor Cocktail and PhosStop Phosphatase Inhibitor Cocktail (Roche) and transferred to 15 mL falcon tubes (on ice). Cells were centrifuged for 5 minutes at 650 x g at 4°C and transferred to fresh 1.5 mL microcentrifuge tubes in 1 mL ice cold PBS containing the inhibitor cocktails described above. Cells were centrifuged again at 855 x g for 5 minutes at 4°C and all PBS was removed. The cell pellets were resuspended in 3 volumes of Buffer C (10 mM HEPES/KOH pH 7.6, 10 mM KCL, 1.5 mM $MgCl_2$, 1 mM EDTA, 1 mM EGTA, 0.5 mM DTT, Protease Inhibitor Cocktail and PhosStop Inhibitor Cocktail) and swelled on ice for 10 minutes. The cells were disrupted by trituration 15 times with a

23G needle and the lystate was centrifuged at 855 x g for 10 minutes. The supernatant (containing the membrane and cytoplasmic fractions) was transferred to a fresh 1.5 mL microcentrifuge tube and centrifuged for another 5 minutes at 855 x g at 4°C to remove any nuclei. The cleared supernatant fraction was then snap frozen on dry ice and stored at -80°C.

To continue nuclear lysis, the pelleted nuclei were washed twice in 200 µL Buffer C and centrifuged at 855 x g at 4°C for 5 minutes between washes. Nuclei were centrifuged again for 3 minutes at 855 x g and any remaining Buffer C was removed using a gel-loading tip. The pelleted nuclei were then resuspended in one volume of Buffer D (20 mM HEPES/KOH pH 7.6, 0.5 M NaCl, 1.5 mM MgCl2, 1 mM EDTA, 1 mM EGTA, 25 % (v/v) glycerol, Protease Inhibitor Cocktail and PhosStop) and incubated on ice for 30 minutes with occasional votexing. The nuclear lysates were cleared by centrifugation at 16,000 x g for 10 minutes at 4°C, transferred to a fresh, cold 1.5 mL microcentrifuge tube, snap frozen on dry ice and stored at -80°C.

2.3.3 Determination of protein quantification

In order to ensure equal protein loading in SDS-PAGE, total protein concentration of protein lysates was determined using the BioRad Protein Assay and measured on a SpectraMax 190 plate reader (Molecular Devices) using the SoftMax® Pro software (Molecular Devices).

2.3.4 SDS polyacrylamide gel electrophoresis (SDS-PAGE)

SDS-PAGE was carried out using the NuPAGE® NOVEX® Bis-Tris 4-12% Precast Gel System (Invitrogen). Protein samples were mixed with 4x NuPAGE® SDS Sample Buffer and heated to 70°C for 10 minutes before loading. Gels were run for 1-1.5 hours at 200V in 1x NuPAGE® MOPS or 1x NuPAGE® MES running buffers, depending on the size of the proteins to be detected. Protein size was estimated using the Full Range Rainbow Molecular Weight Marker (Amersham).

2.3.5 Western blotting

Immobilon-P polyvinylidene difluouride (PVDF, Millipore) membranes were soaked in methanol and then equilibriated in transfer buffer (25 mM Tris, 192 mM glycine and 10% MetOH) for at least 10 minutes. The gel to be transferred, sponges and 4 pieces of Whatman 3M filter paper were also soaked in transfer buffer for at least 10 minutes. Proteins were transferred from the gel to the PVDF membrane in a Bio-Rad TransBlot® electrophoretic transfer cell filled with transfer buffer. 2 filter papers and a sponge were placed either side of the gel and membrane. Transfers were either carried out at 200 mA for 1.5 hours in the presence of an ice block, or at 15 mA overnight at 4°C.

Membranes were blocked for 1 hour at room temperature with gentle shaking in 3% BSA (Sigma)/ Tris buffered saline (TBS). Non-conjugated primary antibodies were diluted according to table 2.12 and incubated overnight at 4°C with gentle rocking. Primary antibodies were washed using 5x 5 minute washes in TBS-Tween® (0.05% v/v Tween®20, Sigma). Secondary antibodies conjugated to horseraddish peroxidase (HRP) (Amersham), as well as primary peroxidase-conjugated antibodies, were incubated in 5% non-fat milk powder (Marvel)/ TBS-Tween® according to table 2.13 for 45-60 minutes at room temperature with gentle rocking. Secondary antibodies were washed using 4x 5 minute washes in TBS- Tween® and a final 5 minute wash in TBS. Protein bands were visualised using ECL or ECL Plus™ (for antibodies recognising SREBP1 (2A4) and SREBP2 (1C6)) western blotting detection reagent (Amersham) and high performance chemiluminescence film (Hyperfilm, Amersham), according to the manufacturer's instructions.

Primary Antibody:	Stock Conc.	Working Dilution:	Source:
4EBP1 Rabbit polyclonal		1:1000	Cell Signaling Technology
ACC (ACC1, ACACA) Rabbit Polyclonal		1:1000	Cell Signaling Technology
ACLY Rabbit Polyclonal		1:1000	Cell Signaling Technology
Akt Rabbit polyclonal		1:1000	Cell Signaling Technology
ATF4 (CREB-2, C-20) Mouse Monoclonal	200 µg/ mL	1:1000	Santa Cruz Biotechnology, Inc
ATF6-alpha (H-280) Rabbit Polyclonal	200 µg/ mL	1:500	Santa Cruz Biotechnology, Inc
beta catenin rabbit polyclonal		1:1000	Cell Signaling Technology
beta-actin HRP Mouse Monoclonal	0.6 mg/mL	1:5000	Sigma
beta-tubulin HRP Rabbit Polyclonal		1:10,000	abcam
Calreticulin Rabbit Polyclonal	1mg/mL	1:1000	StressGen
Cyclin A (H-432) Rabbit Polyclonal	200 µg/ mL	1:500	Santa Cruz Biotechnology, Inc
DP1 (1DP06/ TFD10) Mouse Monoclonal	200ug/ mL	1:500	Stratech Scientific Ltd.
ER alpha (MC-20) Rabbit Polyclonal	200 µg/ mL	1:1000	Santa Cruz Biotechnology, Inc
FASN Mouse Monoclonal	250ug/mL	1:2000	BD Biosciences
GAPDH HRP Mouse Monoclonal		1:2000	abcam
HIF1a Mouse Monoclonal	250ug/mL	1:5,000	BD Biosciences

Lamin B1 (C-20) Goat Polyclonal	200 µg/ mL	1:1000	Santa Cruz Biotechnology, Inc
myc (9E10) Mouse Monoclonal	1.1mg/mL	1:500	CRUK
phospho beta catenin Ser 33/37/ Thr 41 rabbit polyclonal		1:1000	Cell Signaling Technology
phospho 4EBP1 Thr 37/46 rabbit polyclonal		1:1000	Cell Signaling Technology
phospho Akt Ser 473 Rabbit Polyclonal		1:1000	Cell Signaling Technology
phospho RBPS6 Ser 235/236		1:1000	Cell Signaling Technology
phospho RBPS6 Ser 240/244 rabbit polyclonal		1:1000	Cell Signaling Technology
RBPS6 rabbit polyclonal		1:1000	Cell Signaling Technology
SCAP (C-20) Goat Polyclonal	200 µg/ mL	1:1000	BD Biosciences
SREBP1 (2A4) Mouse Monoclonal	0.5mg/mL	1:500	BD Biosciences
SREBP2 (1C6) Mouse Monoclonal	0.5mg/mL	1:500	BD Biosciences

Table 2-12 Primary antibodies used in Western blotting

Secondary Anitbody:	**Stock conc.:**	**Working dilution:**	**Source:**
Donkey anti-rabbit IgG HRP		1: 2000	Amersham
Rabbit anti-goat IgG HRP	0.5mg/mL	1:2000	Dako Cytomation
Sheep anti-mouse IgG HRP		1:2000	Amersham

Table 2-13 Secondary antibodies used in Western blotting

2.3.6 Measuring *de novo* lipid synthesis

U87 cells were seeded in 12-well plates at a density of 1.25 x10^5 cells/ well. The following day, cells were media changed to 0.5 mL media and incubated for a further 24 hours in the appropriate experimental condition. Cells were then incubated with either 2.5 μCi/mL D-[6-^{14}C] glucose (45 mM final concentration, Amersham), 10 μCi/mL [1-^{14}C] acetate (85 μM final concentration, Perkin Elmer) or 2.5 μCi/mL [2-^{14}C] pyruvate (166 μM final concentration, Perkin Elmer) for 4 hours. Cells were washed twice in PBS, trypsinised and transferred to a 15 mL Falcon tube. Following centrifugation at 650 x g to remove the trypsin, cells were lysed in 0.5% Triton-X 100. Lipids were then extracted by successive addition of 2 mL methanol, 2 mL chloroform and 1 mL dH_2O. Samples were vortexed between each addition. Phase separation was achieved by centrifugation at 1,500 x g for 15 minutes. The aqueous phase was removed and the organic phase (lower phase) was transferred to a scintillation vial and allowed to dry overnight. Lipids were dissolved in 5 mL Ultima Gold LSC Cocktail (Perkin Elmer) and counts per minute (CPM) were measured using a LS 6500 Scintillation Counter (Beckmann Coulter). Results were normalised to total protein content (cell mass) (section 2.2.13).

2.3.7 Dual Luciferase® assays

Dual Luciferase Assays (Promega) were used to measure reporter firefly luciferase activity and normalise it to an internal Renilla luciferase control. Cells were transfected with reporter constructs (pSRE-luc: 0.5 μg or pGL2-FASN-luc (wt): 1μg) and the Renilla control (phRL-SV40: 0.5 ng) as described in section 2.2.8. Cells were lysed using the passive lysis method, according to the manufacturer's instructions (Promega). Typically, cells seeded in 12-well plates were lysed in 100 μL PLB for 15 minutes at room temperature on a rocker. 20 μL of lysate were transferred to an opaque 96-well plate and 100 μL Luciferase Assay Reagent II (LARII) was added. The reaction mixture was mixed using a plate mixer and firefly luciferase activity was measured using an EnVision Multilabel Plate Reader (Perkin Elmer). Immediately after reading, 100 μL Stop and Glow® reagent was added, the reaction mixed as above and the renilla activity measured as already described. Renilla activity was used to normalise firefly luciferase activity.

2.3.8 SREBP cleavage assays

SREBP cleavage assays are based on placental alkaline phosphatase (PLAP) assays using a PLAP-SREBP2 fusion construct developed by Sakai and colleagues (Sakai et al., 1998). Upon cleavage of SREBP2 at the S1P and S2P sites, the PLAP is released into the media and PLAP activity can be measured using a chemiluminescent reaction. U2OS-Akt-ER cells were co-transfected with pCMV-PLAP-SREBP2 (1 μg), pCMV-SCAP (2 μg) and the Renilla luciferase control (phRL-SV40: 0.5 ng) as described in section 2.2.8. PLAP activity was measured using the Phospha-Light™ System (Applied Biosystems), according to the manufacturer's instructions. Following culture, 50 μL growth media were transferred to a 1.5 mL microcentrifuge tube and diluted 1:2 in 1x dilution buffer. Samples were heated at 65°C for 30 minutes and then cooled to room temperature by placing on ice for 1 minute. 50 μL of sample were transferred to a well of an opaque 96-well plate and incubated with 50 μL Assay Buffer for 5 minutes at room temperature. 50 μL Reaction Buffer was then added and incubated at room temperature for a further 20 minutes. The resulting PLAP activity was measured using the EnVision Multilabel Plate Reader (Perkin Elmer). PLAP activity was normalised to renilla activity measured in the same experiment (see section 2.3.7).

2.3.9 Measuring Caspase 3/7 activity

As a read-out for apoptosis, caspase 3/7 activity was measured using an assay based on the Apo-ONE assay (Promega). Cells were cultured in 96 well plates in a volume of 100 μL. Following culture for the in the appropriate conditions for the time stated in the figure legends 100 μL caspase assay mix (25 mM HEPES pH7.3, 1 mM EDTA, 100 mM NaCl, 0.1% CHAPS, 5 mM DTT, 0.01mg/mL caspase 3 substrate (Merck)) were added to the wells. Cells were incubated with the caspase assay mix for 1.5 hours at room temperature and were protected from light. Fluorescence was then measured at 485 nm using an EnVision Multilabel Plate Reader (Perkin Elmer). Cells were then fixed in TCA and stained with Sulforhodomine B (Sigma) to determine total protein content (cell mass, 2.2.13). Assay background was measured using media only and each experiment was performed in triplicate.

2.4 Computational and Statistical Analysis

Quantitative data were depicted using GraphPad Prism 5.0c. Paired Student's *t* tests assuming equal or unequal variance and a two-tailed distribution were carried out using Microsoft Excel for statistical analysis. Error bars represent either the standard deviation (SD) or the standard error of the mean (SEM) as described in the figure legends.

Chapter 3. Analysis of the transcriptional response to activation of SREBP1a and SREBP2 in cancer cells

3.1 Introduction

Sterol regulatory element binding proteins (SREBPs) regulate the expression of genes required for the synthesis of fatty acids and cholesterol. Lipid metabolism is perturbed in some diseases, including cancer, and SREBP target genes such as fatty acid synthase (FASN) and stearoyl-coA desaturase (SCD) are upregulated in some forms of human cancer (Li, 2000; Swinnen et al., 2000b; Yoon et al., 2007). A large number of direct transcriptional targets have been identified by studies in genetically manipulated mice and subsequent gene expression microarrays (Horton et al., 2003; Kallin et al., 2007), as well as promoter binding studies (Motallebipour et al., 2009; Reed et al., 2008; Rome et al., 2008; Seo et al., 2011). However, little is known about SREBP isoform-specific transcriptional signatures in cancer cells. SREBP1 has been shown to play a role in tumourigenesis in glioblastoma multiforme (GBM) (Guo et al., 2009b), and this cancer type is associated with hyperactivation of the PI3K/Akt signalling pathway through functional loss of the tumour suppressor protein PTEN (Parsons et al., 2008). This chapter describes the investigation into the transcriptional response to SREBP1a and SREBP2 activation in the human glioblastoma cell line U87.

3.2 Generation of U87.SREBP1a.ER and U87.SREBP2.ER cell lines

The two SREBP1 isoforms share the same DNA binding domain, although it is generally considered that SREBP1a is the stronger transcriptional activator due the longer acidic transactivation domain in its N-terminus (Bengoecheaalonso and Ericsson, 2007; Shimano et al., 1997a). For this reason, the transcriptional response to SREBP1a activation was investigated alongside that of SREBP2 in human glioblastoma cells. In order to identify genes that are regulated in response to activation of SREBP1a or

SREBP2, stable cell lines expressing 4-hydroxytamoxifen (4-OHT) inducible forms of these proteins were generated. The hormone-binding domain of the oestrogen receptor that has been previously engineered to selectively bind the oestrogen antagonist 4-hydroxytamoxifen (4-OHT) instead of its natural ligand 17β-estradiol (ER^{TM})(Littlewood et al., 1995) was used. This was fused N-terminally to the mature N-terminal domain of SREBP1a and SREBP2 (ER.mSREBP1a and ER.mSREBP2). These constructs are described in Figure 3.1. The ER.mSREBP1a and ER.mSREBP2 fusion proteins were then stably expressed in the U87 glioblastoma cell line using retroviral transduction.

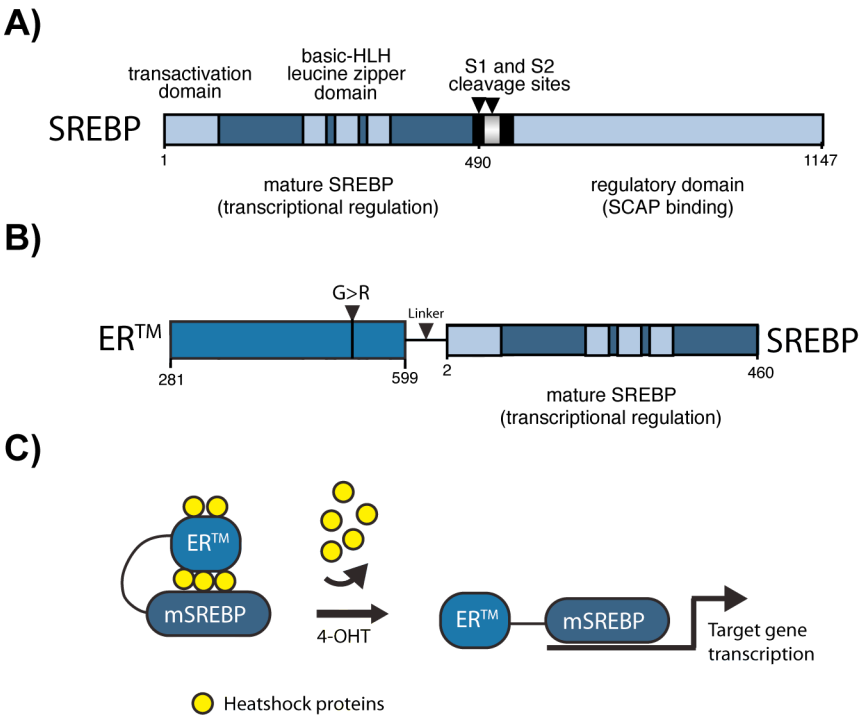

Figure 3-1: Schematic representation of the ER.mSREBP1a and ER.mSREBP2 fusion constructs.
(A) A schematic representation of the full length SREBP proteins, showing the N-terminal transactivation domains, the bHLH DNA binding domain, the C-terminal regulatory region and the S1P and S2P cleavage sites. Numbers correspond to amino acids in SREBP1a B) The hormone binding domain of the murine oestrogen receptor (ER) is fused to the N-terminal of the mature SREBPs (mSREBP), to create a 4-hydroxytamoxifen (4-OHT) inducible construct. The point mutation G>R renders the ER insensitive to its natural ligand, whilst still being able to bind 4-OHT. A 20bp linker connects the ER and the mSREBP, allowing more flexibility. C) Conditional activation of ER.mSREBPs: ER.mSREBPs are constitutively expressed in the cells. In the absence of 4-OHT, the ER-domain is in an inhibitory complex with heat shock 90 proteins (HSP-90). Upon induction with 4-OHT, the ER changes conformation causing the heat shock proteins to dissociate and allowing the ER-mSREBP fusion protein to become transcriptionally active.

It should be noted that the N-terminal fusions used in this thesis correspond to slightly truncated versions of the mature proteins (see Figure 1.2 for the full domain structures of mSREBP1a and mSREBP2). ER.mSREBP1a is lacking the final 31 amino acids in the C-terminus, whilst ER.mSREBP2 lacks the final 17 C-terminal amino acids. These truncations originate from the cDNA originally cloned by the Goldstein and Brown lab (Horton et al., 1998; Shimano et al., 1997a), as demonstrated by DNA sequencing (data not shown: B. Griffiths, GEA, LRI). The constructs used in this thesis still contain the transactivation domains and the DNA binding domains, both of which are required for transcriptional activity. In addition, these constructs still contain the C-terminal residues that are phosphorylated by various kinases that govern the stability of the mature transcription factors (Bengoechea-Alonso and Ericsson, 2009; Bengoechea-Alonso and Ericsson, 2006). However, it is possible that the C-terminal truncations lack previously undescribed residues important for the functional regulation of the mature proteins. It may be difficult, therefore, to compare results obtained using these truncated fusion proteins with some of the more recent literature. Nevertheless, the following sections demonstrate that these fusion proteins do behave in the expected manner and that the ER.mSREBP fusion proteins used in this thesis regulate canonical SREBP target genes.

3.3 Characterisation of U87.ER.mSREBP1a and U87.ER.mSREBP2 cell lines

3.3.1 Activation of ER.mSREBP1a or ER.mSREBP2 reduce cellular proliferation

The U87 cell lines stably expressing ER.mSREBP1a or ER.mSREBP2 (as well as an empty vector control cell line; U87-EV) were characterised. Both constructs could be detected by Western blot using an ER-alpha antibody (Figure 3.2), indicating that the cell lines had been successfully infected and that the proteins were being expressed. Treatment with 4-OHT over a period of 24 hours caused a shift in the mobility of ER.mSREBP1a, but not ER.mSREBP2 (Figure 3.2). This shift could be the result of phosphorylation of the ER.mSREBP1a protein upon activation with 4-OHT.

Next, the effect of long-term SREBP activation on the proliferation of U87 cells was investigated. Cells were treated with solvent (EtOH) or 4-OHT for the times indicated in Figure 3.3 and a cell mass assay was carried out as a measure of cell number. No difference in cell mass was observed between U87.EV cells treated with EtOH or 4-OHT, indicating that treatment with 4-OHT alone had no effect on cell proliferation (Figure 3.3). Interestingly, both the 4-OHT treated ER.mSREBP1a and ER.mSREBP2 cell lines exhibited reduced proliferation at 72 hours compared to their vehicle treated controls and the EV control cell line (Figure 3.3). In addition, the loss of cyclin A, a key cell cycle component, was observed at the 8 hour and 24 hour time points (Figure 3.4). These data indicate that activation of exogenous mSREBP1a and mSREBP2 results in reduced proliferation in these cells, possibly by inhibiting positive cell cycle regulators.

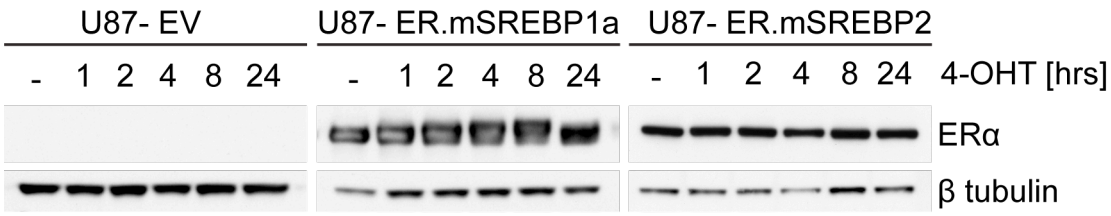

Figure 3-2: Expression of ER.mSREBP1a and ER.mSREBP2 fusion proteins in U87 cells. U87 cells were stably infected with the ER.mSREBP1a and ER.mSREBP2 constructs, as well as an empty vector control (EV). Cells were cultured in 10% FCS and treated with 100 nM 4-OHT for the times indicated. Whole cell lysates were analysed by Western blotting for expression of the ER fusion proteins using an ERα antibody. β tubulin is shown as a loading control.

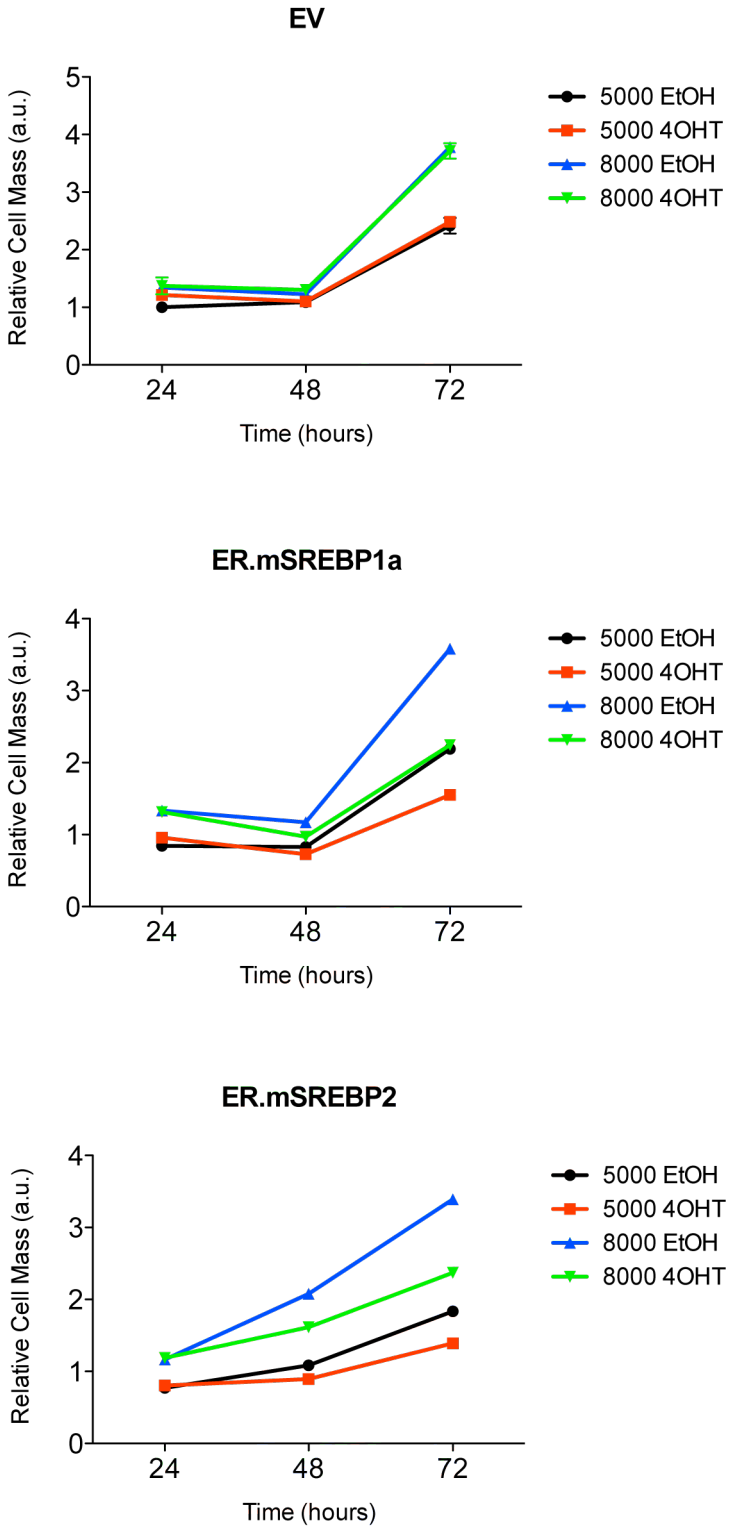

Figure 3-3 Activation of ER.mSREBP1a and ER.mSREBP2 in U87 cells leads to a reduction in growth over time.
U87 stably expressing ER.mSREBP1a and ER.mSREBP2 together with the empty vector control (EV) were seeded in 96-well plates at a density of 5000 or 8000 cells/ well and cultured in 10% FCS in the presence of vehicle (EtOH) or 100 nM 4-OHT over a period of 72 hours. At each time point a cell mass assay was performed. Data shown represents the mean of three biological replicates ± SEM.

Figure 3-4: Activation of ER.mSREBP1a and ER.mSREBP2 in U87 cells results in a reduction in cyclin A.
U87 cells stably expressing ER.mSREBP1a and ER.mSREBP2 together with the empty vector control (EV) were grown in 10% FCS and treated with vehicle (EtOH) or 100 nM 4-OHT for the times indicated. Whole cell lysates were analysed by SDS-PAGE and Western blotting using an antibody against cyclin A. β tubulin is shown as a loading control.

3.3.2 Activation of ER.mSREBP1a and ER.mSREBP2 in U87 cells results in the increased expression of SREBP target genes

In order to assay for transcriptional activity of ER.mSREBP1a and ER.mSREBP2 in U87 cells, the expression of two key SREBP target genes was examined (Figure 3.5). Cells were treated with solvent (EtOH) or 4-OHT for 24 hours. Whole cell lysates were analysed by Western blotting for the expression of FASN and ATP-citrate lyase (ACLY) (Figure 3.5 A). In addition, RNA was extracted from parallel cultures and used for RT-QPCR analysis of both FASN and ACLY (Figure 3.5 B). Treatment with 4-OHT for 24 hours resulted in increased protein and mRNA expression of both FASN and ACLY in cells expressing ER.mSREBP1a as well as cells expressing ER.mSREBP2. Interestingly, activated ER.mSREBP1a appeared to induce both FASN and ACLY expression to a greater extent than ER.mSREBP2. This is in keeping with previous findings that SREBP1a is the stronger transcriptional activator (Bengoecheaalonso and Ericsson, 2007; Shimano et al., 1997a). However, this observation could also be the result of high expression levels of the ER.mSREBP1a protein relative to ER.mSREBP2.

The increase in transcriptional activity of ER.mSREBP1a and ER.mSREBP2 in response to 4-OHT induction was also confirmed using luciferase reporter assays. The pSRE-luc reporter contains three repeats of a classic sterol response element (SRE)/ SP1 binding site fused to the luciferase gene (described in Figure 3.6 A and (Amemiya-

Kudo et al., 2002)). It represents sequences initially designated as repeats 2 and 3 in the promoter region of the low-density lipoprotein receptor (LDLR) gene (Briggs et al., 1993). U87-SREBP1a.ER, U87.SREBP2.ER and U87.EV cell lines were transiently transfected with pSRE-luc and treated with 4-OHT or solvent (EtOH) for 24 hours as indicated in Figure 3.6 B. An increase in the luciferase activity of pSRE-luc was observed in both cell lines expressing ER.mSREBP1a or ER.mSREBP2 following 4-OHT induction (Figure 3.6 B). However, ER.mSREBP1a activation increased luciferase activity to a larger extent than ER.mSREBP2 (Figure 3.6 B). This is consistent with the above observation that activated ER.mSREBP1a induced FASN and ACLY expression to a greater extent than ER.mSREBP2.

When taken together, these data indicate that transcriptional activity of ER.mSREBP1a and ER.mSREBP2 was inducible in a 4-OHT-dependent manner in the U87 cell line.

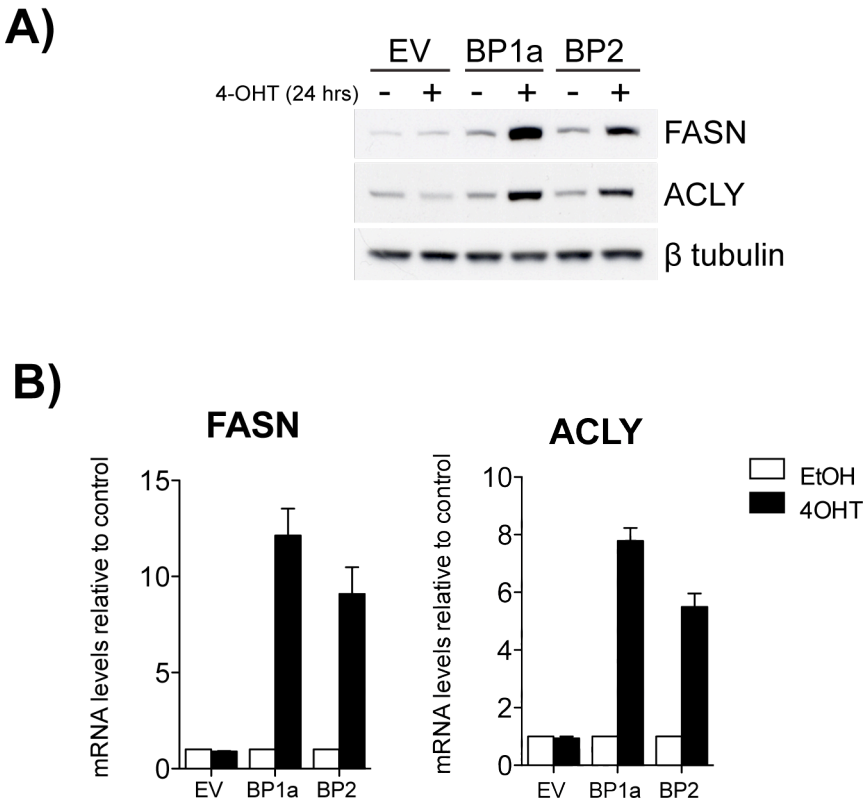

Figure 3-5 Activation of ER.mSREBP1a and ER.mSREBP2 in U87 cells leads to increased expression of SREBP target genes.
U87-EV (EV), U87-ER.mSREBP1a (BP1a) and U87-ER.mSREBP2 (BP2) cells were cultured in 10% FCS for 24 hours in the presence of vehicle (EtOH) or 100 nM 4-OHT. A) Whole cell lysates were analysed by SDS-PAGE and Western blotting with antibodies against FASN and ACLY. β tubulin is shown as a loading control. B) mRNA from cells treated as in (A) was analysed by RT-QPCR and normalised to the loading control. Data shown is the mean of three independent biological replicates ± SEM.

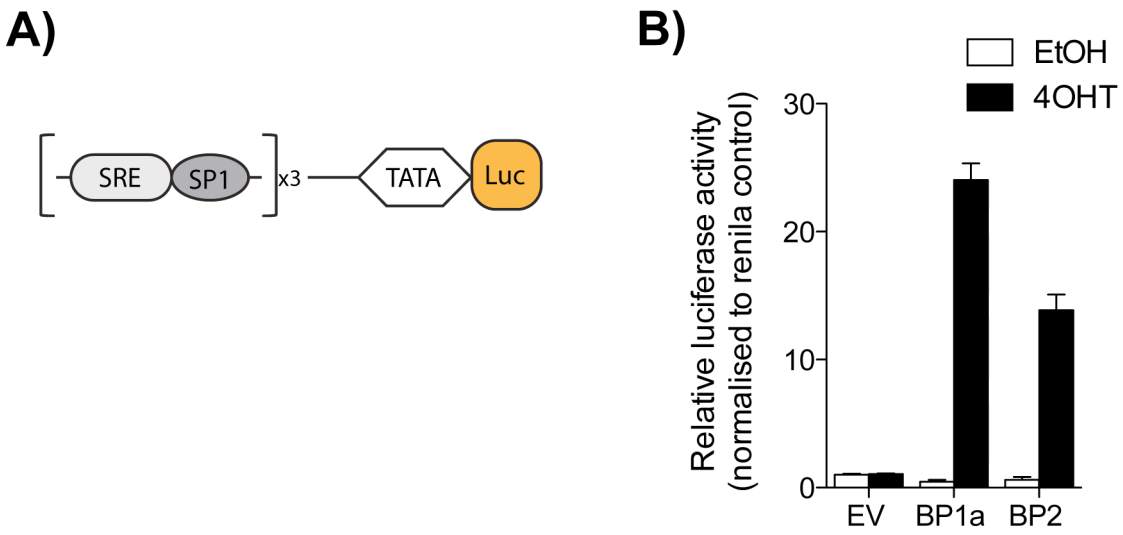

Figure 3-6: Activation of ER.mSREBP1a and ER.mSREBP2 in U87 cells results in increased SRE-luciferase reporter activity.
(A) Schematic representation of the pSRE-luc reporter, where three repeats of the classical SRE-SP1 sequence are fused to a TATA box and the luciferase gene (Amemiya-Kudo et al., 2002). This sequence was formally designated repeats 2 and 3 in the low-density lipoprotein receptor (LDLR) gene promoter (-68/-37) (Briggs et al., 1993). B) U87-EV, U87-ER.mSREBP1a and U87-ER.mSREBP2 cells were co-transfected with the pSRE-luc reporter and phRL-SV40 renilla luciferase as a control. Cells were cultured in 10% FCS in the presence of vehicle (EtOH) or 100 nM 4-OHT for 24 hours and a Dual Luciferase® assay was carried out. Data shown represents the mean luciferase activity normalised to the renilla luciferase control from two biological replicates ± SEM.

3.3.3 Activation of ER.mSREBP1a and ER.mSREBP2 in U87 cells results in the formation of lipid droplets and an increase in *de novo* lipid synthesis

The ability of cells to store energy plays an important role in the cellular response to starvation. Eukaryotic cells store energy in the form of neutral lipids, such as triacylgylcerols (TAGs), and lipid droplets (LDs) provide compartmental storage for TAGs within the cell (Farese and Walther, 2009). Interestingly, activation of SREBPs has been shown to induce the formation of lipid droplets in various models (Seo et al., 2011; Shimano et al., 1996; Wang et al., 2010). Cells expressing ER.mSREBP1a and ER.mSREBP2 were assayed for lipid droplet formation following 4-OHT induced-activation of SREBP using the dye Nile Red. Nile Red specifically binds to neutral lipids found at the core of LDs (Greenspan et al., 1985). Activation of ER.mSREBP1a or ER.mSREBP2 strongly induced the formation of lipid droplets as detected by Nile

Red staining and imaged by confocal microscopy (Figure 3.7). In contrast, no LDs were observed in the control EV cell line after either vehicle (EtOH) or 4-OHT treatment, indicating that the formation of lipid droplets was dependent on SREBP activation. A limited amount of lipid droplet staining was observed in the U87.ER.mSREBP1a cell line when treated with EtOH, however, the size and intensity of the LDs formed upon stimulation with 4-OHT were greatly increased. Although LD formation occurs naturally within the cell, LDs are not always detectable by microscopy. SREBP activation could therefore increase the number of LDs within the cell, or increase the size of LDs so that they become detectable using this technique.

As previously mentioned, SREBPs activate genes involved in fatty acid and cholesterol biosynthesis. In addition, SREBPs are required for *de novo* lipid synthesis (Porstmann et al., 2008). Therefore, *de novo* lipid synthesis was measured in response to SREBP activation. Cells were treated with solvent (EtOH) or 4-OHT for 24 hours before being incubated with radiolabelled glucose (Figure 3.8 A), pyruvate (Figure 3.8 B) or acetate (Figure 3.8 C) for a further 4 hours. Analysis of the incorporation of ^{14}C derived from these radioactive precursors into cellular lipid fractions revealed that activation of ER.mSREBP1a increased the amount of glucose-, pyruvate- and acetate-dependent lipogenesis (Figure 3.8). Interestingly, the relative amounts of all three precursors incorporated into the lipid fraction differed. Incorporation of glucose-derived ^{14}C increased 1.5 fold following ER.mSREBP1a activation (Figure 3.8 A), whereas incorporation of pyruvate-derived ^{14}C was increased by almost 2-fold (Figure 3.8 B). Acetate-derived ^{14}C incorporation showed the largest increase of all three metabolites (Figure 3.8 C). Taken together, these data indicate that activation of ER.mSREBP1a is sufficient to increase *de novo* lipid synthesis in U87 cells, and that mSREBP1a may regulate the incorporation of acetate into lipids more potently than other cellular precursors.

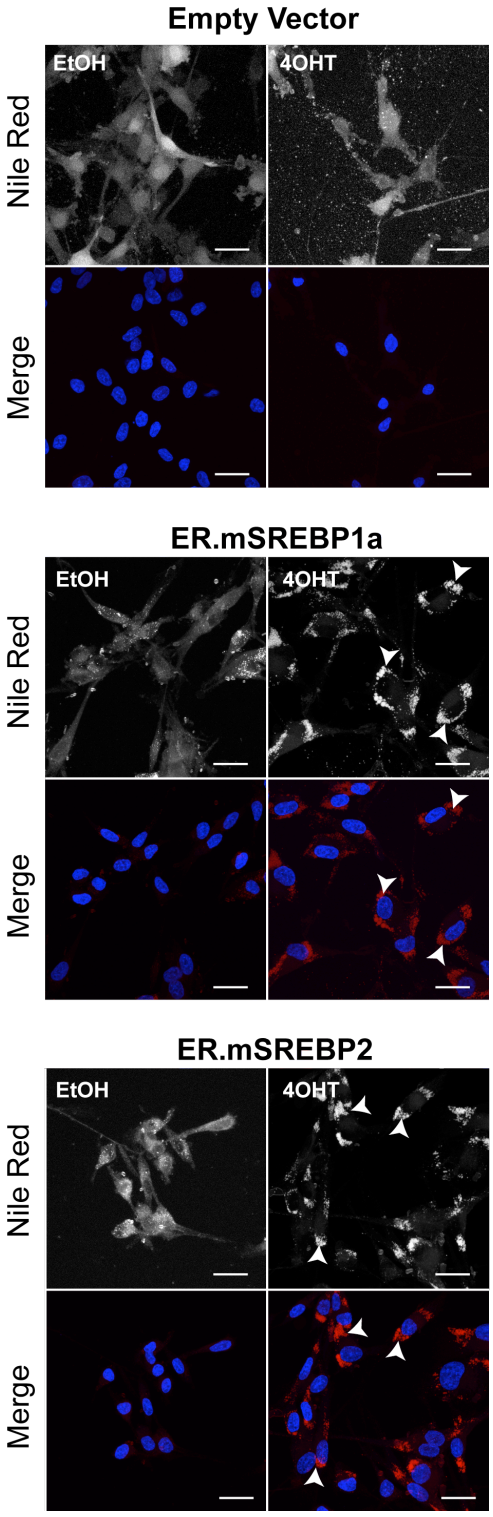

Figure 3-7 Activation of ER.mSREBP1a and ER.mSREBP2 in U87 cells causes increased lipid droplet formation.
U87 cells stably expressing the ER.mSREBP1a and ER.mSREBP2 construts, together with the empty vector control (EV) were seeded onto coverslips. Cells were cultured in 10% FCS for 24 hours in the presence of either vehicle (EtOH) or 100 nM 4-OHT. Cells were fixed and stained with 0.1 µg/mL Nile Red (lipid droplets) and 1 µg/mL DAPI (nuclei) and imaged using confocal microscopy. All images were taken at the same magnification. Arrowheads indicate examples of specific lipid droplet staining. Scale bars represent 20 µm.

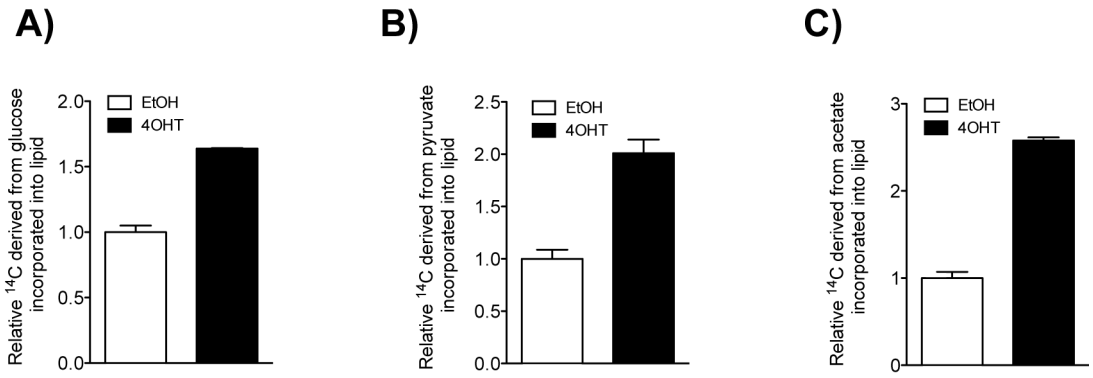

Figure 3-8: Activation of ER.mSREBP1a and ER.mSREBP2 in U87 cells results in increased *de novo* lipogenesis.
U87 cells stably expressing the ER.mSREBP1a and ER.mSREBP2 constructs, together with the empty vector control (EV) were cultured in 10% FCS in the presence of either vehicle (EtOH) or 100 nM 4-OHT for 24 hours. The incorporation of D-[6-^{14}C] glucose (A), [2-^{14}C] pyruvate (B) or [1-^{14}C] acetate (C) into the lipid fraction was then measured. CPM were normalised to cell mass and relative fold change was calculated. Data shown represent the mean of two biological replicates ± SEM.

3.4 Identification of SREBP transcriptional signatures in human glioblastoma cells using gene expression microarray analysis

Having confirmed that the ER.mSREBP1a and ER.mSREBP2 constructs could be activated in a 4-OHT-dependent manner, gene expression microarray analysis was performed using these cell lines in order to identify specific SREBP-dependent transcriptional signatures in a human glioblastoma cell line (U87). Cells from the three cell lines described in the previous sections were treated with 4-OHT to induce SREBP activation for 6 or 24 hours. In addition, cells were treated with solvent (EtOH) as a control. Total RNA was extracted from three independent biological replicates and used for subsequent cDNA synthesis and hybridisation to a HumanRef-8 v2 Expression BeadChip (Illumina, performed by Dr. Charles Mein's laboratory, Bart's and the London Medical School).

Following processing of the Illumina bead intensity data (Phil East, CRUK BABS) it was found that ER.mSREBP1a or ER.mSREBP2 activation lead to a total of 2046 probes being significantly regulated. Using expression values for these probes a

hierarchal clustering analysis was performed to generate a heat map of differentially regulated probes. Three distinct clusters stood out. Upregulation of probes within Cluster A was associated with activation of ER.mSREBP1a (Figure 3.9), whilst upregulation of probes present in cluster B was associated with activation of ER.mSREBP2 (Figure 3.9). However, there was little distinction between the probes downregulated by ER.mSREBP1a or ER.mSREBP2 activation at this clustering level (Figure 3.9, Cluster C). This indicates that whilst ER.mSREBP1a or ER.mSREBP2 activation causes the upregulation of distinct sets of genes, transcriptional downregulation is likely to involve a common mechanism and targets the same genes.

In order to further visualise the distinct effects of either ER.mSREBP1a or ER.mSREBP2 activation on gene expression, gene expression values were used to generate a Venn diagram, showing numbers of genes that were upregulated or downregulated by both transcription factors (Figure 3.10). As indicated by the heat map, the Venn diagrams revealed that more genes were upregulated following activation of either ER.mSREBP1a or ER.mSREBP2 than downregulated. This is expected, as SREBPs are direct activators of transcription. However, SREBP activation still caused the downregulation of a considerable number of genes. This could be the result of the indirect regulation of genes by SREBP activation. It is possible that SREBP may be regulating the activity of negative regulators of the genes downregulated in this microarray data-set (discussed further in section 3.5, page 117). Alternatively, given the effect of SREBP activation on the cell cycle regulator Cyclin A observed in Figure 3.4, together with the decreased proliferation observed in Figure 3.6, downregulation of genes in response to SREBP activation may be the result of cell cycle arrest induced by activation of the exogenous SREBPs. Indeed, overexpression of SREBP1a has previously been shown to induce cell cycle arrest via induction of the cell cycle inhibitor p21 in CHO cells (Nakakuki et al., 2007), as well as in Saos-2 cells (Inoue et al., 2005).

The Venn diagrams also revealed that the number of genes specifically regulated by either SREBP1a or SREBP2 were considerably fewer than the number of transcriptional

targets shared by both proteins. This indicates an overlap of the transcriptional function of SREBP1a and SREBP2 in these cells. However, the number of genes specifically regulated by SREBP2 was higher than those specifically regulated by SREBP1a. This also meant that the total number of genes upregulated by SREBP2 was greater, suggesting that SREBP2 may play a more distinct role in transcriptional regulation in these cells.

Next it was investigated whether the sub-sets of genes that were regulated by SREBP1a and/or SREBP2 had different functions. Gene lists from the sub-sets identified in the Venn diagrams were used for pathway enrichment analysis according to the GeneGo pathways and processes within the Metachore pathway tool (GeneGO) (performed in collaboration with Probir Chakravarty, LRI BABS). Pathways are defined as genes that are directly connected within a defined pathway. As expected, genes upregulated by both SREBP1a and SREBP2 were significantly enriched in pathways associated with lipid metabolism and cholesterol biosynthesis (Figure 3.11, pathways highlighted in orange). Interestingly, the total set of genes upregulated by SREBP2 was enriched in pathways associated with glutathione metabolism, which plays a major role in the cellular response to oxidative stress (Figure 3.11, pathways highlighted in blue). No pathways were significantly enriched in gene sets specifically upregulated by either SREBP1a or SREBP2. This is likely due to the relatively small numbers of genes within these data sets.

The same gene sets described above were subjected to process enrichment analysis. Processes are defined as genes within related pathways that are not directly connected within those pathways. This allows identification of more diverse biological functions. Enriched processes included insulin and leptin signalling, consistent with the well-established role of SREBPs in Akt signal transduction and lipid metabolism. Interestingly, processes enriched within SREBP2 regulated genes included the response to hypoxia and oxidative stress as well as the regulation of angiogenesis. This is consistent with enrichment of the glutathione metabolism pathways observed in Figure 3.11. In addition, process enrichment analysis also revealed that genes upregulated by both SREBP1 and SRBEP2 are associated with inflammation and interferon signalling

(Figure 3.12). These data demonstrate that SREBPs are involved in a range of biological processes.

Next the different subsets of genes were subjected to transcription factor analysis. As expected, the two most significantly associated transcription factors were SREBP1 and SREBP2 (Figure 3.13). Interestingly, the SP1 transcription factor was also highly significantly associated with genes regulated by both SREBP1 and SREBP2. SP1 has been shown to enhance gene SREBP-dependent gene expression and DNA binding sites for this transcription factor are often located in close proximity to SREs within a range of target gene promoters. In addition, other co-regulators of SREBP transcription, nuclear factor Y alpha and beta (NFYA and NFYB), were found to be significantly associated with genes in these data sets. Furthermore, additional transcription factors associated with lipid metabolism were also significantly enriched within these data sets, including HNF4-α and PPAR-α (Figure 3.13).

Pathway and process enrichment analysis of genes that were downregulated following ER.mSREBP1a or ER.mSREBP2 activation showed that many of these genes are associated with cell cycle regulation (see Figures 3.14, 3.15 and 3.16). When taken together with the reduction in proliferation and the loss of cyclin A protein observed in section 3.3.1 (Figure 3.3 and Figure 3.4, respectively), these data strongly suggest that activation of exogenous SREBP results in a reduction in cell proliferation via indirect regulation of cell cycle regulators in glioblastoma cells. In addition, it was found that genes that were downregulated by SREBP1a and SREBP2 were significantly enriched within Notch and Wnt signalling processes. Analysis of transcription factor enrichment within the downregulated genes also revealed the indirect role of SREBPs in cell cycle regulation. In most cases, the two most significantly associated transcription factors were E2F4 and E2F1 (Figure 3.17), transcription factors that are strongly associated with cell cycle regulation.

Interestingly, the hypoxia inducible factor 1-alpha (HIF1α) was associated with genes downregulated by both SREBP1a and SREBP2 (Figure 3.17). This is consistent with

the previous finding that SREBP activation induces expression of genes involved in processes associated with the cellular response to hypoxia and oxidative stress (Figure 3.12).

When taken together, these data indicate that SREBPs are regulating lipid metabolism in the cancer cell line U87. In addition, other metabolic processes are being regulated, including the response to hypoxia and oxidative stress. Most strikingly, activation of SREBPs in U87 cells may lead to a reduction in cellular proliferation, as indicated by the enrichment of cell cycle regulators within the downregulated gene sets. These microarray data may prove to be a useful tool for the future investigation of SREBP function in a human cancer cell line.

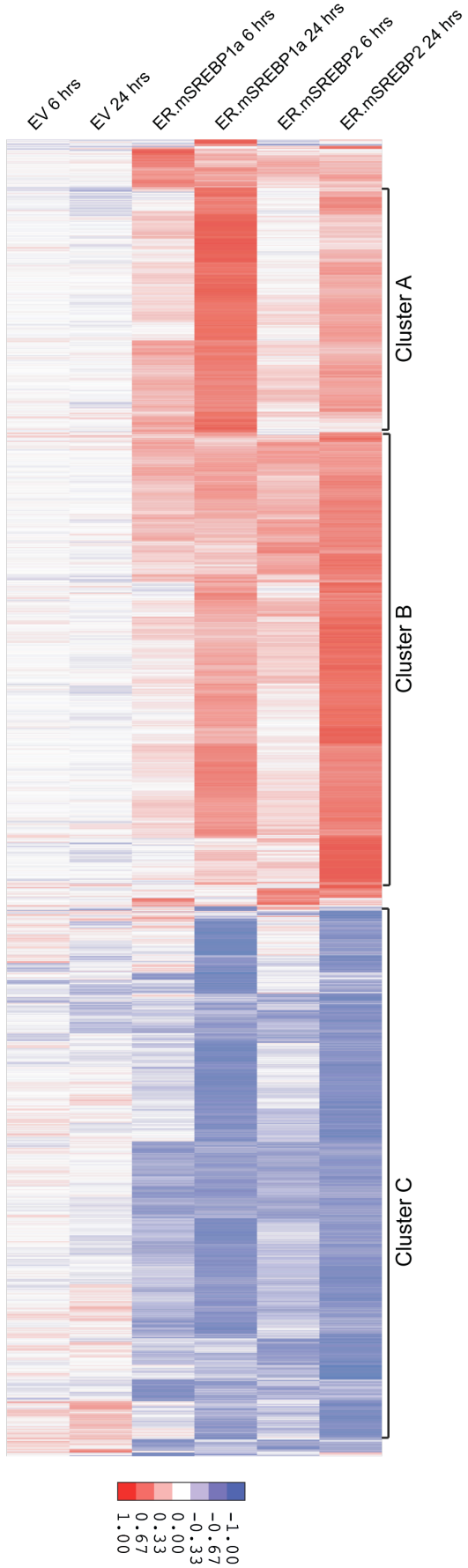
EV 6 hrs
EV 24 hrs
ER.mSREBP1a 6 hrs
ER.mSREBP1a 24 hrs
ER.mSREBP2 6 hrs
ER.mSREBP2 24 hrs
Cluster A
Cluster B
Cluster C
1.00
0.67
0.33
0.00
−0.33
−0.67
−1.00

Figure 3-9: Activation of ER.mSREBP1a and ER.mSREBP2 associates with different subsets of target genes.
Heat-map showing hierarchal clustering of differentially expressed probes following activation of ER.mSREBP1a or ER.mSREBP2 for 6 and 24 hours relative to their control. Total number of probes significantly regulated: 2046. Red indicates increased expression and blue indicates decreased expression relative to the mean centred and scaled expression of the probe compared to the respective sample control. Three selected clusters are highlighted and designated Cluster A, Cluster B and Cluster C.

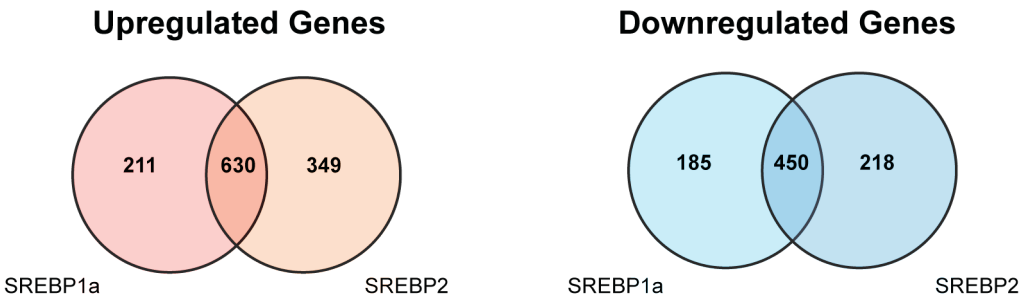

Figure 3-10: Venn diagrams indicating the number of genes regulated following activation of ER.mSREBP1a or ER.mSREBP2 for 6 and 24 hours.
Numbers of genes upregulated (left, orange) or downregulated (right, blue) following activation of ER.mSREBP1a or ER.mSREBP2 for 6 and 24 hours combined are shown. Venn diagrams indicate numbers of genes regulated by ER.mSREBP1a only, ER.mSREBP2 only, genes commonly regulated by both ER.mSREBP1a and ER.mSREBP2, total numbers of genes regulated by ER.mSREBP1a or ER.mSREBP2 and the total number of genes regulated by both ER.mSREBP1a and ER.mSREBP2. Note: numbers shown correspond to numbers of genes, rather than probes.

Pathways associated with SREBP1a upregulated genes

Pathway Name	p.Val	objects
Cholesterol Biosynthesis	3.63E-14	'15/21
Regulation of lipid metabolism_Insulin regulation of fatty acid methabolism	2.18E-05	'12/46
n-6 Polyunsaturated fatty acid biosynthesis	3.89E-05	'8/22
n-3 Polyunsaturated fatty acid biosynthesis	3.89E-05	'8/22
Unsaturated fatty acid biosynthesis	7.37E-05	'7/18
Regulation of lipid metabolism_Regulation of lipid metabolism via LXR, NF-Y and SREBP	9.64E-05	'9/31
Saturated fatty acid biosynthesis	2.65E-04	'3/3

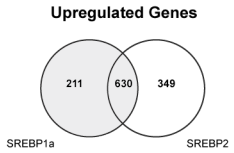

Pathways associated with SREBP2 upregulated genes

Pathway Name	p.Val	objects
Cholesterol Biosynthesis	3.06E-13	'15/21
n-6 Polyunsaturated fatty acid biosynthesis	1.29E-06	'10/22
n-3 Polyunsaturated fatty acid biosynthesis	1.29E-06	'10/22
Regulation of lipid metabolism_Insulin regulation of fatty acid methabolism	3.19E-06	'14/46
Unsaturated fatty acid biosynthesis	1.93E-05	'8/18
Regulation of lipid metabolism_Regulation of lipid metabolism via LXR, NF-Y and SREBP	2.88E-04	'9/31
Saturated fatty acid biosynthesis	4.07E-04	'3/3
Immune response_TREM1 signaling pathway	5.99E-04	'11/48
Immune response_Human NKG2D signaling	7.09E-04	'8/28
Development_PIP3 signaling in cardiac myocytes	9.37E-04	'10/43
Glutathione metabolism / Human version	9.65E-04	'9/36
Apoptosis and survival_BAD phosphorylation	9.65E-04	'9/36
Glutathione metabolism	9.65E-04	'9/36
Arginine metabolism/ Rodent version	9.65E-04	'9/36
Development_IGF-1 receptor signaling	1.13E-03	'10/44

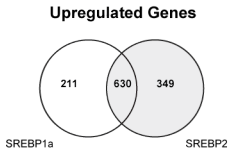

Pathways associated with commonly upregultaed genes

Pathway Name	p.Val	objects
Cholesterol Biosynthesis	1.05E-15	'15/21
n-6 Polyunsaturated fatty acid biosynthesis	6.92E-06	'8/22
n-3 Polyunsaturated fatty acid biosynthesis	6.92E-06	'8/22
Regulation of lipid metabolism_Insulin regulation of fatty acid methabolism	1.29E-05	'11/46
Regulation of lipid metabolism_Regulation of lipid metabolism via LXR, NF-Y and SREBP	1.49E-05	'9/31
Unsaturated fatty acid biosynthesis	1.60E-05	'7/18
Saturated fatty acid biosynthesis	1.31E-04	'3/3
Transcription_Transcription regulation of aminoacid metabolism	1.78E-04	'7/25
Regulation of metabolism_Bile acids regulation of glucose and lipid metabolism via FXR	2.31E-04	'8/34
Regulation of lipid metabolism_Regulation of fatty acid synthase activity in hepatocytes	3.03E-04	'5/13

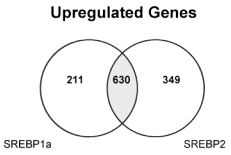

Pathways associated with all upregulated genes

Pathway Name	p.Val	objects
Cholesterol Biosynthesis	3.62E-12	'15/21
Regulation of lipid metabolism_Insulin regulation of fatty acid methabolism	4.35E-06	'15/46
n-6 Polyunsaturated fatty acid biosynthesis	5.98E-06	'10/22
n-3 Polyunsaturated fatty acid biosynthesis	5.98E-06	'10/22
Unsaturated fatty acid biosynthesis	6.53E-05	'8/18

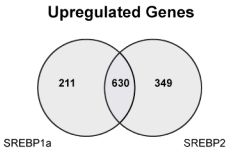

Key:

Lipid Metabolism

Hypoxia and Oxidative Stress

Figure 3-11: Pathway enrichment analysis of genes significantly upregulated by activation of ER.mSREBP1a or ER.mSREBP2.
Tables show pathways that are significantly enriched in each of the sub-sets of genes highlighted in grey in the corresponding Venn diagram. Pathways are colour-coded according to 4 functions (see key). No pathways were significantly enriched in the SREBP1a- or SREBP2-specific sub-sets. Objects: Number of genes in the experimental dataset that are regulated over the total number of genes present in the specified pathway.

Processes associated with SREBP1a upregulated genes

Process Name	p.Val	objects
Inflammation_Interferon signaling	1.38E-06	'20/109
Signal transduction_Leptin signaling	6.29E-05	'15/87
Signal transduction_Insulin signaling	5.41E-04	'15/105
Reproduction_Spermatogenesis, motility and copulation	6.34E-04	'24/215
Regulation of metabolism_Bile acid regulation of lipid metabolism	6.85E-04	'10/55
Reproduction_Male sex differentiation	9.39E-04	'25/234
Inflammation_MIF signaling	1.55E-03	'15/116

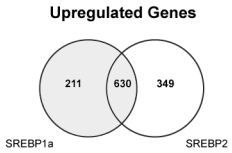

Processes associated with SREBP2 upregulated genes

Process Name	p.Val	objects
Inflammation_Interferon signaling	9.13E-07	'21/109
Signal transduction_Leptin signaling	3.40E-05	'16/87
Regulation of metabolism_Bile acid regulation of lipid metabolism	5.82E-05	'12/55
Signal transduction_Insulin signaling	1.05E-04	'17/105
Reproduction_Spermatogenesis, motility and copulation	1.16E-04	'27/215
Reproduction_Male sex differentiation	4.71E-04	'27/234
Response to hypoxia and oxidative stress	4.74E-04	'16/108
Reproduction_Progesterone signaling	5.85E-04	'23/189
Inflammation_TREM1 signaling	9.56E-04	'17/126
Development_Regulation of angiogenesis	2.04E-03	'23/207
Cell cycle_G1-S Interleukin regulation	2.15E-03	'16/124
Reproduction_Gonadotropin regulation	2.31E-03	'19/160

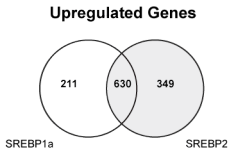

Processes associated with commonly upregulated genes

Process Name	p.Val	objects
Inflammation_Interferon signaling	4.67E-08	'19/109
Signal transduction_Leptin signaling	3.71E-05	'13/87
Reproduction_Spermatogenesis, motility and copulation	4.41E-05	'22/215
Reproduction_Male sex differentiation	5.57E-05	'23/234
Signal transduction_Insulin signaling	6.85E-05	'14/105
Regulation of metabolism_Bile acid regulation of lipid metabolism	2.96E-04	'9/55
Cytoskeleton_Regulation of cytoskeleton rearrangement	2.00E-03	'16/178

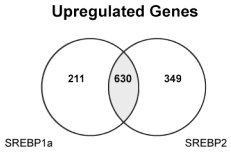

Processes associated with all upregulated genes

Process Name	p.Val	objects
Inflammation_Interferon signaling	8.86E-06	'22/109
Signal transduction_Leptin signaling	4.11E-05	'18/87
Regulation of metabolism_Bile acid regulation of lipid metabolism	1.17E-04	'13/55
Signal transduction_Insulin signaling	5.02E-04	'18/105
Cell cycle_G1-S Interleukin regulation	5.68E-04	'20/124
Inflammation_TREM1 signaling	7.01E-04	'20/126
Reproduction_Spermatogenesis, motility and copulation	8.26E-04	'29/215
Development_Regulation of angiogenesis	9.67E-04	'28/207
Reproduction_Progesterone signaling	1.13E-03	'26/189
Response to hypoxia and oxidative stress	1.90E-03	'17/108
Reproduction_Male sex differentiation	3.09E-03	'29/234

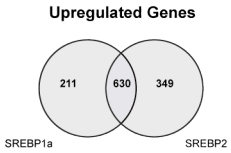

Key:

Lipid Metabolism

Hypoxia and Oxidative Stress

Cell Cycle

Signalling

Figure 3-12: Process enrichment analysis of genes significantly upregulated by activation of ER.mSRBEP1a and ER.mSREBP2.
Tables show processes that are significantly enriched in each of the sub-sets of genes highlighted in grey in the corresponding Venn diagram. Pathways are colour-coded according to 4 functions (see key). No pathways were significantly enriched in the SREBP1a- or SREBP2-specific sub-sets. Objects: Number of genes in the experimental dataset that are regulated over the total number of genes present in the specified pathway.

TFs associated with SREBP1a upregulated genes

Object name	Actual	n	R	N	Expected	Ratio	p-value	z-score
SREBP1 (nuclear)	44	759	221	17765	9.442	4.66	7.11E-18	11.57
SREBP2 (nuclear)	21	759	68	17765	2.905	7.228	3.76E-13	10.87
SP1	169	759	2633	17765	112.5	1.502	1.48E-08	5.9
STAT1	42	759	404	17765	17.26	2.433	1.00E-07	6.156
C/EBPalpha	36	759	381	17765	16.28	2.212	7.47E-06	5.05
NFYA	12	759	86	17765	3.674	3.266	0.0003	4.45

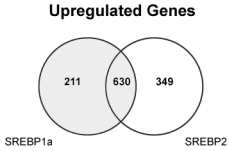

TFs associated with SREBP2 upregulated genes

Object name	Actual	n	R	N	Expected	Ratio	p-value	z-score
SREBP1 (nuclear)	49	870	221	17765	10.82	4.527	2.22E-19	11.97
SREBP2 (nuclear)	22	870	68	17765	3.33	6.606	5.47E-13	10.51
SP1	184	870	2633	17765	128.9	1.427	1.71E-07	5.387
C/EBPalpha	41	870	381	17765	18.66	2.197	1.97E-06	5.361
STAT1	41	870	404	17765	19.78	2.072	8.43E-06	4.947
HNF4-alpha	154	870	2407	17765	117.9	1.306	0.0002	3.669
ATF-4	10	870	58	17765	2.84	3.521	0.0005	4.363
NFYB	12	870	90	17765	4.408	2.723	0.0014	3.718

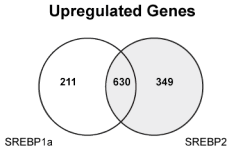

TFs associated with commonly upregulated genes

Object name	Actual	n	R	N	Expected	Ratio	p-value	z-score
SREBP1 (nuclear)	42	568	221	17765	7.066	5.944	5.76E-21	13.44
SREBP2 (nuclear)	20	568	68	17765	2.174	9.199	1.76E-14	12.31
SP1	128	568	2633	17765	84.18	1.52	4.33E-07	5.259
STAT1	33	568	404	17765	12.92	2.555	8.70E-07	5.745
C/EBPalpha	30	568	381	17765	12.18	2.463	5.72E-06	5.245
HNF4-alpha	106	568	2407	17765	76.96	1.377	0.0003	3.619
ChREBP	4	568	16	17765	0.5116	7.819	0.0014	4.959
NFYA	9	568	86	17765	2.75	3.273	0.0017	3.84
NFYB	9	568	90	17765	2.878	3.128	0.0023	3.678
PPAR-alpha	9	568	92	17765	2.942	3.06	0.0027	3.6

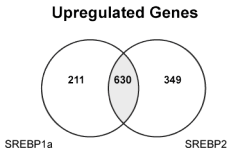

TFs associated with all upregulated genes

Object name	Actual	n	R	N	Expected	Ratio	p-value	z-score
SREBP1 (nuclear)	51	1060	221	17765	13.19	3.868	2.88E-17	10.81
SREBP2 (nuclear)	23	1060	68	17765	4.057	5.669	3.33E-12	9.716
SP1	225	1060	2633	17765	157.1	1.432	4.82E-09	6.052
STAT1	50	1060	404	17765	24.11	2.074	7.73E-07	5.502
C/EBPalpha	47	1060	381	17765	22.73	2.067	1.81E-06	5.306

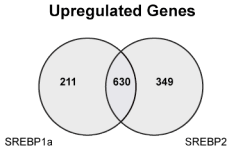

Figure 3-13 Transcription factor enrichment analysis of genes significantly upregulated by activation of ER.mSREBP1a and ER.mSREBP2.
Tables show selected transcription factors (TFs) that are significantly associated with genes present within each of the sub-sets highlighted in grey in the corresponding Venn diagrams. No TFs were significantly associated with genes regulated in the SREBP1a- or SREBP2-specific sub-sets. r: number of targets in the dataset regulated by the chosen transcription factor; n: number of network objects in the dataset; R: number of targets in the complete database regulated by this TF; N: total number of gene-based objects in the complete database; mean: mean value for hypergeometric distribution (n*R/N); z-score: z-score ((r-mean)/sqrt(variance)); p-value: probability to have the given value of r or higher (or lower for negative z-scores).

Pathways associated with SREBP1a downregulated genes

Pathway Name	p.Val	objects
Cell cycle_Role of APC in cell cycle regulation	9.97E-12	'15/32
Cell cycle_Chromosome condensation in prometaphase	7.15E-10	'11/20
Cell cycle_The metaphase checkpoint	8.45E-09	'13/35
Cell cycle_Transition and termination of DNA replication	2.48E-08	'11/26
DNA damage_ATM/ATR regulation of G1/S checkpoint	3.13E-07	'11/32
Development_TGF-beta-dependent induction of EMT via SMADs	8.80E-07	'11/35
Cell cycle_Role of SCF complex in cell cycle regulation	1.07E-06	'10/29
Cell cycle_Start of DNA replication in early S phase	2.16E-06	'10/31
Development_Regulation of epithelial-to-mesenchymal transition (EMT)	2.42E-06	'14/62
Cell cycle_ESR1 regulation of G1/S transition	2.99E-06	'10/32
Cell cycle_Cell cycle (generic schema)	5.68E-06	'8/21
Development_WNT signaling pathway. Part 2	1.26E-05	'12/53
Cell cycle_Regulation of G1/S transition (part 1)	1.66E-05	'10/38
dCTP/dUTP metabolism	8.10E-05	'10/45
Cell cycle_Spindle assembly and chromosome separation	1.78E-04	'8/32
Normal and pathological TGF-beta-mediated regulation of cell proliferation	1.78E-04	'8/32
Cell cycle_Regulation of G1/S transition (part 2)	2.77E-04	'7/26
Development_TGF-beta-dependent induction of EMT via MAPK	5.12E-04	'9/46
Cell cycle_Nucleocytoplasmic transport of CDK/Cyclins	5.14E-04	'5/14
dATP/dITP metabolism	1.50E-03	'9/53
DNA damage_ATM / ATR regulation of G2 / M checkpoint	1.85E-03	'6/26

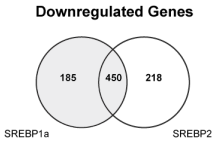

Pathways associated with SREBP2 downregulated genes

Pathway Name	p.Val	objects
Cell cycle_Role of APC in cell cycle regulation	3.17E-08	'12/32
Cell cycle_The metaphase checkpoint	1.02E-07	'12/35
Cell cycle_Chromosome condensation in prometaphase	2.80E-07	'9/20
Cell cycle_Spindle assembly and chromosome separation	3.25E-06	'10/32
Cell cycle_ESR1 regulation of G1/S transition	3.25E-06	'10/32
DNA damage_ATM/ATR regulation of G1/S checkpoint	2.67E-05	'9/32
Development_TGF-beta-dependent induction of EMT via SMADs	5.85E-05	'9/35
Development_WNT signaling pathway. Part 2	7.56E-05	'11/53
Cell cycle_Role of SCF complex in cell cycle regulation	8.86E-05	'8/29
Development_Regulation of epithelial-to-mesenchymal transition (EMT)	3.30E-04	'11/62
CTP/UTP metabolism	4.40E-04	'11/64
Cell cycle_Cell cycle (generic schema)	5.70E-04	'6/21
Cell cycle_Regulation of G1/S transition (part 1)	6.68E-04	'8/38
GTP-XTP metabolism	7.81E-04	'10/58
Cell cycle_Start of DNA replication in early S phase	9.35E-04	'7/31
Development_PDGF signaling via MAPK cascades	1.14E-03	'7/32
Normal and pathological TGF-beta-mediated regulation of cell proliferation	1.14E-03	'7/32
Cell cycle_Regulation of G1/S transition (part 2)	1.94E-03	'6/26
DNA damage_ATM / ATR regulation of G2 / M checkpoint	1.94E-03	'6/26
Cell cycle_Transition and termination of DNA replication	1.94E-03	'6/26

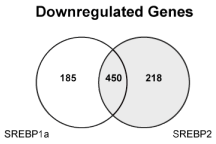

Pathways associated with SREBP1a-specific downregulated genes

Pathway Name	p.Val	objects
Cell cycle_Transition and termination of DNA replication	2.98E-06	'6/26
Cell cycle_Chromosome condensation in prometaphase	2.76E-04	'4/20

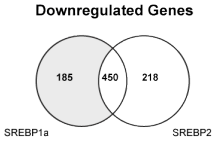

Pathways associated with commonly downregulated genes

Pathway Name	p.Val	objects
Cell cycle_Role of APC in cell cycle regulation	1.34E-08	'11/32
Cell cycle_Chromosome condensation in prometaphase	1.83E-08	'9/20
Cell cycle_The metaphase checkpoint	3.91E-08	'11/35
Development_Regulation of epithelial-to-mesenchymal transition (EMT)	1.92E-05	'11/62
DNA damage_ATM/ATR regulation of G1/S checkpoint	2.03E-05	'8/32
Cell cycle_ESR1 regulation of G1/S transition	2.03E-05	'8/32
Development_WNT signaling pathway. Part 2	2.66E-05	'10/53
Development_TGF-beta-dependent induction of EMT via SMADs	4.11E-05	'8/35
Cell cycle_Role of SCF complex in cell cycle regulation	8.73E-05	'7/29
Cell cycle_Start of DNA replication in early S phase	1.38E-04	'7/31
Cell cycle_Spindle assembly and chromosome separation	1.71E-04	'7/32
Cell cycle_Regulation of G1/S transition (part 1)	5.26E-04	'7/38
Cell cycle_Sister chromatid cohesion	1.01E-03	'5/21
Cell cycle_Cell cycle (generic schema)	1.01E-03	'5/21
Normal and pathological TGF-beta-mediated regulation of cell proliferation	1.21E-03	'6/32
Cell cycle_Nucleocytoplasmic transport of CDK/Cyclins	1.60E-03	'4/14

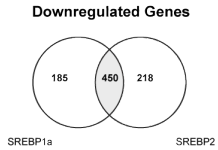

Pathways associated with all downregulated genes

Pathway Name	p.Val	objects
Cell cycle_Role of APC in cell cycle regulation	2.15E-11	'16/32
Cell cycle_Chromosome condensation in prometaphase	8.95E-09	'11/20
Cell cycle_The metaphase checkpoint	1.54E-08	'14/35
Cell cycle_Transition and termination of DNA replication	2.43E-08	'12/26
DNA damage_ATM/ATR regulation of G1/S checkpoint	3.95E-07	'12/32
Cell cycle_ESR1 regulation of G1/S transition	3.95E-07	'12/32
Cell cycle_Role of SCF complex in cell cycle regulation	1.07E-06	'11/29
Development_TGF-beta-dependent induction of EMT via SMADs	1.22E-06	'12/35
Cell cycle_Cell cycle (generic schema)	3.20E-06	'9/21
Cell cycle_Spindle assembly and chromosome separation	3.34E-06	'11/32
Cell cycle_Start of DNA replication in early S phase	1.80E-05	'10/31
Cell cycle_Regulation of G1/S transition (part 1)	2.17E-05	'11/38
Development_WNT signaling pathway. Part 2	2.79E-05	'13/53
Development_Regulation of epithelial-to-mesenchymal transition (EMT)	3.74E-05	'14/62
Normal and pathological TGF-beta-mediated regulation of cell proliferation	1.59E-04	'9/32
Cell cycle_Regulation of G1/S transition (part 2)	1.86E-04	'8/26
dATP/dITP metabolism	5.62E-04	'11/53
dCTP/dUTP metabolism	5.64E-04	'10/45
Transport_RAN regulation pathway	7.63E-04	'6/18
Development_PDGF signaling via MAPK cascades	8.84E-04	'8/32
DNA damage_ATM / ATR regulation of G2 / M checkpoint	1.16E-03	'7/26
Cell cycle_Nucleocytoplasmic transport of CDK/Cyclins	1.52E-03	'5/14
Cell cycle_Role of Nek in cell cycle regulation	2.32E-03	'7/29

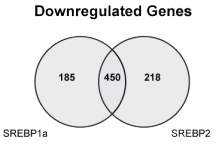

Key:

Cell Cycle

Figure 3-14: Pathway enrichment analysis of genes significantly downregulated by activation of ER.mSREBP1a or ER.mSREBP2.
Tables show pathways that are significantly enriched in each of the sub-sets of genes highlighted in grey in the corresponding Venn diagram. Pathways are colour-coded according to 4 functions (see key). No pathways were significantly enriched in the SREBP2-specific sub-set. Objects: Number of genes in the experimental data set that are regulated over the total number of genes present in the specified pathway.

Processes associated with SREBP1a downregulated genes

Process Name	p.Val	objects
Cell cycle_Core	3.59E-22	'38/114
Cell cycle_S phase	1.47E-20	'41/147
Cell cycle_G2-M	4.28E-15	'41/203
Cell cycle_Mitosis	1.86E-13	'36/177
DNA damage_Checkpoint	7.47E-12	'28/124
Cytoskeleton_Spindle microtubules	3.59E-10	'24/108
DNA damage_BER-NER repair	1.39E-08	'21/100
DNA damage_DBS repair	2.81E-07	'20/108
Signal transduction_WNT signaling	3.23E-06	'24/170
DNA damage_MMR repair	1.54E-05	'12/56
Cell cycle_G1-S	1.75E-05	'22/163
Cell cycle_G1-S Growth factor regulation	1.46E-04	'22/187
Apoptosis_Apoptotic nucleus	2.42E-04	'19/155
Development_EMT_Regulation of epithelial-to-mesenchymal transition	2.44E-04	'23/207
Cell cycle_Meiosis	5.07E-04	'14/102
Reproduction_Feeding and Neurohormone signaling	1.09E-03	'21/202
Signal transduction_NOTCH signaling	2.09E-03	'22/227
Signal Transduction_TGF-beta, GDF and Activin signaling	2.30E-03	'16/145
Development_Regulation of telomere length	2.36E-03	'8/48
DNA damage_Core	2.68E-03	'6/29
Reproduction_Progesterone signaling	2.75E-03	'19/189
Apoptosis_Apoptosis stimulation by external signals	4.59E-03	'14/128
Inflammation_MIF signaling	5.05E-03	'13/116

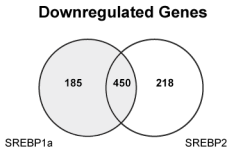

Processes associated with SREBP2 downregulated genes

Process Name	p.Val	objects
Cell cycle_Core	7.90E-15	'31/114
Cell cycle_S phase	1.29E-11	'31/147
Cell cycle_Mitosis	1.97E-11	'34/177
Cell cycle_G2-M	2.32E-10	'35/203
Cytoskeleton_Spindle microtubules	1.32E-07	'21/108
DNA damage_Checkpoint	3.57E-07	'22/124
DNA damage_BER-NER repair	1.43E-05	'17/100
Transcription_mRNA processing	1.86E-04	'20/157
Cell cycle_G1-S Growth factor regulation	2.88E-04	'22/187
Inflammation_MIF signaling	3.31E-04	'16/116
Signal transduction_WNT signaling	5.41E-04	'20/170
Cell cycle_G1-S	8.32E-04	'19/163
DNA damage_MMR repair	2.31E-03	'9/56
Development_EMT_Regulation of epithelial-to-mesenchymal transition	2.67E-03	'21/207
Neurophysiological process_Circadian rhythm	4.12E-03	'8/50
Reproduction_Feeding and Neurohormone signaling	4.43E-03	'20/202

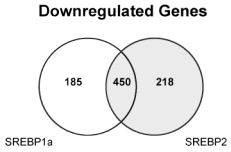

Processes associated with SREBP1a-specific downregulated genes

Process Name	p.Val	objects
Cell cycle_G2-M	5.34E-09	'17/203
Cell cycle_S phase	2.15E-07	'13/147
DNA damage_DBS repair	4.80E-07	'11/108
Cell cycle_Meiosis	1.85E-05	'9/102
Cell cycle_Core	4.51E-05	'9/114
Cell cycle_Mitosis	5.83E-05	'11/177
Cell cycle_G1-S	1.44E-04	'10/163
DNA damage_MMR repair	1.69E-04	'6/56
DNA damage_Checkpoint	4.92E-04	'8/124
DNA damage_BER-NER repair	6.89E-04	'7/100
Cytoskeleton_Spindle microtubules	1.09E-03	'7/108
Apoptosis_Apoptotic nucleus	2.11E-03	'8/155
Apoptosis_Apoptotic mitochondria	4.53E-03	'5/73
Cytoskeleton_Regulation of cytoskeleton rearrangement	4.94E-03	'8/178
Cytoskeleton_Intermediate filaments	6.34E-03	'5/79

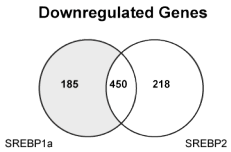

Processes associated with SREBP2-specific downregulated genes

Process Name	p.Val	objects
Protein folding_Folding in normal condition	1.69E-04	'9/116

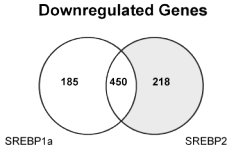

Key:

Cell Cycle

Signalling

Figure 3-15 Process enrichment analysis of genes significantly downregulated by activation of ER.mSREBP1a and ER.mSREBP2.
Tables show processes that are significantly enriched in each of the sub-sets of genes highlighted in grey in the corresponding Venn diagram. Pathways are colour-coded according to 4 functions (see key). Objects: Number of genes in the experimental data set that are regulated over the total number of genes present in the specified pathway.

Processes associated with commonly downregulated genes

Process Name	p.Val	objects
Cell cycle_Core	3.13E-17	'29/114
Cell cycle_S phase	3.16E-13	'28/147
Cell cycle_Mitosis	1.94E-10	'27/177
Cell cycle_G2-M	9.60E-10	'28/203
DNA damage_Checkpoint	3.31E-09	'21/124
Cytoskeleton_Spindle microtubules	3.34E-07	'17/108
DNA damage_BER-NER repair	3.14E-06	'15/100
Signal transduction_WNT signaling	1.60E-04	'17/170
Signal transduction_NOTCH signaling	2.43E-04	'20/227
Cell cycle_G1-S Growth factor regulation	4.98E-04	'17/187
DNA damage_MMR repair	9.35E-04	'8/56
Reproduction_Progesterone signaling	1.56E-03	'16/189
Development_EMT_Regulation of epithelial-to-mesenchymal transition	1.56E-03	'17/207
Reproduction_Feeding and Neurohormone signaling	3.08E-03	'16/202
Inflammation_MIF signaling	3.52E-03	'11/116
Proliferation_Negative regulation of cell proliferation	5.59E-03	'14/177
Proteolysis_Proteolysis in cell cycle and apoptosis	5.85E-03	'11/124
Cell cycle_G1-S Interleukin regulation	5.85E-03	'11/124

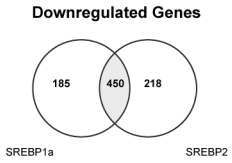

Processes associated with all downregulated genes

Process Name	p.Val	objects
Cell cycle_Core	7.75E-20	'40/114
Cell cycle_S phase	1.21E-18	'44/147
Cell cycle_G2-M	1.12E-15	'48/203
Cell cycle_Mitosis	1.39E-14	'43/177
Cytoskeleton_Spindle microtubules	1.35E-10	'28/108
DNA damage_Checkpoint	8.97E-10	'29/124
DNA damage_BER-NER repair	7.28E-08	'23/100
Cell cycle_G1-S	1.85E-06	'28/163
DNA damage_DBS repair	5.04E-06	'21/108
Signal transduction_WNT signaling	1.30E-05	'27/170
DNA damage_MMR repair	4.79E-05	'13/56
Cell cycle_G1-S Growth factor regulation	1.88E-04	'26/187
Development_EMT_Regulation of epithelial-to-mesenchymal transition	4.10E-04	'27/207
Transcription_mRNA processing	5.23E-04	'22/157
Cell cycle_Meiosis	8.79E-04	'16/102
Development_Regulation of telomere length	8.97E-04	'10/48
Inflammation_MIF signaling	1.34E-03	'17/116
Reproduction_Feeding and Neurohormone signaling	1.44E-03	'25/202
Apoptosis_Apoptotic nucleus	5.77E-03	'19/155

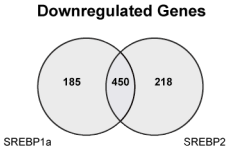

Key:

Cell Cycle

Signalling

Figure 3-16: Process enrichment analysis of genes significantly downregulated by activation of ER.mSRBEP1a and ER.mSREBP2 continued.
Tables show processes that are significantly enriched in each of the sub-sets of genes highlighted in grey in the corresponding Venn diagram. Pathways are colour-coded according to 4 functions (see key). Objects: Number of genes in the experimental data set that are regulated over the total number of genes present in the specified pathway.

TFs associated with SREBP1a downregulated genes

Object name	Actual	n	R	N	Expected	Ratio	p-value	z-score
E2F4	72	556	311	17765	9.734	7.397	4.05E-42	20.46
E2F1	77	556	562	17765	17.59	4.378	1.76E-28	14.63
ZNF143	33	556	134	17765	4.194	7.869	1.13E-20	14.35
c-Myc	120	556	1682	17765	52.64	2.28	2.54E-18	9.913
p53	74	556	916	17765	28.67	2.581	4.88E-14	8.833
HIF1A	30	556	412	17765	12.89	2.327	1.73E-05	4.897
HNF4-alpha	107	556	2407	17765	75.33	1.42	8.85E-05	3.987
p21	2	556	3	17765	0.0939	21.3	0.0029	6.321

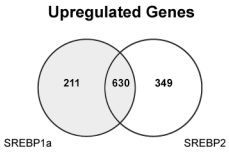

TFs associated with SREBP2 downregulated genes

Object name	Actual	n	R	N	Expected	Ratio	p-value	z-score
E2F4	52	586	311	17765	10.26	5.069	2.14E-22	13.37
c-Myc	133	586	1682	17765	55.48	2.397	2.92E-22	11.12
E2F1	66	586	562	17765	18.54	3.56	1.69E-19	11.39
ZNF143	24	586	134	17765	4.42	5.43	1.18E-11	9.506
p53	64	586	916	17765	30.22	2.118	1.07E-08	6.418
HIF1A	32	586	412	17765	13.59	2.355	7.09E-06	5.138
HNF4-alpha	112	586	2407	17765	79.4	1.411	8.20E-05	4.002

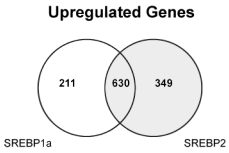

TFs associated with SREBP1a-specific downregulated genes

Object name	Actual	n	R	N	Expected	Ratio	p-value	z-score
E2F4	30	171	311	17765	2.994	10.02	1.32E-21	15.82
E2F1	26	171	562	17765	5.41	4.806	3.01E-11	9.04
MITF	11	171	88	17765	0.8471	12.99	8.02E-10	11.11
ZNF143	11	171	134	17765	1.29	8.528	7.04E-08	8.624
p53	27	171	916	17765	8.817	3.062	1.97E-07	6.318

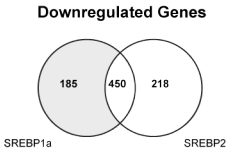

TFs associated with SREBP2-specific downregulated genes

Object name	Actual	n	R	N	Expected	Ratio	p-value	z-score
c-Myc	42	204	1682	17765	19.31	2.174	1.07E-06	5.456
ZNF217	9	204	95	17765	1.091	8.25	1.46E-06	7.636
HSF2	7	204	73	17765	0.8383	8.35	2.04E-05	6.783
HSF1	10	204	224	17765	2.572	3.888	0.0003	4.688

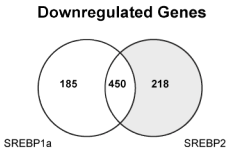

TFs associated with commonly downregulated genes

Object name	Actual	n	R	N	Expected	Ratio	p-value	z-score
E2F4	48	402	311	17765	7.038	6.821	2.55E-26	15.76
E2F1	58	402	562	17765	12.72	4.561	1.78E-22	13.05
c-Myc	96	402	1682	17765	38.06	2.522	6.64E-18	9.983
ZNF143	22	402	134	17765	3.032	7.255	3.16E-13	11.06
E2F3	14	402	77	17765	1.742	8.035	1.70E-09	9.413
HIF1A	24	402	412	17765	9.323	2.574	2.47E-05	4.919
HNF4-alpha	80	402	2407	17765	54.47	1.469	0.0002	3.764

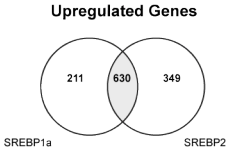

TFs associated with all downregulated genes

Object name	Actual	n	R	N	Expected	Ratio	p-value	z-score
E2F4	76	740	311	17765	12.95	5.867	2.41E-37	18.05
E2F1	85	740	562	17765	23.41	3.631	1.34E-25	13.21
c-Myc	157	740	1682	17765	70.06	2.241	6.38E-23	11.15
ZNF143	35	740	134	17765	5.582	6.27	9.26E-19	12.77
p53	87	740	916	17765	38.16	2.28	3.68E-13	8.294
HIF1A	38	740	412	17765	17.16	2.214	4.10E-06	5.199
p21	2	740	3	17765	0.125	16	0.0051	5.418

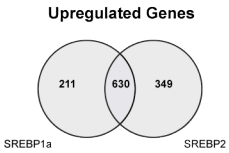

Figure 3-17: Transcription factor enrichment analysis of genes significantly downregulated by activation of ER.mSREBP1a and ER.mSREBP2.
Tables show a selection of transcription factors (TFs) that are significantly associated with genes present within each of the sub-sets highlighted in grey in the corresponding Venn diagrams. r: number of targets in the dataset regulated by the chosen transcription factor; n: number of network objects in the dataset; R: number of targets in the complete database regulated by this TF; N: total number of gene-based objects in the complete database; mean: mean value for hypergeometric distribution (n*R/N); z-score: z-score ((r-mean)/sqrt(variance)); p-value: probability to have the given value of r or higher (or lower for negative z-scores).

3.5 Discussion

Glioblastoma multiforme is a cancer type that is associated with hyperactivation of the PI3K/Akt pathway and SREBP has been shown to play a role in tumourigenesis in this cancer type (Guo et al., 2009b). Despite many direct transcriptional targets being identified for the SREBP family of transcription factors in studies involving genetically manipulated mouse models, relatively little is known about the transcriptional signature of SREBPs in cancer cells. Using a 4-hyrdoxy tamoxifen inducible system, human U87 glioblastoma cells were used to study the transcriptional response to activation of mature SREBP1a and SREBP2.

Activation of mSREBP1a or mSREBP2 induced expression of the known SREBP target genes FASN and ACLY, as well as increasing activity of the pSRE-luciferase reporter, demonstrating that these constructs were transcriptionally active. In order to ensure that expression levels of the exogenous constructs were consistent between the two cell lines, the exogenous proteins were detected by Western blotting using an anti-ER antibody (Figure 3.2). Although this suggests that the expression levels are indeed similar, use of the ER antibody does not allow comparisons to be made between expression levels of the exogenous constructs with those of the endogenous proteins. Since it is the activity of these overexpressed constructs that is inducible, it would be more appropriate to compare the transcriptional activity of the exogenous proteins with that of the endogenous transcription factors. Indeed, activation of ER.mSREBP1a for 24 hours resulted in a 12-fold increase in FASN expression, as detected by RT-QPCR (Figure 3.5B), whilst activation of ER.mSREBP2 increased FASN expression by eight-fold. In comparison, U87 cells cultured in 1% LPDS for 24 hours (a condition which is known to activate the endogenous SREBP transcription factors) showed an eight fold induction of FASN mRNA levels (Figure 4.10C), indicating that the transcriptional activities of ER.mSREBP1a and ER.mSREBP2 are similar to the endogenous proteins. This is an important consideration when evaluating the physiological relevance of the gene expression microarray data presented in Figures 3.9-3.17 (discussed further on in this section).

In addition, activation of ER.mSREBP1a, but not ER.mSREBP2, resulted in a mobility shift in the protein as detected by Western blotting (Figure 3.2). This may indicate post-translational modification of mSREBP1a in response to activation by 4-OHT. Posttranslational modifications of both SREBP1 and SREBP2, including phosphorylation, have been reported (Bengoechea-Alonso and Ericsson, 2009; Bengoechea-Alonso and Ericsson, 2006; Bengoechea-Alonso et al., 2005; Giandomenico et al., 2003; Hirano et al., 2003; Kotzka et al., 2004; Lu, 2006; Punga, 2006; Sundqvist et al., 2005; Sundqvist and Ericsson, 2003; Yellaturu et al., 2009). Furthermore, GSK3-dependent phosphorylation of mSREBP1a on serines 426 and 434 and threonine 430 results in decreased stability of the protein via Fbw7-dependent proteasomal degradation (Bengoechea-Alonso and Ericsson, 2009; Sundqvist et al., 2005). Transcriptional activity of mSREBP1 has been shown to induce its degradation and GSK3-dependent phosphorylation of mSREBP1 increases upon binding of the active transcription factor to promoter elements of its target genes (Punga, 2006; Sundqvist and Ericsson, 2003). Phosphorylation of mSREBP1a could therefore occur in response to its 4-OHT-dependent activation as a direct result of its nuclear translocation and subsequent increased transcriptional activity. Fbw7 has also been reported to regulate the stability of mSREBP2 through GSK3-targeted phosphorylation of serines 432 and 436 (Sundqvist et al., 2005), although no mobility shift of mSREBP2 could be observed upon 4-OHT-dependent activation in the experiment presented here (Figure 3.2).

Activation of either transcription factors resulted in a visible increase in LD staining (as detected by Nile Red staining, Figure 3.7), consistent with results described in mouse livers (Shimano et al., 1996). LD formation is associated with increased lipid storage, specifically of TAGs and cholesterol-esters. Activation of mSREBPs may therefore result in increased cellular TAG levels in U87 cells. It would be interesting to investigate the exact biochemical make-up of these lipid droplets, as differences in lipid species may reveal details about the exact role that SREBP isoforms have in LD formation. Furthermore, SREBP1c has been shown to regulate the expression of the novel lipid droplet protein CIDEA, a member of the cell death-inducing DNA fragmentation factor-α-like effector (CIDE) proteins (Wang et al., 2010). SREBP1c-

mediated expression of CIDEA in mouse liver results in increased lipid droplet formation (Wang et al., 2010). Interestingly, another member of the family, CIDEC, is regulated by SREBP1a or SREBP2 in the microarray presented here (Appendix: Table A3). CIDEC functions in LD formation by regulating LD enlargement (Keller et al., 2008; Puri et al., 2007). Therefore, it is possible that activation of SREBP in U87 cells increases expression of this LD protein, resulting in increased LD formation and TAG storage.

The ability of ER.mSREBP1a activation to induce *de novo* lipid synthesis was also investigated. It was found that activation of ER.mSREBP1a resulted in the increase in glucose-, pyruvate- and acetate-dependent lipid synthesis (Figure 3. 8). This is consistent with the role of SREBP1 in regulating expression of genes required for fatty acid synthesis. It is interesting to note that the fold change of induction differed depending on the precursor. Glucose and pyruvate incorporation into the lipid phase increased to a lesser extent than incorporation of acetate into the lipid phase. This may reflect the different entry points of each precursor into the lipid synthesis pathway. Glucose must first be metabolised to pyruvate, which then enters the TCA cycle. Citrate, a TCA cycle intermediate, is exported from the mitochondria by citrate transporter SLC25A1, an SREBP target gene. Citrate is then converted to acetyl-coA, the major precursor for both cholesterol and fatty acid synthetic pathways. Interestingly, cytosolic acetate can also be directly converted into acetyl-coA by the SREBP target gene ACSS2. This direct conversion of acetate to acetyl-coA could account for the increased incorporation of acetate-derived ^{14}C into the lipid phase. Both ACSS2 and SLC25A1 were upregulated in the microarray performed in this thesis (Appendix: Tables A1 and A4). The difference in incorporation of ^{14}C derived from the three precursors may also reflect SREBP1 target gene activation as most SREBP1 target genes lie within the mevalonate and fatty acid pathways. Therefore, activation of SREBP may result in an increase in flux through these lipogenic pathways, resulting in an increase in acetate-dependent lipid synthesis. The effects of activating mSREBP2 on *de novo* lipid synthesis were not investigated due to limited availability of labelled

metabolites. It would be interesting to examine whether activation of mSREBP2 results in the same increases in *de novo* lipid synthesis as mSREBP1a in these cells.

In order to identify SREBP-dependent transcriptional signatures in U87 human glioblastoma cells, a microarray gene expression analysis following activation of mSREBP1a or mSREBP2 was carried out. Activation of mSREBP1a and mSREBP2 resulted in the upregulation of known SREBP target genes involved in lipid metabolism, including FASN, ACLY, ACACA, ACACB, SCD, INSIG1, HMGCS1, HMGCR, LDLR and G6PD (Appendix: Table A1). The role of SREBPs in lipid synthesis in U87 cells was further confirmed by pathway and process enrichment analysis of the microarray data set. This showed that genes involved in lipid metabolism were significantly enriched following activation of ER.mSREBP1a or ER.mSREBP2.

Interestingly, activation of ER.mSREBP1a resulted in the upregulation of members of the fatty acid binding protein (FABP) family. Specifically, mSREBP1a significantly upregulated expression of FABP3, FABP6 and FABP7. mSREBP2 also upregulated FABP7 expression (Appendix: Table A2). The function of these genes is not fully understood (Schroeder et al., 1998). It has been described that the binding of FABPs to fatty acids facilitates their transport to different cellular compartments, including the nucleus (Mita et al., 2010; Schroeder et al., 1998). In addition, a role for FABP7 in modulating the activity of PPARs has been reported (Mita et al., 2010; Wolfrum et al., 2001). It is interesting to note that FABP7 is the brain specific isoform, and FABP7 increases migration of glioblastoma cells *in vitro* (Liang et al., 2005; Mita et al., 2010), and may be a prognostic marker in GBM patients (Liang et al., 2005). *In silico* analysis predicts the presence of SREs in the promoters of these genes (http://www.genecards.org). FABP3 has been shown to be upregulated by SREBP1a and SREBP1c in human myotubes (Rome et al., 2008), although to date no direct role for SREBP in the expression of FABP7 has been experimentally confirmed. FABPs may represent novel SREBP transcriptional targets, further extending the repertoire of SREBP function in the regulation of lipid metabolism.

In addition to regulation of lipid metabolism, other metabolic processes were also enriched within gene sets upregulated by mSREBP1a or mSREBP2, including glutathione metabolism and the cellular response to hypoxia and oxidative stress. Interestingly, genes associated with the above processes were significantly enriched within sets of genes activated by SREBP2. This suggests that SREBP2 could be involved in the hypoxic response of this cancer cell line. Association of SREBPs and the hypoxic response has been previously described. The fission yeast homologue of SREBP is known to function as an oxygen sensor (Hughes et al., 2005). Moreover, following microarray analysis of genes regulated by SREBPs in human skeletal muscle, SRE binding motifs were found to be significantly associated with transcription factor matrixes relating to hypoxia (Rome et al., 2008). Furthermore, HIF1α was associated with genes downregulated by SREBP2 in the microarray data presented in this thesis. This suggests that SREBP2 may reciprocally regulate genes regulated by HIF1α.

Long-term activation of mSREBP1a and mSREBP2 resulted in the decreased proliferation rates of U87 cells as assayed by Sulforhodamine B staining (cell mass) measured over time (Figure 3.3). In addition, activation of mSREBP1a or mSREBP2 resulted in the loss of cyclin A protein as detected by Western blotting (Figure 3.4. These data indicate that activation of SREBPs in U87 cells leads to decreased proliferation and possibly cell cycle arrest. This is also consistent with gene expression data obtained from the microarray analysis following activation of ER.mSREBP1a or ER.mSREBP2 for 6 or 24 hours. Pathway and process enrichment analysis revealed that a significant number of genes downregulated in response to SREBP activation are involved in cell cycle progression (Figures 3.14, 15 and 16). In addition, transcription factor analysis revealed an association of downregulated genes with members of the E2F family of transcription factors (Figure 3.17). The E2F factors regulate the transcription of genes required for cell cycle progression, including cyclin A (Schulze et al., 1995). Furthermore, activation of SREBPs downregulated expression of two E2F family members. ER.mSREBP1a activation decreased expression of E2F2, whilst ER.mSREBP2 activation decreased E2F4 expression (Appendix: Table A4). These data strongly suggest that prolonged activation of SREBPs results in the downregulation of positive cell cycle regulators. Interestingly, regulation of the cell cycle shares some

regulatory pathways with metabolism (Fritz and Fajas, 2010) and E2Fs have been implicated in lipid metabolism through their role in regulating PPAR γ activity (Fajas et al., 2002). Furthermore, increased E2F activity in Rb-deficient cells causes increased expression of SREBP1c (Shamma et al., 2009). E2F binds directly to the promoter of SREBP1c, resulting in increased expression of prenyltransferases. This aberrant activation of prenyltransferases leads to enhanced isoprenylation and activation of N-Ras, resulting in N-Ras induced cellular senescence in Rb-deficient cells (Shamma et al., 2009).

In addition, expression of the cell cycle inhibitor p21 (CDKN1A) was significantly upregulated following activation of both ER.mSREBP1a and ER.mSREBP2 for 24 hours (Appendix: Table A4). This is consistent with data published by Nakakuki and colleagues, who showed that ectopic SREBP1a could completely inhibit cell growth in chinese hamster ovary (CHO) cells by causing the accumulation of the cell cycle inhibitors p27, p21 and p16 (Nakakuki et al., 2007). However, they did not observe the induction of p21 in response to ectopic expression of SREBP2. Induction of SREBP1a or SREBP2 has been shown to lead to growth arrest via expression of p21 in Saos-2 cells (Inoue et al., 2005). In addition, the p21 promoter, along with several other key cell cycle regulators, is occupied by SREBP1 in HepG2 cells in response to insulin signalling (Reed et al., 2008).

Interestingly, SREBPs have also been shown to be associated with positive cell cycle regulation. mSREBP1a and mSREBP1c are phosphorylated by Cdk1/ Cyclin B in mitotic cells and this phosphorylation results in the stabilisation of the mature transcription factors (Bengoechea-Alonso and Ericsson, 2006; Bengoechea-Alonso et al., 2005). Furthermore, the cell cycle regulator host cell factor C-1 (HCFC1) has been shown to be an SREBP target gene (Motallebipour et al., 2009), although HCSC1 was not regulated by SREBPs in the U87 cells. This suggests that the contribution of SREBPs to cell cycle control is complex, and may vary depending on cell type.

SREBPs regulate target gene transcription through cooperation with other transcriptional regulators, most notably SP1 and NF-Y (Dooley et al., 1998; Jackson et al., 1998; Sanchez et al., 1995). Interestingly, Lu and Archer reported that SP1 positively regulates expression of CDC25A (Lu and Archer, 2010), a phosphatase required for G_1/S-phase transition. Activation of mSREBP1a for 6 or 24 hours, as well as activation of mSREBP2 for 24 hours, resulted in the downregulation of CDC25A in the microarray presented in this thesis (Appendix: Table A4). CDC25A contains an SP1 binding site within its promoter (Lu and Archer, 2010). Transcription factor enrichment analysis also identified SP1 as being associated with downregulated genes (Figure 3.17), suggesting that SREBP could be negatively regulating SP1 activity to inhibit transcription of genes required for cell cycle progression. In addition, association with the transcriptional regulator NF-Y was enriched within both up- and downregulated genes in the microarray presented here (Figures 3.13 and 3.17, respectively). These data are in keeping with the observations of Reed and colleagues, who showed a high degree of overlap between SREBP1 target-gene promoters occupied by SP1 and/or NF-Y (Reed et al., 2008). They suggested that the regulatory circuit of SREBP1, SP1 and NF-Y is highly interconnected and that the binding sites of all three transcription factors are found within promoters for other transcription factor genes, suggesting that these factors can regulate gene expression in an indirect manner (Reed et al., 2008).

Taken together, these data support the conclusion that SREBPs not only regulate genes required for fatty acid and cholesterol biosynthesis, but also other aspects of lipid metabolism, such as lipid droplet formation. In addition, SREBPs play a role in other crucial cellular processes, including cell cycle regulation, redox regulation and cellular stress response (Figure 3.18).

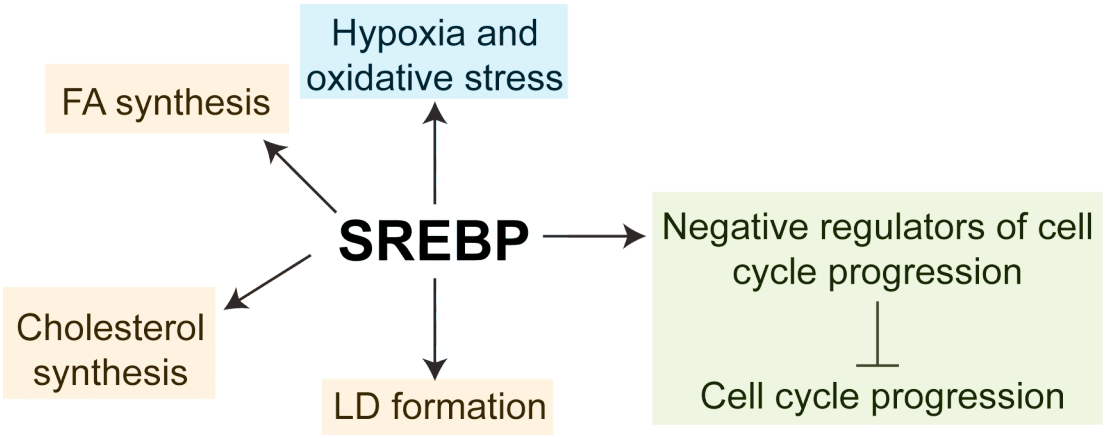

Figure 3-18: Summary of the function of genes regulated by SREBPs as identified by the gene expression microarray analysis presented in this thesis.
Groups of genes representing different cellular processes were identified, including processes already known to be regulated by SREBPs (FA biosynthesis, cholesterol biosynthesis, cell cycle progression) as well as novel processes (hypoxia and oxidative stress, lipid droplet formation).

Chapter 4. The role of SREBPs in the hypoxic response of cancer cells

4.1 Introduction

Many cancers reactivate *de novo* fatty acid biosynthesis and the role of the lipogenic phenotype in cancer has been reviewed (Menendez and Lupu, 2007). Numerous reports have shown that SREBP target genes are upregulated in cancer cells. Overexpression of FASN is a frequent occurrence in breast and prostate cancers and is associated with poor prognosis (Kuhajda et al., 1994; Swinnen et al., 2000a; Swinnen et al., 2000b; Yoon et al., 2007). In addition, SREBP participates in the upregulation of FASN in colorectal neoplasia (Li et al., 2000). Genetic depletion of SCD has been shown to reduce breast cancer cell proliferation (Luyimbazi et al., 2010) and overexpression of SCD has been observed in prostate cancer (Fritz et al., 2010). A role for SREBP in tumourigenesis in glioblastoma multiforme (GBM) has also been reported (Guo et al., 2009a; Guo et al., 2009b).

Most solid tumours exhibit regions of poor oxygenation and hypoxia is considered to be a key regulatory factor in tumour growth (Harris, 2002). Although prolonged hypoxia leads to cell death in both non-cancer and cancer cells, cancer cells have adapted certain metabolic pathways in response to hypoxia in order to promote their survival (Harris, 2002). Interestingly, SREBPs have been implicated in oxygen sensing mechanisms in budding yeast (Hughes et al., 2005; Lee et al., 2009) and a number of reports suggest that SREBPs and/ or their target genes are involved in the hypoxic response of tumour cells (Furuta et al., 2008; Yoshii et al., 2009). However, the exact role of SREBPs in the hypoxia response of cancer cells is not known. The cancer type glioblastoma multiforme (GBM) is associated with hyper-activation of the PI3K/ Akt signalling pathway and this tumour type shows extensive hypoxic regions (Evans et al., 2004; Parsons et al., 2008). This chapter describes the investigation of the role of SREBPs in the hypoxic response of the human glioblastoma U87 cell line.

4.2 Hypoxia induces differential expression of SREBP isoforms and their target genes

4.2.1 Expression of SCD and fatty acid binding proteins is increased under hypoxia whilst FASN expression is decreased

In order to investigate the role that SREBPs may play in the hypoxic response of the human glioblastoma U87 cell line, cells were cultured in normoxic (20% O_2) or hypoxic conditions (<0.5% O_2) for a period of 24 hours. RNA from these cells was extracted and used in subsequent RT-QPCR analyses. Expression of SREBP target genes within different functional groups was investigated. Unexpectedly, SREBP target genes showed differential expression in hypoxia. In hypoxic conditions, genes required for fatty acid and cholesterol biosynthesis (FASN, ACLY, ACACA, ACACB, and HMGCR) were significantly downregulated, with the exception of HMGCS1, which showed no change in mRNA expression levels (Figure 4.1A). In contrast, it was found that expression of SCD, the enzyme that catalyses the desaturation of SFA, was upregulated in hypoxic conditions. Expression of the fatty acid binding proteins FABP3 and FABP7 were also increased in response to hypoxia (Figure 4.1B). Induction of the HIF1α target gene, VEGFA, was used as positive control for hypoxic conditions (Figure 4.1C).

4.2.2 Expression of SREBF1c mRNA, but not SREBF1a or SREBF2, is decreased in hypoxia

Since SREBP target genes exhibited differential expression in response to hypoxic conditions, it was hypothesised that different SREBP isoforms may play a role in the transcriptional regulation of these target genes. Therefore, the expression of the three SREBP isoforms was investigated. Antibodies recognising SREBP1 cannot distinguish between SREBP1a and SREBP1c. Therefore, the expression of SREBF1a and SREBF1c (as well as SREBF2) mRNA was measured using isoform-specific RT-QPCR. Primers from the Quantitect system detecting SREBF1 bind the exon boundary between exons 1a and 2a. Primers that bind specifically to SREBF1c mRNA were designed. These were chosen to be complementary to exon 1c, which is not present in sequences within SREBF1a mRNA (see Figure 1.2, introduction). Therefore, the

expression of SREBF1a and SREBF1c mRNA could be individually examined. Interestingly, the mRNA expression in response to hypoxia was different for all three isoforms. Following 24 hours of culture in hypoxic conditions, mRNA expression of SREBF1a remained unchanged, whereas SREBF1c mRNA was significantly decreased (Figure 4.2A). In contrast, expression of SREBF2 mRNA was increased in response to hypoxia (Figure 4.2A), although it did not reach statistical significance. In order to investigate whether loss of SREBF1c mRNA occurred in a time-dependent manner, cells were cultured in hypoxia for the times indicated in Figure 4.2 B. RT-QPCR analysis revealed that SREBF1c mRNA expression decreased after 2 hours in hypoxic conditions, and this continued to decrease over time, suggesting that loss of SREBP1c may lead to the decreased expression of the SREBP target genes examined in Figure 4.1.

Taken together, these gene expression data indicate that the loss of SREBP1c may account for the loss of expression of genes involved in fatty acid synthesis and cholesterol biosynthesis. In addition, the maintenance of SREBF1a expression together with the increased expression of SREBF2 may play a role in the increased expression of SCD, FABP3 and FABP7 that was observed in response to hypoxia.

4.2.3 Hypoxia reduces nuclear accumulation of SREBP1

As described in section 1.3 (Introduction), SREBPs are produced as inactive precursors and undergo a two-step proteolytic cleavage process in the Golgi. The cleaved N-terminal fragment (mature SREBP: mSREBP) translocates to the nucleus, where it binds to the promoters of target genes as a homodimer. Nuclear accumulation of mSREBPs is thus an indicator of their activation, and should reflect increased transcriptional activity. In order to determine whether the changes in mRNA expression observed above also resulted in changes in SREBP protein, U87 cells grown in hypoxia for 24 hours were subjected to nuclear fractionation to enrich nuclear mSREBPs. The nuclear extracts contain only disrupted nuclei while cytoplasmic material and membrane components are found in the supernatant fraction. Whole cell lysates were prepared in parallel to assay for expression of FASN as a positive control of SREBP

activity. To enhance the formation of mSREBP, cells were grown in 1% lipoprotein deficient serum (LPDS). This serum condition starves cells of sterols and results in the nuclear accumulation of active mSREBPs. In addition, in order to prevent proteasome-dependent degradation of the mSREBPs in the nucleus, cells were treated with the proteasome inhibitor MG-132 for 1.5 hours prior to lysis, as is standard in protocols for the analysis of mSREBPs.

As expected, culture in medium containing 1% LPDS increased nuclear accumulation of mSREBP1 in U87 cells (Figure 4.3 A). It is interesting to note that the mature SREBP1 protein was detected as a doublet. The lower band was induced by 1% LPDS and completely lost in hypoxia, whilst although the upper band was reduced in hypoxic conditions, it was not lost completely. When taken together with the mRNA expression data shown in Figure 4.2, this may indicate that the lower band could correspond to SREBP1c, whilst the upper band may correspond to SREBP1a. SREBP2 was not detectable in the supernatant fraction using the SREBP2 antibody (clone 1C6) in U87 cells under these conditions. In addition, the epitope lies in the C-terminal of SREBP2, making it impossible to detect the mature nuclear protein with this antibody. As a positive control of hypoxic conditions, HIF1α was detected in the nuclear extract. HIF1α stabilisation was not affected by lipoprotein deficient serum (Figure 4.3 A). It should be noted that HIF1α was detectable in the normoxia samples, most likely due to the treatment of the cells with the proteasome inhibitor MG-132 which causes the stabilisation of HIF1α protein in normoxic conditions.

Detection of full-length precursor protein (flSREBP1) in the supernatant fraction revealed that flSREBP1 was induced by culturing cells in 1% LPDS and that it was completely lost in response to oxygen deprivation (Figure 4.3 B). Analysis of FASN expression in whole cell lysates showed that hypoxia reduces FASN in these conditions. However, culture of cells in 1% LPDS still increased FASN expression when compared to levels in cells cultured in 10% FCS (Figure 4.3C).

4.2.4 Hypoxia decreases expression of SCAP mRNA, but not protein

Since SREBPs can transcriptionally regulate their own promoters (Horton et al., 2003), hypoxia may result in a reduction in SREBP processing, which could in turn lead to a reduction in SREBF mRNA over a prolonged period. SCAP is required for cleavage of the full-length SREBPs into the active mature transcription factors as it regulates ER-Golgi translocation of SREBPs (Nohturfft et al., 2000; Sakai et al., 1997). Therefore, the effect of hypoxia on SCAP expression was investigated. Interestingly, SCAP mRNA expression was significantly reduced in cells that were cultured in hypoxia for 24 hours (Figure 4.4 A). This change in expression in hypoxic conditions was then analysed over time. A reduction in SCAP mRNA was not observed until cells had been exposed to hypoxic conditions for 24 hours (Figure 4.4 B). Surprisingly, when protein levels were analysed, there was no reduction in SCAP protein over time. (Figure 4.4 C). These data suggest that SCAP has a relatively long half-life, as loss of mRNA does not result in immediate loss of protein. The maintenance of SCAP protein levels suggests that the loss of mSREBP1 in hypoxic cells is not due to low SCAP expression in cells cultured in hypoxic conditions.

4.2.5 Activation of exogenous SREBP1a and SREBP2 is sufficient to drive expression of SREBP-target genes down-regulated in hypoxia

Since SREBP1 protein is lost in hypoxia and selected SREBP target gene expression is downregulated in hypoxic conditions, it was then asked whether exogenous SREBP can induce expression of these genes under hypoxia. The U87 ER.mSREBP1a and ER.mSREBP2 cell lines described in chapter 3 were grown in hypoxia for 24 hours in the presence or absence of 4-OHT. Total RNA was extracted and used for RT-QPCR analysis (Figure 4.5A). Activation of either ER.mSREBP1a or ER.mSREBP2 in hypoxia for 24 hours was sufficient to induce the expression of FASN, ACLY, ACACA, and HMGCR; target genes that were downregulated in Figure 4.1. In addition, induction of ER.mSREBP1a or ER.mSREBP2 increased expression of HMGCS1 in hypoxia. However, expression of all genes was still slightly lower in the hypoxic cells (Figure 4.5A), suggesting decreased transcriptional activity of the exogenous mSREBPS in hypoxic cells. Alternatively, the overall activity of the promoter may be reduced in hypoxia.

When the mRNA expression of the HIF1α target gene VEGFA was analysed as a positive control for hypoxic conditions, it was found that activation of mSREBP1a or mSREBP2 decreased VEGFA expression in normoxia (Figure 4.5 B). This is consistent with a published report showing that overexpression of exogenous SREBP suppresses VEGFA promoter activity (Motoyama et al., 2006). However, activation of mSREBP1a and mSREBP2 in hypoxia resulted in a slight increase in VEGFA expression compared to the EV control. This could indicate that SREBPs influence the expression of a canonical HIF1α target in hypoxic conditions.

4.2.6 SREBP1 and SREBP2 are both required for hypoxia-induced expression of FABP7

Since the expression of the SREBP target genes SCD, FABP3 and FABP7 was induced in hypoxic conditions, it was next investigated whether SREBPs are indeed required for their induction in hypoxia. In addition, the role of HIF1α in the hypoxia-dependent induction of SCD, FABP3 and FABP7 was examined. Pools of small interfering RNAs (siRNAs) targeting HIF1α, SREBP1, or SREBP2 were transiently transfected into U87 cells. Non-targeting siRNA was used as a control. Silencing was allowed to establish for 96 hours before cells were transferred to hypoxic conditions for a further 24 hours. Total RNA was then extracted and used for RT-QPCR analysis. Silencing of SREBP1, SREBP2 and HIF1α reduced normoxic expression of SCD (Figure 4.6 A), consistent with SCD expression being regulated by these transcription factors. Depletion of SREBP1 and HIF1α in hypoxia reduced the expression of SCD to basal normoxic levels (Figure 4.6 A), suggesting a role for these transcription factors in the hypoxia-dependent induction of both genes. However, silencing of SREBP2 did not have an effect on SCD and FABP3 expression in hypoxia (Figure 4.6 A). Silencing of HIF1α slightly decreased FABP7 mRNA levels in both oxygen conditions compared to control. Unexpectedly, silencing of both SREBP1 and SREBP2 alone resulted in the inhibition of FABP7 expression in both normoxic and hypoxic cells, suggesting that both isoforms are required for FABP7 expression. This gene may therefore represent a novel class of SREBP target gene, where both SREBP isoforms are acting together to induce FABP7 expression.

Although the hypoxia-dependent induction of SCD and FABP3 was not completely blocked in SREBP1 or HIF1α depleted cells, this may be due to the remaining expression of the transcription factors, since complete silencing was not achieved (Figure 4.7 B). However, it cannot be ruled out that other transcriptional regulators may be involved.

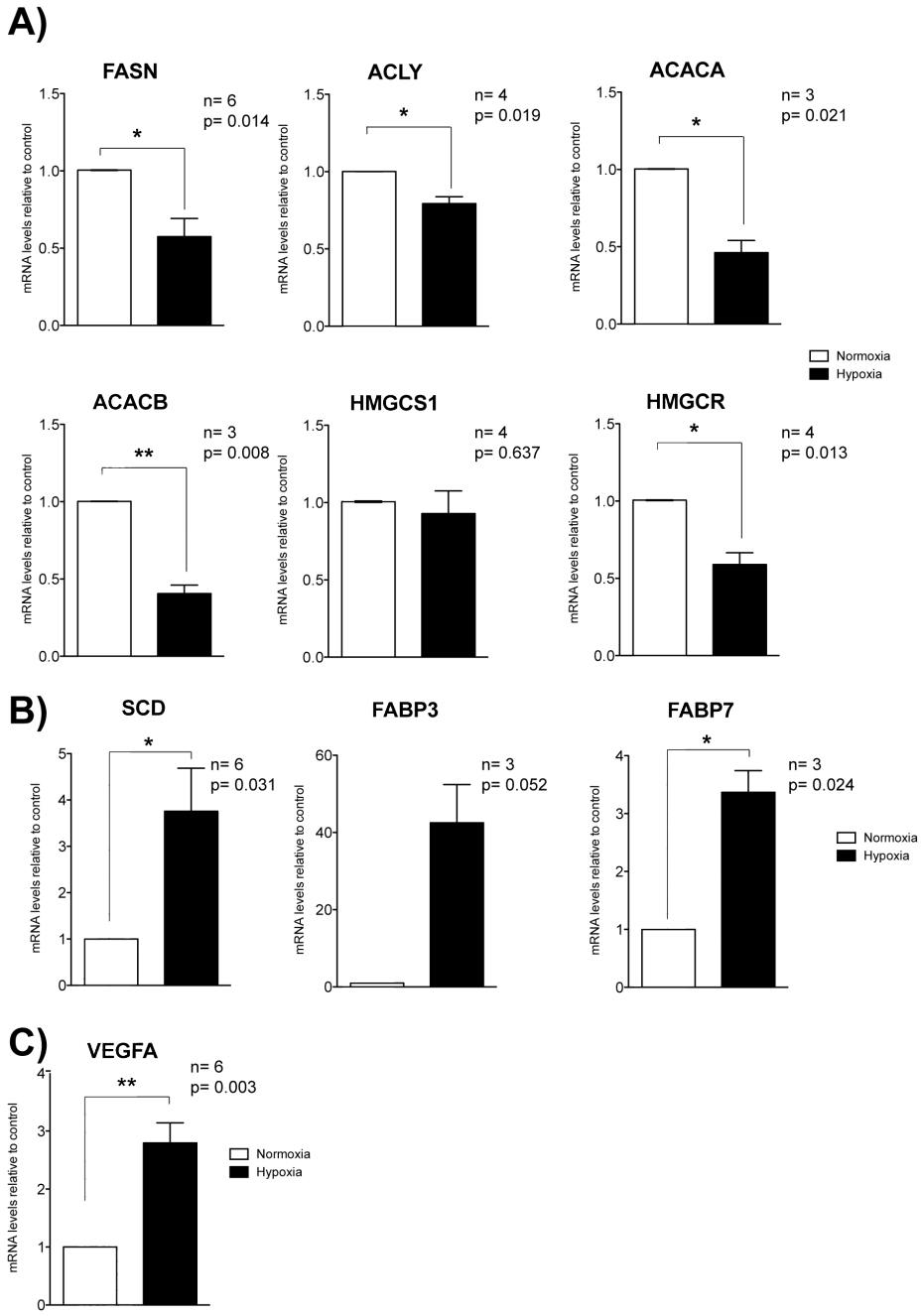

Figure 4-1: Hypoxia induces differential SREBP target-gene expression.
U87 cells were grown in normoxia or hypoxia for 24 hours and total RNA was extracted. mRNA levels of several SREBP target genes were measured using RT-QPCR and normalised to β actin as a loading control. Data shown represents the average of at least three independent biological replicates ± SEM. n numbers for each gene are given and p values were calculated using paired student's t tests. Asterisks indicate statistical significance (*: <0.05, **:<0.005). A) Genes required for fatty acid and cholesterol biosynthesis are down-regulated in hypoxia. B) Genes involved in the fate of fatty acids are up-regulated in hypoxia C) The HIF1α target VEGFA is shown as a positive control for hypoxic conditions.

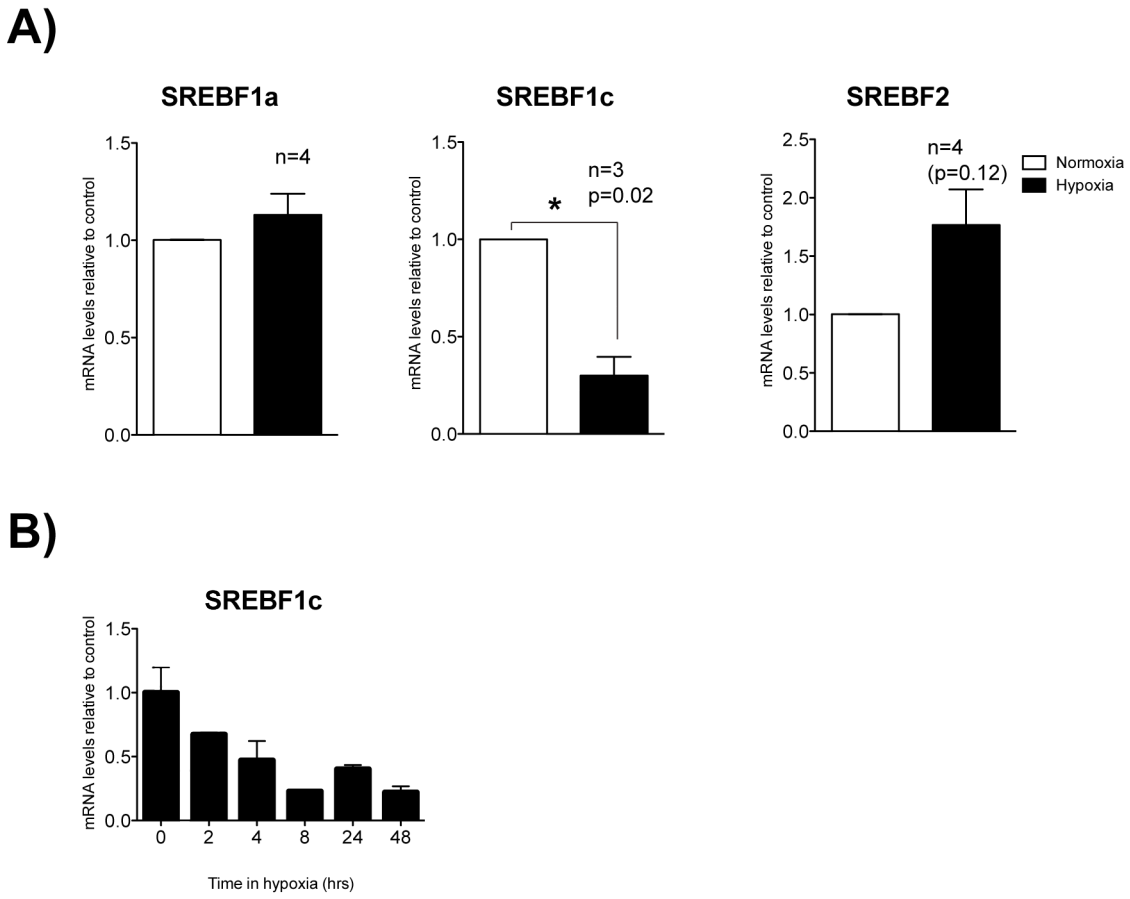

Figure 4-2: Hypoxia leads to a loss of SREBF1c mRNA.
(A) U87 cells were grown in normoxia or hypoxia for 24 hours. RNA was extracted and used for RT-QPCR analysis of SREBF1a, SREBF1c and SREBF2. Expression was normalised to β actin as a loading control. Data shown are the means of at least 3 independent biological replicates ± SEM. Asterisks indicate statistical significance. P values were calculated using a student's paired t test. (B) U87 cells were grown in hypoxia for the times indicated. mRNA levels of SREBF1c were analysed by RT-QPCR using β actin as a loading control. Data shown are the means of two biological replicates ± SD.

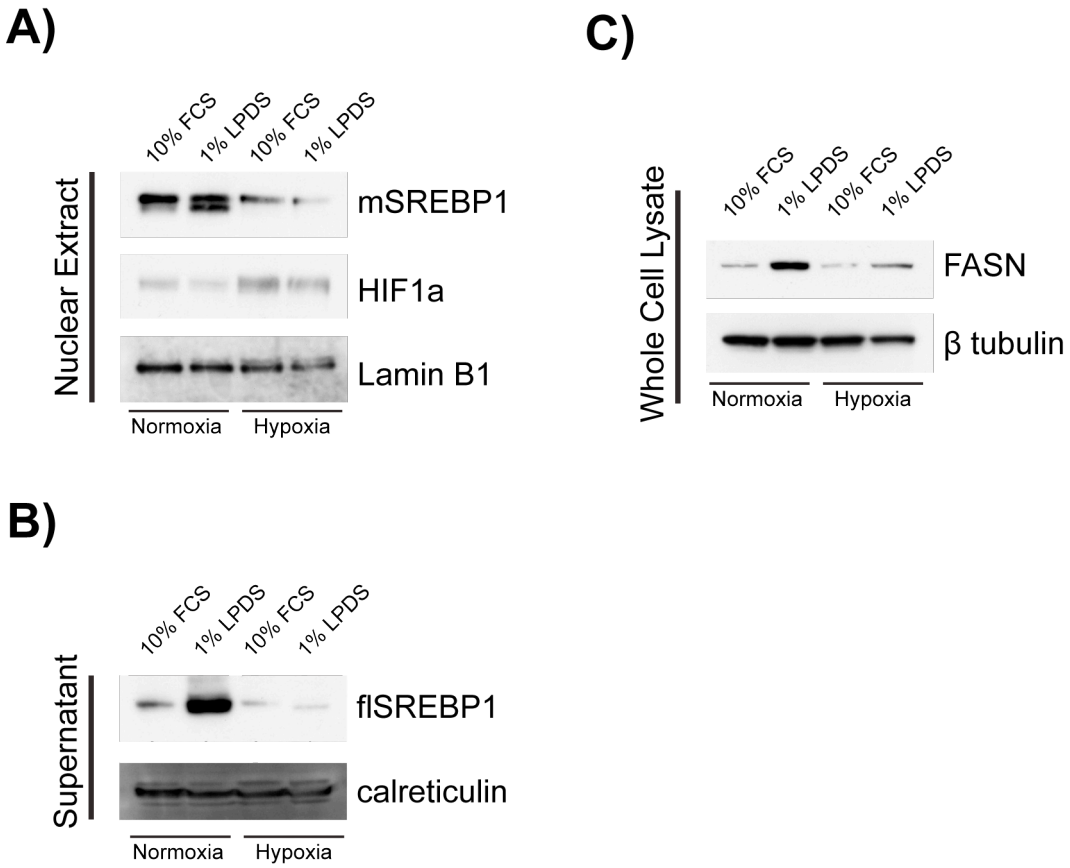

Figure 4-3: Hypoxia leads to a loss of SREBP1 protein.
U87 cells were grown in normoxia or hypoxia for 24 hours in either 10% FCS or 1% LPDS (lipoprotein deficient serum). Cells were harvested and subjected to nuclear fractionation. A) Nuclear extracts were analysed by Western blotting using antibodies against SREBP1 and HIF1α. Lamin B1 is shown as a nuclear specific loading control. B) The supernatant fraction containing the membranes and cytoplasm was analysed by Western blotting using antibodies against SREBP1. Calreticulin is shown as a membrane specific loading control. C) Whole cell protein lysates were harvested in parallel and analysed as described in A and B using an antibody against FASN. β tubulin is shown as a loading control.

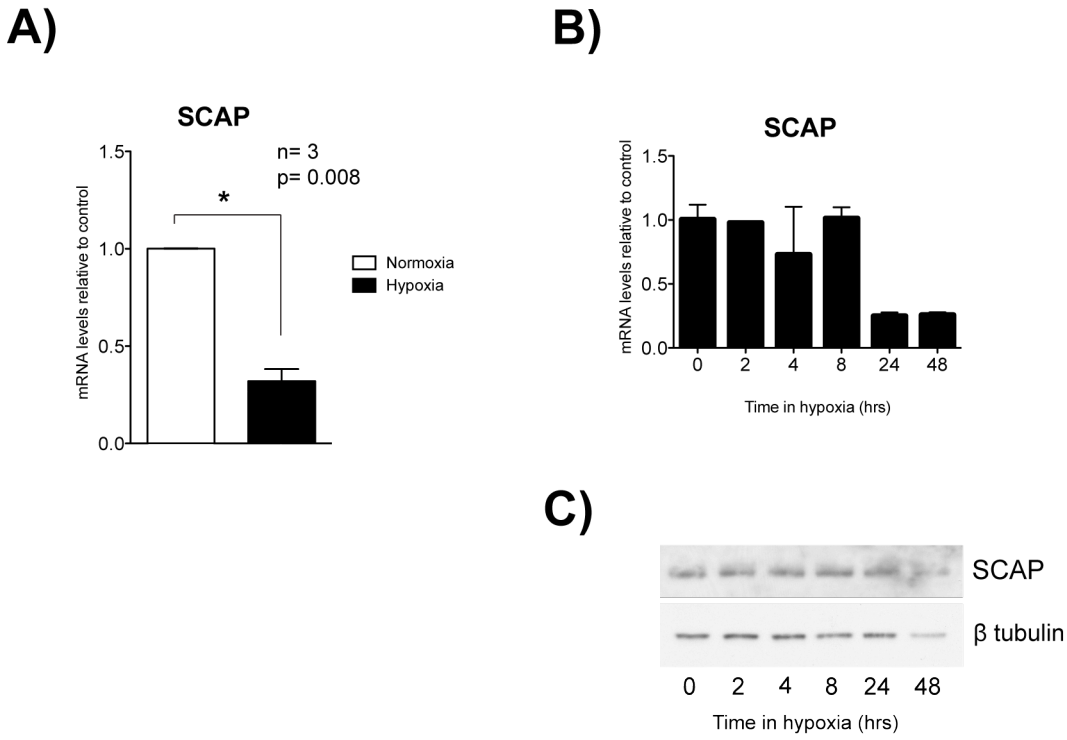

Figure 4-4: Hypoxia leads to a loss of SCAP mRNA but not protein.
(A) U87 cells were grown in normoxia or hypoxia for 24 hours and total RNA was extracted and subjected to RT-QPCR analysis. SCAP mRNA expression was normalised to β actin as a loading control (A). Data shown is the mean of three biological replicates ± SEM. (B) U87 cells were grown in hypoxia for the times indicated. SCAP mRNA was analysed using RT-QPCR and normalised to β actin as a loading control. Data shown are the means of two technical replicates ± SD. (C) Whole cell lysates extracted from cells grown in parallel to those in (B) were analysed by Western blotting for SCAP protein expression. β tubulin is shown as a loading control.

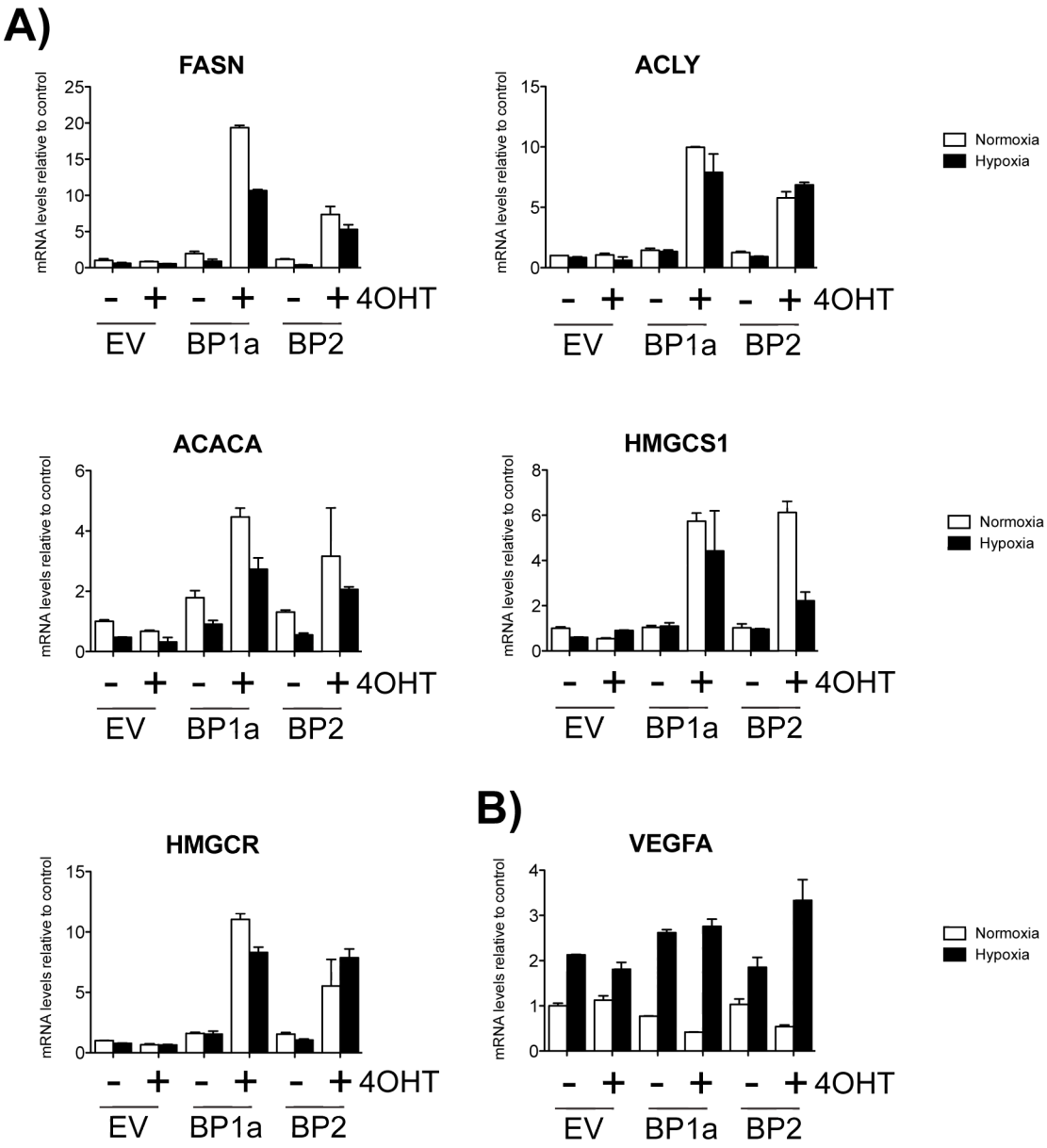

Figure 4-5: Activation of ER.mSREBP1a or ER.mSREBP2 is sufficient to drive SREBP-target gene expression in hypoxia.
U87-EV, U87-ER.mSREBP1a and U87-ER.mSREBP2 cells were grown in hypoxia or normoxia in the presence or absence of 4-hydroxytamoxifen (4OHT). Total RNA was extracted and mRNA expression levels of the SREBP target genes FASN, ACLY, ACACA, HMGCS1 and HMGCR was analysed using RT-QPCR (A). (B) mRNA expression of VEGFA was analysed as a control for hypoxic conditions. Data was normalised to β actin as a loading control. Data shown are the means of two technical replicates ± SD. EV: U87.EV; BP1a: U87.ER.mSREBP1a; BP2: U87.ER.mSREBP2. These data have been observed in two independent biological replicates.

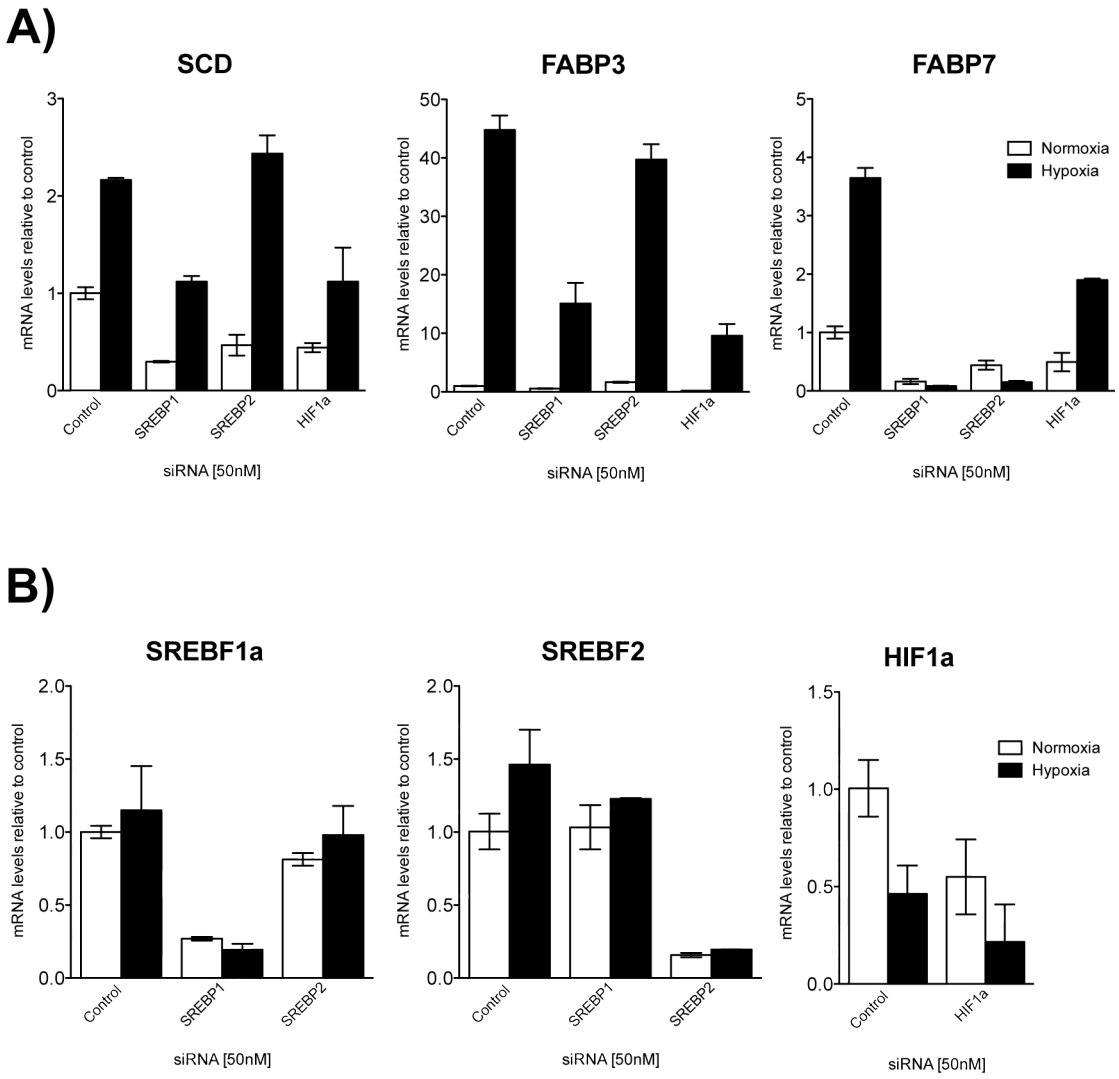

Figure 4-6: SREBP1 and SREBP2 are both required for expression of FABP7 in hypoxia. U87 cells were transiently transfected with pools of siRNA oligos targeting HIF1α, SREBP1, or SREBP2, alongside a non-targeting siRNA control. Silencing was established for 96 hours before cells were grown in hypoxia for 24 hours. Total RNA was extracted and subjected to RT-QPCR analysis. (A) mRNA expression of SREBP target genes SCD, FABP3 and FABP7. (B) mRNA expression of SREBF1a, SREBF2 and HIF1α was analysed as a control for gene silencing. mRNA expression levels were normalised to β actin as a loading control. Data shown are the means of two technical replicates ± SD. These data have been observed in two independent biological replicates.

4.3 Hypoxia activates the sterol regulatory element luciferase reporter

In order to further investigate the contribution that SREBPs play in the transcriptional regulation in hypoxia, the activity of the sterol regulatory element luciferase reporter (pSRE-luc, described in chapter 3) was examined under hypoxic conditions. U87 cells were transiently transfected with the pSRE-luc plasmid and a renilla luciferase control (pRL-SV40). Cells were then cultured in hypoxia for 24 hours. As a positive control of pSRE-luc activity, cells were cultured in 1% LPDS. In cells that were exposed to hypoxia, the luciferase activity of the SRE-reporter was significantly increased in both cells cultured in 10% FCS and those cultured in 1% LPDS (Figure 4.7). Cells cultured in 1% LPDS showed an overall increase in SRE-reporter activity compared to cells cultured in 10% FCS (Figure 4.7), indicating that the induction of the luciferase reporter was indeed being regulated under conditions known to activate SREBPs.

4.3.1 Activation of the SRE-luciferase reporter in hypoxia is partially dependent on SREBP1 and HIF1α

Since increased activation of the SRE-luciferase reporter was observed in hypoxia, the contribution of SREBP1, SREBP2 and HIF1α towards induction of this reporter activity was investigated. U87 cells were transiently transfected with pools of siRNA oligos targeting HIF1α, SREBP1, or SREBP2, as well as a non-targeting control. Silencing was allowed to establish for 48 hours before cells were transiently transfected with the pSRE-luc and pRL-SV40 plasmids. 24 hours later, cells were placed into hypoxia for a further 24 hours. Parallel cultures were grown in order to extract RNA to assay for gene silencing (Figure 4.8 B). As previously observed, hypoxia induced luciferase activity of the SRE-reporter in control-transfected cells (Figure 4.8 A). Silencing of HIF1α or SREBP1 decreased the overall activity of the reporter in normoxic conditions. However, silencing of SREBP2 alone did not affect SRE-reporter activity in either normoxic or hypoxic cells. Interestingly, silencing of SREBP1 or HIF1α alone reduced luciferase reporter activity in hypoxic conditions when compared to the basal activity observed in normoxic control-transfected cells. This is consistent with the mRNA

expression data observed for SCD (Figure 4.6 A), suggesting a role for HIF1α and SREBP1 in the hypoxia-dependent induction of the SRE-luciferase reporter.

Since SREBP1 and HIF1α are playing a role in the hypoxia-dependent induction of SRE-reporter activity, it was next asked whether there may be co-operation between SREBP1 and HIF1α under hypoxic conditions in U87 cells. In order to address this possibility, the effects of combined silencing of SREBP1 and HIF1α on SRE-reporter activity in hypoxia were investigated. U87 cells were transfected with siRNAs and cultured as described above. Preliminary results suggested that combined silencing of SREBP1 and HIF1α was not sufficient to block the hypoxia-dependent induction of luciferase activity, although combined silencing of both genes reduced the overall luciferase reporter activity when compared to silencing of either gene alone (Figure 4.9 A). Although these data could indicate that SREBP1 may be co-operating with HIF1α to induce SRE-luciferase reporter activity in hypoxic cells, the influence of other transcriptional regulators cannot be excluded.

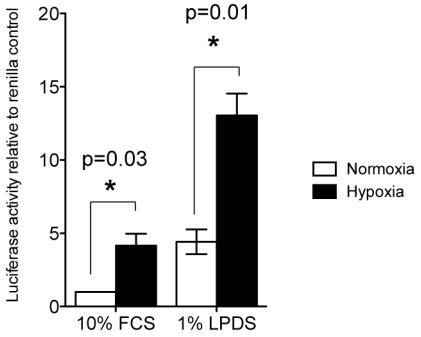

Figure 4-7: Hypoxia increases SRE luciferase reporter activity.
U87 cells were transiently transfected with the pSRE-luc reporter and pRL-SV40 renilla plasmids. Cells were grown in normoxia or hypoxia in 10% FCS or 1% LPDS (lipoprotein deficient serum) for 24 hours. Luciferase activity was measured and normalised to the renilla control. Data shown is the mean of four independent biological replicates ± SEM. Asterisks indicate statistical significance and p values from paired student's t tests are shown.

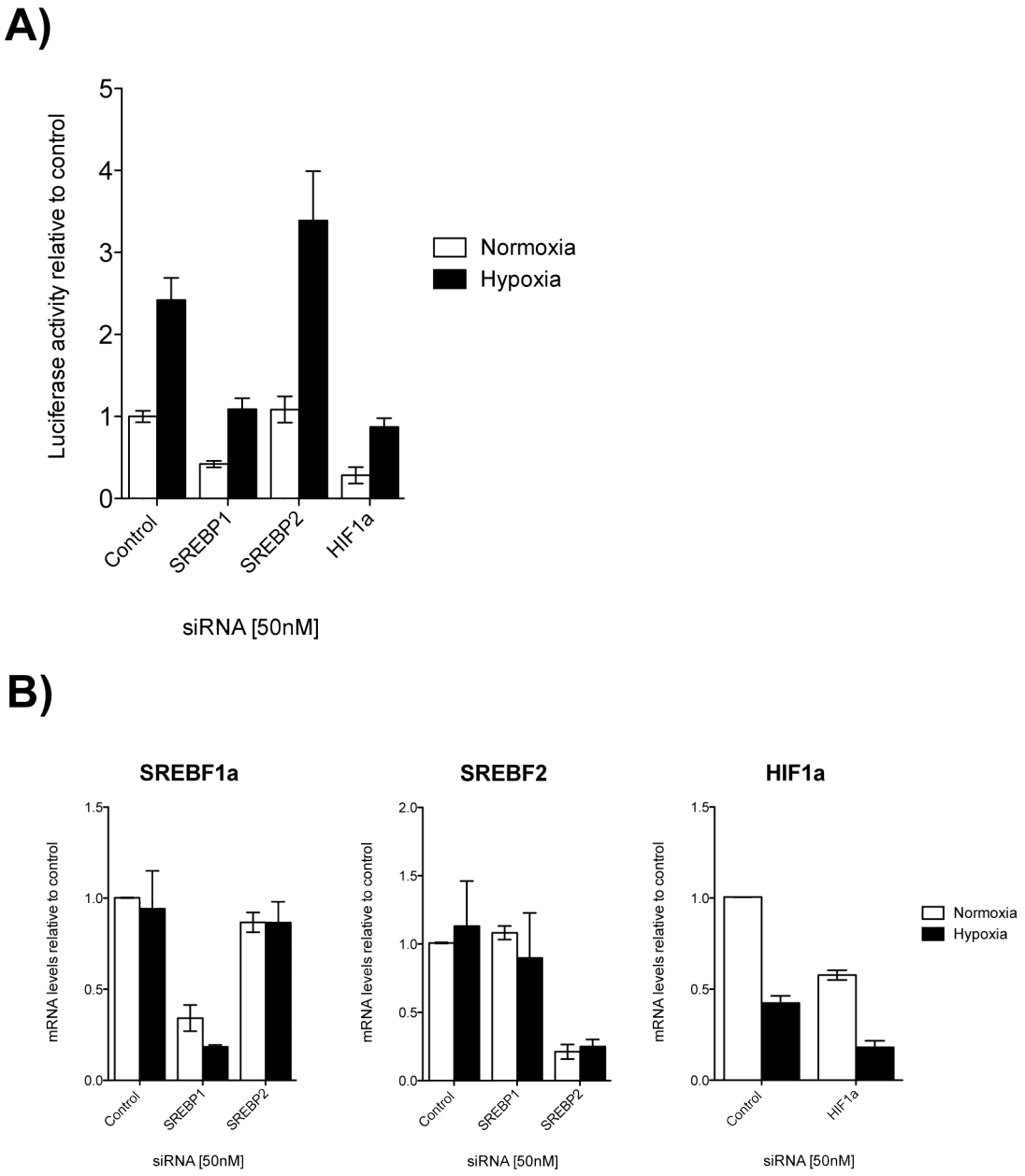

Figure 4-8: The hypoxia-dependent induction of the SRE luciferase reporter is partially dependent on SREBP1 and HIF1α.
U87 cells were transiently transfected with siRNAs targeting HIF1α, SREBP1, SREBP2, as well as a non-targeting control. 24 hours later, cells were transiently transfected with pSRE-luc and pRL-SV40 plasmids. Cells were grown in normoxia or hypoxia for 24 hours and luciferase activity was measured and normalised to the renilla control (A). Data shown are the means of two independent biological replicates ± SEM. (B) Gene silencing was confirmed in U87 cells that were transiently transfected with siRNAs as in (A) and grown in normoxia or hypoxia for 24 hours. mRNA expression levels of SREBP1, SREBP2 and HIF1α were normalised to β tubulin. Data shown is the mean of two biological replicates ± SEM.

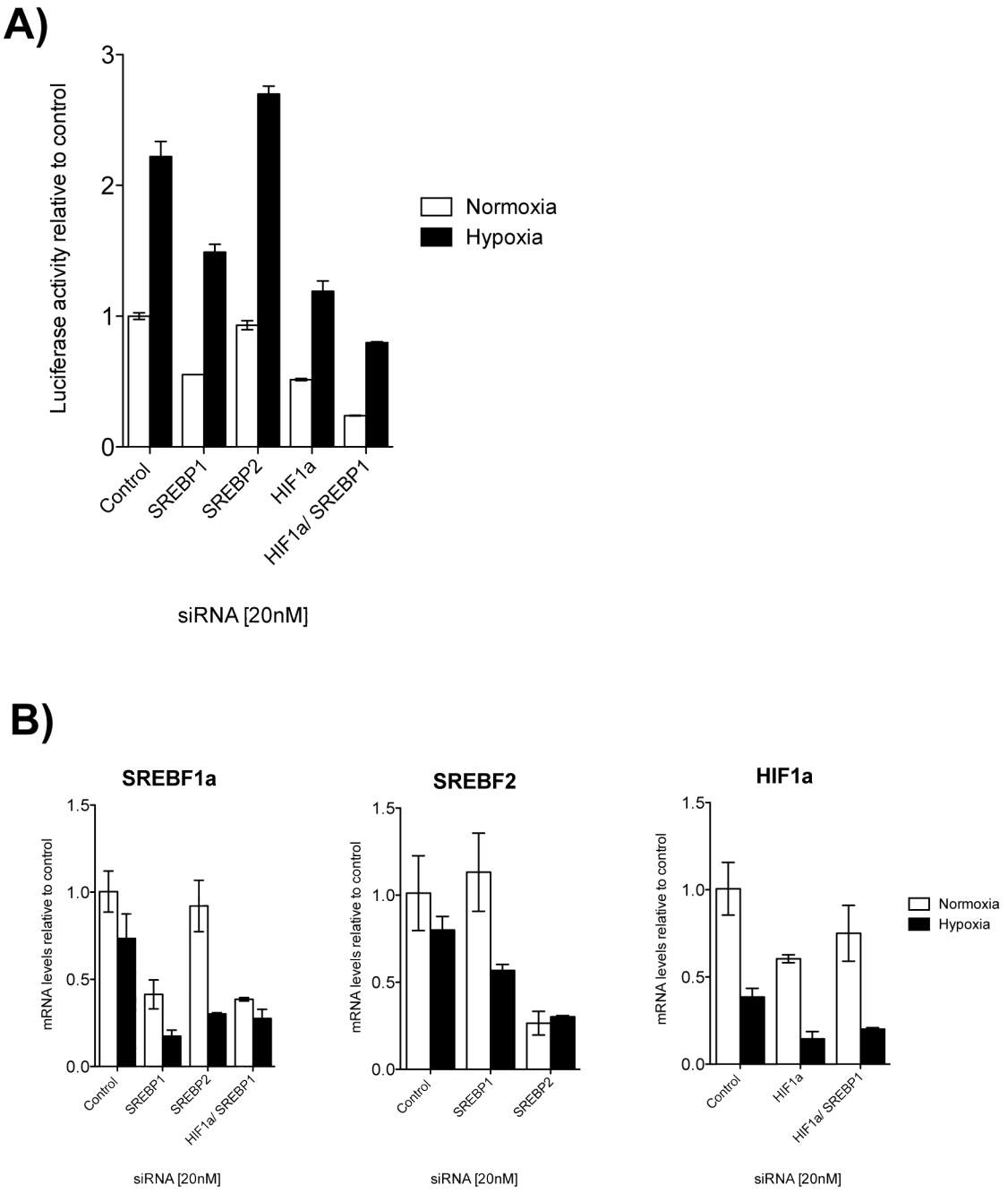

Figure 4-9: Combined silencing of SREBP1 and HIF1α partially reduce the hypoxia-dependent induction of SRE-reporter activity.
(A) U87 cells were transiently transfected with pools of siRNA oligos targeting SREBP1, SREBP2, and SREBP1 and HIF1a combined, as well as a non-targeting control. 24 hours later, cells were transiently transfected with pSRE-luc and pRL-SV40 plasmids. Cells were placed in hypoxia for 24 hours and luciferase activity was measured and normalised to the renilla control. Data shown are the means of three technical replicates ± SD. (B) Gene silencing was confirmed by RT-QPCR. mRNA expression levels of SREBF1a, SREBF2 and HIF1α were normalised to β actin. Data shown is the mean of two technical replicates ± SD.

4.4 Hypoxia alters *de novo* lipid synthesis

4.4.1 Lipoprotein deficient serum induces pyruvate-dependent *de novo* lipid synthesis in hypoxic cells

It has been shown that under hypoxic conditions, a number of metabolic changes and adaptations take place in cancer cells. Since expression of some SREBP target genes required for fatty acid and cholesterol biosynthesis was downregulated under hypoxia, it was hypothesised that *de novo* lipogenesis is reduced in hypoxic cells. Cells were cultured in hypoxia for 24 hours before being incubated with ^{14}C- labelled pyruvate or acetate for a further four hours. Incorporation of ^{14}C derived from pyruvate or acetate into the lipid fraction was measured and normalised to total cell mass. As a positive control, cells were cultured in 1% LPDS. Interestingly hypoxia had differential effects on pyruvate- and acetate-dependent lipid synthesis. Hypoxia significantly reduced the amount of pyruvate-dependent lipid synthesis in U87 cells cultured in both 10% FCS and 1% LPDS (Figure 4.10 A). A small, yet significant increase in acetate-dependent lipid synthesis was observed in hypoxic cells cultured in full serum (Figure 4.10 B), however, no change in lipid synthesis was observed in acetate-derived lipids in hypoxic cells cultured in 1% LPDS (Figure 4.10 B). These data suggest that a change in the carbohydrate intermediates used for lipid synthesis occurs in hypoxic conditions

Interestingly, cells cultured in 1% LPDS exhibited higher incorporation of carbohydrate-derived ^{14}C into the lipid phase than cells cultured in 10% FCS, regardless of the oxygen levels (Figure 4.10 A and B). This indicates that lipoprotein deficient conditions induce *de novo* lipid synthesis in U87 cells even in hypoxic conditions and is consistent with the induction of SREBP target genes FASN and ACACA in response to lipoprotein depletion (Figure 4.10 C).

4.4.2 Hypoxia regulates expression of PDK1, ACSS2 and PDK4

In order to gain more insight into the regulation of lipid synthesis in hypoxia in U87 cells, mRNA expression of the key enzyme that regulates pyruvate entry into the TCA cycle (PDK1) was analysed. In addition, expression of ACSS2, the enzyme that

synthesises cytoplasmic acetyl-CoA from acetate, was measured. Cells were cultured in hypoxia for 24 hours and total RNA was extracted and used for RT-QPCR analysis. As expected from the observed decrease in pyruvate-dependent lipid synthesis in hypoxic conditions, PDK1 was upregulated under hypoxia (Figure 4.11), indicating that entry of pyruvate into the TCA cycle is reduced in hypoxic cells. This is consistent with the findings of Kim and colleagues as well as Papandreou and colleagues who both demonstrated that hypoxia results in a HIF1α-dependent induction of PDK1 expression (Kim et al., 2006; Papandreou et al., 2006). However, there was no significant difference in PDK1 expression between cells cultured in 10% FCS or 1% LPDS. Levels of ACSS2 mRNA in hypoxic cells cultured in both 10% FCS and 1% LPDS (Figure 4.11) were reduced in a small, yet statistically significant manner. This indicates that increased acetate-dependent lipid synthesis is not due to increased ACSS2 expression under hypoxic conditions. Culture of cells in 1% LPDS significantly increased expression of ACSS2 when compared to cells cultured in 10% FCS (Figure 4.11). This increase correlates with the increase in acetate-dependent lipid synthesis observed in cells cultured in 1% LPDS (Figure 4.10 B). In contrast, expression of PDK4 was significantly reduced under hypoxia (Figure 4.11). Since PDK4 is a PPARα target gene (Mandard et al., 2004), decreased expression may indicate a decrease in PPARα transcriptional activity and therefore decreased β-oxidation.

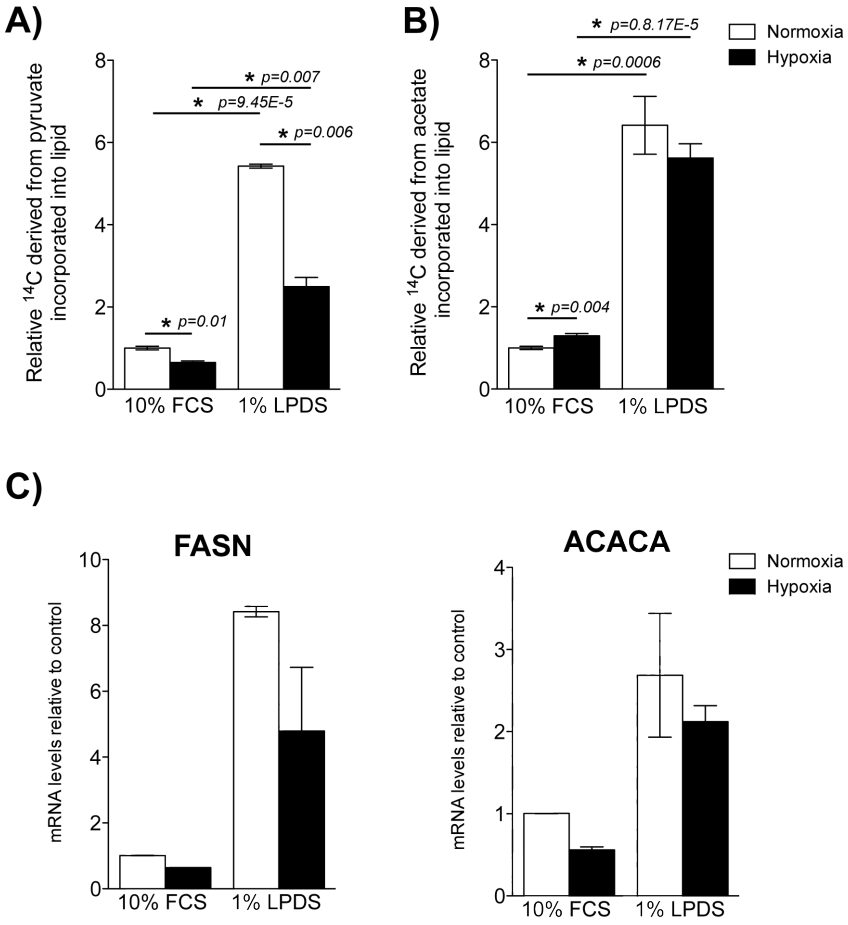

Figure 4-10: Hypoxia decreases pyruvate-dependent lipid synthesis but increases acetate-dependent lipid synthesis.
U87 cells were grown in normoxia or hypoxia for 24 hours and incorporation of ^{14}C-pyruvate (A) or ^{14}C-acetate (B) into the lipid phase was measured and normalised to cell mass. (C) Cells cultured in the same conditions as in (A) were analysed for expression of the SREBP target genes FASN and ACACA by RT-QPCR. Data shown is the mean of at least three independent biological replicates. p values from paired student's t tests are shown. Asterisks indicate statistical significance.

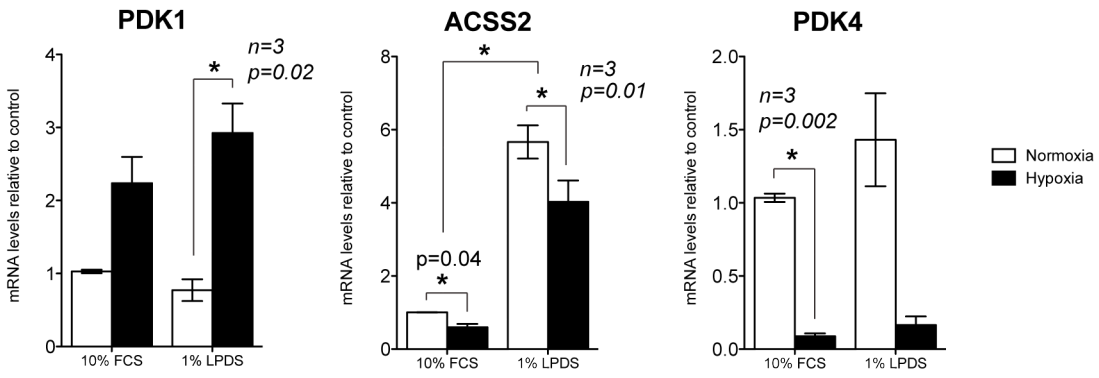

Figure 4-11: Hypoxia increases expression of PDK1 and inhibits PDK4 expression.
U87 cells were grown in 10% FCS or 1% LPDS (lipoprotein deficient serum) in normoxia or hypoxia for 24 hours. Total RNA was extracted and subjected to RT-QPCR analysis. mRNA expression levels for PDK1, PDK4 and ACSS2 were normalised to β tubulin as a loading control. Data shown is the mean of three independent biological replicates ± SEM. Asterisks indicate statistical significance according to the student's paired t test. n numbers and p values are displayed.

4.5 Hypoxia increases lipid droplet formation in an SREBP1-independent manner

4.5.1 Hypoxia increases lipid droplet staining

It has been known for sometime that hypoxic cells induce lipid droplet (LD) formation (Gordon et al., 1977; Whitmer et al., 1978) and HIF1α induces expression of the LD protein HIG2 (Gimm et al., 2010). This presumably increases capacity for lipid storage in response to the inhibition of lipid catabolism (β-oxidation). In the previous sections it was demonstrated that expression of SREBP target genes required for fatty acid synthesis were largely downregulated under hypoxic conditions, while the expression of three genes involved in fatty acid desaturation and transport and were induced in hypoxic cells in an SREBP1-dependent manner. In addition, a decrease in *de novo* pyruvate-dependent lipid synthesis was observed. This could indicate that hypoxia induces a change in the fate of lipids in U87 cells. Therefore it was investigated whether LD formation in U87 cells requires SREBP-dependent gene expression.

Cells were cultured in hypoxia for 24 hours in the serum conditions indicated in Figure 4.12. Cells were fixed and stained with DAPI to detect nuclei. In addition, cells were

stained with Nile Red, a dye that specifically detects neutral lipids, such as those found in LDs. LD staining was quantified using Array Scan technology, which uses an algorithm to quantify lipid droplet staining normalised to cell number (described in materials and methods). Hypoxia induced lipid droplet staining in cells cultured in 10% FCS (Figure 4.12). Hypoxia-induced LD staining was also observed in cells cultured in reduced serum or reduced lipoprotein conditions, although the levels of LD staining in hypoxia were significantly less than cells cultured in full serum (Figure 4.12). These data suggest that cell culture medium components (including fatty acids) are required for maximum LD formation in hypoxia.

4.5.2 SREBP-activation enhances lipid droplet induction in hypoxia

It was next investigated whether SREBPs play a role in LD formation in hypoxia. LD formation in response to activation of exogenous ER.mSREBP1a and ER.mSREBP2 was examined. U87-EV, U87-ER.mSREBP1a and U87-ER.mSREBP2 cells were grown in normoxia or hypoxia either in full serum or 1% LPDS for 48 hours in the presence or absence of 4-OHT. Cells were stained with DAPI and Nile Red and LD formation was quantified using the Array Scan. As previously observed, hypoxia induced the formation of lipid droplets in both 10% FCS and 1% LPDS and the induction in cells cultured in 1% LPDS was lower when compared with 10% FCS (Figure 4.13). Interestingly, activation of ER.mSREBP1a or ER.mSREBP2 enhanced LD staining in hypoxia. Activation of mSREBP1a or mSREBP2 increased lipid droplet formation in both serum conditions, although induction in cells cultured in 1% LPDS was lower than those cultured in full serum. This indicates that the SREBP-dependent induction of LDs requires components of cell culture medium.

4.5.3 SREBP1-depletion does not prevent lipid droplet induction in hypoxia

Since activation of exogenous SREBP was able to enhance the formation of LDs under hypoxia, it was next investigated whether LD formation in hypoxia was SREBP-dependent. Because SREBP1 silencing performed in experiments described in sections 4.2.6 and 4.3 was incomplete, and residual SREBP1 expression was observed, a stable

silencing strategy was used. U87 cells stably expressing a doxycycline inducible short hairpin RNA (shRNA) targeting SREBP1 were generated by lentiviral transduction. As a control, cells expressing a doxycycline inducible non-targeting shRNA (scrambled: scr) were also generated. Following 72 hours of treatment with doxycycline, flSREBP1 protein and mRNA levels were reduced in these cells compared to the EtOH treated control, demonstrating induction of the shRNA (Figure 4.14 A and B). SREBP1 protein and mRNA expression remained unchanged following induction of the scrambled control (sh-Scr) (Figure 4.14 A and B). In order to assess the contribution of SREBP1 to lipid droplet formation under hypoxia, these cells were cultured for 72 hours in the presence or absence of doxycycline and then placed in normoxic or hypoxic conditions for a further 24 hours. In addition, cells exposed to hypoxia for 24 hours were returned to normoxia for an additional 24 hours (reoxygenation) in order to analyse the effect of reoxygenation on LDs. Consistent with previous observations, hypoxia significantly increased LD staining in both cell lines (Figure 4.14 C). Interestingly, LD staining was significantly reduced following re-oxygenation, indicating that the induction of LDs in response to hypoxia is reversible (Figure 4.14 C, grey bars). Induction of SREBP1 silencing did not affect hypoxia-dependent LD induction. However, the decrease in LD staining in cells expressing sh-SREBP1 following reoxygenation was slightly blocked. This suggests that loss of SREBP1 may lead to a delay in the recovery of cells exposed to hypoxia.

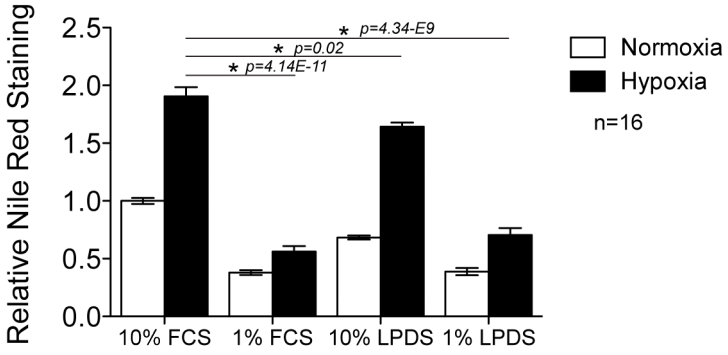

Figure 4-12: Hypoxia increases lipid droplet formation.
U87 cells were grown in 96-well plates in hypoxia or normoxia in the four serum conditions indicated for 24 hours. Cells were fixed and stained with DAPI (nuclei) and Nile Red (lipid droplets) and scanned using the Array Scan VTI. Data shown represents the mean of 16 replicates. Asterisks indicate statistical significance. P values from paired student's t tests are shown.

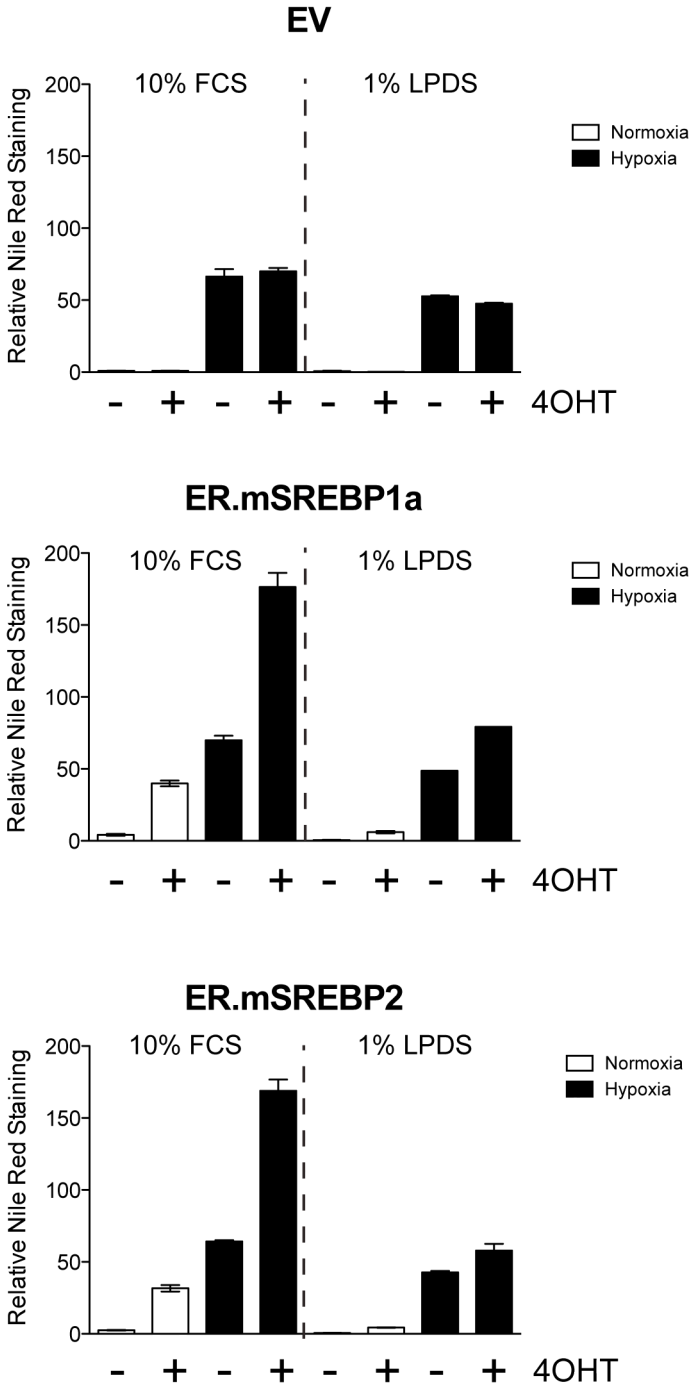

Figure 4-13: SREBP activation is sufficient to induce lipid droplet formation in hypoxia. U87-EV, U87-ER.mSREBP1a and U87-ER.mSREBP2 cells were grown in 96-well plates. Cells were cultured in 10% FCS or 1% LPDS in the presence or absence of 4-hydroxytamoxifen (4OHT) and in hypoxia or normoxia for 24 hours. Cells were fixed and stained with DAPI (nuclei) and Nile Red (lipid droplets) and staining was quantified using the Array Scan VTI. Data shown is the mean from three biological replicates ± SEM.

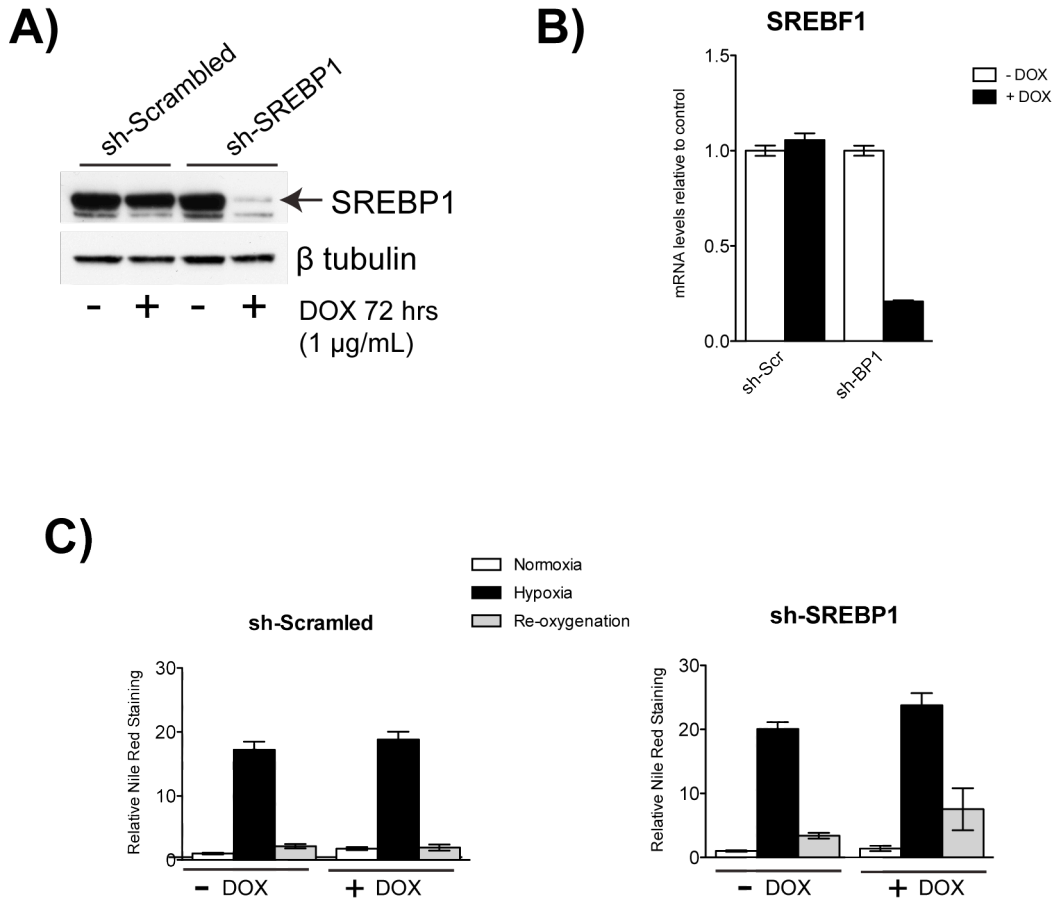

Figure 4-14: Ablation of SREBP1 does not prevent lipid droplet formation in hypoxia.
(A) U87 cells were stably infected with shRNAs targeting either SREBP1 or a non-targeting control (Scrambled). Cells were cultured in the presence or absence of doxycycline (1 μg/ mL) for 72 hours and whole cell lysates were analysed by Western blotting and an antibody recognising SREBP1. β tubulin is shown as a loading control. (B) RNA was extracted from cells treated as in (A) and subjected to RT-QPCR analysis. mRNA expression levels of SREBP1 were normalised to β actin as a loading control. (C) Cells expressing shRNAs targeting SREBP1 or a scrambled control were grown in the presence or absence of doxycycline for 72 hours. Cells were then cultured in normoxia or hypoxia for 24 hours. In addition, cells that were cultured in hypoxia for 24 hours were given 24 hours to recover in normoxic conditions (re-oxygenation). Cells were grown in 96-well plates, fixed and stained with DAPI (nuclei) and Nile Red (lipid droplets) and lipid droplet staining was quantified using the Array Scan VTI. Data shown are the means of 9 replicates ± SEM.

4.6 Silencing of SREBP1 increases apoptosis in low lipoprotein conditions

The data presented so far strongly suggest that SREBPs are being regulated in response to hypoxia. It was therefore investigated whether SREBP1 is required for the survival of U87 cells under hypoxic conditions. Cells that were stably expressing doxycycline inducible shRNA targeting SREBP1 or a non-targeting control were cultured in the presence or absence of doxycycline for 72 hours to induce shRNA expression. Cells were then grown in medium containing 10% FCS or 1% LPDS in normoxia or hypoxia for 48 hours. The experiment presented in Figure 4.15 indicates that although hypoxia tended to increase overall levels of apoptosis, silencing of SREBP1 did not affect cell viability in medium supplemented with 10% FCS. Culture of cells in medium containing 1% LPDS increased overall levels of apoptosis, suggesting that removal of serum lipoproteins may be detrimental to U87 cells. The culturing of cells in hypoxic conditions in medium containing 1% LPDS further increased the levels of apoptosis, suggesting that the combination of a lack of oxygen and external fatty acids is detrimental to U87 cells. Depletion of SREBP1 in cells cultured in 1% LPDS in either normoxia or hypoxia resulted in a large increase in apoptosis. This indicates that activation of SREBP1 in response to low serum lipoprotein conditions may be important for the survival of U87 cells, in both normoxia and hypoxia.

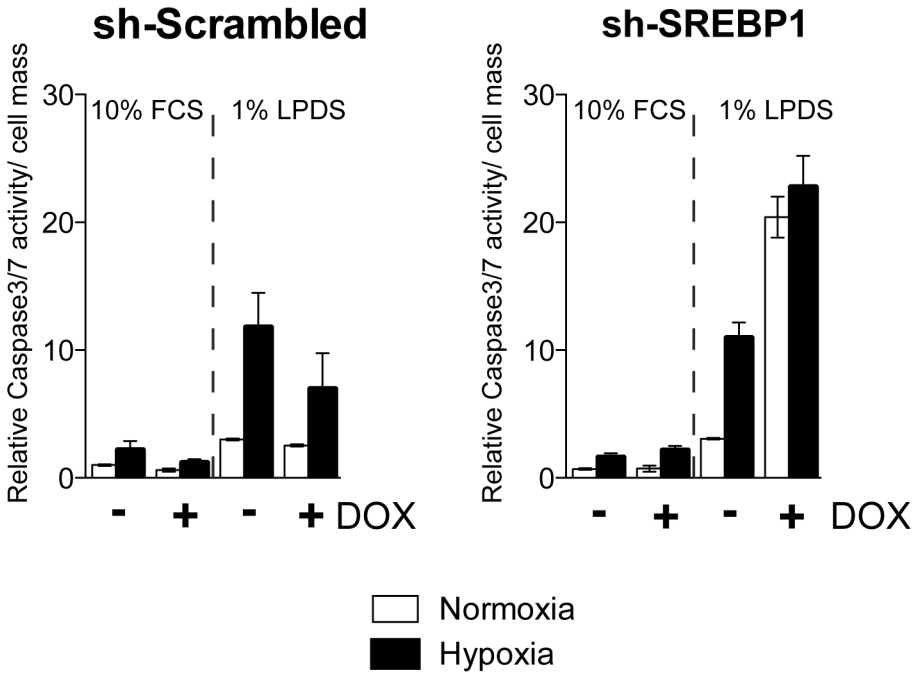

Figure 4-15: Silencing of SREBP1 increases apoptosis in low lipoprotein conditions
U87 cells stably expressing doxycycline-inducible shRNAs targeting SREBP1 or a Scrambled control were grown in the presence or absence of doxycycline (1µg/ mL) for 72 hours. Cells were then seeded into 96 well plates and allowed to attach before being cultured in either 10% FCS or 1% LPDS for 16 hours. Cells were placed into hypoxia or normoxia for 48 hours. Caspase 3/7 activity was measured using the Apo1 assay and normalised to total protein content (cell mass). This experiment was performed by B. Griffiths (LRI, GEA). Data represent the mean of three replicates ± SEM.

4.7 Discussion

Altered lipid metabolism is a common feature of cancer cells and solid tumours often exhibit areas of low oxygen tension, due to poorly developed tumour vasculature. Glioblastoma multiforme is a cancer associated with areas of hypoxia, and SREBP has been shown to play a role in the tumourigenic potential of this cancer type. Although there are reports demonstrating a role for altered lipid metabolism in the hypoxic response of cancer cells, some of these data are conflicting, suggesting that lipid metabolism may be altered in a tumour-type specific manner. The aim of this chapter of the thesis was to investigate the role of SREBPs and lipid metabolism in the hypoxic response of the human glioblastoma U87 cell line.

The expression of a selected group of SREBP target genes was investigated under hypoxic conditions. Unexpectedly, hypoxia induced differential expression of the SREBP target genes examined (Figure 4.1). Most SREBP target genes encoding enzymes involved in the initial stages of fatty acid and cholesterol biosynthesis were downregulated in hypoxia. For example, expression of the rate-limiting enzyme in fatty acid biosynthesis (ACACA), as well as the rate-limiting enzyme for cholesterol biosynthesis (HMGCR), was downregulated under hypoxic conditions. In contrast, expression of the SREBP target gene SCD, as well FABP3 and FABP7, was increased in a hypoxia-dependent manner. Upon analysis of SREBP isoform expression in hypoxia it was found that hypoxia decreased expression of SREBF1c but not SREBF1a or SREBF2 at the mRNA level (Figure 4.2). Indeed, expression of SREBF2 mRNA was slightly increased in response to hypoxia. In addition, hypoxia resulted in the decreased expression of flSREBP1 protein (Figure 4.3). Hypoxia also reduced nuclear mSREBP1 levels. It is unclear if the doublets observed in Figure 4.3 correspond to the individual SREBP1 isoforms. Although the molecular weights of the two isoforms are not different enough to be resolved by SDS PAGE, denaturation of some proteins results in altered migration in SDS PAGE. Another possibility is that the two bands observed by Western blotting represent different phosphorylation-species of nuclear mSREBP1. Treatment with λ phosphatase could reveal whether this is in fact the case.

These data indicate the complex nature of lipid metabolism in hypoxia in U87 cells. It is tempting to speculate that loss of SREBP1c expression is responsible for the change in expression of a specific subset of SREBP target genes that are downregulated. Specific silencing of individual SREBP1 isoforms in normoxic conditions may provide more information as to the SREBP1c-dependency of this observation. Furthermore, it will be interesting to investigate whether the hypoxia-induced changes in SREBP isoform expression are HIF dependent. Chromatin-immunoprecipiation (ChIP) studies of the promoters of the different SREBP isoforms in hypoxia may yield important clues as to their regulation under hypoxia in U87 cells. In addition, analysis of SREBP expression following stabilisation of HIF1α using DMOG, an inhibitor of PHD activity, could indicate a HIF1α-dependent mechanism.

Interestingly, expression of SREBP1c and FASN was also specifically downregulated in response to hypoxia in human hepatoma Hep3B cells (Choi et al., 2008). This hypoxia-mediated inhibition of SREBP1c expression was dependent on HIF1α-induced expression of Stra13/DEC1 and DEC2. These two transcriptional repressors directly compete with SREBP1c for binding to the promoter of the SREBF1c gene in hypoxia (Choi et al., 2008), thereby resulting in decreased SREBP1c expression. It would be interesting to investigate the expression of Stra13/DEC1 and DEC2 in U87 cells in hypoxic conditions in order to further understand the regulation of SREBP expression in the cellular response to hypoxia in these cells. In addition, an early paper reported that the SCAP promoter contained a binding site for SREBP1c (Nakajima et al., 1999). Therefore, the downregulation of SCAP mRNA expression in response to hypoxia that was observed in Figure 4.4 may be due to the loss of SREBP1c. However, further experiments are required to demonstrate that the loss of SREBP target gene expression is dependent on decreased SREBP1c expression.

Decreased expression of SREBP target genes under hypoxic conditions is consistent with a report by Rankin and colleagues, who demonstrate that in murine liver expression of SREBP1c, HMGCS1, FASN and ACACA is decreased in a HIF2α-dependent manner (Rankin et al., 2009). The decreased expression of SCAP was also

observed in this study, consistent with data presented in this thesis (Figure 4.4). The role of HIF2α was not investigated in this thesis and the possible contribution of HIF2α to the changes in gene expression should be investigated. In contrast to observations throughout this thesis, Rankin et al also observed a decrease in expression of SCD in response to HIF2α activation. SCD is considered to be a PPARα target gene (Mandard et al., 2004) and the authors show that decreased SCD expression is due to decreased expression of PPARα and perturbed β-oxidation (Rankin et al., 2009). SCD catalyses the rate limiting step in the production of MUFA from SFA and the expression of SCD is regulated by the ratio of SFAs:PUFAs (Ntambi, 1999). In addition, the reaction catalysed by SCD requires molecular oxygen (Ntambi, 1999). Therefore, the absence of oxygen could lead to a build up of SFAs due to the decreased catalytic activity of SCD. The change in the SFA:PUFA ratio would release the PUFA-dependent inhibition of SCD expression and allow SREBP to bind to and activate the SCD promoter. Whether or not the limited amount of oxygen present would be sufficient to catalyse the desaturation of SFA in response to increased SCD expression is not known. It would be interesting to investigate changes in the levels of SFAs, MUFAs and PUFAs in U87 cells following hypoxia in order to understand the role of SCD in the hypoxic response of cancer cells.

The decreased expression of HMGCR observed in this chapter (Figure 4.1) is also consistent with the observations of Nguyen and colleagues who demonstrated that HIF1α induces expression of INSIGS, resulting in the degradation of HMGCR in response to hypoxia in Chinese hamster ovary (CHO) cells (Nguyen et al., 2007). This report suggests that hypoxia results in a build up of lanosterol and the authors propose that the degradation of HMGCR represents an oxygen sensing mechanism. However, this study was not performed in cancer cells. In contrast, it has been shown that hypoxic-induction of HIF1α in response to $CoCl_2$ results in increased expression and activity of HMGCR in human hepatocellular carcinoma HepG2 cells (Pallottini et al., 2008). It should be noted that these observations were made in chemically-induced pseudo-hypoxia and true hypoxia may result in a different cellular response.

Increased expression of FASN and SREBP1, mediated by hypoxia-dependent Akt activation, has been reported in the hypoxic response of breast cancer cell lines (Furuta et al., 2008). The lack of induction of FASN expression and SREBP1 in response to hypoxia in U87 cells may represent a tissue-specific response. In addition, no change in Akt phosphorylation on serine 473 was observed in hypoxia in U87 cells (data not shown), suggesting that hypoxia does not increase Akt activity in these cells. This may account for the difference in SREBP1 and FASN expression observed in response to hypoxia in breast cancer cell lines compared with the U87 glioblastoma cell line in this thesis.

Increased expression of the potential SREBP target genes FABP3 and FABP7 was observed in hypoxic conditions (Figure 4.1). FABP3 and FABP7 were regulated by activation of ER.mSREBP1a and ER.mSREBP2 in Chapter 3. Interestingly, FABP7 is upregulated in GBM and plays a role in migration of U87 cells *in vitro*, indicating a role in GBM invasion (Liang et al., 2005; Mita et al., 2010). Silencing of either SREBP1 or SREBP2 was sufficient to inhibit hypoxia-dependent FABP7 expression (Figure 4.6), indicating that FABP7 is an SREBP target gene in U87 cells.

Induction of FABP3 and SCD in response to hypoxia was partially dependent on SREBP (Figure 4.6). Although induction under hypoxic conditions was still observed following silencing of SREBP1 or HIF1α, expression of both genes was substantially reduced. This indicates that both HIF1α and SREBP1 may play a role in the transcriptional induction of SCD and FABP3 in hypoxia. Consistent with this hypothesis, SREBP1a and SREBP1c transcriptionally regulate FABP3 in human myotubes (Rome et al., 2008). In addition, FABP3 contains an HIF1β regulatory element within its promoter and is also regulated by hypoxia (Biron-Shental et al., 2007). Analysis of expression of SCD and FABP3 in response to hypoxia following combined silencing of HIF1α and SREBP1 may reveal whether there is cooperation between HIF1α and SREBP1 in the transcriptional response to hypoxia. In addition, the role of HIF2α in the expression of SCD and FABP3 could be investigated.

The activity of the pSRE-luc reporter in hypoxia was also investigated and increased luciferase activity was observed in hypoxic conditions (Figure 4.7). This suggests that despite the decreased expression of SREBP1c and some SREBP target genes, transcriptional activity of SREBP1a and SREBP2 in hypoxia is still present. The regulation of the pSRE-luc reporter by SREBP1, SREBP2 and HIF1α was also investigated. Silencing of HIF1α or SREBP1, but not SREBP2, decreased reporter activity in hypoxic conditions to that of basal activity (Figure 4.8). Combined silencing of HIF1α and SREBP1 resulted in a further decrease in reporter activity, although induction in response to hypoxia was not blocked completely (Figure 4.9). Since the pSRE-luc reporter also contains binding sites for SP1, regulation of the reporter by SP1 in response to hypoxia cannot be ruled out. Furthermore, both HIF1α and SREBP1 are known to interact with additional transcriptional regulators. Experiments with a mutated version of the pSRE-luc without the SP1 binding sites should be performed in order to confirm the contribution of SREBPs to the hypoxic induction of this reporter. In addition, it would be interesting to investigate whether hypoxia induces activity of the FASN-luc reporter (Amemiya-Kudo et al., 2002), since hypoxia decreases expression of FASN mRNA.

Taken together, these results clearly show that some SREBP targets, as well as SREBP1c itself, are downregulated following hypoxia. At the same time, SREBPs are essential for the hypoxia-dependent induction of other genes (i.e. FABP7). It is possible that hypoxia induces post-translational modifications in individual SREBP isoforms, thereby altering their transcriptional activity resulting in the induction of specific subsets of genes. Alternatively, SREBPs could be recruited to specific promoters in hypoxic cells by other transcription factors such as HIF1α or SP1. Detailed analysis of the promoters of FABP7, FABP3 and SCD may lead to the identification of additional binding sites involved in the regulation of these genes.

Since hypoxia resulted in decreased expression of SREBP target genes involved in lipid biosynthesis, it was investigated whether *de novo* lipid synthesis was affected by hypoxic conditions. Hypoxia reduced pyruvate-dependent lipid synthesis in U87 cells in

a manner consistent with the induction of PDK1 (Figures 4.10 and 4.11) (Kim et al., 2006; Papandreou et al., 2006). However, acetate-dependent lipid synthesis in hypoxia is unaltered in lipoprotein deficient conditions, and in full serum conditions acetate-dependent lipid synthesis is moderately increased in hypoxia. Since activation of SREBP1a in these cells (Chapter 3) induces *de novo* lipid synthesis, it should be demonstrated that SREBPs are required for this acetate-dependent lipid synthesis in hypoxia. It is possible that the increased acetate-dependent lipid synthesis is a response to the reduction of pyruvate-dependent lipid synthesis in these conditions.

Expression of the SREBP target gene ACSS2 was also examined. ACSS2 catalyses the activation of cytosolic acetate for lipid synthesis and is induced by hypoxia in tumour cells (Yoshii et al., 2009). However, expression of ACSS2 in U87 cells was slightly downregulated in hypoxia (Figure 4.11). Since the possibility that ACSS2 is required for acetate-dependent lipid synthesis cannot yet be ruled out, ACSS2 silencing experiments would be useful. However, the culture of cells in lipoprotein deficient conditions increased both pyruvate- and acetate-dependent lipid synthesis when compared to full serum conditions (Figure 4.10 A and B), regardless of oxygen levels. This indicates that in conditions where external fatty acids are limited, *de novo* lipid synthesis is still able to take place. This is consistent with the upregulation of SREBP target genes observed in lipoprotein deplete conditions in hypoxia compared to full serum (Figure 4. 10 C). Finally, the expression of the PPARα target gene PDK4 was analysed (Figure 4.11). The observed hypoxia-dependent decrease in PDK4 expression could indicate reduced PPARα activity and suggests a reduction in fatty acid β-oxidation. However, expression analysis of other β-oxidation genes such as CPT1 would be beneficial to support this conclusion. In addition, β-oxidation itself could be measured to investigate whether hypoxia inhibits the break down of fatty acids in U87 cells.

Hypoxia induces lipid accumulation and storage in the form of lipid droplets (LDs) and increased LD formation in response to hypoxia in U87 cells was observed (Figure 4.12). Interestingly, in contrast to lipid synthesis and expression of SREBP target genes, LD

formation was dramatically reduced in lipoprotein-depleted conditions, suggesting that LD formation in hypoxia may be the result of increased fatty acid uptake. Indeed, HIF1α has been shown to result in activation of PPARγ, whose target genes include the lipid transporter CD36, as well as the rate-limiting enzyme in TAG synthesis GPAT (Krishnan et al., 2009). The authors of this study concluded that HIF1α activation leads to increased PPARγ activity, thus resulting in increased lipid uptake, TAG synthesis and increased storage of lipids in LDs. This supports the idea put forward by other publications (Gimm et al., 2010; Rankin et al., 2009). In experiments described in chapter 3 it was observed that SREBP activation is sufficient to induce LD formation in U87 cells (Figure 3.7), consistent with previously published findings that SREBP induces LD formation in various models (Seo et al., 2011; Shimano et al., 1996; Wang et al., 2010). Activation of mSREBP1a or mSREBP2 in hypoxia greatly enhanced LD formation in 10% FCS but not in 1% LPDS (Figure 4.13), suggesting that SREBPs induce LD formation only in the presence of external lipids. However, LD formation was unaltered in hypoxia after SREBP1 shRNA-mediated depletion in U87 cells (Figure 4.14 C), indicating that factors other than SREBP1 are also involved in LD formation in hypoxia. Interestingly, the loss of LDs in response to reoxygenation was moderately reduced in cells in which SREBP1 had been silenced (Figure 4.14 C). This suggests that SREBP1 may be involved in the mobilisation of TAGs from LDs, which fits with observations made by Seo and colleaugues who demonstrated that serum depletion resulted in reduced mobilisation of TAGs from LDs upon silencing of SREBP2 in HeLa cells (Seo et al., 2011).

Experiments in this chapter demonstrated that SREBP1 is involved in the hypoxia-dependent induction of SCD, FABP3 and FABP7 (Figure 4.6) and together the data suggest a role for SREBPs and lipid metabolism in the hypoxic response of cancer cells. Therefore, it was hypothesised that SREBP1 may be required for U87 viability in hypoxia. Although hypoxia increased overall levels of apoptosis, SREBP1 silencing did not affect cell viability in full serum conditions. However, SREBP1 depletion by shRNA in low lipoprotein conditions caused a large increase in apoptosis, suggesting that SREBP1 is important for cell viability in these conditions (Figure 4.15). Demonstrating failure of hypoxia-dependent FABP7 induction upon SREBP1 silencing

in these conditions would support this hypothesis. Additional confirmation would be provided by a similar induction of apoptosis after SCD, FABP3, or FABP7 silencing in the same conditions. Furthermore, rescue experiments following SREBP1 silencing could also be performed. If SCD-induction is SREBP-dependent in these conditions, addition of the MUFA oleate may rescue the apoptotic effect. Similarly, the rescue of apoptosis following overexpression of FABP7 in SREBP1-depleted cells would demonstrate a role for the SREBP-dependent induction of FABP7 in U87 cell survival in hypoxia.

The exact mechanism by which SREBP1 promotes cell survival under oxygen and nutrient-deprived conditions remains to be elucidated. It is unlikely that the pro-survival function of SREBP1 in this context is due to a single target gene. Given the observation that SREBP1-depletion increases cell death only in response to a reduction in both oxygen and serum components, it would be beneficial to analyse SREBP-target gene expression under these conditions. Gene expression microarray analysis in cells in which SREBP1 has been silenced would allow for the identification of SREBP-target genes that are required for cancer cell survival under conditions of oxygen and nutrient stress. Furthermore, the exact components of serum that are present in 10% FCS but not in 1% LPDS should be identified in order to further clarify the role of SREBP1 in cell survival in response to nutrient and oxygen deprivation. Throughout this thesis commercial LPDS was used, although the manufacturer does not make the exact components of this serum available. Removing the lipoproteins and other lipids from FCS used in parallel experiments would enable us to determine which lipids and/or lipoproteins are required for cell survival under hypoxic conditions.

It is also possible that SREBP functions to protect the cells from reactive oxygen species (ROS), which are produced by the mitochondria under hypoxic conditions and can sensitise the cells to apoptosis (Dang et al., 2008). Gene expression microarray analysis carried out in Chapter 3 revealed a number of genes involved in oxidative stress to be regulated by SREBPs (Figure 3.12). Determination of intracellular ROS levels could be carried out to demonstrate that loss of SREBP1 under these conditions

increases levels of ROS. If the failure of the cell to detoxify cellular ROS plays a role in the apoptosis observed in SREBP1-silenced cells, it may be possible to rescue cell death following SREBP1-silencing in 1% LPDS and hypoxia by treating the cells with a ROS scavenger.

The regulation of lipid metabolism in U87 cells in hypoxia is clearly complex (see Figure 4.16 for a summary of the hypotheses presented in this thesis). The data presented here suggest that hypoxia may induce a switch in SREBP-isoform expression. In addition, hypoxia may increase the transcriptional activity of SREBP1a, resulting in the increased expression of FABP7, thereby increasing fatty acid uptake and TAG synthesis. This would be similar to the induction of PPARγ expression by HIF1α, which results in the increase of fatty acid uptake and TAG biosynthesis (Krishnan et al., 2009). FABPs have been implicated in the regulation of PPAR transcriptional activity (Mita et al., 2010; Wolfrum et al., 2001), which allows for the possibility that the hypoxia-induced expression of SREBP1-dependent FABP7 results in PPARγ transcriptional activation, and a subsequent increase in fatty acid uptake and TAG synthesis. Further experiments are required to link the formation of lipid droplets in hypoxia directly to SREBP. It would be interesting to investigate the purpose of hypoxia-induced LD formation in this context to determine whether LDs are simply a consequence of increased fatty acid uptake and decreased β oxidation, or if LD formation in hypoxia protects the cells from lipotoxicity and/or plays a role in cell recovery following reoxygenation.

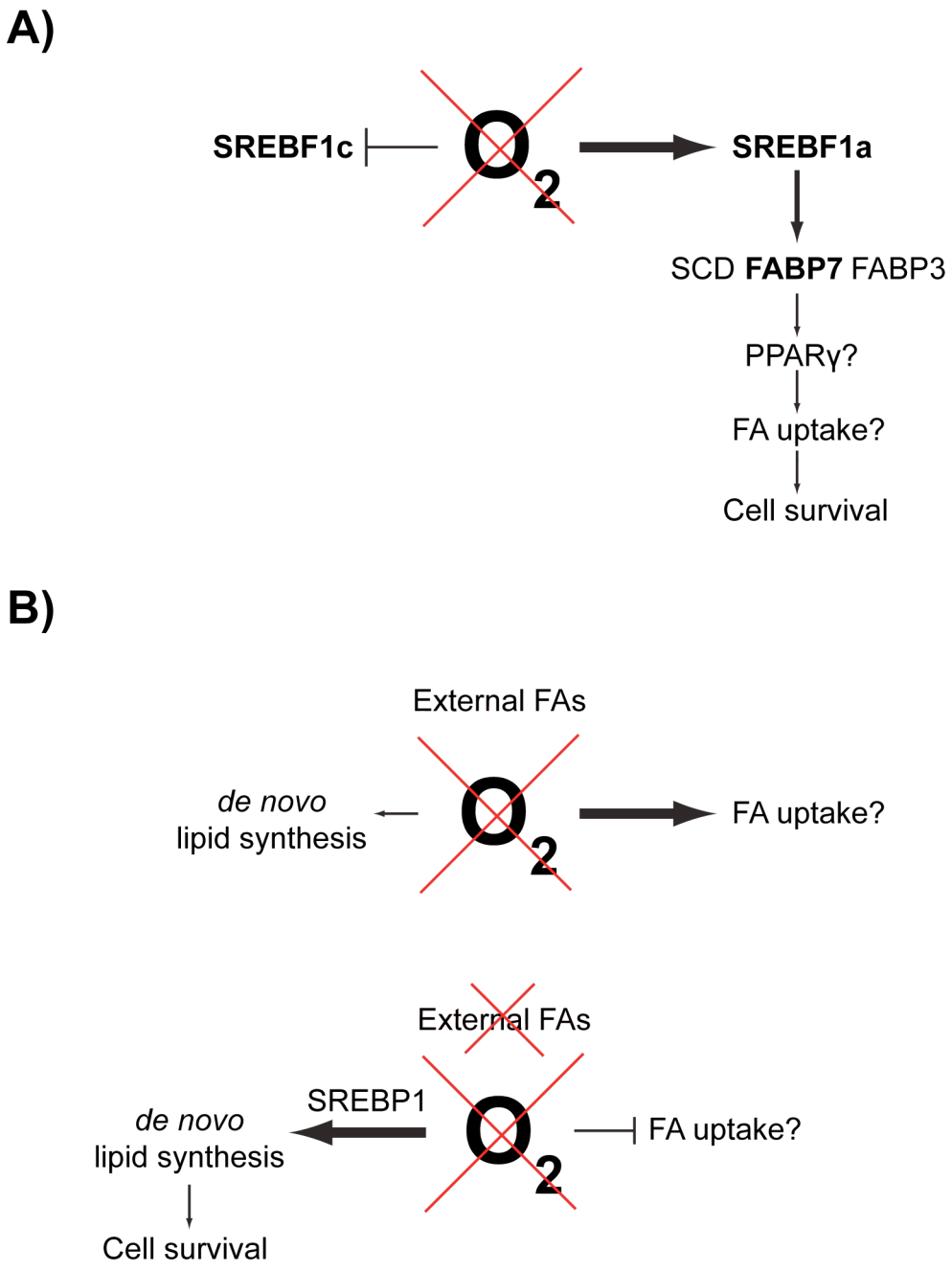

Figure 4-16: Schematic summary of the effect of hypoxia on SREBP1 isoform expression and activity and the proposed role of SREBP in cell survival in hypoxic conditions.
(A) Hypoxia results in the decreased expression of SREBF1c mRNA and an increase in SREBP1a transcriptional activity. This leads to an increase in SREBP1-dependent expression of FABP7, as well as expression of SCD and FABP3. Increased FABP7 expression may be required for PPARγ transcriptional activity and subsequent increase in FA uptake. This may represent a mechanism of survival for cells under hypoxic conditions. (B) In hypoxic conditions *de novo* lipid synthesis is reduced, but not inhibited completely. It is possible that in hypoxia FA uptake is the main source of lipids for the cell. However, removal of external FAs under low oxygen conditions forces the cell to switch back to *de novo* lipid synthesis, for which SREBP1 may be required. Ablation of SREBP1 in these conditions leads to cell death.

Chapter 5. Regulation of SREBPs by the Akt/ mTORC1 pathway

5.1 Introduction

The Akt/ PKB serine/ threonine kinase plays a vital role in many cellular processes including metabolism, proliferation, cell survival and growth control (Manning and Cantley, 2007). Akt is activated by the lipid kinase phosphoinositide 3-kinase (PI3K) in response to growth factors (Engelman et al., 2006). Insulin activates Akt via the insulin receptor (IR) and Akt is a critical mediator of the metabolic changes resulting from insulin signalling (Manning and Cantley, 2007). Aberrant activation of the PI3K/ Akt signalling pathway via the constitutive activation of oncogenic Ras or the loss of the tumour suppressor protein PTEN is frequently observed in human cancers (Altomare and Testa, 2005).

It has previously been shown that Akt regulates the expression of genes involved in lipogenesis through SREBP1 activation (Porstmann et al., 2005). In addition, a requirement for mTORC1 in Akt-dependent lipogenesis has been demonstrated (Porstmann et al., 2008). Furthermore, Akt induces nuclear accumulation of mSREBP1, and the induction of the SREBP1 target genes FASN and ACLY following Akt activation is blocked by rapamycin, indicating the requirement for mTORC1 (Porstmann et al., 2008). Other groups have since established a role for mTORC1 in lipid metabolism and demonstrated that this is mediated by SREBPs. There are a number of reports that support a role for mTORC1 in the regulation of SREBP. mTORC1 has been implicated at multiple levels in the control of SREBP activity including regulation of SREBP1 transcription (Li et al., 2010), ER-Golgi translocation (Ma et al., 2007), flSREBP1 processing (Düvel et al., 2010) and stability of the mature protein (Porstmann et al., 2008). However, the mechanism by which Akt and mTORC1 regulate SREBPs is still unknown. In this chapter, new results demonstrating the regulation of SREBPs by mTORC1 are presented.

5.2 Inhibition of mTORC1 differentially affects SREBP protein and mRNA levels

In order to gain further insight into the regulation of SREBPs by Akt and mTORC1, the RPE-Akt-ER inducible cell line was used. Human retinal pigment epithelial cells (RPEs) that have been immortalised using the human telomerase gene (RPE-hTERT) are considered to be a good cellular system in which to study biochemical and physiological aspects of cell growth, due to their untransformed phenotype and indefinite life span (Bodnar et al., 1998). RPE-hTERT cells that stably express an inducible, truncated form of Akt1 (myrAkt) fused to the oestrogen receptor (ER) have been described previously (RPE-Akt-ER) (Porstmann et al., 2005). This truncated Akt lacks the PH domain and is instead targeted to the membrane via an N-terminal Src myristolation sequence independently of PI3K activation (Figure 5.1 B). Treatment with 4-OHT results in rapid and sustained activation of the kinase activity of the Akt-ER fusion protein (Figure 5.1 C) (Kohn et al., 1998).

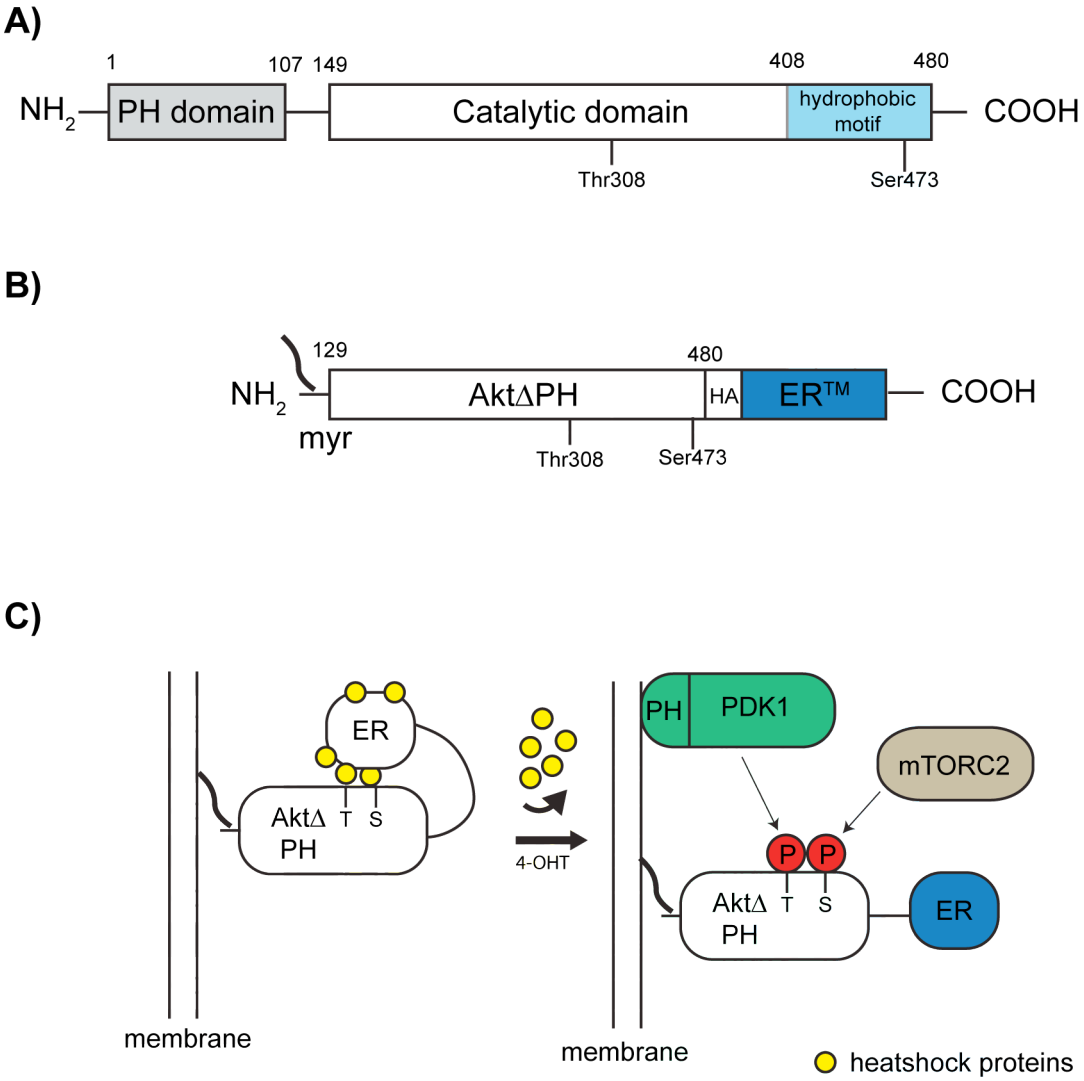

Figure 5-1: Schematic representation of the myr-Akt-ER construct used in this thesis.
(A) Domain structure of wild-type Akt showing the plekstrin homology (PH) domain, catalytic domain and the hydrophobic motif. Phosphorylation sites involved in Akt activation are indicated. (B) Schematic representation of the truncated ΔPH form of Akt fused to the mutant murine oestrogen receptor (ER) showing the N-terminal Src myristolation sequence (myr). (C) Conditional activation of myr-Akt-ER: Akt-ER is directed to the membrane by the myristolated residue, thereby rendering it independent from its upstream regulator PI3K. In the absence of 4-hydroxytamoxifen (4-OHT) the ER domain is in an inhibitory complex with heatshock proteins. Upon treatment with 4-OHT the ER changes conformation, causing the dissociation of heatshock proteins and the two phosphorylation sites become accessible for their corresponding kinases. PDK1: 3-phosphoinositide-dependent kinase 1; mTORC2: mammalian target of rapamycin complex 2; ER: oestrogen receptor.

5.2.1 Nuclear accumulation of mSREBP1 following Akt activation is rapamycin sensitive

Since SREBP processing and activation is negatively regulated by high cellular sterol concentrations, RPE-Akt-ER cells were grown in 1% lipoprotein deficient serum (LPDS) in order to allow processing and nuclear accumulation of mSREBP. This condition also limits the activation of endogenous Akt. In addition, in order to prevent proteasome-dependent degradation of the mSREBPs in the nucleus, cells were treated with the proteasome inhibitor MG-132 for 1.5 hours prior to lysis, as is standard in protocols for the analysis of mSREBPs.

In order to investigate the role of mTORC1 in nuclear accumulation of mSREBP1 in response to Akt activation, RPE-Akt-ER cells were treated with solvent (EtOH) or 4-OHT for 24 hours in the presence or absence of the mTORC1-specific inhibitor rapamcyin. Treatment with 4-OHT resulted in increased phosphorylation of Akt on serine 473 (S473), and phosphorylation of the ribosomal protein S6 was completely abolished upon treatment with rapamycin (Figure 5.2 A), demonstrating that both Akt activation and mTORC1 inhibition were successful. Activation of Akt for 24 hours induced accumulation of mSREBP1 in whole cell lysates (Figure 5.2 A). In addition, Akt increased flSREBP1 levels, as well as expression of the SREBP target gene FASN (Figure 5.2 A). This increase was attenuated by rapamycin treatment (Figure 5.2 A). Analysis of mSREBP1 enriched in nuclear fractions showed that Akt induced nuclear accumulation of mSREBP1 and that this was reduced in the presence of rapamycin (Figure 5.2 B).

5.2.2 Inhibition of mTORC1 differentially affects mRNA expression of SREBF isoforms

Several groups have reported that mTORC1 regulates SREBF mRNA expression (Li et al., 2010; Ma et al., 2007; Peng et al., 2002; Yecies et al., 2011) and Akt activation has been shown to increase expression of SREBF1a and SREBF1c, but not SREBF2 mRNA (Porstmann et al., 2005). In order to investigate the effect of mTORC1 inhibition on the Akt-dependent induction of SREBP mRNA, RPE-Akt-ER cells were cultured in 1%

LPDS. Cells were treated with solvent (EtOH) or 100 nM 4-OHT in the presence or absence of 50 nM rapamycin for 24 hours. Total RNA was extracted and analysed by RT-QPCR. As previously described by Porstmann and colleagues (Porstmann et al., 2008), Akt activation increased expression of both SREBF1a and SREBF1c mRNA expression, but had no effect on SREBF2 mRNA expression levels (Figure 5.3 A). In addition, mRNA expression of SREBP target genes SCD and FASN was up-regulated following Akt activation (Figure 5.3 B). Interestingly, rapamycin treatment had differential effects on the mRNA expression levels of the three SREBF isoforms. SREBF1a mRNA was significantly reduced by rapamycin treatment in EtOH treated cells (Figure 5.3 A). However, in cells that had activated Akt, rapamycin was not able to significantly decrease mRNA expression. In contrast, SREBF1c mRNA levels were significantly decreased following rapamycin treatment, regardless of Akt activation status (Figure 5.3 A). These data indicate that mTORC1 activity may differ towards the two SREBP1 isoforms. Levels of SREBF2 mRNA expression were unaffected by both Akt activation and rapamycin treatment, suggesting that SREBF2 mRNA is not regulated downstream of Akt or mTORC1 in this model system.

Since the nuclear accumulation of mSREBP1 occurs within 2 hours of Akt activation (Porstmann et al., 2008), it was next investigated whether short-term activation of Akt and mTORC1 influence SREBF mRNA expression. RPE-Akt-ER cells were cultured in 1% LPDS for 16 hours and pre-treated with rapamycin for 30 minutes before being treated with solvent (EtOH) or 4-OHT for 2 hours. Expression of SREBF1a, SREBF1c and SREBF2 mRNA was analysed by RT-QPCR (Figure 5.4). Both SREBF1a and SREBF1c mRNA levels increased in response to Akt-activation, although this did not reach statistical significance. This indicates that Akt activation may induce SREBF1 mRNA expression quite rapidly. In contrast to long-term mTORC1 inhibition, Akt activation for 2 hours in the presence of rapamycin failed to reduce SREBF1c mRNA expression, but SREBF1a mRNA expression was significantly reduced. Expression of SREBF2 mRNA remained unaffected following Akt activation and mTORC1 inhibition, providing further evidence that SREBF2 mRNA is not regulated downstream of Akt or mTORC1 in these cells. Taken together, these data indicate that over time, mTORC1 inhibition differentially affects SREBF1a and SREBF1c mRNA expression.

SREBF1a is rapidly upregulated in response to Akt/mTORC1 activation while SREBF1c is upregulated only after longer-term activation. This may indicate that regulation of SREBF1a by Akt is more direct, whilst increased SREBF1c expression may be a result of increased SREBF1a expression.

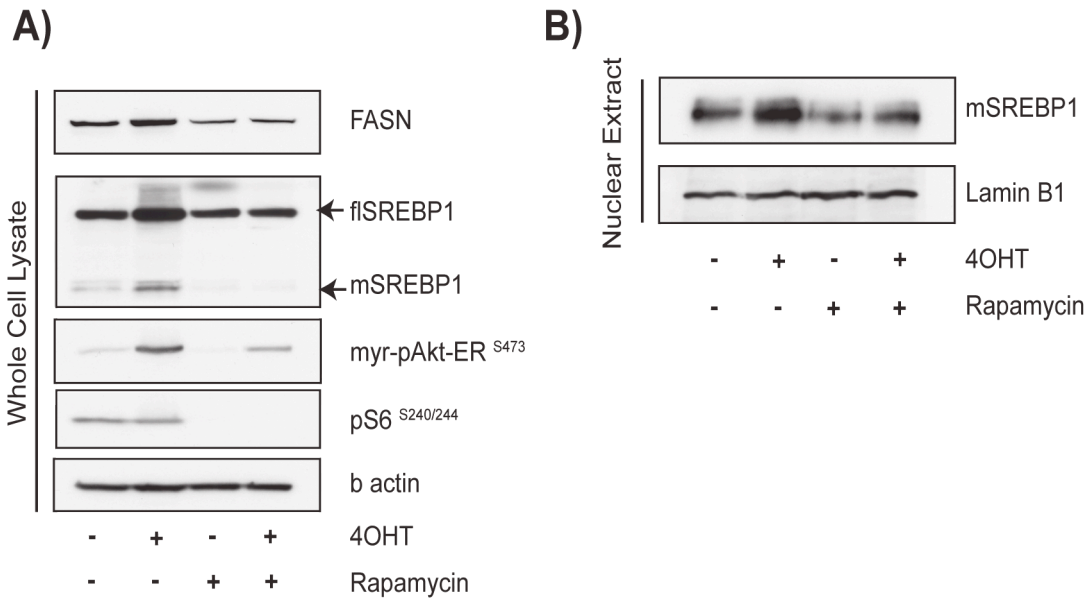

Figure 5-2: Akt activation leads to rapamycin-sensitive accumulation of mSREBP1 in the nucleus.
RPE-Akt-ER cells were grown in 1% LPDS and treated with solvent (EtOH) or 100 nM 4-OHT in the presence or absence of rapamycin (50 nM) for 24 hours. Cells were harvested and subjected to nuclear fractionation. Cell lysates were analysed by Western blotting. (A) Whole cell lysates from cells treated in parallel to those in (B) showing total levels of flSREBP1 and mSREBP1. FASN expression is shown as a positive control for SREBP1 transcriptional activity. Phosphorylated Akt (pAktSer473) and S6 (pS6Ser240/244) were assayed as controls for 4-OHT and rapamcyin treatment. β actin is shown as a loading control. (B) Nuclear fractions showing levels of mature SREBP1 (mSREBP1). Lamin B1 is shown as a nuclear specific loading control.

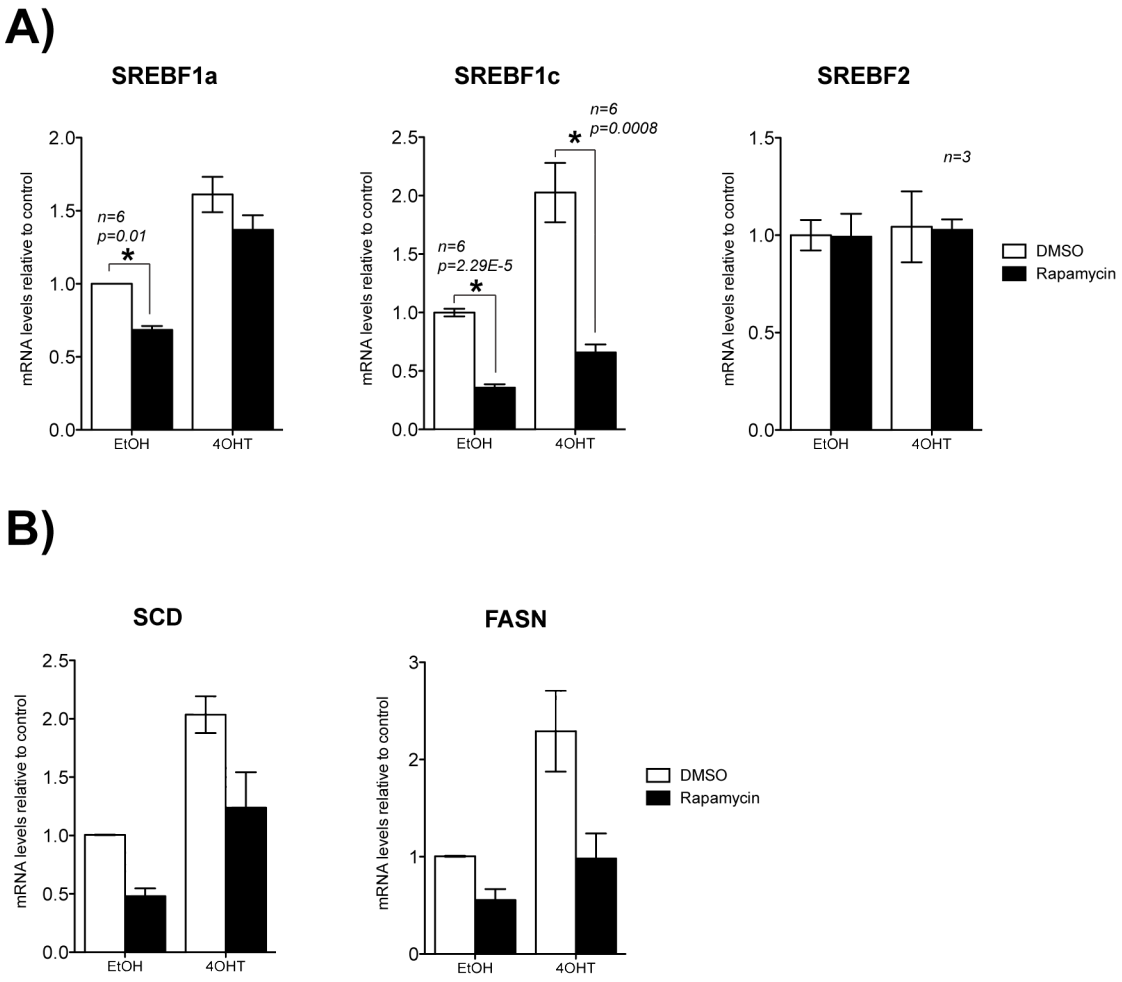

Figure 5-3: Rapamycin differentially affects mRNA expression of SREBF isoforms.
RPE-Akt-ER cells were grown in 1% LPDS and treated with solvent (EtOH) or 100 nM 4-OHT in the presence or absence of rapamycin (50 nM) for 24 hours. Total RNA was extracted and used for RT-QPCR analysis. (A) mRNA expression levels of SREBF1a, SREBF1c and SREBF2 were normalised to B2M as a loading control. Data shown represents the mean of at least three individual biological replicates ± SEM. Asterisks indicate statistical significance. P values calculated using paired student's t tests and n number for each gene are shown. (B) mRNA expression levels of SREBP target genes SCD and FASN were normalised to B2M as a loading control. Data shown is the mean of three individual biological replicates ± SEM.

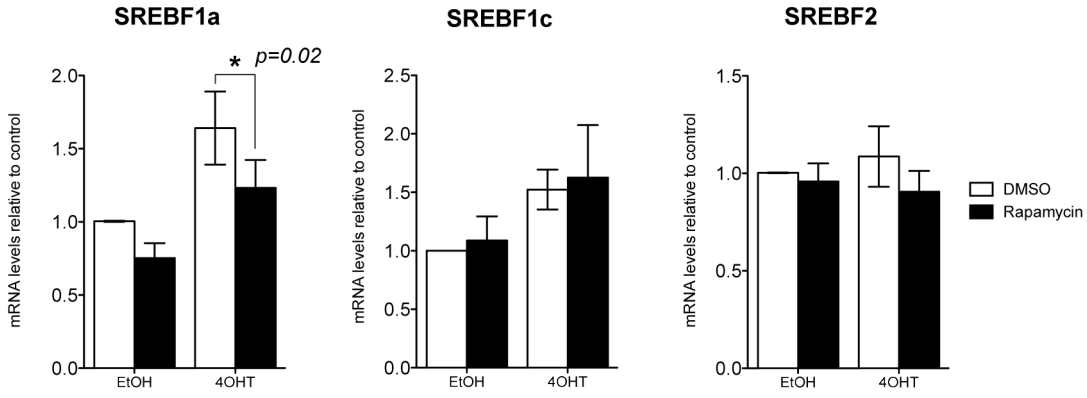

Figure 5-4: Short-term Akt activation leads to an increase in SREBF1a and SREBF1c mRNA but not SREBF2 mRNA expression.
RPE-Akt-ER cells were cultured overnight in 1% LPDS. The following day cells were pre-treated with vehicle (DMSO) or rapamycin for 30 minutes before being treated with solvent (EtOH) or 100 nM 4-OHT for 2 hours. RNA was extracted and used for RT-QPCR analysis. Expression levels of SREBF1a, SREBF1c and SREBF2 mRNA were normalied to B2M as a loading control. Data shown is the mean of 3 independent biological replicates ± SEM. Asterisk indicates statistical significance. P values were calculated using student's paired t tests.

5.3 Amino acid stimulation increases mSREBP1 nuclear accumulation and this may be dependent on mTORC1 activity

Having established that pharmacological inhibition of mTORC1 is sufficient to decrease nuclear accumulation of mSREBP1, it was investigated whether activation of mTORC1 was able to increase mSREBP1 nuclear accumulation. mTORC1 is a mediator of nutrient response and its activity has been shown to be positively regulated by amino acids. Amino acid stimulation leads to increased co-localisation of mTORC1 with GTP-loaded Rheb and therefore increases mTORC1 activity (Kim et al., 2008; Sancak et al., 2008). In order to investigate whether activation of mTORC1 is sufficient to regulate SREBP1, the effect of amino acid stimulation on the accumulation of nuclear mSREBP1 was analysed.

RPE-hTERT cells were serum starved for 16 hours and then starved of amino acids for the final 3 hours, before amino acids were added back to the medium for 1 hour. Whole cell lysates and nuclear fractions were analysed by Western blotting. Stimulation with

amino acids increased nuclear accumulation of mSREBP1 (Figure 5.5 A), as well as flSREBP1 in whole cell lysate (Figure 5.5 B). Increased S6 phosphorylation was observed in response to amino acid stimulation, consistent with increased mTORC1 activity (Figure 5.5 B). Interestingly, phosphorylation of Akt on serine 473 was decreased following amino acid stimulation (Figure 5.5 B), indicating that increased SREBP1 expression in response to amino acid stimulation is independent of Akt activation.

In order to confirm that this increase was indeed dependent on mTORC1 activity, RPE-hTERT cells were stimulated with amino acids in the presence or absence of rapamycin. In the absence of amino acids, rapamycin was not able to further reduce the levels of nuclear mSREBP1 (Figure 5.6A). Upon stimulation with amino acids, levels of mSREBP1 in the nucleus were increased, supporting the observations in Figure 5.5. Rapamycin had a moderate effect on the levels of nuclear mSREBP1 in the amino acid stimulated cells (Figure 5.6A), indicating that this increase may be mTORC1-dependent. In addition, increased levels of mSREBP1 and flSREBP1 were observed in whole cell lysates following stimulation with amino acids, although the effects of rapamycin on both mSREBP1 and flSREBP1 are more difficult to interpret, as the samples in this particular experiment do not appear to be accurately loaded (Figure 5.6B). Although this experiment was performed twice, it should be repeated in order to confirm that mTORC1 activity is indeed required for the increase in mSREBP1 observed in response to amino acid stimulation. It would then be possible to determine if these differences are statistically significant using densitometry. Phosphorylation of Akt in amino acid stimulated cells was decreased, again suggesting that Akt is inactive under these conditions (Figure 5.6B). Together, these data indicate that amino acid stimulation results in an increase in nuclear mSREBP1 and that this may be dependent on mTORC1 activity. However, it cannot be ruled out that amino acids are capable of increasing nuclear mSREBP1 accumulation in an Akt/mTORC1-independent manner and further experiments would be required to show this.

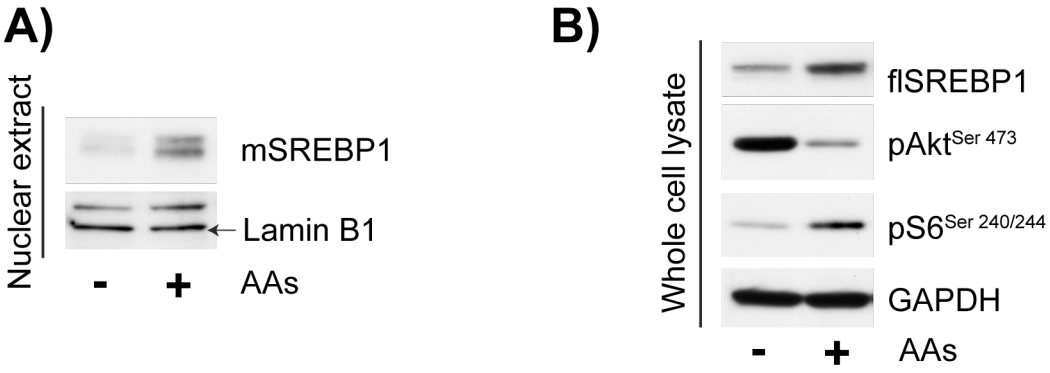

Figure 5-5: Amino acid stimulation and activation of mTORC1 is sufficient to induce mSREBP1 nuclear accumulation.
RPE-hTERT cells were serum starved overnight and starved of amino acids for 3 hours. Amino acids were then added back for 1 hour and cells were subjected to nuclear fractionation and analysis by Western blot. (A) Nuclear fraction showing expression of mSREBP1. Lamin B1 is shown as a loading control. (B) Whole cell lysates showing expression of flSREBP1 and phosphorylation of Akt (pAkt^{Ser473}). Phosphorylation of S6 (pS6$^{Ser240/244}$) is shown as a control of mTORC1 activity. GAPDH is shown as a loading control.

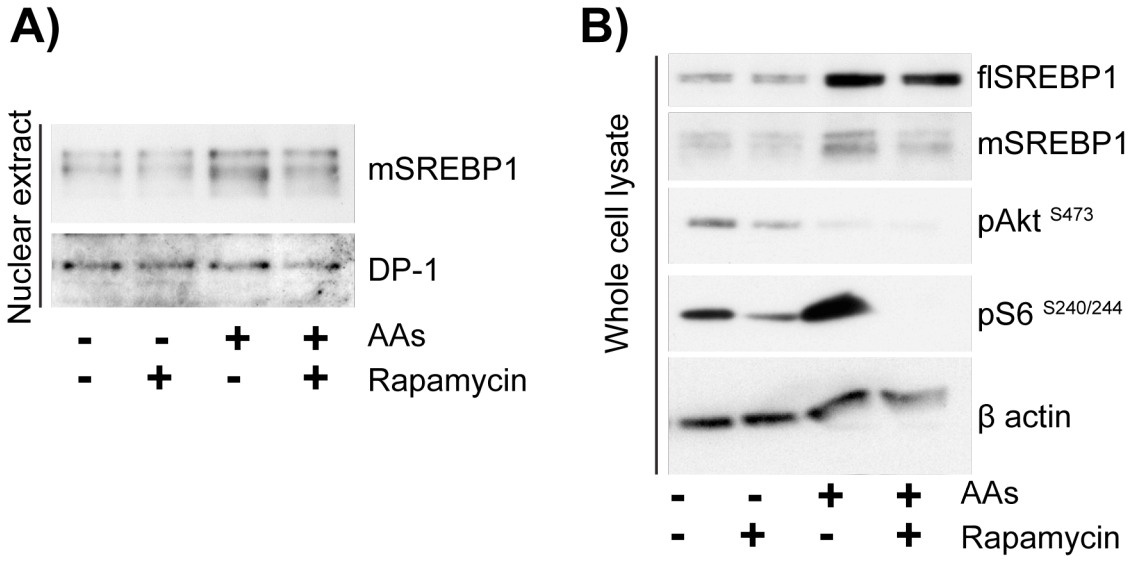

Figure 5-6: Amino acid induced mSREBP1 nuclear accumulation may be dependent on mTORC1 activity.
RPE-hTERT cells were serum starved overnight and starved of amino acids for 1 hour. Cells were pre-treated with vehicle (DMSO) or rapamycin (50 nM) for 30 minutes before amino acids were added back for 1 hour. Cells were harvested and subjected to nuclear fractionation. (A) Nuclear fraction showing expression of mSREBP1. DP1 is shown as loading control. (B) Whole cell lysates from cells treated in parallel to those in (A) showing expression of flSREBP1, mSREBP1 and phosphorylation of Akt (pAkt^{Ser473}). Phosphorylation of pS6$^{S240/244}$ is shown as a control for mTORC1 activity. β actin is shown as a loading control.

5.4 S6 kinases are not required for SREBP1 processing

Since it remains unclear whether mTORC1 is acting directly on SREBP or via a downstream signalling component following Akt activation, the requirement for the mTORC1 target S6K in SREBP processing was investigated.

5.4.1 Silencing of S6K does not prevent the Akt-dependent induction of mSREBP1 accumulation

RPE-Akt-ER cells were transiently transfected with siRNAs targeting mTOR, 4EBP1, S6K1, S6K2 and a combination of sequences targeting both S6K1 and S6K2. Cells were cultured in 1%LPDS and Akt was activated in the presence or absence of rapamycin. Whole cell lysates were analysed by Western blotting for the accumulation of mSREBP1. Akt activation induced accumulation of mSREBP1 (Figure 5.7, lanes a and b). Silencing of mTOR blocked the Akt-dependent induction of mSREBP1 and reduced expression of the SREBP target gene ACLY (Figure 5.7, lanes c and d). FASN was still induced following Akt activation, this could be as a result of incomplete mTOR silencing, as indicated by residual phosphorylation of S6 (Figure 5.7, lanes c and d). This could also account for the lack of complete loss of mSREBP1 in response to mTOR silencing. Depletion of the mTORC1 downstream target 4EBP1 did not result in a reduction in the Akt-dependent increase in mSREBP1 accumulation or the increase in ACLY or FASN expression (Figure 5.7, lanes e and f), indicating that 4EBP1 does not play a role in the regulation of SREBP1. However, the silencing efficiency of 4EBP1 was not investigated. Silencing of S6K1 did not affect the Akt-dependent induction of SREBP1 accumulation, and phosphorylation of S6 remained unaffected (Figure 5.7, lanes g and h). This could be a result of S6K2 compensating for loss of S6K1 activity as S6K2 has been shown to compensate for loss of S6K1 activity in mice harbouring a deletion of the S6K1 gene (Shima et al., 1998). In contrast, S6K2 silencing alone reduced Akt-dependent accumulation of mSREBP1 as well as FASN and ACLY induction and reduced S6 phosphorylation (Figure 5.7, lanes i and j). Combined silencing of both S6K1 and S6K2 reduced S6 phosphorylation but increased overall expression of mSREBP1 (Figure 5.7, lanes k and l). It is unlikely that co-silencing of S6K1 with S6K2 causes a re-activation of S6K2 function since the reduction in of S6

phosphorylation was unaffected. Silencing of any of the TOR signalling components investigated here did not affect Akt-dependent induction of flSREBP1 expression, suggesting that Akt and mTORC1 may regulate flSREBP1 and mSREBP1 in different ways.

5.4.2 Genetic ablation of S6 kinases does not prevent SREBP1 processing

It is possible that the residual phosphorylation of S6 following silencing of S6K1 and S6K2 may be sufficient to regulate SREBP1 downstream of mTORC1. Primary mouse embryonic fibroblasts (MEFs) from mice carrying a deletion in both S6K1 and S6K2 genes, in which S6 phosphorylation is completely abolished, were used in order to investigate this further.

It was first determined whether SREBP1 was sensitive to rapamycin treatment in immortalised MEFs which were cultured in 10% FCS or 1% LPDS as a positive control for SREBP1 processing. Cells were treated either with insulin or with rapamycin for 24 hours to induce Akt signalling or mTORC1 inhibition, respectively. Accumulation of mSREBP1 in response to insulin treatment was observed in cells cultured in 1% LPDS but not full serum (Figure 5.8, lanes a-d). Phosphorylation of Akt on serine 473 was increased in 1% LPDS but not 10% FCS (Figure 5.8, lanes a-d), confirming activation of Akt. It is likely that full serum already induces maximal activation of Akt, and therefore no change in phosphorylation levels are observed. Treatment of cells with rapamycin resulted in decreased mSREBP1 levels in both serum conditions, although a more potent effect of rapamycin treatment on mSREBP1 was observed in cells cultured in 1% LPDS (Figure 5.8, lanes e-h). Phosphorylation of S6 on serine 240/244 was abolished by rapamycin treatment in both serum conditions (Figure 5.8, lanes e-f). A slight increase in flSREBP1 was observed in response to insulin treatment in cells cultured in 1% LPDS (Figure 5.8, lanes a and b) and rapamycin treatment partially reduced flSREBP1 levels in cells cultured in 1% LPDS (Figure 5.8, lanes e and f). These data indicate that regulation of the Akt-mTORC1-SREBP1 signalling axis observed in RPEs is also found in immortalised MEFs.

Next the effect of genetic ablation of S6K1 and S6K2 on mSREBP1 accumulation was investigated. Primary MEFs from mice in which both genes have been deleted (Pende et al., 2004) were cultured in 10% FCS or 1% LPDS and treated with rapamycin for 24 hours. Whole cell lysates were analysed by Western blotting. Primary wild-type MEFs from wild-type littermates were treated in parallel. Wild-type cells cultured in 1% LPDS showed an accumulation of mSREBP1, although rapamycin treatment did not affect this (Figure 5.9, lanes a and b). Low levels of mSREBP1 were present in cells cultured in 10% FCS, although a non-specific band was detected by the SREBP1 antibody (Figure 5.9, lanes c and d). No effect of rapamycin on mSREBP1 was observed in these cells, despite phosphorylation of S6 on being completely abolished upon rapamycin treatment (Figure 5.9, lanes a-d). MEFs lacking S6K1 and S6K2 cultured in 1% LPDS still showed accumulation of mSREBP1, indicating that processing of SREBP1 was still intact in these cells. The absence of S6 kinases was confirmed as no S6 phosphorylation was detected in these cells (Figure 5.9, lanes e-h). Processed mSREBP1 was still detected in S6K knockout cells cultured in 10% FCS (Figure 5.9, lanes g and h), although the bands detected by the SREBP1 antibody were altered in the same manner as in the wild-type cells.

When taken together with the silencing data in the RPE-Akt-ER cells, these data suggest that S6 kinases are not required for SREBP1 processing, since mSREBP1 is still detected in cells lacking both S6K1 and S6K2. However, it is possible that S6 kinases contribute to mSREBP1 accumulation under conditions of mTORC1 hyperactivation.

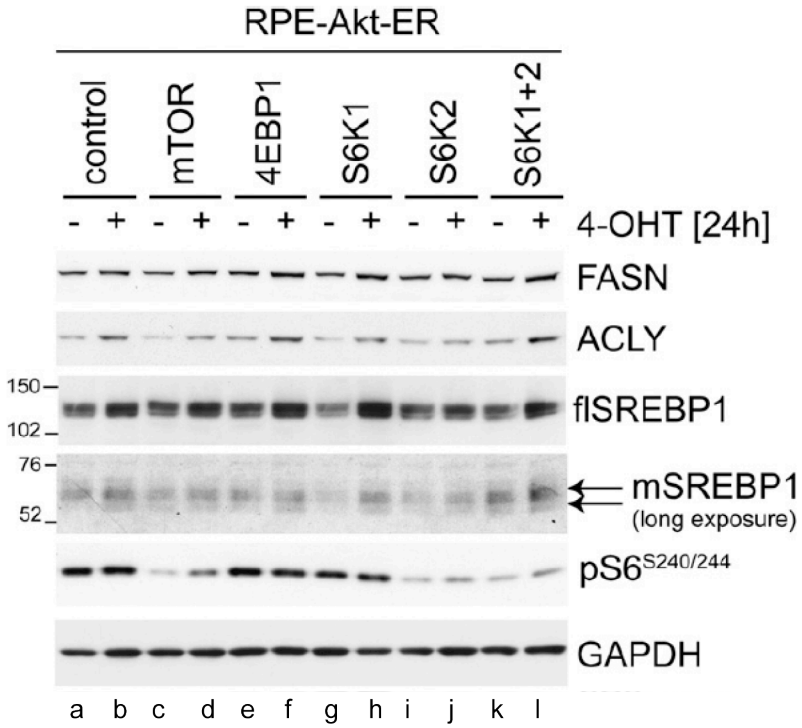

Figure 5-7: Silencing of S6K1 or S6K2 does not block Akt-dependent accumulation of mature SREBP.
RPE-myrAkt-ER cells were transfected with siRNA oligonucleotides targeting the expression of mTOR, 4EBP1, S6K1, S6K2 or a mixture of the oligonucleotides targeting S6K1 and S6K2. Three days post-transfection, cells were transferred to medium supplemented with 1% lipoprotein deficient serum (LPDS) and treated with 100 nM 4-hydroxytamoxifen (4-OHT) or solvent (ethanol) for 24 h. Whole cell extracts were analysed by Western blotting using antibodies against the proteins indicated. GAPDH was used as a loading control. This experiment was performed by B. Griffiths (LRI, GEA). Reprinted from Advances in Enzyme Regulation, (Lewis et al., 2011), © 2011, with permission from Elsevier.

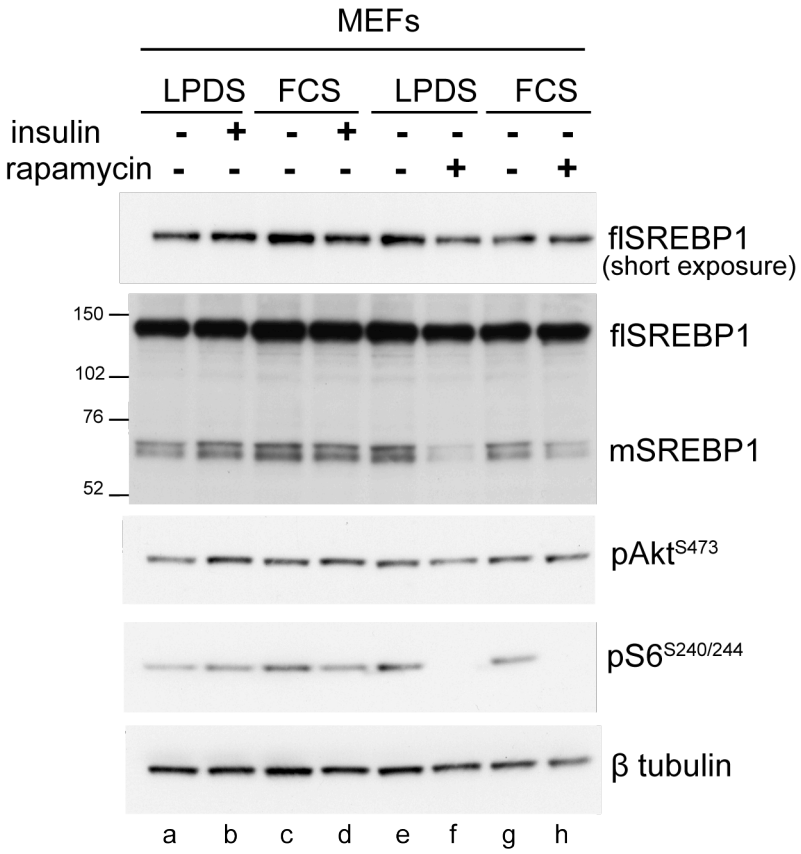

Figure 5-8: Rapamycin reduces mSREBP1 accumulation in immortalised MEFs.
Immortalised MEFs were grown in medium containing 10% FCS or 1% LPDS in the presence or absence of rapamycin (50 nM) or insulin (10 mg/ml) for 24 h. Cells were treated with 25 mg/ml ALLN for 2 h before harvesting. Whole cell lysates were analysed by Western blot using antibodies against the proteins indicated. β tubulin was used as a loading control. Figure adapted from Advances in Enzyme Regulation, (Lewis et al., 2011), © 2011, with permission from Elsevier.

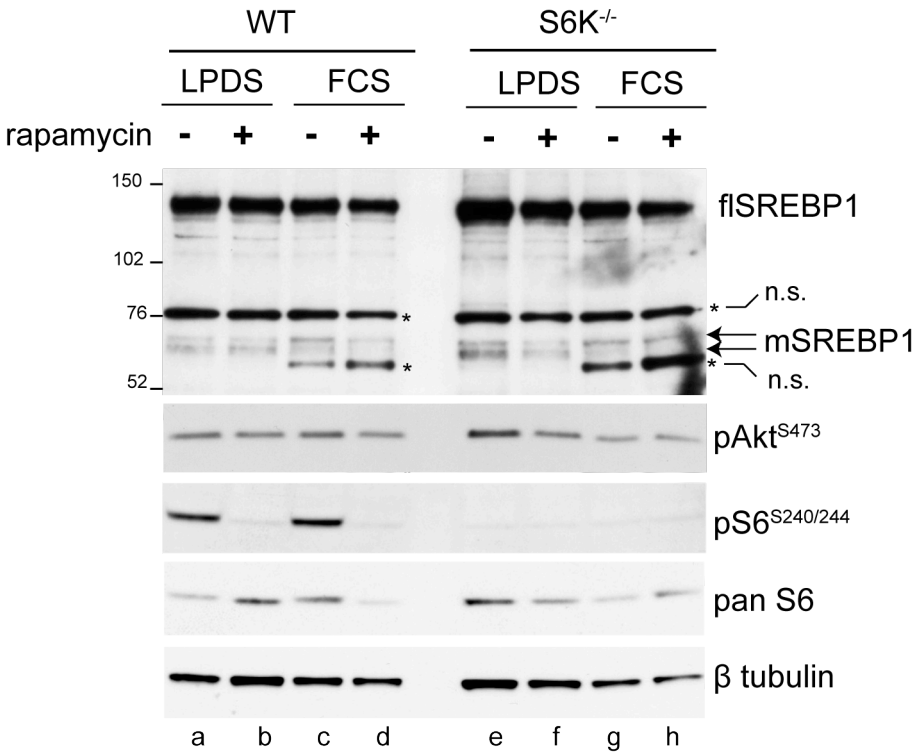

Figure 5-9: Genetic deletion of S6K does not prevent processing of SREBP1.
Primary MEFs from WT and S6K1/S6K2 double knockout MEFs were grown in medium containing 10% FCS or 1% LPDS and treated with rapamycin (50 nM) for 24 h. Cells were treated with 25 mg/ml ALLN for 2 h before harvesting. Whole cell lysates were analysed by Western blotting using antibodies against the proteins indicated. β tubulin was used as a loading control. Figure adapted from Advances in Enzyme Regulation, (Lewis et al., 2011), © 2011, with permission from Elsevier.

5.5 Regulation of SREBP processing components by Akt and mTORC1

The results presented so far in this chapter have focussed on the nuclear accumulation of mSREBP1 in response to activation of Akt and mTORC1. However, it still remains unclear whether Akt and mTORC1 are directly regulating SREBP processing in the RPE-Akt-ER system. In order to address the role of Akt and mTORC1 on SREBP processing in RPE-Akt-ER cells, the effects of Akt activation and mTORC1 inhibition on components required for SREBP processing were investigated.

5.5.1 mTORC1 influences SCAP mRNA expression

The SREBP cleavage activating protein (SCAP) is required for the ER-Golgi translocation of the precursor SREBP protein under low sterol conditions (Nohturfft et al., 1999; Nohturfft et al., 2000; Sakai et al., 1997). RPE-Akt-ER cells were cultured in 10% FCS or 1% LPDS and treated with solvent (EtOH) or 4-OHT in the presence or absence of rapamycin for 24 hours. Whole cell lysates were analysed by Western blotting and total RNA was analysed by RT-QPCR (Figure 5.10). As a positive control for Akt activation and mTORC1 inhibition, lysates were analysed for phospho-Akt and phospho-S6, as well as mSREBP1 accumulation. Figure 5.10 B shows that activation of Akt resulted in an increase in Akt phosphorylation on serine 473 and treatment with rapamycin abolished S6 phosphorylation (Figure 5.10 B). In addition, levels of mSREBP1 were increased in response to Akt activation and rapamycin treatment reduced mSREBP1 levels.

Activation of Akt or treatment with rapamycin did not alter SCAP protein levels (Figure 5.10 A). Interestingly, although mRNA expression levels of SCAP were not affected by Akt activation, short-term rapamcyin treatment (2 hours; Figure 5.10 C) and long-term treatment (24 hours; Figure 5.10 D) moderately reduced levels of SCAP mRNA in 4-OHT treated cells. As observed in Chapter 4 (Figure 4.4), a reduction in SCAP mRNA does not result in a reduction in SCAP protein levels, suggesting that SCAP is a very stable protein. It is therefore unlikely that the effect of mTORC1 inhibition on mSREBP1 is occurring through loss of SCAP mRNA. However, a slight shift in SCAP mobility was observed between cells cultured in 10% FCS and 1% LPDS and may be lost following rapamycin treatment (Figure 5.10 A), indicating that mTORC1 may influence the conformational change that SCAP protein undergoes in response to low sterol conditions. These data indicate that increased accumulation of mSREBP1 in response to Akt activation and the decrease in response to mTORC1 inhibition do not occur through changes in SCAP expression.

5.5.2 Activation of Akt and inhibition of mTORC1 do not prevent activity of the proteases required for SREBP cleavage

The site-1 (S1P) and site-2 (S2P) proteases are both required for the regulation of the two-step proteolytic cleavage that SREBP undergoes in the Golgi. It was therefore investigated whether Akt or mTORC1 could affect the activity of these proteins. Activating transcription factor 6-alpha (ATF6α) is regulated by S1P and S2P cleavage in response to ER stress (Shen and Prywes, 2005; Ye et al., 2000). In order to investigate whether Akt or mTORC1 regulate the activity of S1P or S2P, cells were treated with tunicamycin, an inducer of ER stress and a known activator of ATF6α processing. RPE-Akt-ER cells were cultured in 1% LPDS for 16 hours before they were pre-treated with vehicle or rapamycin for 30 minutes before being treated with vehicle or tunicamycin for a further 30 minutes. Akt activation was then induced for 5 hours. Whole cell lysates were analysed for ATF6α cleavage by Western blotting. Akt activation alone did not induce ATF6α cleavage (Figure 5.11, lanes a and b). Cleaved ATF6α protein (N- nuclear fragment) was observed in all cells treated with tunicamycin, regardless of Akt activation status (Figure 5.11, lanes c-f), indicating that Akt activation does not influence the activity of S1P or S2P. Inhibition of mTORC1 through treatment with rapamycin did not alter levels of activated ATF6α (N) (Figure 5.11, lanes e and f). This confirms that inhibition of mTORC1 does also not regulate the activity of the proteases required for ATF6α and SREBP cleavage. In addition to the formation of the 50 kDa nuclear ATF6α fragment (N), treatment with tunicamycin alone also resulted in a decrease in the glycosylated precursor protein (P) and caused an increase in the levels of non-glycosylated precursor (P*) protein (Figure 5.11, lanes c and d). This corresponds to the movement of ATF6α from the ER to the Golgi upon induction of ER stress (Shen and Prywes, 2005; Ye et al., 2000). These data indicate that Akt or mTORC1 do not influence the proteolytic activity of the S1P and S2P proteases.

5.5.3 mTORC1 inhibition reduces the mRNA expression of INSIG1 but not INSIG2

The insulin-induced genes INSIG1 and INSIG2 also regulate the processing and activation of SREBPs. In sterol-saturated conditions, a conformational change in SCAP

results in its interaction with INSIG proteins, which prevents translocation of the SCAP/SREBP complex and retains SREBP in the ER (Brown et al., 2002; Yang et al., 2002). It was therefore investigated whether levels of INSIG are influenced by Akt activation and/or mTORC1 inhibition. Due to the lack of sensitive INSIG antibodies, mRNA expression of INSIG1 and INSIG2 was determined in response to Akt activation and inhibition of mTORC1. RPE-Akt-ER cells were cultured in 1% LPDS and treated with vehicle (EtOH) or 4-OHT in the presence or absence of rapamycin for 24 hours. Total RNA was analysed by RT-QPCR analysis. Expression of INSIG1 was significantly increased following Akt activation (Figure 5.12 A) and this induction was significantly reduced upon rapamycin treatment (Figure 5.12 A). However, INSIG1 is also an SREBP target gene (Horton et al., 2003). Therefore, the change in expression of INSIG1 following long-term Akt activation and mTORC1 inhibition is most likely due to regulation of SREBP activity. Expression of INSIG2 mRNA did not change (Figure 5.10 A), indicating both that Akt and mTORC1 are not signalling through INSIG2 expression and that INSIG2 is not an SREBP target gene.

Since SREBP transcriptionally regulates INSIG1 it was next investigated whether short-term Akt activation and mTORC1 inhibition influenced mRNA expression levels of the INSIGs. RPE-Akt-ER cells were cultured in 1% LPDS for 16 hours and were pre-treated with rapamycin for 30 minutes before being treated with solvent (EtOH) or 4-OHT for 2 hours. mRNA expression of INSIG1 and INSIG2 was analysed. Akt activation or rapamycin treatment did not alter mRNA expression of INSIG2 (Figure 5.12 B). In addition, Akt activation significantly increased INSIG1 expression. This could indicate that Akt activation results in increased transcriptional activity of SREBPs after only 2 hours (Figure 5.12 B). In contrast, rapamycin treatment did not significantly reduce mRNA expression of INSIG1, indicating that inhibition of mTORC1 is not able to block the transcriptional activity of SREBP following short-term inhibition. However, other regulators of INSIG1 expression in response to Akt activation cannot be ruled out.

.

5.5.4 Akt and mTORC1 do not regulate processing of exogenous SREBP2

It remains unclear whether endogenous SREBP processing is regulated by Akt or mTORC1. Therefore the effects of Akt and mTORC1 on exogenous SREBP were investigated. Since the general mechanisms of SREBP processing are conserved between the different isoforms, it was investigated whether Akt or mTORC1 influence the processing of an exogenous PLAP-SREBP2 fusion construct. pCMV-PLAP-SREBP2(513-1141) encodes a fusion protein in which the signal peptidase cleavage site and catalytic domain of placental alkaline phosphatase (PLAP) is joined to the luminal loop of SREBP2 on the NH_2-terminal side of the S1P cleavage site (see Figure 5.13 A) (Sakai et al., 1998). Expression of this fusion protein results in the catalytic domain of PLAP being located in the ER lumen, flanked on either side by the signal peptidase and S1P cleavage sites (Sakai et al., 1998). Low sterol conditions lead to cleavage of this fusion protein at both sites, resulting in PLAP secretion into the medium where its activity can be readily detected. Sakai and colleagues have demonstrated that in the absence of exogenous SCAP, relatively little PLAP is secreted into the medium. Expression of increasing amounts of exogenous SCAP results in a linear increase in the amount of PLAP secretion indicating an increase in the amount of PLAP-SREBP2 processing (Sakai et al., 1998).

Using this system to assay SREBP2 cleavage, no PLAP activity could be detected in RPE-Akt-ER cells (data not shown). This may be because the PLAP-SREBP2 construct was not successfully expressed in RPE cells. Instead, U2OS-Akt-ER cells were co-transfected with pCMV-PLAP-SREBP2(513-1141) and increasing amounts of an exogenous SCAP expression construct (pCMV-SCAP), along with the renilla luciferase control (pRL-SV40). Cells were cultured in 0.5% BSA to induce sterol starvation and the PLAP activity in the cell culture medium was analysed using a chemiluminescence PLAP assay. PLAP activity was normalised to renilla luciferase activity as a control. Expression of PLAP-SREBP2 alone resulted in very little PLAP activity (Figure 5.13 B), whereas co-expression of PLAP-SREBP2 with increasing amounts of SCAP (0.5-1.5 µg) produced a dose-dependent increase in PLAP activity, indicating that PLAP-SREBP2 was cleaved in these cells (Figure 5.13 B). It was next investigated whether PLAP-SREBP2 cleavage was induced in U2OS-Akt-ER cells by sterol starvation alone.

Cells were co-transfected with pCMV-PLAP-SREBP2(513-1141) and pCMV- SCAP and cultured either in full serum (10% FCS) or 0.5% BSA. Cells cultured in full serum produced less PLAP activity than cells cultured in 0.5% BSA (Figure 5.13 C), indicating that sterol starvation was sufficient to induce PLAP-SREBP2 cleavage in these cells.

In order to address whether Akt activation and mTORC1 inhibition could affect PLAP-SREBP2 processing, U2OS-Akt-ER cells were co-transfected with pCMV-PLAP-SREBP2 and pCMV-SCAP, along with the renilla luciferase control, and cultured in 0.5% BSA. Cells were treated with vehicle (EtOH) or 4-OHT in the presence or absence of the mTORC1 inhibitor rapamycin for 24 hours. Conditioned medium was then analysed for PLAP activity and this was normalised to renilla luciferase activity. There was no clear effect on the amount of PLAP activity in cells treated with EtOH or 4-OHT, nor with rapamycin treatment on PLAP activity (Figure 5.13 D).

Since the inability of Akt or mTORC1 to affect PLAP-SREBP2 cleavage in U2OS-Akt-ER cells might be due to the possibility that SREBP2 is not regulated by this pathway in this cell line. In order to address whether Akt and mTORC1 influenced SREBP2 expression levels in U2OS cells, U2OS-Akt-ER cells were treated as described above and whole cell lysates were analysed for levels of flSREBP2 and processed SREBP2 (pSREBP2) by Western blotting. Levels of pSREBP2 were low in cells cultured in 10% FCS, and levels of flSREBP2 did not change in response to Akt activation (Figure 5.13 E, lanes a and b). In contrast, cells cultured in 0.5% BSA showed an increase in pSREBP2 and a decrease in flSREBP2 compared to cells cultured in full serum (Figure 5.13 E, compare lanes a and b with c and d), indicating that low sterol conditions induce SREBP2 processing in these cells However, activation of Akt did not affect levels of pSREBP2 or flSREBP2 (Figure 5.13 E, lanes c and d). In addition, treatment of the cells with rapamycin had no effect on levels of pSREBP2. When taken together, these data suggest that SREBP2 is not regulated downstream of Akt or mTORC1 in U2OS cells. Furthermore, these data indicate that Akt and mTORC1 do not target the common

components of SREBP processing machinery that are conserved between SREBP1 and SREBP2.

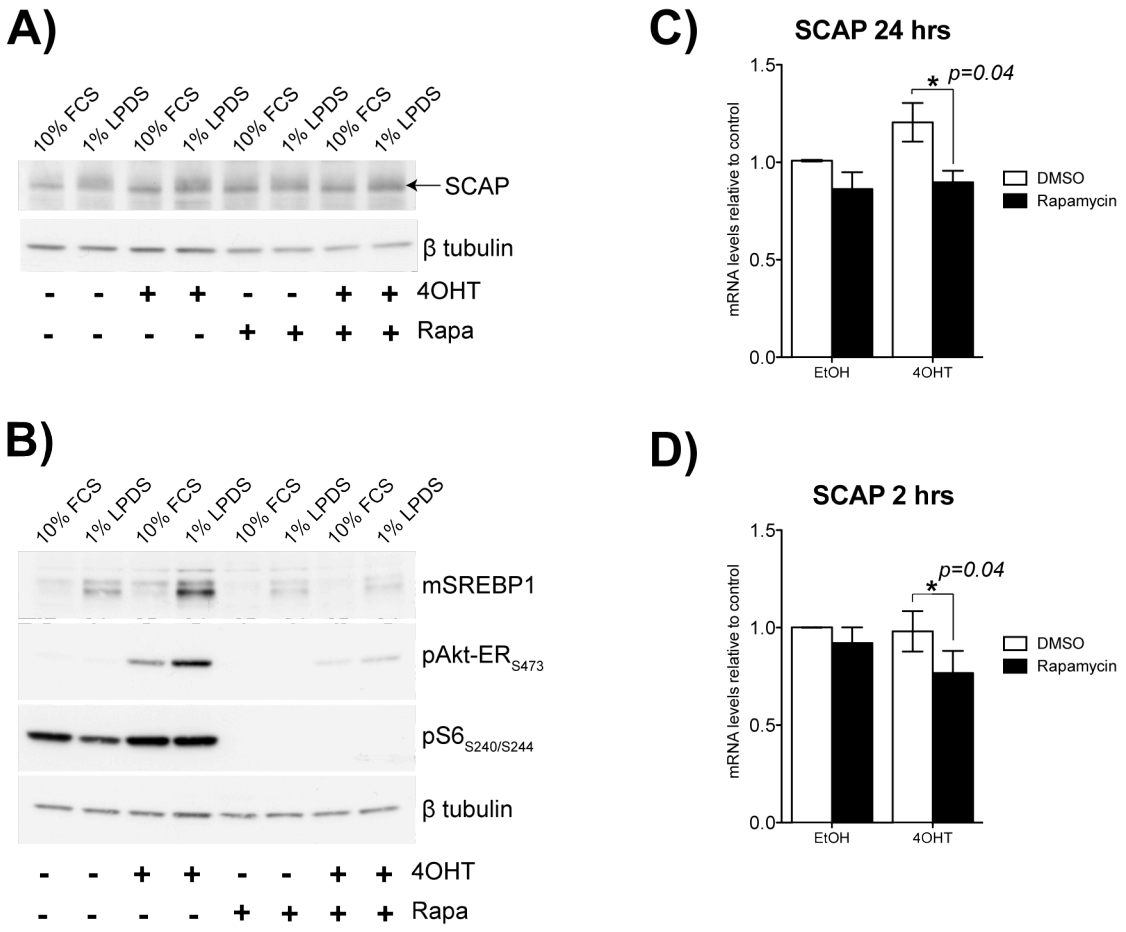

Figure 5-10: Akt and mTORC1 do not affect mSREBP1 levels by altering SCAP expression.
RPE-Akt-ER cells were cultured either in 10% FCS or medium supplemented with 1% LPDS. Cells were treated with solvent (EtOH) or 100 nM 4-OHT in the presence or absence of rapamycin (50 nM) for 24 hours. (A) Whole cell extracts were analysed by Western blotting for SCAP expression. β tubulin was used as a loading control. (B) Whole cell extracts from cells treated as in (A) were analysed by Western blotting for expression of mSREBP1, pAkt-ER^{Ser473} and pS6$^{Ser240/244}$ as a positive control for inhibitor function. β tubulin was used as a loading control. (C) RNA extracted from cells cultured in 1% LPDS and treated as in (A) and (B) was analysed by RT-QPCR for SCAP expression. Data shown is the mean of three independent biological replicates ± SEM normalized to B2M expression as a loading control. Asterisk indicates statistical significance. P values were calculated using a paired student's t test. (D) RPE-Akt-ER cells were cultured in 1% LPDS gor 16 hours. Cells were pre-treated with rapamycin (50 nM) for 30 minutes before being treated with either solvent (EtOH) or 100 nM 4-OHT for 2 hours. RNA was extracted and used for RT-QPCR analysis of SCAP expression. Data shown is the mean of three independent biological replicates ± SEM normalized to B2M expression as a loading control. Asterisk indicates statistical significance. P values were calculated using a paired student's t test.

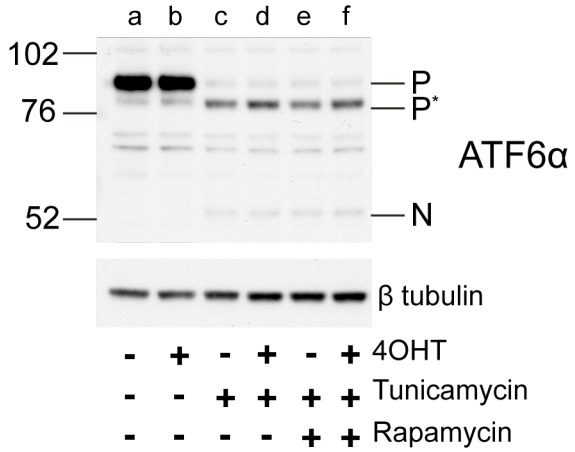

Figure 5-11: Akt activation and mTORC1 inhibition do not alter the activity of proteases required for cleavage activation of SREBPs.
RPE-Akt-ER cells were cultured in 1% LPDS overnight. Cells were then pre-treated with rapamycin (50 nM) for 30 minutes before being treated either with vehicle (DMSO) or tunicamycin (5 µg/ mL) for a further 30 minutes. Akt activation was induced by addition of 100 nM 4-OHT for 5 hours. Cells were treated with MG-132 (25 µM) for 1.5 hours prior to lysis. Whole cell extracts were analysed by Western blotting for cleavage of ATF6α. β tubulin was used as a loading control. Molecular weight markers are shown (left). P: Unprocessed precursor protein; P*: Unprocessed non-glycosylated precursor protein; N: Processed (nuclear) ATF6α.

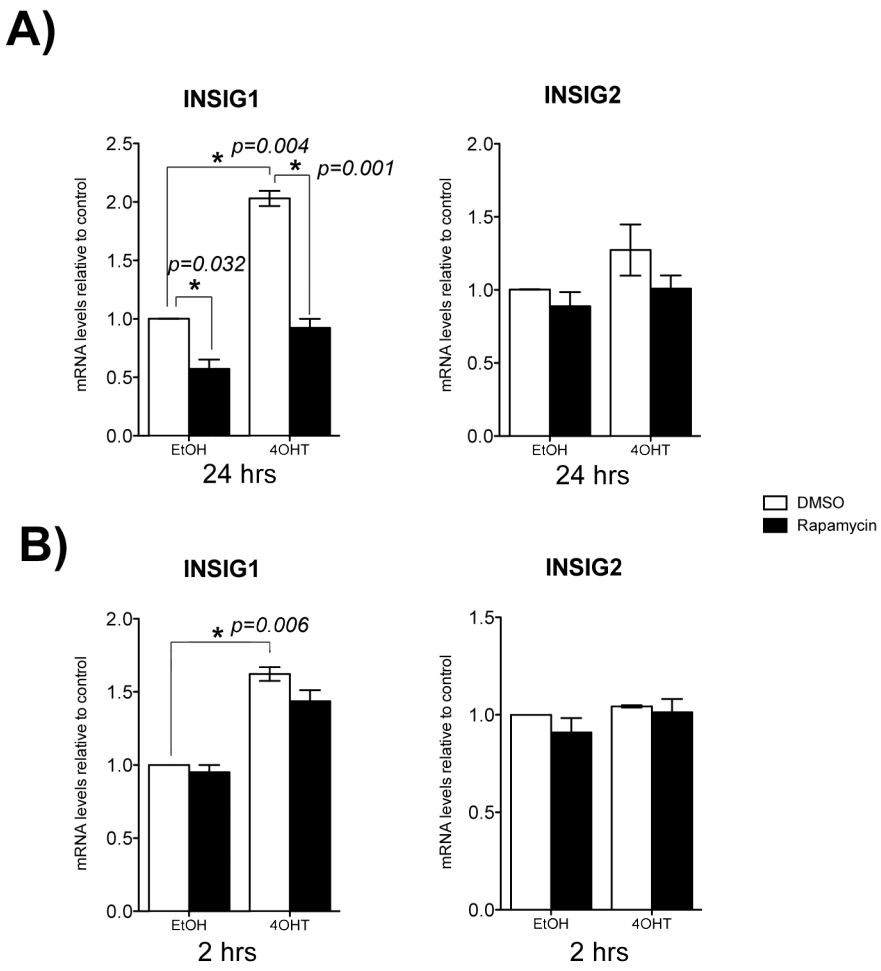

Figure 5-12: Inhibition of mTORC1 reduces mRNA expression of INSIG1 but not INSIG2. RPE-Akt-ER cells were cultured in 1% LPDS and treated with vehicle (EtOH) or 100 nM 4-OHT in the presence or absence of rapamcyin for 24 hours (A) or 2 hours (B). RNA was extracted and used for RT-QPCR analysis of INSIG1 and INSIG2 expression. Data shown is the mean of three biological replicates ± SEM normalised to B2M expression. Asterisks indicate statistical significance. P values were calculated using a paired student's t test.

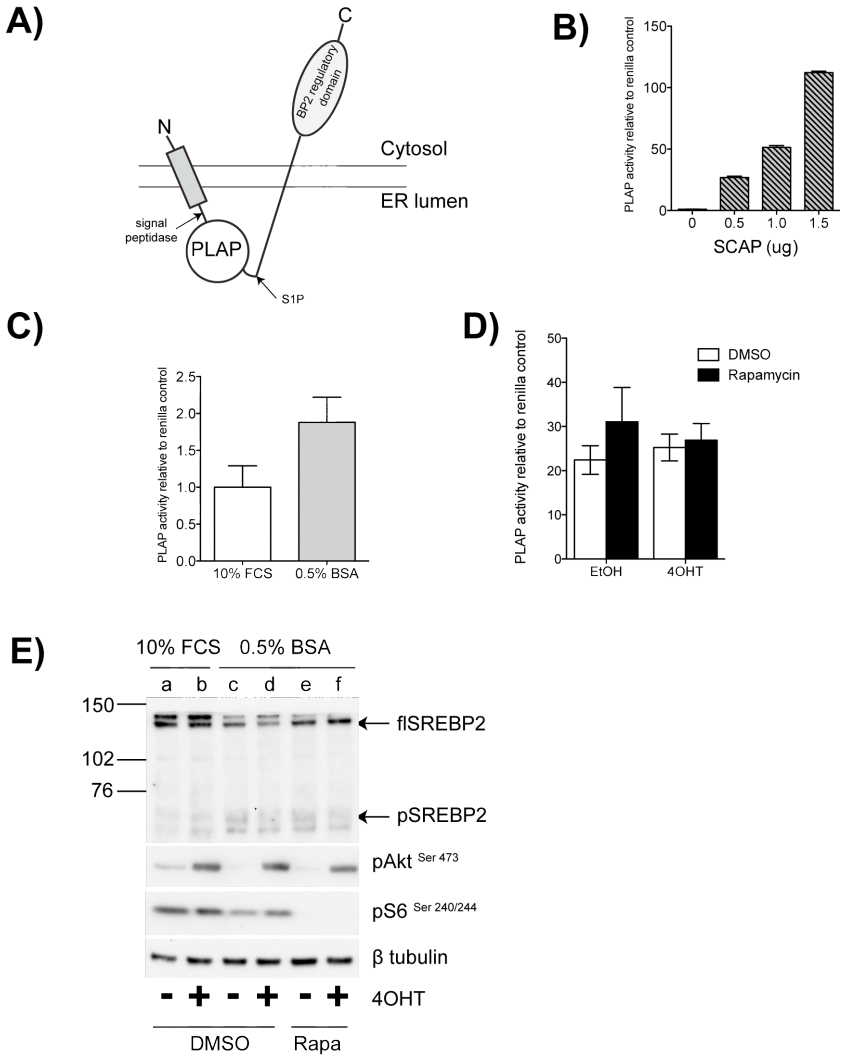

Figure 5-13: Akt and mTORC1 do not regulate SREBP2 in U2OS-Akt-ER cells.
(A) Schematic representation of the pCMV-PLAP-SREBP2 construct described in (Sakai et al., 1998). PLAP: placental alkaline phosphatase. (B) U2OS-Akt-ER cells were transiently transfected with pCMV-PLAP-SREBP2 and increasing amounts of pCMV-SCAP (0.5 µg- 1.5 µg). Cells were cultured in 0.5% BSA overnight and conditioned medium was assayed for PLAP activity and normalised to the renilla luciferase control. Data shown is the mean of three technical replicates ± SEM. (C) U2OS-Akt-ER cells were co-transfected with pCMV-PLAP-SREBP2 and pCMV-SCAP. Cells were cultured in either 10% FCS or 0.5% BSA overnight. PLAP activity in the medium was measured as described above. Data shown is the mean of three independent biological replicates ± SEM. (D) US2S-Akt-ER cells were co-transfected with PLAP-SREBP2 and SCAP and cultured in 0.5% BSA. Cells were treated with vehicle (EtOH) or 100 nM 4-OHT for 24 hours in the presence or absence of rapamycin (50 nM). Data shown is the mean of three independent biological replicates ± SEM. (E) Whole cell lysates from U2OS-Akt-ER cells treated as in D were analysed for expression of flSREBP2 and processed SREBP2 (pSREBP2). β tubulin was used as a loading control.

5.6 Analysis of SREBP1 sub-cellular localisation in response to Akt activation and mTORC1 inhibition

The transcriptional activity of mSREBP is dependent on the nuclear localisation of the protein. It is possible that Akt and mTORC1 influence the sub-cellular localisation of mSREBP. In order to address this possibility, confocal microscopy was used to determine subcellular localisation of SREBP1. Previous attempts to visualise endogenous SREBPs in RPE cells using the antibody recognising the 2A4 epitope were not successful (C.Santos, GEA, unpublished observations). Therefore, SREBP1 was visualised in U2OS-Akt-ER cells using an alternative N-terminal SREBP1 antibody (K10). Cells were seeded onto coverslips and cultured in 0.5% BSA and treated with solvent (EtOH) or 4-OHT in the presence or absence of rapamycin for 24 hours. As a negative control of mSREBP1 nuclear localisation, cells were cultured in 10% FCS in parallel. Cells were fixed and stained with DAPI (nuclei) and anti-SREBP1 (K-10) and imaged using confocal microscopy. The cytoplasmic localisation of SREBP1 was not clear due to high background staining. However, it was observed that serum starvation (0.5% BSA) resulted in a slight increase in the intensity of SREBP1 staining in the nucleus when compared with cells cultured in 10% FCS (Figure 5.14). This staining appeared more intense upon Akt activation and was localised mainly to the nucleus (Figure 5.14). Treatment with rapamycin decreased overall SREBP1 staining in both EtOH and 4-OHT treated cells (Figure 5.14). These support the observations that Akt increases nuclear localisation (Figure 5.2), although it remains difficult to conclude whether this is due to increased processing. Co-localisation studies using markers for the ER and Golgi apparatus would be useful to demonstrate SREBP1 localisation to these organelles.

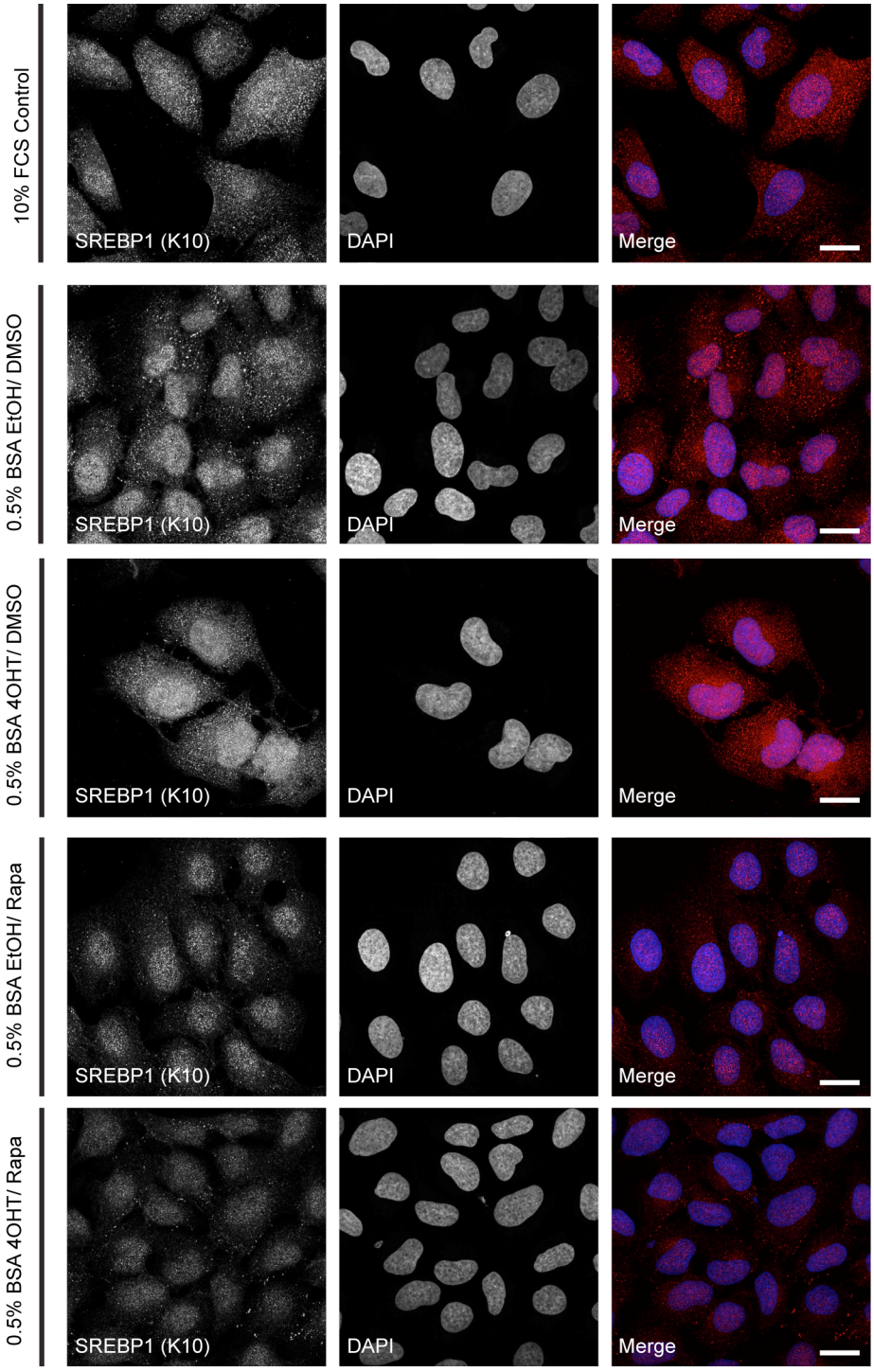

Figure 5-14: Rapamycin decreases overall staining of SREBP1 in confocal microscopy studies.
U2OS-Akt-ER cells grown on coverslips were cultured in 10% FCS or 0.5% BSA and treated with EtOH or 100 nM 4-OHT in the presence or absence of 50 nM rapamycin for 24 hours. Cells were fixed and stained with DAPI (nuclei) and an antibody recognising SREBP1 (clone K10). Images were acquired using confocal microscopy. Scale bars represent 20 μm.

5.7 Effects of Akt and mTORC1 on SREBP protein stability

Levels of nuclear SREBP1 are increased in response to Akt activation following inhibition of mTORC1 (Figure 5.2). A major mechanism that regulates the transcriptional activity of mSREBPs is their proteasomal-dependent degradation (see chapter 1, introduction). GSK3-dependent phosphorylation of 3 sites within the C-terminus of mSREBP enables binding of the Fbw7 ubiquitin ligase and induces degradation of the mSREBP protein (Bengoechea-Alonso and Ericsson, 2009; Sundqvist et al., 2005). Since insulin signalling regulates this GSK3-dependent phosphorylation (Bengoechea-Alonso and Ericsson, 2009), it was hypothesised that Akt may regulate the stability of mature SREBP.

5.7.1 Activation of Akt increases stability of mature SREBP1a in an mTORC1-independent manner

So far, three phosphorylation sites for GSK3 have been identified in mSREBP (Bengoechea-Alonso and Ericsson, 2009; Sundqvist et al., 2005). The phosphorylation of S434 by GSK3 acts as a priming phosphorylation, resulting in the subsequent phosphorylation of S430 and T426 (Bengoechea-Alonso and Ericsson, 2009). It is these two sites that when phosphorylated are recognised by Fbw7 and target mSREBP for degradation. In order to investigate the effects of Akt activation and mTORC1 inhibition on SREBP stability, a DNA construct encoding a myc-tagged mSREBP1a protein containing mutated GSK3-phosphorylation sites (myc-mSREBP1a$^{T426A/S430A}$) was used. RPE-Akt-ER cells were transiently transfected with either pcDNA3-myc-mSREBP1a(wt) or pcDNA3-myc-mSREBP1a$^{T426A/S430A}$. 24 hours following transfection, cells were re-seeded, placed in 1% LPDS and treated with solvent (EtOH) or 4-OHT in the presence or absence of rapamycin for 24 hours. Whole cell lysates were analysed by Western blotting using an antibody recognising the myc-tag. Importantly, cells were not treated with proteasome inhibitors, as this would mask the effects of Akt activation. Activation of Akt increased levels of the wild-type myc-mSREBP1a protein and treatment with rapamycin decreased overall expression of wild-type myc-mSREBP1a (Figure 5.15 B), consistent with what has been observed for endogenous protein (Figure 5.2). In contrast, levels of myc-mSREBP1a$^{T426A/S430A}$

remained unchanged following activation of Akt (Figure 5.15 B) strongly suggesting that Akt activation regulates mSREBP1a protein stability through a mechanism requiring T426/S430 phosphorylation. This indicates that Akt may regulate the stability of mSREBP1a in an mTORC1-independent manner, presumably via the phosphorylation and inhibition of GSK3. However, upon rapamycin treatment, a slight decrease in protein levels of myc-mSREBP1a$^{T426A/S430A}$ could be observed. This indicates that mTORC1 may regulate exogenous mSREBP1a stability independently of GSK3-mediated phosphorylation.

5.7.2 Akt increases transcriptional activity of exogenous mSREBP1a

Since Akt increases stability of mSREBP1a in a rapamycin-independent manner, it was investigated whether inhibition of mTORC1 was able to affect the transcriptional activity of the protein. RPE-Akt-ER cells transfected with either wild-type pcDNA3-myc-mSREBP1a, pcDNA3-myc-mSREBP1a$^{T426A/S430A}$ or empty vector control (pcDNA3) were co-transfected with the FASN luciferase reporter in order to assay for SREBP1a transcriptional activity (FASN-luc, Figure 5.16 A; described in (Bennett et al., 1995)). Cells were cultured in 1% LPDS and treated with solvent (EtOH) or 4-OHT in the presence or absence of rapamycin for 24 hours. Luciferase activity of the FASN-luc reporter was measured and normalised to activity of the renilla luciferase control. Expression of either mature SREBP1a constructs increased luciferase activity when compared to the empty vector control (Figure 5.16B), demonstrating that the mSREBP1a constructs are transcriptionally active. Expression of myc-mSREBP1a$^{T426A/S430A}$ increased overall luciferase reporter activity compared to cells expressing wild-type myc-mSREBP1a (Figure 5.16 B), demonstrating that increased stability of mSREBP1a results in increased transcriptional activity. Interestingly, Akt activation significantly increased luciferase reporter activity not only in wild-type, but also in mutant expressing cells, indicating that Akt may not only be increasing the stability of the mature protein but also promoter activation. In addition, rapamycin treatment reduced reporter activity in cells expressing either wild-type protein or mutant mSREBP1a (Figure 5.16 B), suggesting that rapamycin can affect mSREBP1a independently of Akt/GSK3.

These data suggest that Akt activation increases the stability of mSREBP1a through inhibition of GSK3-dependent phosphorylation and degradation. In addition, Akt also increases the transcriptional activity of mSREBP1a independently of GSK3 phosphorylation. Inhibition of mTORC1 via treatment with rapamycin may affect stability of mSREBP1 independently of GSK3 phosphorylation and reduce its transcriptional activity. This indicates that Akt may regulate SREBP1a in mTORC1-dependent, as well as an mTORC1-independent, manner.

5.7.3 mTORC1 activity is required for mSREBP1 accumulation following GSK3 inhibition

Activation of mTORC1 has been shown to result in the inactivation of GSK3 (Peyrollier et al., 2000). In addition, it has been shown that under conditions of mTORC1 hyper-activation in cells that lack its upstream regulators TSC1/2, GSK3 becomes a direct target for S6K (Zhang et al., 2006a). In order to further investigate whether rapamycin-dependent loss of mSREBP1 is dependent on GSK3 activity, the effects of mTORC1 inhibition in the presence of a GSK3 inhibitor on the nuclear accumulation of endogenous mSREBP1 were analysed. RPE-hTERT cells were cultured in 1% LPDS in the presence or absence of the GSK3 kinase inhibitor SB-216763 and treated with vehicle (DMSO) or rapamycin for 24 hours. Cells were subjected to nuclear fractionation and analysis by Western blotting (Figure 5.17 A). Whole cell lysates from cells treated in parallel were analysed as a control of inhibitor function (Figure 5.17 B). Phosphorylated levels of the GSK-3 target protein β catenin were reduced in response to treatment with SB-216763 and β catenin was stabilised, indicating that GSK-3 activity was reduced in the presence of the inhibitor (Figure 5.17 B). Rapamycin completely blocked phosphorylation of S6 in cells treated with rapamycin alone and reduced levels of S6 phosphorylation in cells treated with the GSK3 inhibitor (Figure 5.17 B). However, cells treated with GSK3 inhibitor alone showed reduced pS6 levels when compared with control cells, indicating that inhibition of GSK3 itself reduces S6 phosphorylation (Figure 5.17 B). GSK3 inhibition resulted in increased nuclear accumulation of mSREBP1, as well an increase in the full-length

protein in whole cell lysates. This is consistent with an increase in mSREBP1 stability (Figure 5.17 A). However, GSK3 inhibition increased levels of the nuclear protein DP1, used as a loading control in this experiment. These data have been observed at least twice, although further repetition would allow statistical analysis. GSK3-inhibitor treatment has been shown to increase DP1 levels on other occasions (data not shown), making it unlikely that the differences in mSREBP1 levels are as a result of unequal loading. Nevertheless, in order to fully confirm this result, this experiment should be repeated using an alternative loading control. Rapamycin treatment reduced the accumulation of nuclear mSREBP1 in cells treated with vehicle and with the GSK3 inhibitor, indicating that inhibition of mTORC1 prevents induction of nuclear mSREBP1 levels in the presence of a GSK3 inhibitor.

5.7.4 Effects of rapamycin on nuclear accumulation of mSREBP1 are blocked in the presence of the proteasome inhibitor MG-132

In experiments investigating the nuclear accumulation of mSREBP1, cells have been treated with the proteasome inhibitor MG-132 in the final 1.5-2 hours before lysis to preserve the levels of nuclear mSREBP1. Since rapamycin reduces mSREBP1 nuclear accumulation in the presence of a GSK3 inhibitor, it was also investigated whether mTORC1 inhibition can reduce nuclear mSREBP1 accumulation following prior treatment with MG-132. RPE-hTERT cells were cultured overnight in 1% LPDS before being pre-treated for 30 minutes with MG-132. Cells were then treated with solvent or rapamycin for the times indicated (Figure 5.18 A). Nuclear fractions, supernatant fractions and whole cell lysates from cells treated in parallel were analysed by Western blotting for accumulation of mSREBP1 and flSREBP1. mSREBP1 was not detected in cells that were not treated with MG-132 (Figure 5.18 A, lane a). Treatment of cells with MG-132 for only 1.5 hours resulted in a substantial increase in the levels of mSREBP1 in cells treated with or without rapamycin (Figure 5.18 A, compare lane a with b and e), confirming that mSREBP1 is turned over rapidly. Treatment with MG-132 for increasing amounts of time increased the nuclear accumulation of mSREBP1, consistent with an increase in protein stability (Figure 5.18 A, lanes a-d). However, treatment of cells with rapamycin failed to reduce levels of nuclear mSREBP1 (Figure 5.18 A, lanes e-g), indicating that when mSREBP1 is already stabilised, inhibition of mTORC1 is not

sufficient to reduce mSREBP1 accumulation. This is in contrast to the finding that mTORC1 inhibition is still able to decrease levels of nuclear mSREBP1 in cells treated with a GSK3 inhibitor (Figure 5.17). This suggests that MG-132 and GSK3 may function in different ways to regulate the stability of mSREBP1. It may be that GSK3 inhibition blocks Fbw7 dependent mSREBP1 degradation, whilst mSREBP1 degradation following mTORC1 inhibition is likely to be Fbw7-indpendent. However, it should be noted that cells were treated with the GSK3 inhibitor for 24 hours, whereas MG-132 treatment was relatively short (6.5 hours) due to the detrimental effect of long-term proteasome inhibition on cells.

In the supernatant fractions, it was observed that treatment with MG-132 resulted in increased levels of flSREBP1 over time, similar to that observed for mSREBP1 in the nuclear fractions (Figure 5.18 A, lanes a-d). Interestingly, this increase in flSREBP1 was less pronounced in cells treated with rapamycin (Figure 5.18 A, lanes e-g), indicating that even in the presence of MG-132, rapamycin is able to reduce expression of flSREBP1, providing further evidence that rapamycin may differentially regulate flSREBP1 and mSREBP1.

It was then investigated whether MG132 is still able to block the effects of rapamycin on mSREBP1 accumulation in the presence of activated Akt. RPE-Akt-ER cells were cultured in 1% LPDS and treated with solvent (EtOH) or 4-OHT for 16 hours. Cells were then treated with MG-132 and rapamcyin as previously described. Nuclear mSREBP1 levels were increased after 1.5 hours of MG132 treatment (Figure 5.18 B, lane c) and increased further after 3.5 hours of MG-132 treatment (Figure 5.18 B, lanes b-c). However, accumulation of nuclear mSREBP1 remained the same after treatment of MG-132 for 6.5 hours (Figure 5.18 B, lanes b-d), indicating that there was no further increase in mSREBP1 stability in the presence of activated Akt. In contrast, levels of flSREBP1 expression continued to increase following treatment with MG-132 over time (Figure 5.18 B, supernatant fraction, lanes a-e). However, rapamycin treatment prevent this increase in flSREBP1 levels (Figure 5.18 B, supernatant fraction, lanes f-h). This

may indicate that rapamycin prevents the transcriptional activity of mSREBP1, preventing feed-forward transcriptional regulation of its promoter.

The data presented in this section indicate that activated Akt induces stabilisation of mSREBP1 in a GSK3-dependent, mTORC1 independent manner, yet inhibition of SREBP1 transcriptional activity is still reduced by rapamycin. Inhibition of the proteasome prevents rapamycin-dependent loss of nuclear mSREBP1, suggesting that mTORC1 signalling may be regulating mSREBP1 stability in a GSK3-independent, yet proteasome-dependent manner.

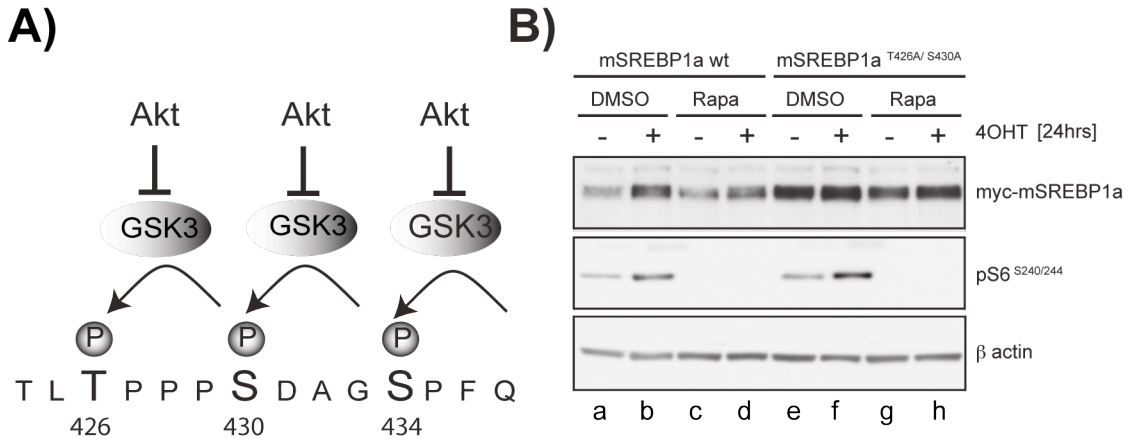

Figure 5-15: Activation of Akt increases stability of mature exogenous SREBP1a in an mTORC1-independent manner.
(A) Schematic representation of Akt-mediated phosphorylation of GSK3 suggesting one mechanism of regulation of mSREBP1 stability. Three key phosphorylation sites are depicted. Adapted from (Bengoechea-Alonso and Ericsson, 2009). (B) RPE-Akt-ER cells were transiently transfected with myc-mSREBP1 wt or mSREBP1$^{T426A/\ S430A}$, a mutant form of the protein that cannot be phosphorylated by GSK3. Cells were then cultured in 1% LPDS and treated with 100nM 4-OHT in the presence or absence of rapamycin (50 nM) for 24 hours. Whole cell lysates were analysed for the expression of myc-mSREBP1a.

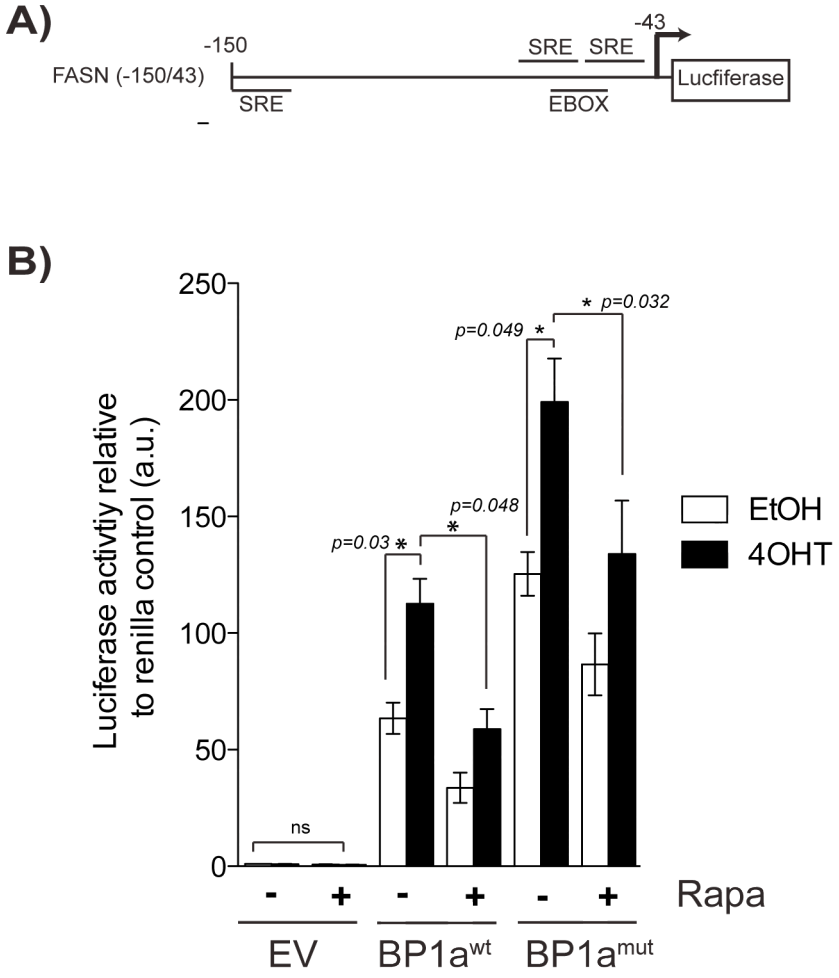

Figure 5-16: Akt increases transcriptional activity of mSREBP1a.
(A) A schematic representation of the fatty acid synthase (FASN) promoter luciferase reporter construct used in (B). (B) RPE-Akt-ER cells were transiently transfected with the FASN-luc reporter construct and the pRL-SV40 renilla control together with either empty vector control pcDNA3 (EV), myc-mSREBP1a wt ($BP1a^{wt}$) or myc-mSREBP1a$^{T426A/\ S430A}$ ($BP1a^{mut}$) as indicated. Cells were cultured in 1% LPDS and treated with 100 nM 4-OHT in the presence or absence of rapamycin (50 nM) for 24 hours. Luciferase activity was measured and normalised to the renilla control. Data were normalised to the EV control and show relative fold change. Data shown is the mean of three independent biological replicates ± SEM. Asterisks indicate statistical significance.

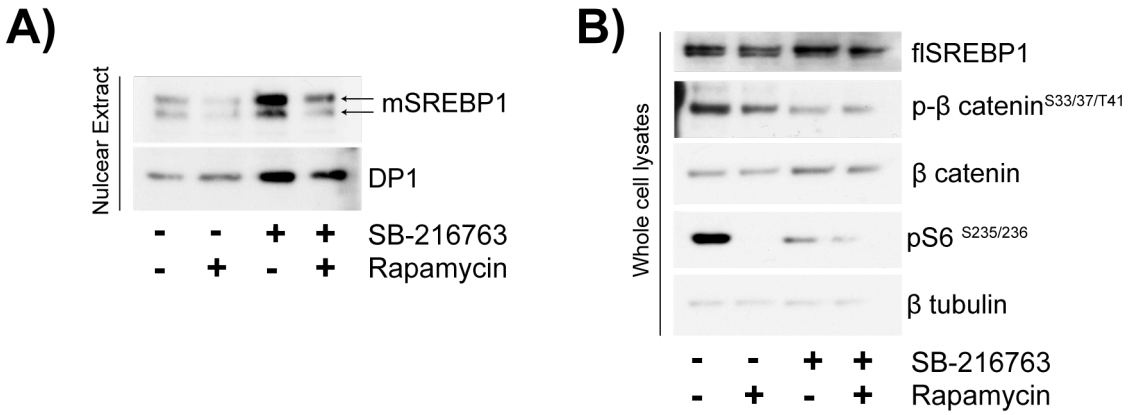

Figure 5-17: Inhibition of GSK3 does not prevent the effects of mTORC1 inhibition on nuclear accumulation of mSREBP1.
RPE-hTERT cells were cultured in 1% LPDS and treated with vehicle (DMSO) or the GSK3 inhibitor SB-216763 (5 μM) in the presence or absence rapamycin (50 nM) for 24 hours. Cells were subjected to nuclear fractionation and analysed by Western blotting. (A) Nuclear fractions showing mSREBP1 expression. DP1 is shown as a nuclear-specific loading control. (B) Whole cell lysates treated from cells treated in parallel to those in (A). Antibodies were used to detect S6 phosphorylation (pS6 $^{S235/236}$) as a control of rapamycin treatment and phosphorylation of β catenin (p-β catenin $^{S33/37/T41}$) as well as β-catenin as controls for GSK3 inhibition. β tubulin is shown as a loading control.

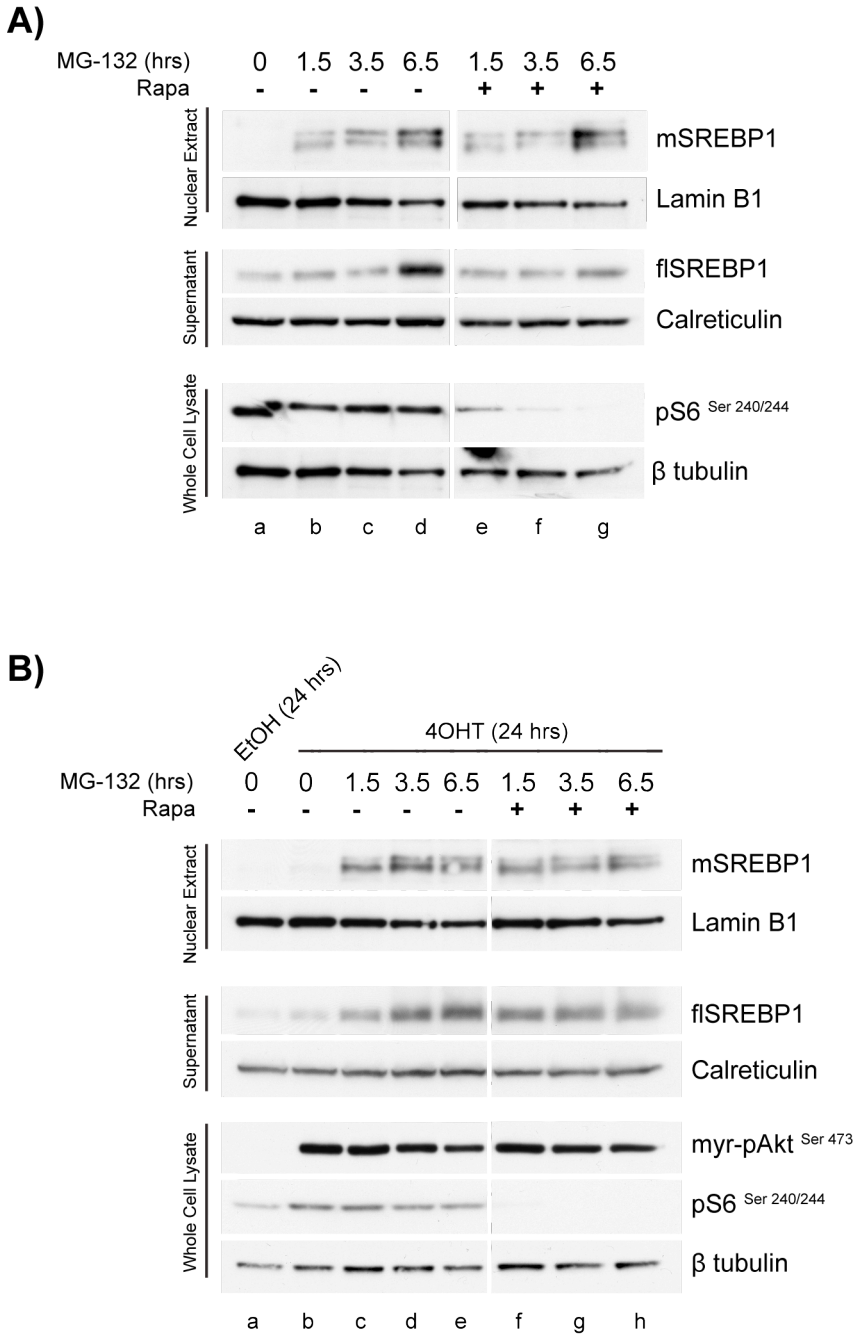

Figure 5-18: MG-132 increases nuclear accumulation of mSREBP1 in a time-dependent manner and this is not prevented by rapamycin.
(A) RPE-hTERT cells were cultured overnight in 1% LPDS. Cells were then pre-treated with vehicle (DMSO) or rapamycin (50 nM) for 30 minutes before being treated with or without 25 μM MG-132 for the times indicated. Nuclear fractions, supernatant fractions and whole cell extracts treated in parallel were analysed by Western blotting for expression of, mSREBP1, flSREBP1and pS6$^{Ser240/244}$. Lamin B1, Calreticulin and β tubulin were used as loading controls for nuclear extracts, supernatant fractions and whole cell extracts, respectively. (B) RPE-Akt-ER cells were cultured in 1% LPDS overnight in the presence of solvent (EtOH) or 100 nM 4-OHT. Cells were then treated as in (A). Nuclear fractions, supernatant fractions and whole cell extracts were analysed by Western blotting for the expression of mSREBP1, flSREBP1, myr-pAkt^{Ser473} and pS6$^{Ser240/244}$. Lamin B1, calreticulin and β tubulin were used as loading controls.

5.8 Discussion

It has been established by the GEA lab that SREBPs are regulated downstream of Akt (Porstmann et al., 2005) and that Akt-dependent activation of SREBP requires mTORC1 activity (Porstmann et al., 2008). In addition, mTORC1-dependent regulation of lipogenesis occurs through SREBP1-activation in liver (Düvel et al., 2010). The regulatory mechanisms governing SREBP activation are likely to be complex, and could involve many factors. In this chapter, several possible mechanisms by which Akt and mTORC1 regulate SREBPs were investigated.

First, it was demonstrated that Akt-dependent nuclear accumulation of mSREBP1 was attenuated following mTORC1 inhibition (Figure 5.2). In addition, treatment with rapamycin resulted in decreased levels of flSREBP1 protein (Figure 5.2). This is consistent with previously published results (Porstmann et al., 2008), confirming that Akt and mTORC1 regulate nuclear accumulation of mSREBP1. It remains unclear whether Akt and mTORC1 affect all three SREBP isoforms in a similar manner. Akt activation increases SREBP2 protein expression in RPE cells, and silencing of mTORC1 components do not alter levels of flSREBP2 protein (Porstmann et al., 2008). However, the effects of mTORC1 inhibition were not investigated in this study. It is important to assess the effects of mTORC1 inhibition on SREBP2 protein levels in this system in order to conclude that mTORC1 differentially affects SREBP isoform expression. Unfortunately, the antibodies used in this thesis could not accurately detect SREBP2 protein levels in RPE cells. In addition, as the SREBP1 antibody cannot distinguish between SREBP1a and SREBP1c, RT-QPCR analysis of individual isoform expression was carried out. It was demonstrated that SREBF1a and SREBF1c mRNA expression was increased following 24 hrs Akt activation, whereas activation of Akt did not effect SREBF2 mRNA expression (Figure 5.3 and 5.4). This is consistent with previously published data (Porstmann et al., 2005). It was shown that SREBF1a is rapidly upregulated in response to Akt activation while SREBF1c is upregulated only after longer-term activation. This suggests that Akt regulates SREBF1 isoforms differentially. It is possible that Akt rapidly upregulates expression of SREBF1a in a more direct manner, resulting in SREBF1a transcriptional-dependent regulation of

SREBF1c. Indeed, SREBF1c is regulated mostly at the transcriptional level (Eberle et al., 2004).

mRNA expression of the two SREBF1 isoforms was differentially regulated in response to mTORC1 inhibition (Figures 5.3-5.4). Overall, rapamycin more potently inhibited expression of SREBF1c mRNA than SREBF1a. Rapamycin-dependent inhibition of SREBF1 mRNA expression has been observed previously in human BJAB B-lymphoma cells and murine CTLL-2 T lymphocytes (Peng et al., 2002) and insulin induced SREBF1c mRNA expression in rat livers and cultured hepatocytes requires mTORC1 (Li et al., 2010). No effects of mTORC1 inhibition using rapamycin were observed on SREBF2 mRNA expression (Figure 5.3-5.4). This demonstrates that in human RPE cells SREBF2 mRNA expression is independent of Akt and mTORC1 activity. This is in contrast to what has been observed in human HepG2 cells (Ma et al., 2007). However, rapamycin has been shown to reduce LDLR expression in CHO cells in an SREBP2-independent manner (Sharpe and Brown, 2008). In NIH3T3 cells, inhibitors of mTORC1 were shown to decrease SREBF2 mRNA expression but not SREBF1 expression (Peterson et al., 2011), suggesting that mTORC1 regulation of SREBP isoforms may be cell-type specific.

A report by Düvel and colleagues demonstrated that expression of the SREBP2 target gene MVK is decreased by rapamycin treatment in TSC2 null MEFs (Düvel et al., 2010). However, expression of SREBP2 itself was not analysed. In addition, they showed that silencing of SREBP1 or SREBP2 in this context reduced MVK expression, indicating that there is overlap between SREBP targets. This is also supported by the microarray data presented in chapter 3 of this thesis, where both SREBP1a and SREBP2 activation upregulated expression of MVK in U87 cells. Therefore, it remains unclear whether mTORC1 activity affects SREBP2 activation.

It was also shown that amino acid stimulation was sufficient to induce nuclear accumulation of mSREBP1 (Figure 5.5) This is consistent with results published in NIH3T3 cells and MEFs, where amino acid withdrawal results in the decreased

expression of SREBP target genes (Peterson et al., 2011). It remains unclear from the experiments presented in this thesis whether the increase in mSREBP1 levels in response to amino acid stimulation is in fact mTORC1-dependent and these experiments should be repeated. It is possible that amino acids may be able to influence levels of both flSREBP1 and mSREBP1 in an Akt/mTORC1-independent manner. Although it has recently been shown that glutamine can induce SREBP activation (Inoue et al., 2011), the effects of glutamine on SREBP1 can be ruled out in the experiments presented in this thesis as there was no glutamine present in the amino acid free medium and the mixture of amino acids used for amino acid stimulation was glutamine free.

It may still be possible that this increase in flSREBP1 and nuclear mSREBP1 in response to amino acid stimulation is a result of increased SREBP translation through the mTORC1 pathway. Indeed, mTORC1-mediated *de novo* protein synthesis is one of the most important biological consequences of this pathway in response to activation by nutrients and growth factors (Wullschleger et al., 2006). Interestingly, the SREBP targets FASN and ACC have been shown to be upregulated at the translational level in an mTORC1-dependent manner in breast cancer cells (Yoon et al., 2007), demonstrating that the lipid synthesis pathway is a target for mTORC1-dependent translational control. In addition, mTORC1 regulates HIF1α translation (Bernardi et al., 2006), demonstrating the regulation of a transcription factor at the translational level. Although attempts were made to investigate whether mTORC1 regulates translation of SREBPs, technical difficulties hampered these experiments. Therefore, it cannot be excluded that SREBP regulation by mTORC1 is at the translational level.

The involvement of downstream effectors of mTORC1 on SREBP1 activation was investigated. It was shown that S6K is required for SREBP processing in the experimental systems used, as mSREBP1 could still be detected even in MEFs in which S6K1 and S6K2 had been genetically deleted (Figure 5.9). This is in contrast to the data published by Düvel and colleagues where they show that processing of SREBP1 is dependent on S6K1 activity in MEFs lacking the mTORC1 inhibitor TSC2 (Düvel et

al., 2010). However, this model results in the uncoupling of mTORC1 activity from Akt signalling. Furthermore, constitutive activation of mTORC1 by genetic ablation of the negative regulators TSC1 or TSC2 is likely to cause adaptations due to extensive feedback regulation within the mTORC pathway (Efeyan and Sabatini, 2010). Another report has suggested that SREBP activation downstream of mTORC1 is not dependent on S6 kinases in MCF7 and MDA-MB- 468 cell lines, and that mTORC1 signalling proceeds through the 4-EBP1 axis in these cells (Luyimbazi et al., 2010). It should be noted, however, that experiments with primary S6K1/S6K2 knockout MEFs presented in this thesis did not include insulin stimulation, and it cannot be excluded that the downstream activation of SREBP1 in response to Akt activation signals through mTORC1 and S6K1. Together, these data indicate that SREBP activation downstream of Akt and mTORC1 is complex and may differ according to cell type, as well as between immortalised and primary cells.

The discussion of data presented in Figures 5.5-5.9 has so far focussed on the ability of Akt and mTORC1 to influence levels of nuclear mSREBP1. Nuclear mSREBP1 is difficult to detect, and whenever possible mSREBP1 was enriched using nuclear fractionation. However, differences in the levels of mSREBP1 remain partial in the Western blots presented. Although experiments presented in Figures 5.5-5.8 have been performed twice, it may be beneficial to repeat these experiments in order to determine if differences are statistically significant using densitometry. Data presented in Figure 5.9 represents only one experiment, due to the limited availability of the primary cell line used. Alternatively, given the much stronger effects of Akt activation and amino acid stimulation on the full-length precursor protein levels compared with the levels of the mature transcription factor (Figures 5.5-5.9) it may be that flSREBP1 is being regulated under these conditions. The increased nuclear mSREBP1 observed could therefore be a result of increased precursor protein.

Potential mechanisms for mTORC1 regulating SREBP activity include the regulation of SREBP processing. Therefore, effects of Akt activation and mTORC1 inhibition on components of the SREBP processing machinery were investigated. It was shown that

SCAP mRNA expression was reduced following rapamycin treatment (Figure 5.10). This has been observed previously in HepG2 cells (Ma et al., 2007). SCAP protein levels were unaffected by Akt activation or mTORC1 inhibition in this thesis. It is therefore unlikely that changes in SCAP expression form part of the Akt/mTORC1 regulatory mechanism governing SREBP activity in RPE cells. However, a slight shift in SCAP protein migration was observed in cells cultured in 1% LPDS. Rapamycin treatment partially inhibited this, suggesting that mTORC1 may affect the conformational change in SCAP that occurs in response to sterol depletion. Interestingly, it has been shown recently that SCAP is phosphorylated on Ser 850 and that this phosphorylation is sensitive to an inhibitor of mTORC1 (Torin1) (Hsu et al., 2011). Therefore it cannot be ruled out that mTORC1-dependent phosphorylation of SCAP affects the ability of SCAP to facilitate SREBP-dependent ER-Golgi translocation. It has also been shown that Akt phosphorylates Sec24, a component of the COPII complex (Sharpe et al., 2010). It has been proposed that this phosphorylation increases incorporation of the SCAP/SREBP complex into budding vesicles (Sharpe et al., 2010). Co-immunoprecipitation experiments were used to investigate whether Akt and mTORC1 can regulate the interaction of SCAP and SREBP proteins. However, despite immunoprecipitation of SCAP and SREBP with their corresponding antibodies, co-immunoprecipitation of the two proteins together could not be established and therefore it has not been possible to evaluate any effect of Akt and mTORC1 on this interaction (data not shown). Thus, it remains unclear whether Akt and mTORC1 could be influencing the ability of SCAP to interact with SREBPs.

SREBP activation requires a two-step proteolytic cleavage of SREBP. This cleavage is carried out by the S1P and S2P proteases. It was investigated whether this cleavage process was influenced by Akt and mTORC1 activity. The activity of S1P and S2P proteases was not affected by either activation of Akt or inhibition of mTORC1, as demonstrated by the cleavage of ATF6α in the presence of rapamycin (Figure 5.11). Effects of Akt and mTORC1 activity on INSIG mRNA expression levels were also investigated (Figure 5.12). It was found that INSIG1 mRNA was affected by Akt activation and mTORC1 inhibition in a similar manner to SREBF1 mRNA expression levels. INSIG1 is an SREBP target gene and it is therefore likely that these changes are

due to the effects of Akt and mTORC1 on SREBP activity. Interestingly, activation of Akt for 2 hours was sufficient to increase INSIG1 expression, yet rapamycin had no effect. However, longer-term rapamycin treatment resulted in decreased INSIG1 expression. This indicates that the Akt-mediated effects on SREBP activation occur more rapidly than mTORC1 inhibition. INSIG2 mRNA expression was unaffected by Akt activation or mTORC1 inhibition. However, a recent report demonstrates that Akt suppresses the liver-specific transcript INSIG2a in primary mouse hepatocytes resulting in an mTORC1-independent, Akt-dependent increase in SREBF1c expression (Yecies et al., 2011). It would be interesting to investigate the effects of Akt activation and mTORC1 inhibition on the interaction between INSIGs and SCAP/SREBP complexes in the experimental system used in this thesis.

The direct involvement of mTORC1 in the cleavage of SREBPs was investigated. As the mechanisms that regulate processing of SREBPs are conserved, an exogenous PLAP-SREBP2 construct was used. A change in the processing of exogenous PLAP-SREBP2 in U2OS-Akt-ER cells was not observed in response to Akt activation or mTORC1 inhibition (Figure 5.13). Sterol starvation did increase PLAP-SREBP2 processing in these cells, demonstrating that sterol responsive processing of SREBP2 is intact in these cells. In contrast to RPE-Akt-ER cells, SREBP2 protein levels were detectable in the U2OS-Akt-ER cell line, although Akt activation and mTORC1 inhibition did not have any effect on levels of flSREBP2 or processed SREBP2. These data suggest that although SREBP2 processing is sterol responsive in this cell line, it is independent of Akt and mTORC1 activity. It should be investigated whether a PLAP-SREBP1 fusion construct is regulated in the same manner.

The subcellular localisation of mSREBP1 was analysed in response to Akt activation and mTORC1 inhibition (Figure 5.14). Sterol depletion resulted in an increased intensity of SREBP1 staining in the nucleus and Akt activation increased this. Rapamycin treatment resulted in the reduction of overall SREBP1 staining. These data indicate that inhibition of mTORC1 activity reduces total SREBP1 protein levels, and support previous observations made throughout this thesis. As no clear cytoplasmic

staining of SREBP1 was observed, it may be suggested that rapamycin does not sequester mSREBP1 to another cellular compartment. However, this analysis should be treated with caution as the antibody staining resulted in high background. This problem with the ability of antibodies to detect endogenous SREBP in immunofluorescence is perhaps reflected in the relatively few publications showing cellular localisation of endogenous SREBP. Most studies that have analysed subcellular localisation of SREBP have used exogenous, epitope-tagged SREBP.

The effects of Akt and mTORC1 signalling on SREBP1 stability were investigated. It was shown that activation of Akt increased the GSK3-regulated stability of exogenous mSREBP1a in a rapamycin-independent manner, although the transcriptional activity of exogenous mSRBEP1a remained rapamycin-sensitive (Figures 5.15 and 5.16). This indicates that rapamycin does not affect the stability of mSREBP1a protein in a GSK3-dependent manner. This would be consistent with recently published data, showing that inhibition of mTORC1 prevents SREBP-transcriptional activity through a lipin1 dependent mechanism (Peterson et al., 2011). Inhibition of mTORC1 results in dephosphorylation of lipin1 and its subsequent translocation to the nucleus where it prevents SREBP transcriptional activity (Peterson et al., 2011).

In addition, rapamycin decreased nuclear accumulation of endogenous mSREBP1 in a GSK3-independent manner (Figure 5.17). Although GSK3-inhibition resulted in decreased S6 phosphorylation, this may be accounted for by the slight non-specific effects of the GSK3 inhibitor SB-216763 on S6K1 activity (Bain et al., 2007). Despite this, inhibition of GSK3 was demonstrated by decreased β-catenin phosphorylation (Figure 5.17). Rapamycin treatment reduced mSREBP1 nuclear accumulation in the presence of the GSK3 inhibitor, confirming that inhibition of mTORC1 prevents nuclear accumulation of mSREBP1 in a GSK3-independent manner.

The very low stability of SREBP is a crucial factor when investigating mSREBP protein levels. In order to detect mSREBP1 by Western blot, cells are generally treated with a proteasome inhibitor (MG-132) for 1.5 hours prior to lysis. Since rapamycin reduces

nuclear accumulation of mSREBP1 independently of GSK3 activity, it was investigated whether the effects of rapamycin are proteasome dependent (Figure 5.18). Inhibition of the proteasome increased mSREBP1 nuclear accumulation in a time-dependent manner. However, rapamycin did not prevent this accumulation, suggesting that inhibition of mTORC1 effects mSREBP1 stability in a GSK3-independent, proteasome-dependent manner. This finding is in contrast to data published by Düvel and colleaugues, who show that rapamycin-dependent inhibition of mSREBP1 is independent of proteasomal activity (Düvel et al., 2010). Interestingly, the levels of flSREBP1 were increased following proteasome inhibition, but rapamycin reduced flSREBP1 levels in the presence of MG-132. These data could support the model whereby mTORC1 inhibition decreases mSREBP1 transcriptional activity, as SREBF1 is an SREBP target gene.

It should be noted that throughout this thesis experiments were performed using long-term rapamycin treatment (i.e. 24 hours). As previously mentioned in the introduction, it has been shown in some cases that prolonged rapamycin treatment results in the inhibition of mTORC2, and the effects of rapamycin are no longer mTORC1-specific (Sarbassov et al., 2006). Under these conditions, rapamycin inhibits the formation of mTORC2 as well as Akt activity (Sarbassov et al., 2006). However, in the experiments presented in this thesis rapamycin treatment was often performed together with activation of Akt in order to prevent inhibition of Akt. Furthermore, previous data published by the GEA lab has shown that short-term rapamycin treatment does prevent nuclear accumulation of mSREBP1 in RPE-Akt-ER cells (Porstmann et al., 2008), and that the effects of long-tern rapamycin treatment observed by Sarbassov and colleagues do not occur in the RPE-Akt-ER cells (T.Porstmann, personal communication). Nevertheless, it may be beneficial to repeat certain experiments with shorter rapamycin treatment (2 hours) in order to separate out the indirect and direct effects of mTORC1 inhibition.

The data presented here demonstrate that regulation of SREBP by the Akt and mTORC1 signalling pathway is complex (see Figure 5.19). However, the data strongly support a model whereby Akt activation stabilises mSREBP1 through inhibition of

GSK3, and mTORC1 affects mSREBP1 stabilisation through a GSK3-independent mechanism. These effects result in an increase in SREBP transcriptional activity. Although this appears to be a rather complex mechanism, it allows for SREBP activation downstream of mTORC1 independently of Akt activity.

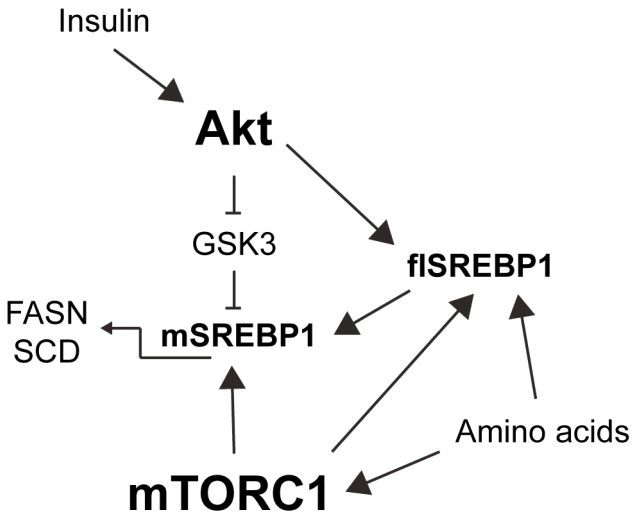

Figure 5-19: Model showing the complex regulation of SREBP1 by Akt, mTORC1 and amino acids.
The regulation of SREBP by Akt and mTORC1 is complex. Experiments presented in this thesis suggest that Akt promotes the stability of mSREBP1 by inactivating GSK3. In addition, it is likely that mTORC1 regulates stability of mSREBP1, but in a GSK-3 independent manner. mTORC1 may also regulate the full length precursor protein. Amino acids may signal to flSREBP1 through mTORC1, although an mTORC1-independent mechanism is also possible. Increase in levels of mSREBP1 results in an increase in SREBP1 target genes, such as FASN and SCD.

Chapter 6. Final Discussion

The original observations of Otto Warburg were made over half a century ago, but in the last decade the role of altered cell metabolism has taken the cancer research field by storm. Initially, interest focussed primarily on the altered glycolytic state of cancer cells, but more recent research has demonstrated the importance of altered lipid metabolism in tumourigenesis. This has been largely fuelled by discoveries that regulators of lipid metabolism are downstream of canonical oncogenic pathways, in particular the PI3K/Akt/mTORC1 pathway.

The SREBP family of transcription factors are master regulators of lipid metabolism, controlling the expression of genes encoding enzymes required for fatty acid and cholesterol biosynthesis. Although there is ample evidence for altered lipid metabolism in cancer, surprisingly little is known about the role of SREBPs in this context. The data presented in this thesis reinforces the importance of SREBPs as master regulators of lipid synthesis, as well as providing insight into their involvement in the regulation of other cellular processes, such as cell cycle progression, redox regulation and cellular stress response. Identification of FABP7 as a SREBP target gene in glioblastoma cells also demonstrates a role for SREBPs in other aspects of lipid metabolism in addition to fatty acid and cholesterol biosynthesis. The data-set generated from the microarray analysis will be an important tool for further investigation of the role of SREBPs in promoting survival by regulating previously unidentified sub-sets of genes that are important in processes other than lipid metabolism in cancer cells.

Hypoxia is a feature of many solid tumours and altered lipid metabolism has been shown to occur in hypoxic conditions. Experiments performed in this thesis have shown that lipid metabolism in glioblastoma cells in hypoxia is indeed altered, and suggest a change in the SREBP-regulated transcriptional programme in response to hypoxia. Although further work is required to fully understand the changes in lipid metabolism in hypoxia and the role it may have for cancer cell survival, the data presented in this thesis point to a metabolic switch resulting in decreased lipid synthesis and increased

lipid storage. In addition, the hypoxia-induced transcriptional programme observed here may have particular relevance to the clinical manifestations of GBM. The regulation of FABP7 by SREBP could be of particular importance given its observed overexpression in GBM and association with poor clinical prognosis and patient outcome (Liang et al., 2005; Mita et al., 2010). In addition, the increased expression of FABP7 in glioblastoma cells in hypoxia may also be of significant importance. Clinical trials are underway for the use of an anti-human VEGF antibody (Bevacizumab: Bev) in the treatment of GBM. However, the efficacy of inhibiting angiogenesis in GBM is controversial and to date no significant impact on overall patient survival has been observed (Keunen et al., 2011). A study in a clinically relevant model of GBM in rats has demonstrated that anti-angiogenic treatment results in an increased hypoxic tumour microenvironment along with HIF1α stabilisation and increased glycolysis (Keunen et al., 2011). In addition, this switch in metabolism is accompanied by increased invasiveness of tumour cells into the normal brain tissue (Keunen et al., 2011). Since SREBP may be required for cell survival in hypoxia and under conditions of nutrient-depletion, it is possible that combination therapy which includes compounds targeting the SREBP pathway may be more efficacious than single treatment alone.

The PI3K/mTORC1 pathway is a target for anti-cancer therapies and although rapalogues are yielding some success in the clinic, the development of mTORC1 inhibitors as anti-cancer drugs is still in early days (Garcia-Echeverria, 2011). Furthermore, the need to consider signalling crosstalk and feedback mechanisms within the pathway is becoming more evident (Garcia-Echeverria, 2011). Activation of SREBP downstream of mTORC1 may have important implications for cancer treatments targeting this pathway. Therefore, understanding the exact mechanism of regulation of SREBPs by mTORC1 is of great importance. The data presented here contribute to the understanding of this mechanism by showing that mTORC1 regulates the expression of SREBP isoforms in a differential manner. Furthermore, mTORC1 regulates the transcriptional activity of SREBP and may regulate the stability of the mature protein in a GSK3-independent, proteasome-dependent manner. The regulation of SREBP by the PI3K/Akt/mTORC1 axis is likely to be highly complex, and may depend on the exact nature of the signalling input. The PI3K/mTORC1 pathway is one of the most

frequently deregulated signalling pathways in cancer. The diverse genetic aberrations that contribute to its hyperactivation could have differential effects on its downstream transcriptional effectors, including SREBP, in a tissue-specific manner. Continued experimentation is therefore required to elucidate the mechanism by which SREBP is regulated by this important signalling axis.

The regulation of SREBPs downstream of the PI3K/Akt/mTORC1 pathway as well as their important role in the cellular response to hypoxia demonstrates the importance of these transcription factors in regulating cellular homeostasis. The implications that this may have on cancer progression are becoming evident and this is reflected in the increasing interest in SREBPs in the research field of cancer cell metabolism.

Appendix and Supplementary Data

The following pages contain tables of selected individual genes that were significantly regulated following activation of mSREBP1a and mSREBP2 in U87 cells. Genes were identified by gene expression microarray analysis, described in Chapter 3. Tables show fold change gene expression following activation of mSREBP1a or mSREBP2 for 6 or 24 hours.

List of Tables:

Microarray Data (CD-ROM)

A full list of significantly regulated genes can be found on the CD-ROM submitted with this thesis, along with the complete pathway and process enrichment analysis described in Chapter 3.

Table A1: Selected known SREBP target genes upregulated following activation of mSREBP1 or mSREBP2 in U87 cells, as identified by gene expression microarray analysis

	SREBP1a 6 hrs		SREBP1a 24 hours		SREBP2 6 hours		SREBP2 24 hours	
Gene	Fold Change	P-Value	Fold Change	P-Value	Fold Change	P-Value	Fold Change	P-Value
INSIG1	4.884981963	9.70E-013	5.764211207	1.50E-013	3.918716379	1.06E-011	3.855844663	1.31E-011
SCD	2.899424096	1.10E-005	4.93791534	4.41E-008	2.294739706	0.000177229	3.515873922	1.27E-006
HMGCR	2.728357578	3.61E-005	4.564723497	1.54E-007	2.749519927	3.16E-005	3.064248574	9.15E-006
ACACB	1.704215603	0.00023517	4.034625243	2.58E-010			4.637174791	1.13E-010
HMGCS1	2.554137844	0.000355993	3.889680233	4.94E-006	3.40621688	1.48E-005	3.406188424	1.48E-005
LDLR	2.646757269	1.02E-007	3.87207295	6.64E-010	2.669970468	8.62E-008	3.353271948	3.74E-009
FASN	2.066560069	0.001276179	3.846163827	1.40E-006			2.599676208	8.96E-005
ACLY	1.672799121	4.64E-005	3.1547262	6.63E-010	1.526803663	0.00035933	2.453578743	2.96E-008
ACSS2			3.08144678	3.32E-006			3.360302379	1.29E-006
MVK	2.402972639	6.70E-005	2.483582167	4.24E-005	2.827159855	7.20E-006	2.602873864	2.16E-005
SLC25A1			2.40266723	0.004667788			2.727111465	0.0016487
ACACA			2.261387719	4.97E-008			1.996336975	6.11E-007
G6PD			2.161008279	2.16E-005			2.306305138	8.37E-006

Table A2: Genes encoding fatty acid binding proteins upregulated following activation of mSREBP1 or mSREBP2 in U87 cells, as identified by gene expression microarray analysis

	SREBP1a 6 hrs		SREBP1a 24 hours		SREBP2 6 hours		SREBP2 24 hours	
Gene	Fold Change	P-Value	Fold Change	P-Value	Fold Change	P-Value	Fold Change	P-Value
FABP7			5.294662989	1.41E-007			4.377335034	3.83E-006
FABP3			1.451450609	0.000610155				
FABP6			1.256394135	0.003891958				

Table A3: Genes encoding lipid droplet proteins upregulated following activation of mSREBP1 or mSREBP2 in U87 cells, as identified by gene expression microarray analysis

	SREBP1a 6 hrs		SREBP1a 24 hours		SREBP2 6 hours		SREBP2 24 hours	
Gene	Fold Change	P-Value	Fold Change	P-Value	Fold Change	P-Value	Fold Change	P-Value
CIDEC	1.618236019	3.17E-005	3.211396286	1.54E-011			1.82111244	2.21E-006

Table A4: Genes encoding cell cycle regulators regulated following activation of mSREBP1 or mSREBP2 in U87 cells, as identified by gene expression microarray analysis

	SREBP1a 6 hrs		SREBP1a 24 hours		SREBP2 6 hours		SREBP2 24 hours	
Gene	Fold Change	P-Value	Fold Change	P-Value	Fold Change	P-Value	Fold Change	P-Value
CDKN1A/p21			1.963890032	0.002093217			1.775161988	0.006928
CDC25A	-1.49833416	0.000918073	-1.874851681	1.10E-005			-1.648241124	0.000127
E2F2			-2.516020502	0.002199902				
CCNA2/ Cyclin A2			-2.929226235	6.80E-007			-1.938623029	0.000193
E2F4							-1.762834987	0.004418

Reference List

Accioly, M.T., Pacheco, P., Maya-Monteiro, C.M., Carrossini, N., Robbs, B.K., Oliveira, S.S., Kaufmann, C., Morgado-Diaz, J.A., Bozza, P.T., and Viola, J.P. (2008). Lipid bodies are reservoirs of cyclooxygenase-2 and sites of prostaglandin-E2 synthesis in colon cancer cells. Cancer Research *68*, 1732-1740.

Alessi, D.R., James, S.R., Downes, C.P., Holmes, A.B., Gaffney, P.R., Reese, C.B., and Cohen, P. (1997). Characterization of a 3-phosphoinositide-dependent protein kinase which phosphorylates and activates protein kinase Balpha. Current Biology *7*, 261-269.

Altomare, D.A., and Testa, J.R. (2005). Perturbations of the AKT signaling pathway in human cancer. Oncogene *24*, 7455-7464.

Amemiya-Kudo, M. (2000). Promoter Analysis of the Mouse Sterol Regulatory Element-binding Protein-1c Gene. The Journal of Biological Chemistry *275*, 31078-31085.

Amemiya-Kudo, M., Shimano, H., Hasty, A.H., Yahagi, N., Yoshikawa, T., Matsuzaka, T., Okazaki, H., Tamura, Y., Iizuka, Y., Ohashi, K., Osuga, J.-i., Harada, K., Gotoda, T., Sato, R., Kimura, S., Ishibashi, S., and Yamada, N. (2002). Transcriptional activities of nuclear SREBP-1a, -1c, and -2 to different target promoters of lipogenic and cholesterogenic genes. The Journal of Lipid Research *43*, 1220-1235.

Andjelkovic, M., Alessi, D.R., Meier, R., Fernandez, A., Lamb, N.J., Frech, M., Cron, P., Cohen, P., Lucocq, J.M., and Hemmings, B.A. (1997). Role of translocation in the activation and function of protein kinase B. The Journal of Biological Chemistry *272*, 31515-31524.

Arito, M., Horiba, T., Hachimura, S., Inoue, J., and Sato, R. (2008). Growth Factor-induced Phosphorylation of Sterol Regulatory Element-binding Proteins Inhibits Sumoylation, Thereby Stimulating the Expression of Their Target Genes, Low Density Lipoprotein Uptake, and Lipid Synthesis. The Journal of Biological Chemistry *283*, 15224-15231.

Arsham, A.M., Howell, J.J., and Simon, M.C. (2003). A novel hypoxia-inducible factor-independent hypoxic response regulating mammalian target of rapamycin and its targets. The Journal of Biological Chemistry *278*, 29655-29660.

Azzout-Marniche, D., Bécard, D., Guichard, C., Foretz, M., Ferré, P., and Foufelle, F. (2000). Insulin effects on sterol regulatory-element-binding protein-1c (SREBP-1c) transcriptional activity in rat hepatocytes. Biochemical Journal *350 Pt 2*, 389-393.

Bain, J., Plater, L., Elliott, M., Shpiro, N., Hastie, C.J., Mclauchlan, H., Klevernic, I., Arthur, J.S.C., Alessi, D.R., and Cohen, P. (2007). The selectivity of protein kinase inhibitors: a further update. Biochemical Journal *408*, 297-315.

Baranowski, M. (2008). Biological role of liver X receptors. Journal of physiology and pharmacology : an official journal of the Polish Physiological Society *59 Suppl 7*, 31-55.

Baron, A., Migita, T., Tang, D., and Loda, M. (2004). Fatty acid synthase: a metabolic oncogene in prostate cancer? Journal of Cellular Biochemistry *91*, 47-53.

Bartz, F., Kern, L., Erz, D., Zhu, M., Gilbert, D., Meinhof, T., Wirkner, U., Erfle, H., Muckenthaler, M., Pepperkok, R., and Runz, H. (2009). Identification of Cholesterol-Regulating Genes by Targeted RNAi Screening. Cell Metabolism *10*, 63-75.

Bauer, D.E., Hatzivassiliou, G., Zhao, F., Andreadis, C., and Thompson, C.B. (2005). ATP citrate lyase is an important component of cell growth and transformation. Oncogene *24*, 6314-6322.

Beckner, M.E., Fellows-Mayle, W., Zhang, Z., Agostino, N.R., Kant, J.A., Day, B.W., and Pollack, I.F. (2009). Identification of ATP citrate lyase as a positive regulator of glycolytic function in glioblastomas. International Journal of Cancer *126*, 2282-2295.

Belanger, A.J., Luo, Z., Vincent, K.A., Akita, G.Y., Cheng, S.H., Gregory, R.J., and Jiang, C. (2007). Hypoxia-inducible factor 1 mediates hypoxia-induced cardiomyocyte lipid accumulation by reducing the DNA binding activity of peroxisome proliferator-activated receptor alpha/retinoid X receptor. Biochemical and Biophysical Research Communications *364*, 567-572.

Bellacosa, A., Chan, T.O., Ahmed, N.N., Datta, K., Malstrom, S., Stokoe, D., McCormick, F., Feng, J., and Tsichlis, P. (1998). Akt activation by growth factors is a multiple-step process: the role of the PH domain. Oncogene *17*, 313-325.

Bellacosa, A., Testa, J.R., Staal, S.P., and Tsichlis, P.N. (1991). A retroviral oncogene, akt, encoding a serine-threonine kinase containing an SH2-like region. Science *254*, 274-277.

Bengoechea-Alonso, M., and Ericsson, J. (2009). A phosphorylation cascade controls the degradation of active SREBP1. The Journal of Biological Chemistry *284*, 5885-5895.

Bengoechea-Alonso, M.T., and Ericsson, J. (2006). Cdk1/cyclin B-mediated phosphorylation stabilizes SREBP1 during mitosis. Cell Cycle *5*, 1708-1718.

Bengoechea-Alonso, M.T., Punga, T., and Ericsson, J. (2005). Hyperphosphorylation regulates the activity of SREBP1 during mitosis. Proceedings of the National Academy of Sciences USA *102*, 11681-11686.

Bengoecheaalonso, M., and Ericsson, J. (2007). SREBP in signal transduction: cholesterol metabolism and beyond. Current Opinion in Cell Biology *19*, 215-222.

Bennett, M.K. (2004). Selective Association of Sterol Regulatory Element-binding Protein Isoforms with Target Promoters in Vivo. The Journal of Biological Chemistry *279*, 37360-37367.

Bennett, M.K., Lopez, J.M., Sanchez, H.B., and Osborne, T.F. (1995). Sterol regulation of fatty acid synthase promoter. Coordinate feedback regulation of two major lipid pathways. The Journal of Biological Chemistry *270*, 25578-25583.

Bernardi, R., Guernah, I., Jin, D., Grisendi, S., Alimonti, A., Teruya-Feldstein, J., Cordon-Cardo, C., Simon, M.C., Rafii, S., and Pandolfi, P.P. (2006). PML inhibits HIF-1alpha translation and neoangiogenesis through repression of mTOR. Nature *442*, 779-785.

Bertout, J.A., Patel, S.A., and Simon, M.C. (2008). The impact of O2 availability on human cancer. Nature Reviews Cancer *8*, 967-975.

Berwick, D.C., Hers, I., Heesom, K.J., Moule, S.K., and Tavare, J.M. (2002). The identification of ATP-citrate lyase as a protein kinase B (Akt) substrate in primary adipocytes. The Journal of Biological Chemistry *277*, 33895-33900.

Biron-Shental, T., Schaiff, W.T., Ratajczak, C.K., Bildirici, I., Nelson, D.M., and Sadovsky, Y. (2007). Hypoxia regulates the expression of fatty acid-binding proteins in primary term human trophoblasts. American Journal of Obstetrics and Gynecology *197*, 516 e511-516.

Bodnar, A.G., Ouellette, M., Frolkis, M., Holt, S.E., Chiu, C.P., Morin, G.B., Harley, C.B., Shay, J.W., Lichtsteiner, S., and Wright, W.E. (1998). Extension of life-span by introduction of telomerase into normal human cells. Science *279*, 349-352.

Bostrom, P., Magnusson, B., Svensson, P.A., Wiklund, O., Boren, J., Carlsson, L.M., Stahlman, M., Olofsson, S.O., and Hulten, L.M. (2006). Hypoxia converts human macrophages into triglyceride-loaded foam cells. Arteriosclerosis, Thrombosis and Vascular Biology *26*, 1871-1876.

Bozza, P.T., and Viola, J.P.B. (2010). Lipid droplets in inflammation and cancer. Prostaglandins, Leukotrienes, and Essential Fatty Acids *82*, 243-250.

Briggs, M.R., Yokoyama, C., Wang, X., Brown, M.S., and Goldstein, J.L. (1993). Nuclear protein that binds sterol regulatory element of low density lipoprotein receptor promoter. I. Identification of the protein and delineation of its target nucleotide sequence. The Journal of Biological Chemistry *268*, 14490-14496.

Brown, A.J., Sun, L., Feramisco, J.D., Brown, M.S., and Goldstein, J.L. (2002). Cholesterol addition to ER membranes alters conformation of SCAP, the SREBP escort protein that regulates cholesterol metabolism. Molecular Cell *10*, 237-245.

Brown, M.S., and Goldstein, J.L. (1997). The SREBP pathway: regulation of cholesterol metabolism by proteolysis of a membrane-bound transcription factor. Cell *89*, 331-340.

Brown, M.S., and Goldstein, J.L. (1999). A proteolytic pathway that controls the cholesterol content of membranes, cells, and blood. Proceedings of the Natational Academy of Sciences USA *96*, 11041-11048.

Brown, N., Stefanovicracic, M., Sipula, I., and Perdomo, G. (2007). The mammalian target of rapamycin regulates lipid metabolism in primary cultures of rat hepatocytes. Metabolism *56*, 1500-1507.

Brugarolas, J., Lei, K., Hurley, R.L., Manning, B.D., Reiling, J.H., Hafen, E., Witters, L.A., Ellisen, L.W., and Kaelin, W.G., Jr. (2004). Regulation of mTOR function in response to hypoxia by REDD1 and the TSC1/TSC2 tumor suppressor complex. Genes and Development *18*, 2893-2904.

Cagen, L.M., Deng, X., Wilcox, H.G., Park, E.A., Raghow, R., and Elam, M.B. (2005). Insulin activates the rat sterol-regulatory-element-binding protein 1c (SREBP-1c) promoter through the combinatorial actions of SREBP, LXR, Sp-1 and NF-Y cis-acting elements. Biochemical Journal *385*, 207-216.

Carpten, J.D., Faber, A.L., Horn, C., Donoho, G.P., Briggs, S.L., Robbins, C.M., Hostetter, G., Boguslawski, S., Moses, T.Y., Savage, S., Uhlik, M., Lin, A., Du, J., Qian, Y.W., Zeckner, D.J., Tucker-Kellogg, G., Touchman, J., Patel, K., Mousses, S., Bittner, M., Schevitz, R., Lai, M.H., Blanchard, K.L., and Thomas, J.E. (2007). A transforming mutation in the pleckstrin homology domain of AKT1 in cancer. Nature *448*, 439-444.

Chan, S. (2004). Targeting the mammalian target of rapamycin (mTOR): a new approach to treating cancer. British Journal of Cancer *91*, 1420-1424.

Chan, S., Scheulen, M.E., Johnston, S., Mross, K., Cardoso, F., Dittrich, C., Eiermann, W., Hess, D., Morant, R., Semiglazov, V., Borner, M., Salzberg, M., Ostapenko, V., Illiger, H.J., Behringer, D., Bardy-Bouxin, N., Boni, J., Kong, S., Cincotta, M., and Moore, L. (2005). Phase II study of temsirolimus (CCI-779), a novel inhibitor of mTOR, in heavily pretreated patients with locally advanced or metastatic breast cancer. Jouranl of Clinical Oncology *23*, 5314-5322.

Chang, Y., Wang, J., Lu, X., Thewke, D.P., and Mason, R.J. (2005). KGF induces lipogenic genes through a PI3K and JNK/SREBP-1 pathway in H292 cells. The Journal of Lipid Research *46*, 2624-2635.

Chen, C., Pore, N., Behrooz, A., Ismail-Beigi, F., and Maity, A. (2001). Regulation of glut1 mRNA by hypoxia-inducible factor-1. Interaction between H-ras and hypoxia. The Journal of Biological Chemistry *276*, 9519-9525.

Choi, S.M., Cho, H.-J., Cho, H., Kim, K.H., Kim, J.B., and Park, H. (2008). Stra13/DEC1 and DEC2 inhibit sterol regulatory element binding protein-1c in a hypoxia-inducible factor-dependent mechanism. Nucleic Acids Research *36*, 6372-6385.

Coffer, P.J., and Woodgett, J.R. (1991). Molecular cloning and characterisation of a novel putative protein-serine kinase related to the cAMP-dependent and protein kinase C families. European Journal of Biochemistry *201*, 475-481.

Cross, D.A., Alessi, D.R., Cohen, P., Andjelkovich, M., and Hemmings, B.A. (1995). Inhibition of glycogen synthase kinase-3 by insulin mediated by protein kinase B. Nature *378*, 785-789.

Dang, C.V., Kim, J.-w., Gao, P., and Yustein, J. (2008). The interplay between MYC and HIF in cancer. Nature Reviews Cancer *8*, 51-56.

Deberardinis, R., Lum, J., Hatzivassiliou, G., and Thompson, C. (2008). The Biology of Cancer: Metabolic Reprogramming Fuels Cell Growth and Proliferation. Cell Metabolism *7*, 11-20.

Demoulin, J.-B. (2004). Platelet-derived Growth Factor Stimulates Membrane Lipid Synthesis Through Activation of Phosphatidylinositol 3-Kinase and Sterol Regulatory Element-binding Proteins. The Journal of Biological Chemistry *279*, 35392-35402.

Denko, N.C. (2008). Hypoxia, HIF1 and glucose metabolism in the solid tumour. Nature Reviews Cancer *8*, 705-713.

Dibble, C.C., Asara, J.M., and Manning, B.D. (2009). Characterization of Rictor phosphorylation sites reveals direct regulation of mTOR complex 2 by S6K1. Molecular and Cellular Biology *29*, 5657-5670.

Dobrosotskaya, I.Y. (2002). Regulation of SREBP Processing and Membrane Lipid Production by Phospholipids in Drosophila. Science *296*, 879-883.

Dooley, K.A., Millinder, S., and Osborne, T.F. (1998). Sterol regulation of 3-hydroxy-3-methylglutaryl-coenzyme A synthase gene through a direct interaction between sterol regulatory element binding protein and the trimeric CCAAT-binding factor/nuclear factor Y. The Journal of Biological Chemistry *273*, 1349-1356.

Dummler, B., and Hemmings, B.A. (2007). Physiological roles of PKB/Akt isoforms in development and disease. Biochemical Society Transactions *35*, 231-235.

Düvel, K., Yecies, J.L., Menon, S., Raman, P., Lipovsky, A.I., Souza, A.L., Triantafellow, E., Ma, Q., Gorski, R., Cleaver, S., Vander Heiden, M.G., Mackeigan, J.P., Finan, P.M., Clish, C.B., Murphy, L.O., and Manning, B.D. (2010). Activation of a Metabolic Gene Regulatory Network Downstream of mTOR Complex 1. Molecular Cell *39*, 171-183.

Eberle, D., Hegarty, B., Bossard, P., Ferre, P., and Foufelle, F. (2004). SREBP transcription factors: master regulators of lipid homeostasis. Biochimie *86*, 839-848.

Efeyan, A., and Sabatini, D.M. (2010). mTOR and cancer: many loops in one pathway. Current Opinion in Cell Biology *22*, 169-176.

Eisen, M.B., Spellman, P.T., Brown, P.O., and Botstein, D. (1998). Cluster analysis and display of genome-wide expression patterns. Proceedins of the National Academy of Sciences USA *95*, 14863-14868.

Engelman, J.A. (2009). Targeting PI3K signalling in cancer: opportunities, challenges and limitations. Nature Reviews Cancer *9*, 550-562.

Engelman, J.A., Luo, J., and Cantley, L.C. (2006). The evolution of phosphatidylinositol 3-kinases as regulators of growth and metabolism. Nature Reviews Genetics *7*, 606-619.

Evans, S.M., Judy, K.D., Dunphy, I., Jenkins, W.T., Hwang, W.T., Nelson, P.T., Lustig, R.A., Jenkins, K., Magarelli, D.P., Hahn, S.M., Collins, R.A., Grady, M.S., and Koch, C.J. (2004). Hypoxia is important in the biology and aggression of human glial brain tumors. Clinical Cancer Research *10*, 8177-8184.

Fajas, L., Landsberg, R.L., Huss-Garcia, Y., Sardet, C., Lees, J.A., and Auwerx, J. (2002). E2Fs regulate adipocyte differentiation. Developmental Cell *3*, 39-49.

Farese, R.V., and Walther, T.C. (2009). Lipid droplets finally get a little R-E-S-P-E-C-T. Cell *139*, 855-860.

Favaro, E., Lord, S., Harris, A.L., and Buffa, F.M. (2011). Gene expression and hypoxia in breast cancer. Genome Medicine *3*, 55.

Fernandez-Alvarez, A., Alvarez, M.S., Gonzalez, R., Cucarella, C., Muntane, J., and Casado, M. (2011). Human SREBP1c expression in liver is directly regulated by peroxisome proliferator-activated receptor alpha (PPARα). The Journal of Biological Chemistry *286*, 21466-21477.

Fleischmann, M., and Iynedjian, P.B. (2000). Regulation of sterol regulatory-element binding protein 1 gene expression in liver: role of insulin and protein kinase B/cAkt. Biochemical Journal *349*, 13-17.

Forsythe, J.A., Jiang, B.H., Iyer, N.V., Agani, F., Leung, S.W., Koos, R.D., and Semenza, G.L. (1996). Activation of vascular endothelial growth factor gene transcription by hypoxia-inducible factor 1. Molecular and Cellular Biology *16*, 4604-4613.

Fritz, V., Benfodda, Z., Rodier, G., Henriquet, C., Iborra, F., Avances, C., Allory, Y., de la Taille, A., Culine, S., Blancou, H., Cristol, J.P., Michel, F., Sardet, C., and Fajas, L. (2010). Abrogation of de novo lipogenesis by stearoyl-CoA desaturase 1 inhibition interferes with oncogenic signaling and blocks prostate cancer progression in mice. Molecular Cancer Therapeutics *9*, 1740-1754.

Fritz, V., and Fajas, L. (2010). Metabolism and proliferation share common regulatory pathways in cancer cells. Oncogene *29*, 4369-4377.

Furuta, E., Pai, S.K., Zhan, R., Bandyopadhyay, S., Watabe, M., Mo, Y.-Y., Hirota, S., Hosobe, S., Tsukada, T., Miura, K., Kamada, S., Saito, K., Iiizumi, M., Liu, W., Ericsson, J., and Watabe, K. (2008). Fatty acid synthase gene is up-regulated by hypoxia via activation of Akt and sterol regulatory element binding protein-1. Cancer Research *68*, 1003-1011.

Garcia-Echeverria, C. (2011). Blocking the mTOR pathway: a drug discovery perspective. Biochemical Society Transactions *39*, 451-455.

Gentleman, R.C., Carey, V.J., Bates, D.M., Bolstad, B., Dettling, M., Dudoit, S., Ellis, B., Gautier, L., Ge, Y., Gentry, J., Hornik, K., Hothorn, T., Huber, W., Iacus, S., Irizarry, R., Leisch, F., Li, C., Maechler, M., Rossini, A.J., Sawitzki, G., Smith, C., Smyth, G., Tierney, L., Yang, J.Y., and Zhang, J. (2004). Bioconductor: open software development for computational biology and bioinformatics. Genome Biology *5*, R80.

Giandomenico, V., Simonsson, M., Grönroos, E., and Ericsson, J. (2003). Coactivator-dependent acetylation stabilizes members of the SREBP family of transcription factors. Molecular and Cellular Biology *23*, 2587-2599.

Gibot, L., Follet, J., Metges, J.-P., Auvray, P., Simon, B., Corcos, L., and Le Jossic-Corcos, C. (2009). Human caspase 7 is positively controlled by SREBP-1 and SREBP-2. Biochemical Journal *420*, 473-483.

Gimm, T., Wiese, M., Teschemacher, B., Deggerich, A., Schödel, J., Knaup, K.X., Hackenbeck, T., Hellerbrand, C., Amann, K., Wiesener, M.S., Höning, S., Eckardt, K.-U., and Warnecke, C. (2010). Hypoxia-inducible protein 2 is a novel lipid droplet protein and a specific target gene of hypoxia-inducible factor-1. The FASEB Journal *24*, 4443-4458.

Goldstein, J., Deboseboyd, R., and Brown, M. (2006). Protein Sensors for Membrane Sterols. Cell *124*, 35-46.

Goldstein, J.L., Rawson, R.B., and Brown, M.S. (2002). Mutant mammalian cells as tools to delineate the sterol regulatory element-binding protein pathway for feedback regulation of lipid synthesis. Archives of Biochemistry and Biophysics *397*, 139-148.

Gong, Y., Lee, J.N., Lee, P.C., Goldstein, J.L., Brown, M.S., and Ye, J. (2006). Sterol-regulated ubiquitination and degradation of Insig-1 creates a convergent mechanism for feedback control of cholesterol synthesis and uptake. Cell Metabolism *3*, 15-24.

Gordon, G.B., Barcza, M.A., and Bush, M.E. (1977). Lipid accumulation of hypoxic tissue culture cells. American Journal of Pathology *88*, 663-678.

Greenspan, P., Mayer, E.P., and Fowler, S.D. (1985). Nile red: a selective fluorescent stain for intracellular lipid droplets. The Journal of Cell Biology *100*, 965-973.

Greer, E.L., and Brunet, A. (2005). FOXO transcription factors at the interface between longevity and tumor suppression. Oncogene *24*, 7410-7425.

Guertin, D., and Sabatini, D. (2007). Defining the Role of mTOR in Cancer. Cancer Cell *12*, 9-22.

Guertin, D.A., and Sabatini, D.M. (2009). The pharmacology of mTOR inhibition. Science Signaling *2*, pe24.

Guo, D., Hildebrandt, I., Prins, R., Soto, H., Mazzotta, M., Dang, J., Czernin, J., Shyy, J., Watson, A., Phelps, M., Radu, C., Cloughesy, T., and Mischel, P. (2009a). The AMPK agonist AICAR inhibits the growth of EGFRvIII-expressing glioblastomas by inhibiting lipogenesis. Proceedings of the National Academy of Sciences USA *106*, 12932-7.

Guo, D., Prins, R.M., Dang, J., Kuga, D., Iwanami, A., Soto, H., Lin, K.Y., Huang, T.T., Akhavan, D., Hock, M.B., Zhu, S., Kofman, A.A., Bensinger, S.J., Yong, W.H., Vinters, H.V., Horvath, S., Watson, A.D., Kuhn, J.G., Robins, H.I., Mehta, M.P., Wen, P.Y., Deangelis, L.M., Prados, M.D., Mellinghoff, I.K., Cloughesy, T.F., and Mischel, P.S. (2009b). EGFR Signaling Through an Akt-SREBP-1-Dependent, Rapamycin-Resistant Pathway Sensitizes Glioblastomas to Antilipogenic Therapy. Science Signaling *2*, ra82-ra82.

Haar, E.V., Lee, S.-I., Bandhakavi, S., Griffin, T.J., and Kim, D.-H. (2007). Insulin signalling to mTOR mediated by the Akt/PKB substrate PRAS40. Nature Cell Biology *9*, 316-323.

Hanahan, D., and Weinberg, R.A. (2000). The hallmarks of cancer. Cell *100*, 57-70.

Hanahan, D., and Weinberg, R.A. (2011). Hallmarks of cancer: the next generation. Cell *144*, 646-674.

Hannah, V.C., Ou, J., Luong, A., Goldstein, J.L., and Brown, M.S. (2001). Unsaturated fatty acids down-regulate srebp isoforms 1a and 1c by two mechanisms in HEK-293 cells. The Journal of Biological Chemistry *276*, 4365-4372.

Hardt, M., Chantaravisoot, N., and Tamanoi, F. (2011). Activating mutations of TOR (target of rapamycin). Genes to Cells *16*, 141-151.

Harris, A.L. (2002). Hypoxia--a key regulatory factor in tumour growth. Nature Reviews Cancer *2*, 38-47.

Hatzivassiliou, G., Zhao, F., Bauer, D.E., Andreadis, C., Shaw, A.N., Dhanak, D., Hingorani, S.R., Tuveson, D.A., and Thompson, C.B. (2005). ATP citrate lyase inhibition can suppress tumor cell growth. Cancer Cell *8*, 311-321.

Hegarty, B.D., Bobard, A., Hainault, I., Ferre, P., Bossard, P., and Foufelle, F. (2005). Distinct roles of insulin and liver X receptor in the induction and cleavage of sterol regulatory element-binding protein-1c. Proceedings of the National Academy of Sciences USA *102*, 791-796.

Heinonen, H., Nieminen, A., Saarela, M., Kallioniemi, A., Klefström, J., Hautaniemi, S., and Monni, O. (2008). Deciphering downstream gene targets of PI3K/mTOR/p70S6K pathway in breast cancer. BMC Genomics *9*, 348.

Hilvo, M., Denkert, C., Lehtinen, L., Müller, B., Brockmöller, S., Seppänen-Laakso, T., Budczies, J., Bucher, E., Yetukuri, L., Castillo, S., Berg, E., Nygren, H., Sysi-Aho, M., Griffin, J.L., Fiehn, O., Loibl, S., Richter-Ehrenstein, C., Radke, C., Hyötyläinen, T., Kallioniemi, O., Iljin, K., and Oresic, M. (2011). Novel Theranostic Opportunities Offered by Characterization of Altered Membrane Lipid Metabolism in Breast Cancer Progression. Cancer Research *71*, 3236-3245.

Hirano, Y., Murata, S., Tanaka, K., Shimizu, M., and Sato, R. (2003). Sterol regulatory element-binding proteins are negatively regulated through SUMO-1 modification independent of the ubiquitin/26 S proteasome pathway. The Journal of Biological Chemistry *278*, 16809-16819.

Hirano, Y., Yoshida, M., Shimizu, M., and Sato, R. (2001). Direct demonstration of rapid degradation of nuclear sterol regulatory element-binding proteins by the ubiquitin-proteasome pathway. The Journal of Biological Chemistry *276*, 36431-36437.

Horton, J.D. (2002). Sterol regulatory element-binding proteins: transcriptional activators of lipid synthesis. Biochemical Society Transactions *30*, 1091-1095.

Horton, J.D., Goldstein, J.L., and Brown, M.S. (2002). SREBPs: activators of the complete program of cholesterol and fatty acid synthesis in the liver. The Journal of Clinical Investigation *109*, 1125-1131.

Horton, J.D., Shah, N.A., Warrington, J.A., Anderson, N.N., Park, S.W., Brown, M.S., and Goldstein, J.L. (2003). Combined analysis of oligonucleotide microarray data from transgenic and knockout mice identifies direct SREBP target genes. Proceedings of the National Academy of Sciences USA *100*, 12027-12032.

Horton, J.D., Shimomura, I., Brown, M.S., Hammer, R.E., Goldstein, J.L., and Shimano, H. (1998). Activation of cholesterol synthesis in preference to fatty acid synthesis in liver and adipose tissue of transgenic mice overproducing sterol regulatory element-binding protein-2. The Journal of Clinical Investigation *101*, 2331-2339.

Howard, B.V., Howard, W.J., and Bailey, J.M. (1974). Acetyl coenzyme A synthetase and the regulation of lipid synthesis from acetate in cultured cells. The Journal of Biological Chemistry *249*, 7912-7921.

Howell, J.J., and Manning, B.D. (2011). mTOR couples cellular nutrient sensing to organismal metabolic homeostasis. Trends in Endocrinology and Metabolism *22*, 94-102.

Hresko, R.C., and Mueckler, M. (2005). mTOR.RICTOR is the Ser473 kinase for Akt/protein kinase B in 3T3-L1 adipocytes. The Journal of Biological Chemistry *280*, 40406-40416.

Hsu, P.P., Kang, S.A., Rameseder, J., Zhang, Y., Ottina, K.A., Lim, D., Peterson, T.R., Choi, Y., Gray, N.S., Yaffe, M.B., Marto, J.A., and Sabatini, D.M. (2011). The mTOR-regulated phosphoproteome reveals a mechanism of mTORC1-mediated inhibition of growth factor signaling. Science *332*, 1317-1322.

Hua, X., Nohturfft, A., Goldstein, J.L., and Brown, M.S. (1996). Sterol resistance in CHO cells traced to point mutation in SREBP cleavage-activating protein. Cell *87*, 415-426.

Hua, X., Wu, J., Goldstein, J.L., Brown, M.S., and Hobbs, H.H. (1995). Structure of the human gene encoding sterol regulatory element binding protein-1 (SREBF1) and localization of SREBF1 and SREBF2 to chromosomes 17p11.2 and 22q13. Genomics *25*, 667-673.

Hua, X., Yokoyama, C., Wu, J., Briggs, M.R., Brown, M.S., Goldstein, J.L., and Wang, X. (1993). SREBP-2, a second basic-helix-loop-helix-leucine zipper protein that stimulates transcription by binding to a sterol regulatory element. Proceedings of the National Academy of Sciences USA *90*, 11603-11607.

Huang, J., and Manning, B.D. (2008). The TSC1-TSC2 complex: a molecular switchboard controlling cell growth. Biochemical Journal *412*, 179-190.

Hughes, A., Todd, B., and Espenshade, P. (2005). SREBP Pathway Responds to Sterols and Functions as an Oxygen Sensor in Fission Yeast. Cell *120*, 831-842.

Hull, F.E., Radloff, J.F., and Sweeley, C.C. (1975). beta-Hydroxy fatty acid production during fatty acid oxidation by heart mitochondria. Recent Advances in Studies on Cardiac Structural Metabolism *7*, 13-21.

Ide, T., Shimano, H., Yahagi, N., Matsuzaka, T., Nakakuki, M., Yamamoto, T., Nakagawa, Y., Takahashi, A., Suzuki, H., Sone, H., Toyoshima, H., Fukamizu, A., and Yamada, N. (2004). SREBPs suppress IRS-2-mediated insulin signalling in the liver. Nature Cell Biology *6*, 351-357.

Igal, R.A. (2010). Stearoyl-CoA desaturase-1: a novel key player in the mechanisms of cell proliferation, programmed cell death and transformation to cancer. Carcinogenesis *31*, 1509-1515.

Inoki, K., Li, Y., Xu, T., and Guan, K.L. (2003). Rheb GTPase is a direct target of TSC2 GAP activity and regulates mTOR signaling. Genes and Development *17*, 1829-1834.

Inoue, J., Ito, Y., Shimada, S., Satoh, S.-i., Sasaki, T., Hashidume, T., Kamoshida, Y., Shimizu, M., and Sato, R. (2011). Glutamine stimulates the gene expression and processing of sterol regulatory element-binding proteins, thereby increasing the expression of their target genes. FEBS Journal *278*, 2739-50.

Inoue, N., Shimano, H., Nakakuki, M., Matsuzaka, T., Nakagawa, Y., Yamamoto, T., Sato, R., Takahashi, A., Sone, H., Yahagi, N., Suzuki, H., Toyoshima, H., and Yamada, N. (2005). Lipid synthetic transcription factor SREBP-1a activates p21WAF1/CIP1, a universal cyclin-dependent kinase inhibitor. Molecular and Cellular Biology *25*, 8938-8947.

Jacinto, E., Facchinetti, V., Liu, D., Soto, N., Wei, S., Jung, S.Y., Huang, Q., Qin, J., and Su, B. (2006). SIN1/MIP1 maintains rictor-mTOR complex integrity and regulates Akt phosphorylation and substrate specificity. Cell *127*, 125-137.

Jackson, S.M., Ericsson, J., Mantovani, R., and Edwards, P.A. (1998). Synergistic activation of transcription by nuclear factor Y and sterol regulatory element binding protein. Journal of Lipid Research *39*, 767-776.

Jiang, P., Du, W., Wang, X., Mancuso, A., Gao, X., Wu, M., and Yang, X. (2011). p53 regulates biosynthesis through direct inactivation of glucose-6-phosphate dehydrogenase. Nature Cell Biology *13*, 310-316.

Jones, P.F., Jakubowicz, T., and Hemmings, B.A. (1991). Molecular cloning of a second form of rac protein kinase. Cell Regulation *2*, 1001-1009.

Kahn, B.B., Alquier, T., Carling, D., and Hardie, D.G. (2005). AMP-activated protein kinase: ancient energy gauge provides clues to modern understanding of metabolism. Cell Metabolism *1*, 15-25.

Kallin, A., Johannessen, L.E., Cani, P.D., Marbehant, C.Y., Essaghir, A., Foufelle, F., Ferré, P., Heldin, C.-H., Delzenne, N.M., and Demoulin, J.-B. (2007). SREBP-1 regulates the expression of heme oxygenase 1 and the phosphatidylinositol-3 kinase regulatory subunit p55 gamma. The Journal of Lipid Research *48*, 1628-1636.

Kamei, Y., Miura, S., Suganami, T., Akaike, F., Kanai, S., Sugita, S., Katsumata, A., Aburatani, H., Unterman, T.G., Ezaki, O., and Ogawa, Y. (2008). Regulation of SREBP1c gene expression in skeletal muscle: role of retinoid X receptor/liver X receptor and forkhead-O1 transcription factor. Endocrinology *149*, 2293-2305.

Keller, P., Petrie, J.T., De Rose, P., Gerin, I., Wright, W.S., Chiang, S.H., Nielsen, A.R., Fischer, C.P., Pedersen, B.K., and MacDougald, O.A. (2008). Fat-specific protein 27 regulates storage of triacylglycerol. The Journal of Biological Chemistry *283*, 14355-14365.

Keunen, O., Johansson, M., Oudin, A., Sanzey, M., Rahim, S.A.A., Fack, F., Thorsen, F., Taxt, T., Bartos, M., Jirik, R., Miletic, H., Wang, J., Stieber, D., Stuhr, L., Moen, I., Rygh, C.B., Bjerkvig, R., and Niclou, S.P. (2011). Anti-VEGF treatment reduces blood supply and increases tumor cell invasion in glioblastoma. Proceedings of the National Academy of Sciences USA *108*, 3749-3754.

Kim, E., Goraksha-Hicks, P., Li, L., Neufeld, T.P., and Guan, K.-L. (2008). Regulation of TORC1 by Rag GTPases in nutrient response. Nature Cell Biology *10*, 935-945.

Kim, J.B., Sarraf, P., Wright, M., Yao, K.M., Mueller, E., Solanes, G., Lowell, B.B., and Spiegelman, B.M. (1998). Nutritional and insulin regulation of fatty acid synthetase and leptin gene expression through ADD1/SREBP1. Journal of Clinical Investigation *101*, 1-9.

Kim, J.B., Spotts, G.D., Halvorsen, Y.D., Shih, H.M., Ellenberger, T., Towle, H.C., and Spiegelman, B.M. (1995). Dual DNA binding specificity of ADD1/SREBP1 controlled by a single amino acid in the basic helix-loop-helix domain. Moleulcar and Cellular Biology *15*, 2582-2588.

Kim, J.W., Tchernyshyov, I., Semenza, G.L., and Dang, C.V. (2006). HIF-1-mediated expression of pyruvate dehydrogenase kinase: a metabolic switch required for cellular adaptation to hypoxia. Cell Metabolism *3*, 177-185.

Koh, M.Y., Darnay, B.G., and Powis, G. (2008). Hypoxia-associated factor, a novel E3-ubiquitin ligase, binds and ubiquitinates hypoxia-inducible factor 1alpha, leading to its oxygen-independent degradation. Molecular and Cellular Biology *28*, 7081-7095.

Kohn, A.D., Barthel, A., Kovacina, K.S., Boge, A., Wallach, B., Summers, S.A., Birnbaum, M.J., Scott, P.H., Lawrence, J.C., Jr., and Roth, R.A. (1998). Construction and characterization of a conditionally active version of the serine/threonine kinase Akt. The Journal of Biological Chemistry *273*, 11937-11943.

Kotzka, J., Lehr, S., Roth, G., Avci, H., Knebel, B., and Muller-Wieland, D. (2004). Insulin-activated Erk-mitogen-activated protein kinases phosphorylate sterol regulatory element-binding Protein-2 at serine residues 432 and 455 in vivo. The Journal of Biological Chemistry *279*, 22404-22411.

Kotzka, J., Müller-Wieland, D., Roth, G., Kremer, L., Munck, M., Schürmann, S., Knebel, B., and Krone, W. (2000). Sterol regulatory element binding proteins (SREBP)-1a and SREBP-2 are linked to the MAP-kinase cascade. Journal of Lipid Research *41*, 99-108.

Krishnan, J., Suter, M., Windak, R., Krebs, T., Felley, A., Montessuit, C., Tokarska-Schlattner, M., Aasum, E., Bogdanova, A., Perriard, E., Perriard, J.-C., Larsen, T., Pedrazzini, T., and Krek, W. (2009). Activation of a HIF1alpha-PPARgamma axis underlies the integration of glycolytic and lipid anabolic pathways in pathologic cardiac hypertrophy. Cell Metabolism *9*, 512-524.

Kuhajda, F.P., Jenner, K., Wood, F.D., Hennigar, R.A., Jacobs, L.B., Dick, J.D., and Pasternack, G.R. (1994). Fatty acid synthesis: a potential selective target for antineoplastic therapy. Proceedings of the Natlional Academy of Sciences U S A *91*, 6379-6383.

Lee, C.-Y.S., Stewart, E.V., Hughes, B.T., and Espenshade, P.J. (2009). Oxygen-dependent binding of Nro1 to the prolyl hydroxylase Ofd1 regulates SREBP degradation in yeast. The EMBO Journal *28*, 135-143.

Lee, J.N., Song, B., DeBose-Boyd, R.A., and Ye, J. (2006). Sterol-regulated degradation of Insig-1 mediated by the membrane-bound ubiquitin ligase gp78. The Journal of Biological Chemistry *281*, 39308-39315.

Lee, J.P., Brauweiler, A., Rudolph, M., Hooper, J.E., Drabkin, H.A., and Gemmill, R.M. (2010). The TRC8 Ubiquitin Ligase Is Sterol Regulated and Interacts with Lipid and Protein Biosynthetic Pathways. Molecular Cancer Research *8*, 93-106.

Lee, S.J., Sekimoto, T., Yamashita, E., Nagoshi, E., Nakagawa, A., Imamoto, N., Yoshimura, M., Sakai, H., Chong, K.T., Tsukihara, T., and Yoneda, Y. (2003). The structure of importin-beta bound to SREBP-2: nuclear import of a transcription factor. Science *302*, 1571-1575.

Lewis, C.A., Griffiths, B., Santos, C.R., Pende, M., and Schulze, A. (2011). Genetic ablation of S6-kinase does not prevent processing of SREBP1. Advances in Enzyme Regulation *51*, 280-290.

Li, J. (2000). Sterol Regulatory Element-Binding Protein-1 Participates in the Regulation of Fatty Acid Synthase Expression in Colorectal Neoplasia. Experimental Cell Research *261*, 159-165.

Li, J., Bosch-Marce, M., Nanayakkara, A., Savransky, V., Fried, S.K., Semenza, G.L., and Polotsky, V.Y. (2006). Altered metabolic responses to intermittent hypoxia in mice with partial deficiency of hypoxia-inducible factor-1alpha. Physiological Genomics *25*, 450-457.

Li, J., Grigoryev, D.N., Ye, S.Q., Thorne, L., Schwartz, A.R., Smith, P.L., O'Donnell, C.P., and Polotsky, V.Y. (2005a). Chronic intermittent hypoxia upregulates genes of lipid biosynthesis in obese mice. Journal of Applied Physiology *99*, 1643-1648.

Li, J., Thorne, L.N., Punjabi, N.M., Sun, C.K., Schwartz, A.R., Smith, P.L., Marino, R.L., Rodriguez, A., Hubbard, W.C., O'Donnell, C.P., and Polotsky, V.Y. (2005b). Intermittent hypoxia induces hyperlipidemia in lean mice. Circulation Research *97*, 698-706.

Li, J.N., Mahmoud, M.A., Han, W.F., Ripple, M., and Pizer, E.S. (2000). Sterol regulatory element-binding protein-1 participates in the regulation of fatty acid synthase expression in colorectal neoplasia. Experimental Cell Research *261*, 159-165.

Li, S., Brown, M.S., and Goldstein, J.L. (2010). Bifurcation of insulin signaling pathway in rat liver: mTORC1 required for stimulation of lipogenesis, but not inhibition of gluconeogenesis. Proceedings of the National Academy of Sciences USA *107*, 3441-6.

Li, X., Monks, B., Ge, Q., and Birnbaum, M.J. (2007). Akt/PKB regulates hepatic metabolism by directly inhibiting PGC-1alpha transcription coactivator. Nature *447*, 1012-1016.

Li, Y., Xu, S., Mihaylova, M.M., Zheng, B., Hou, X., Jiang, B., Park, O., Luo, Z., Lefai, E., Shyy, J.Y.-J., Gao, B., Wierzbicki, M., Verbeuren, T.J., Shaw, R.J., Cohen, R.A., and Zang, M. (2011). AMPK Phosphorylates and Inhibits SREBP Activity to Attenuate Hepatic Steatosis and Atherosclerosis in Diet-Induced Insulin-Resistant Mice. Cell Metabolism *13*, 376-388.

Liang, G. (2002). Diminished Hepatic Response to Fasting/Refeeding and Liver X Receptor Agonists in Mice with Selective Deficiency of Sterol Regulatory Element-binding Protein-1c. The Journal of Biological Chemistry *277*, 9520-9528.

Liang, Y., Diehn, M., Watson, N., Bollen, A.W., Aldape, K.D., Nicholas, M.K., Lamborn, K.R., Berger, M.S., Botstein, D., Brown, P.O., and Israel, M.A. (2005). Gene expression profiling reveals molecularly and clinically distinct subtypes of glioblastoma multiforme. Proceedings of the National Academy of Sciences USA *102*, 5814-5819.

Lim, J.H., Lee, Y.M., Chun, Y.S., Chen, J., Kim, J.E., and Park, J.W. (2010). Sirtuin 1 modulates cellular responses to hypoxia by deacetylating hypoxia-inducible factor 1 alpha. Molecular Cell *38*, 864-878.

Lin, S.M., Du, P., Huber, W., and Kibbe, W.A. (2008). Model-based variance-stabilizing transformation for Illumina microarray data. Nucleic Acids Research *36*, e11.

Listenberger, L.L., Han, X., Lewis, S.E., Cases, S., Farese, R.V., Jr., Ory, D.S., and Schaffer, J.E. (2003). Triglyceride accumulation protects against fatty acid-induced lipotoxicity. Proceedings of the National Academy of Sciences USA *100*, 3077-3082.

Littlewood, T.D., Hancock, D.C., Danielian, P.S., Parker, M.G., and Evan, G.I. (1995). A modified oestrogen receptor ligand-binding domain as an improved switch for the regulation of heterologous proteins. Nucleic Acids Research *23*, 1686-1690.

Liu, L., Cash, T.P., Jones, R.G., Keith, B., Thompson, C.B., and Simon, M.C. (2006). Hypoxia-induced energy stress regulates mRNA translation and cell growth. Molecular Cell *21*, 521-531.

Liu, X., Qiao, A., Ke, Y., Kong, X., Liang, J., Wang, R., Ouyang, X., Zuo, J., Chang, Y., and Fang, F. (2010). FoxO1 represses LXRα-mediated transcriptional activity of SREBP-1c promoter in HepG2 cells. FEBS Letters *584*, 4330-4.

Locke, G.A., Cheng, D., Witmer, M.R., Tamura, J.K., Haque, T., Carney, R.F., Rendina, A.R., and Marcinkeviciene, J. (2008). Differential activation of recombinant human acetyl-CoA carboxylases 1 and 2 by citrate. Archives of Biochemistry and Biophysics *475*, 72-79.

Logette, E., Le Jossic-Corcos, C., Masson, D., Solier, S., Sequeira-Legrand, A., Dugail, I., Lemaire-Ewing, S., Desoche, L., Solary, E., and Corcos, L. (2005). Caspase-2, a novel lipid sensor under the control of sterol regulatory element binding protein 2. Molecular and Cellular Biology *25*, 9621-9631.

Long, X., Lin, Y., Ortiz-Vega, S., Yonezawa, K., and Avruch, J. (2005). Rheb binds and regulates the mTOR kinase. Current Biology *15*, 702-713.

Lu, C.-W., Lin, S.-C., Chen, K.-F., Lai, Y.-Y., and Tsai, S.-J. (2008). Induction of pyruvate dehydrogenase kinase-3 by hypoxia-inducible factor-1 promotes metabolic switch and drug resistance. The Journal of Biological Chemistry *283*, 28106-28114.

Lu, M. (2006). Sterol regulatory element-binding protein 1 is negatively modulated by PKA phosphorylation. AJP: Cell Physiology *290*, C1477-C1486.

Lu, S., and Archer, M.C. (2010). Sp1 coordinately regulates de novo lipogenesis and proliferation in cancer cells. International Journal of Cancer *126*, 416-425.

Luong, A., Hannah, V.C., Brown, M.S., and Goldstein, J.L. (2000). Molecular characterization of human acetyl-CoA synthetase, an enzyme regulated by sterol regulatory element-binding proteins. The Journal of Biological Chemistry *275*, 26458-26466.

Luyimbazi, D., Akcakanat, A., McAuliffe, P.F., Zhang, L., Singh, G., Gonzalez-Angulo, A.M., Chen, H., Do, K.-A., Zheng, Y., Hung, M.-C., Mills, G.B., and Meric-Bernstam, F. (2010). Rapamycin Regulates Stearoyl CoA Desaturase 1 Expression in Breast Cancer. Molecular Cancer Therapeutics *9*, 2770-84.

Ma, K.L., Ruan, X.Z., Powis, S.H., Chen, Y., Moorhead, J.F., and Varghese, Z. (2007). Sirolimus modifies cholesterol homeostasis in hepatic cells: a potential molecular mechanism for sirolimus-associated dyslipidemia. Transplantation *84*, 1029-1036.

Ma, Y.Y., Wei, S.J., Lin, Y.C., Lung, J.C., Chang, T.C., Whang-Peng, J., Liu, J.M., Yang, D.M., Yang, W.K., and Shen, C.Y. (2000). PIK3CA as an oncogene in cervical cancer. Oncogene *19*, 2739-2744.

Magana, M.M., Lin, S.S., Dooley, K.A., and Osborne, T.F. (1997). Sterol regulation of acetyl coenzyme A carboxylase promoter requires two interdependent binding sites for sterol regulatory element binding proteins. Journal of Lipid Research *38*, 1630-1638.

Majmundar, A.J., Wong, W.J., and Simon, M.C. (2010). Hypoxia-inducible factors and the response to hypoxic stress. Molecular Cell *40*, 294-309.

Mandard, S., Müller, M., and Kersten, S. (2004). Peroxisome proliferator-activated receptor alpha target genes. Cellular and Molecular Life Sciences *61*, 393-416.

Manning, B., and Cantley, L. (2007). AKT/PKB Signaling: Navigating Downstream. Cell *129*, 1261-1274.

Massion, P.P., Kuo, W.L., Stokoe, D., Olshen, A.B., Treseler, P.A., Chin, K., Chen, C., Polikoff, D., Jain, A.N., Pinkel, D., Albertson, D.G., Jablons, D.M., and Gray, J.W. (2002). Genomic copy number analysis of non-small cell lung cancer using array comparative genomic hybridization: implications of the phosphatidylinositol 3-kinase pathway. Cancer Research *62*, 3636-3640.

Matthews, K.A., Ozdemir, C., and Rawson, R.B. (2010). Activation of sterol regulatory element binding proteins in the absence of Scap in Drosophila melanogaster. Genetics *185*, 189-198.

Maxwell, P.H., Dachs, G.U., Gleadle, J.M., Nicholls, L.G., Harris, A.L., Stratford, I.J., Hankinson, O., Pugh, C.W., and Ratcliffe, P.J. (1997). Hypoxia-inducible factor-1 modulates gene expression in solid tumors and influences both angiogenesis and tumor growth. Proceedings of the National Academy of Sciences USA *94*, 8104-8109.

Menendez, J.A., and Lupu, R. (2007). Fatty acid synthase and the lipogenic phenotype in cancer pathogenesis. Nature Reviews Cancer *7*, 763-777.

Mita, R., Beaulieu, M.J., Field, C., and Godbout, R. (2010). Brain fatty acid-binding protein and omega-3/omega-6 fatty acids: mechanistic insight into malignant glioma cell migration. The Journal of Biological Chemistry *285*, 37005-37015.

Moasser, M.M. (2007). The oncogene HER2: its signaling and transforming functions and its role in human cancer pathogenesis. Oncogene *26*, 6469-6487.

Moore, S., Knudsen, B., True, L.D., Hawley, S., Etzioni, R., Wade, C., Gifford, D., Coleman, I., and Nelson, P.S. (2005). Loss of stearoyl-CoA desaturase expression is a frequent event in prostate carcinoma. International Journal of Cancer *114*, 563-571.

Morgenstern, J.P., and Land, H. (1990). Advanced mammalian gene transfer: high titre retroviral vectors with multiple drug selection markers and a complementary helper-free packaging cell line. Nucleic Acids Research *18*, 3587-3596.

Motallebipour, M., Enroth, S., Punga, T., Ameur, A., Koch, C., Dunham, I., Komorowski, J., Ericsson, J., and Wadelius, C. (2009). Novel genes in cell cycle control and lipid metabolism with dynamically regulated binding sites for sterol regulatory element-binding protein 1 and RNA polymerase II in HepG2 cells detected by chromatin immunoprecipitation with microarray detection. FEBS Journal *276*, 1878-1890.

Motoyama, K., Fukumoto, S., Koyama, H., Emoto, M., Shimano, H., Maemura, K., and Nishizawa, Y. (2006). SREBP inhibits VEGF expression in human smooth muscle cells. Biochemical and Biophysical Research Communications *342*, 354-360.

Mukodani, J., Ishikawa, Y., and Fukuzaki, H. (1990). Effects of hypoxia on sterol synthesis, acyl-CoA:cholesterol acyltransferase activity, and efflux of cholesterol in cultured rabbit skin fibroblasts. Arteriosclerosis *10*, 106-110.

Munday, M.R. (2002). Regulation of mammalian acetyl-CoA carboxylase. Biochemical Society Transactions *30*, 1059-1064.

Murphy, C., Ledmyr, H., Ehrenborg, E., and Gåfvels, M. (2006). Promoter analysis of the murine squalene epoxidase gene. Identification of a 205 bp homing region regulated by both SREBPS and NF-Y. Biochimica et Biophysica Acta (BBA) - Molecular and Cell Biology of Lipids *1761*, 1213-1227.

Nagoshi, E., Imamoto, N., Sato, R., and Yoneda, Y. (1999). Nuclear import of sterol regulatory element-binding protein-2, a basic helix-loop-helix-leucine zipper (bHLH-Zip)-containing transcription factor, occurs through the direct interaction of importin beta with HLH-Zip. Molecular Biology of the Cell *10*, 2221-2233.

Nagoshi, E., and Yoneda, Y. (2001). Dimerization of sterol regulatory element-binding protein 2 via the helix-loop-helix-leucine zipper domain is a prerequisite for its nuclear localization mediated by importin beta. Molecular and Cellular Biology *21*, 2779-2789.

Nakajima, T., Hamakubo, T., Kodama, T., Inazawa, J., and Emi, M. (1999). Genomic structure and chromosomal mapping of the human sterol regulatory element binding protein (SREBP) cleavage-activating protein (SCAP) gene. Journal of Human Genetics *44*, 402-407.

Nakakuki, M., Shimano, H., Inoue, N., Tamura, M., Matsuzaka, T., Nakagawa, Y., Yahagi, N., Toyoshima, H., Sato, R., and Yamada, N. (2007). A transcription factor of lipid synthesis, sterol regulatory element-binding protein (SREBP)-1a causes G1 cell-cycle arrest after accumulation of cyclin-dependent kinase (cdk) inhibitors. FEBS Journal *274*, 4440-4452.

Narita, Y., Nagane, M., Mishima, K., Huang, H.J., Furnari, F.B., and Cavenee, W.K. (2002). Mutant epidermal growth factor receptor signaling down-regulates p27 through activation of the phosphatidylinositol 3-kinase/Akt pathway in glioblastomas. Cancer Research *62*, 6764-6769.

Nguyen, A.D., McDonald, J.G., Bruick, R.K., and DeBose-Boyd, R.A. (2007). Hypoxia stimulates degradation of 3-hydroxy-3-methylglutaryl-coenzyme A reductase through accumulation of lanosterol and hypoxia-inducible factor-mediated induction of insigs. The Journal of Biological Chemistry *282*, 27436-27446.

Nohturfft, A., Debose-Boyd, R.A., Scheek, S., Goldstein, J.L., and Brown, M.S. (1999). Sterols regulate cycling of SREBP cleavage-activating protein (SCAP) between endoplasmic reticulum and Golgi. Proceedings of the National Academy of Sciences USA *96*, 11235-11240.

Nohturfft, A., Yabe, D., Goldstein, J.L., Brown, M.S., and Espenshade, P.J. (2000). Regulated step in cholesterol feedback localized to budding of SCAP from ER membranes. Cell *102*, 315-323.

Nohturfft, A., and Zhang, S.C. (2009). Coordination of lipid metabolism in membrane biogenesis. Annual Review of Cell and Developmental Biology *25*, 539-566.

Nomura, D.K., Long, J.Z., Niessen, S., Hoover, H.S., Ng, S.-W., and Cravatt, B.F. (2010). Monoacylglycerol Lipase Regulates a Fatty Acid Network that Promotes Cancer Pathogenesis. Cell *140*, 49-61.

Ntambi, J.M. (1999). Regulation of stearoyl-CoA desaturase by polyunsaturated fatty acids and cholesterol. The Journal of Lipid Research *40*, 1549-1558.

Ntambi, J.M., and Miyazaki, M. (2004). Regulation of stearoyl-CoA desaturases and role in metabolism. Progress in Lipid Research *43*, 91-104.

Oh, S.Y. (2003). Acetyl-CoA Carboxylase Gene Is Regulated by Sterol Regulatory Element-binding Protein-1 in Liver. The Journal of Biological Chemistry *278*, 28410-28417.

Osborne, T.F., and Espenshade, P.J. (2009). Evolutionary conservation and adaptation in the mechanism that regulates SREBP action: what a long, strange tRIP it's been. Genes and Development *23*, 2578-2591.

Ou, J., Tu, H., Shan, B., Luk, A., Debose-Boyd, R.A., Bashmakov, Y., Goldstein, J.L., and Brown, M.S. (2001). Unsaturated fatty acids inhibit transcription of the sterol regulatory element-binding protein-1c (SREBP-1c) gene by antagonizing ligand-dependent activation of the LXR. Proceedings of the National Academy of Sciences USA *98*, 6027-6032.

Pallottini, V., Guantario, B., Martini, C., Totta, P., Filippi, I., Carraro, F., and Trentalance, A. (2008). Regulation of HMG-CoA reductase expression by hypoxia. Journal of Cellular Biochemistry *104*, 701-709.

Papandreou, I., Cairns, R.A., Fontana, L., Lim, A.L., and Denko, N.C. (2006). HIF-1 mediates adaptation to hypoxia by actively downregulating mitochondrial oxygen consumption. Cell Metabolism *3*, 187-197.

Parks, S.K., Chiche, J., and Pouyssegur, J. (2011). pH control mechanisms of tumor survival and growth. Journal of Cell Physiology *226*, 299-308.

Parraga, A., Bellsolell, L., Ferre-D'Amare, A.R., and Burley, S.K. (1998). Co-crystal structure of sterol regulatory element binding protein 1a at 2.3 A resolution. Structure *6*, 661-672.

Parsons, D.W., Jones, S., Zhang, X., Lin, J.C., Leary, R.J., Angenendt, P., Mankoo, P., Carter, H., Siu, I.M., Gallia, G.L., Olivi, A., McLendon, R., Rasheed, B.A., Keir, S., Nikolskaya, T., Nikolsky, Y., Busam, D.A., Tekleab, H., Diaz, L.A., Jr., Hartigan, J., Smith, D.R., Strausberg, R.L., Marie, S.K., Shinjo, S.M., Yan, H., Riggins, G.J., Bigner, D.D., Karchin, R., Papadopoulos, N., Parmigiani, G., Vogelstein, B., Velculescu, V.E., and Kinzler, K.W. (2008). An integrated genomic analysis of human glioblastoma multiforme. Science *321*, 1807-1812.

Pende, M., Um, S.H., Mieulet, V., Sticker, M., Goss, V.L., Mestan, J., Mueller, M., Fumagalli, S., Kozma, S.C., and Thomas, G. (2004). S6K1(-/-)/S6K2(-/-) mice exhibit perinatal lethality and rapamycin-sensitive 5'-terminal oligopyrimidine mRNA translation and reveal a mitogen-activated protein kinase-dependent S6 kinase pathway. Molecular and Cellular Biology *24*, 3112-3124.

Peng, T., Golub, T.R., and Sabatini, D.M. (2002). The immunosuppressant rapamycin mimics a starvation-like signal distinct from amino acid and glucose deprivation. Molecular and Cellular Biology *22*, 5575-5584.

Peterson, T.R., Sengupta, S.S., Harris, T.E., Carmack, A.E., Kang, S.A., Balderas, E., Guertin, D.A., Madden, K.L., Carpenter, A.E., Finck, B.N., and Sabatini, D.M. (2011). mTOR Complex 1 Regulates Lipin 1 Localization to Control the SREBP Pathway. Cell *146*, 408-420.

Peyrollier, K., Hajduch, E., Blair, A.S., Hyde, R., and Hundal, H.S. (2000). L-leucine availability regulates phosphatidylinositol 3-kinase, p70 S6 kinase and glycogen synthase kinase-3 activity in L6 muscle cells: evidence for the involvement of the mammalian target of rapamycin (mTOR) pathway in the L-leucine-induced up-regulation of system A amino acid transport. Biochemical Journal *350 Pt 2*, 361-368.

Ponugoti, B., Kim, D.H., Xiao, Z., Smith, Z., Miao, J., Zang, M., Wu, S.Y., Chiang, C.M., Veenstra, T.D., and Kemper, J.K. (2010). SIRT1 deacetylates and inhibits SREBP-1C activity in regulation of hepatic lipid metabolism. The Journal of Biological Chemistry *285*, 33959-33970.

Porstmann, T., Griffiths, B., Chung, Y.-L., Delpuech, O., Griffiths, J.R., Downward, J., and Schulze, A. (2005). PKB/Akt induces transcription of enzymes involved in cholesterol and fatty acid biosynthesis via activation of SREBP. Oncogene *24*, 6465-81.

Porstmann, T., Santos, C., Griffiths, B., Cully, M., Wu, M., Leevers, S., Griffiths, J., Chung, Y., and Schulze, A. (2008). SREBP Activity Is Regulated by mTORC1 and Contributes to Akt-Dependent Cell Growth. Cell Metabolism *8*, 224-236.

Porstmann, T., Santos, C.R., Lewis, C., Griffiths, B., and Schulze, A. (2009). A new player in the orchestra of cell growth: SREBP activity is regulated by mTORC1 and contributes to the regulation of cell and organ size. Biochemical Society Transactions *37*, 278-283.

Potter, C.J., Pedraza, L.G., and Xu, T. (2002). Akt regulates growth by directly phosphorylating Tsc2. Nature Cell Biology *4*, 658-665.

Puigserver, P. (2005). Tissue-specific regulation of metabolic pathways through the transcriptional coactivator PGC1-alpha. International Journal of Obesity (Lond) *29 Suppl 1*, S5-9.

Punga, T. (2006). Phosphorylation and Ubiquitination of the Transcription Factor Sterol Regulatory Element-binding Protein-1 in Response to DNA Binding. The Journal of Biological Chemistry *281*, 25278-25286.

Puri, V., Konda, S., Ranjit, S., Aouadi, M., Chawla, A., Chouinard, M., Chakladar, A., and Czech, M.P. (2007). Fat-specific protein 27, a novel lipid droplet protein that enhances triglyceride storage. The Journal of Biological Chemistry *282*, 34213-34218.

Radhakrishnan, A., Ikeda, Y., Kwon, H.J., Brown, M.S., and Goldstein, J.L. (2007). Sterol-regulated transport of SREBPs from endoplasmic reticulum to Golgi: oxysterols block transport by binding to Insig. Proceedings of the National Academy of Sciences USA *104*, 6511-6518.

Rankin, E.B., Rha, J., Selak, M.A., Unger, T.L., Keith, B., Liu, Q., and Haase, V.H. (2009). Hypoxia-inducible factor 2 regulates hepatic lipid metabolism. Molecular and Cellular Biology *29*, 4527-4538.

Reed, B.D., Charos, A.E., Szekely, A.M., Weissman, S.M., Snyder, M., and Frankel, W.N. (2008). Genome-Wide Occupancy of SREBP1 and Its Partners NFY and SP1 Reveals Novel Functional Roles and Combinatorial Regulation of Distinct Classes of Genes. PLoS Genetics *4*, e1000133.

Reiling, J.H., and Hafen, E. (2004). The hypoxia-induced paralogs Scylla and Charybdis inhibit growth by down-regulating S6K activity upstream of TSC in Drosophila. Genes and Development *18*, 2879-2892.

Robey, R.B., and Hay, N. (2006). Mitochondrial hexokinases, novel mediators of the antiapoptotic effects of growth factors and Akt. Oncogene *25*, 4683-4696.

Rome, S., Lecomte, V., Meugnier, E., Rieusset, J., Debard, C., Euthine, V., Vidal, H., and Lefai, E. (2008). Microarray analyses of SREBP-1a and SREBP-1c target genes identify new regulatory pathways in muscle. Physiological Genomics *34*, 327-337.

Roth, G., Kotzka, J., Kremer, L., Lehr, S., Lohaus, C., Meyer, H.E., Krone, W., and Müller-Wieland, D. (2000). MAP kinases Erk1/2 phosphorylate sterol regulatory element-binding protein (SREBP)-1a at serine 117 in vitro. The Journal of Biological Chemistry *275*, 33302-33307.

Rysman, E., Brusselmans, K., Scheys, K., Timmermans, L., Derua, R., Munck, S., Van Veldhoven, P.P., Waltregny, D., Daniëls, V.W., Machiels, J., Vanderhoydonc, F., Smans, K., Waelkens, E., Verhoeven, G., and Swinnen, J.V. (2010). De novo lipogenesis protects cancer cells from free radicals and chemotherapeutics by promoting membrane lipid saturation. Cancer Research *70*, 8117-8126.

Sakai, J., Duncan, E.A., Rawson, R.B., Hua, X., Brown, M.S., and Goldstein, J.L. (1996). Sterol-regulated release of SREBP-2 from cell membranes requires two sequential cleavages, one within a transmembrane segment. Cell *85*, 1037-1046.

Sakai, J., Nohturfft, A., Cheng, D., Ho, Y.K., Brown, M.S., and Goldstein, J.L. (1997). Identification of complexes between the COOH-terminal domains of sterol regulatory element-binding proteins (SREBPs) and SREBP cleavage-activating protein. The Journal of Biological Chemistry *272*, 20213-20221.

Sakai, J., Rawson, R.B., Espenshade, P.J., Cheng, D., Seegmiller, A.C., Goldstein, J.L., and Brown, M.S. (1998). Molecular identification of the sterol-regulated luminal protease that cleaves SREBPs and controls lipid composition of animal cells. Molecular Cell *2*, 505-514.

Sancak, Y., Bar-Peled, L., Zoncu, R., Markhard, A.L., Nada, S., and Sabatini, D.M. (2010). Ragulator-Rag complex targets mTORC1 to the lysosomal surface and is necessary for its activation by amino acids. Cell *141*, 290-303.

Sancak, Y., Peterson, T.R., Shaul, Y.D., Lindquist, R.A., Thoreen, C.C., Bar-Peled, L., and Sabatini, D.M. (2008). The Rag GTPases Bind Raptor and Mediate Amino Acid Signaling to mTORC1. Science *320*, 1496-1501.

Sancak, Y., Thoreen, C., Peterson, T., Lindquist, R., Kang, S., Spooner, E., Carr, S., and Sabatini, D. (2007). PRAS40 Is an Insulin-Regulated Inhibitor of the mTORC1 Protein Kinase. Molecular Cell *25*, 903-915.

Sanchez, H.B., Yieh, L., and Osborne, T.F. (1995). Cooperation by sterol regulatory element-binding protein and Sp1 in sterol regulation of low density lipoprotein receptor gene. The Journal of Biological Chemistry *270*, 1161-1169.

Sarbassov, D., Ali, S., Sengupta, S., Sheen, J., Hsu, P., Bagley, A., Markhard, A., and Sabatini, D. (2006). Prolonged Rapamycin Treatment Inhibits mTORC2 Assembly and Akt/PKB. Molecular Cell *22*, 159-168.

Sarbassov, D.D., Guertin, D.A., Ali, S.M., and Sabatini, D.M. (2005). Phosphorylation and regulation of Akt/PKB by the rictor-mTOR complex. Science *307*, 1098-1101.

Sato, R., Inoue, J., Kawabe, Y., Kodama, T., Takano, T., and Maeda, M. (1996). Sterol-dependent transcriptional regulation of sterol regulatory element-binding protein-2. The Journal of Biological Chemistry *271*, 26461-26464.

Sato, R., Okamoto, A., Inoue, J., Miyamoto, W., Sakai, Y., Emoto, N., Shimano, H., and Maeda, M. (2000). Transcriptional regulation of the ATP citrate-lyase gene by sterol regulatory element-binding proteins. The Journal of Biological Chemistry *275*, 12497-12502.

Sato, R., Yang, J., Wang, X., Evans, M.J., Ho, Y.K., Goldstein, J.L., and Brown, M.S. (1994). Assignment of the membrane attachment, DNA binding, and transcriptional activation domains of sterol regulatory element-binding protein-1 (SREBP-1). The Journal of Biological Chemistry *269*, 17267-17273.

Sauter, G., Maeda, T., Waldman, F.M., Davis, R.L., and Feuerstein, B.G. (1996). Patterns of epidermal growth factor receptor amplification in malignant gliomas. American Journal of Pathology *148*, 1047-1053.

Scaglia, N., Chisholm, J.W., and Igal, R.A. (2009). Inhibition of stearoylCoA desaturase-1 inactivates acetyl-CoA carboxylase and impairs proliferation in cancer cells: role of AMPK. PLoS ONE *4*, e6812.

Schroeder, F., Jolly, C.A., Cho, T.H., and Frolov, A. (1998). Fatty acid binding protein isoforms: structure and function. Chemistry and Physics of Lipids *92*, 1-25.

Schulze, A., Zerfass, K., Spitkovsky, D., Middendorp, S., Berges, J., Helin, K., Jansen-Durr, P., and Henglein, B. (1995). Cell cycle regulation of the cyclin A gene promoter is mediated by a variant E2F site. Proceedings of the National Academy of Sciences USA *92*, 11264-11268.

Semenza, G.L., Jiang, B.H., Leung, S.W., Passantino, R., Concordet, J.P., Maire, P., and Giallongo, A. (1996). Hypoxia response elements in the aldolase A, enolase 1, and lactate dehydrogenase A gene promoters contain essential binding sites for hypoxia-inducible factor 1. The Journal of Biological Chemistry *271*, 32529-32537.

Sengupta, S., Peterson, T.R., and Sabatini, D.M. (2010). Regulation of the mTOR Complex 1 Pathway by Nutrients, Growth Factors, and Stress. Molecular Cell *40*, 310-322.

Seo, Y.-K., Jeon, T.-I., Chong, H.K., Biesinger, J., Xie, X., and Osborne, T.F. (2011). Genome-wide Localization of SREBP-2 in Hepatic Chromatin Predicts a Role in Autophagy. Cell Metabolism *13*, 367-375.

Shah, O.J., and Hunter, T. (2006). Turnover of the active fraction of IRS1 involves raptor-mTOR- and S6K1-dependent serine phosphorylation in cell culture models of tuberous sclerosis. Molecular and Cellular Biology *26*, 6425-6434.

Shah, O.J., Wang, Z., and Hunter, T. (2004). Inappropriate activation of the TSC/Rheb/mTOR/S6K cassette induces IRS1/2 depletion, insulin resistance, and cell survival deficiencies. Current Biology *14*, 1650-1656.

Shamma, A., Takegami, Y., Miki, T., Kitajima, S., Noda, M., Obara, T., Okamoto, T., and Takahashi, C. (2009). Rb Regulates DNA damage response and cellular senescence through E2F-dependent suppression of N-ras isoprenylation. Cancer Cell *15*, 255-269.

Sharpe, L.J., and Brown, A.J. (2008). Rapamycin down-regulates LDL-receptor expression independently of SREBP-2. Biochemical and Biophysical Research Communications *373*, 670-674.

Sharpe, L.J., Luu, W., and Brown, A.J. (2010). Akt Phosphorylates Sec24: New Clues into the Regulation of ER-to-Golgi Trafficking. Traffic *12*, 19-27.

Shaw, R.J., Bardeesy, N., Manning, B.D., Lopez, L., Kosmatka, M., DePinho, R.A., and Cantley, L.C. (2004). The LKB1 tumor suppressor negatively regulates mTOR signaling. Cancer Cell *6*, 91-99.

Shaw, R.J., and Cantley, L.C. (2006). Ras, PI(3)K and mTOR signalling controls tumour cell growth. Nature *441*, 424-430.

Shayesteh, L., Lu, Y., Kuo, W.L., Baldocchi, R., Godfrey, T., Collins, C., Pinkel, D., Powell, B., Mills, G.B., and Gray, J.W. (1999). PIK3CA is implicated as an oncogene in ovarian cancer. Nature Genetics *21*, 99-102.

Shen, J., and Prywes, R. (2005). ER stress signaling by regulated proteolysis of ATF6. Methods *35*, 382-389.

Sheng, Z., Otani, H., Brown, M.S., and Goldstein, J.L. (1995). Independent regulation of sterol regulatory element-binding proteins 1 and 2 in hamster liver. Proceedings of the National Academy of Sciences USA *92*, 935-938.

Shima, H., Pende, M., Chen, Y., Fumagalli, S., Thomas, G., and Kozma, S.C. (1998). Disruption of the p70(s6k)/p85(s6k) gene reveals a small mouse phenotype and a new functional S6 kinase. The EMBO Journal *17*, 6649-6659.

Shimano, H., Horton, J.D., Hammer, R.E., Shimomura, I., Brown, M.S., and Goldstein, J.L. (1996). Overproduction of cholesterol and fatty acids causes massive liver enlargement in transgenic mice expressing truncated SREBP-1a. The Journal of Clinical Investigation *98*, 1575-1584.

Shimano, H., Horton, J.D., Shimomura, I., Hammer, R.E., Brown, M.S., and Goldstein, J.L. (1997a). Isoform 1c of sterol regulatory element binding protein is less active than isoform 1a in livers of transgenic mice and in cultured cells. The Journal of Clinical investigation *99*, 846-854.

Shimano, H., Shimomura, I., Hammer, R.E., Herz, J., Goldstein, J.L., Brown, M.S., and Horton, J.D. (1997b). Elevated levels of SREBP-2 and cholesterol synthesis in livers of mice homozygous for a targeted disruption of the SREBP-1 gene. The Journal of Clinical Investigation *100*, 2115-2124.

Shimomura, I., Bashmakov, Y., Ikemoto, S., Horton, J.D., Brown, M.S., and Goldstein, J.L. (1999). Insulin selectively increases SREBP-1c mRNA in the livers of rats with streptozotocin-induced diabetes. Proceedings of the National Academy of Sciences USA *96*, 13656-13661.

Shimomura, I., Shimano, H., Horton, J.D., Goldstein, J.L., and Brown, M.S. (1997). Differential expression of exons 1a and 1c in mRNAs for sterol regulatory element binding protein-1 in human and mouse organs and cultured cells. The Journal of Clinical Investigation *99*, 838-845.

Sone, H., Shimano, H., Sakakura, Y., Inoue, N., Amemiya-Kudo, M., Yahagi, N., Osawa, M., Suzuki, H., Yokoo, T., Takahashi, A., Iida, K., Toyoshima, H., Iwama, A., and Yamada, N. (2002). Acetyl-coenzyme A synthetase is a lipogenic enzyme controlled by SREBP-1 and energy status. American Journal of Physiology Endocrinology and Metabolism *282*, E222-230.

Sonveaux, P., Vegran, F., Schroeder, T., Wergin, M.C., Verrax, J., Rabbani, Z.N., De Saedeleer, C.J., Kennedy, K.M., Diepart, C., Jordan, B.F., Kelley, M.J., Gallez, B., Wahl, M.L., Feron, O., and Dewhirst, M.W. (2008). Targeting lactate-fueled respiration selectively kills hypoxic tumor cells in mice. The Journal of Clinical Investigation *118*, 3930-3942.

Sowter, H.M., Raval, R.R., Moore, J.W., Ratcliffe, P.J., and Harris, A.L. (2003). Predominant role of hypoxia-inducible transcription factor (Hif)-1alpha versus Hif-2alpha in regulation of the transcriptional response to hypoxia. Cancer Research *63*, 6130-6134.

Stephens, L., Anderson, K., Stokoe, D., Erdjument-Bromage, H., Painter, G.F., Holmes, A.B., Gaffney, P.R., Reese, C.B., McCormick, F., Tempst, P., Coadwell, J., and

Hawkins, P.T. (1998). Protein kinase B kinases that mediate phosphatidylinositol 3,4,5-trisphosphate-dependent activation of protein kinase B. Science *279*, 710-714.

Sun, L.-P. (2005). Insig Required for Sterol-mediated Inhibition of Scap/SREBP Binding to COPII Proteins in Vitro. The Journal of Biological Chemistry *280*, 26483-26490.

Sun, L.-P., Seemann, J., Goldstein, J.L., and Brown, M.S. (2007). From the Cover: Sterol-regulated transport of SREBPs from endoplasmic reticulum to Golgi: Insig renders sorting signal in Scap inaccessible to COPII proteins. Proceedings of the National Academy of Sciences USA *104*, 6519-6526.

Sundqvist, A., Bengoecheaalonso, M., Ye, X., Lukiyanchuk, V., Jin, J., Harper, J., and Ericsson, J. (2005). Control of lipid metabolism by phosphorylation-dependent degradation of the SREBP family of transcription factors by SCF. Cell Metabolism *1*, 379-391.

Sundqvist, A., and Ericsson, J. (2003). Transcription-dependent degradation controls the stability of the SREBP family of transcription factors. Proceedings of the National Academy of Sciences USA *100*, 13833-13838.

Swinnen, J.V., Brusselmans, K., and Verhoeven, G. (2006). Increased lipogenesis in cancer cells: new players, novel targets. Current Opinion in Clinical Nutrition and Metabolic Care *9*, 358-365.

Swinnen, J.V., Heemers, H., Deboel, L., Foufelle, F., Heyns, W., and Verhoeven, G. (2000a). Stimulation of tumor-associated fatty acid synthase expression by growth factor activation of the sterol regulatory element-binding protein pathway. Oncogene *19*, 5173-5181.

Swinnen, J.V., Vanderhoydonc, F., Elgamal, A.A., Eelen, M., Vercaeren, I., Joniau, S., Van Poppel, H., Baert, L., Goossens, K., Heyns, W., and Verhoeven, G. (2000b). Selective activation of the fatty acid synthesis pathway in human prostate cancer. International Journal of Cancer *88*, 176-179.

Taghibiglou, C., Martin, H.G.S., Rose, J.K., Ivanova, N., Lin, C.H.C., Lau, H.L., Rai, S., Wang, Y.T., and Rankin, C.H. (2009). Essential role of SBP-1 activation in oxygen deprivation induced lipid accumulation and increase in body width/length ratio in Caenorhabditis elegans. FEBS Letters *583*, 831-834.

Takeuchi, Y., Yahagi, N., Izumida, Y., Nishi, M., Kubota, M., Teraoka, Y., Yamamoto, T., Matsuzaka, T., Nakagawa, Y., Sekiya, M., Iizuka, Y., Ohashi, K., Osuga, J.-i., Gotoda, T., Ishibashi, S., Itaka, K., Kataoka, K., Nagai, R., Yamada, N., Kadowaki, T., and Shimano, H. (2010). Polyunsaturated fatty acids selectively suppress sterol regulatory element-binding protein-1 through proteolytic processing and autoloop regulatory circuit. The Journal of Biological Chemistry *285*, 11681-11691.

Tarling, E., Salter, A., and Bennett, A. (2004). Transcriptional regulation of human SREBP-1c (sterol-regulatory-element-binding protein-1c): a key regulator of lipogenesis. Biochemical Society Transactions *32*, 107-109.

Tee, A.R., Manning, B.D., Roux, P.P., Cantley, L.C., and Blenis, J. (2003). Tuberous sclerosis complex gene products, Tuberin and Hamartin, control mTOR signaling by acting as a GTPase-activating protein complex toward Rheb. Current Biology *13*, 1259-1268.

Teran-Garcia, M., Adamson, A.W., Yu, G., Rufo, C., Suchankova, G., Dreesen, T.D., Tekle, M., Clarke, S.D., and Gettys, T.W. (2007). Polyunsaturated fatty acid suppression of fatty acid synthase (FASN): evidence for dietary modulation of NF-Y binding to the Fasn promoter by SREBP-1c. Biochemical Journal *402*, 591.

Thewke, D.P., Panini, S.R., and Sinensky, M. (1998). Oleate potentiates oxysterol inhibition of transcription from sterol regulatory element-1-regulated promoters and maturation of sterol regulatory element-binding proteins. The Journal of Biological Chemistry *273*, 21402-21407.

Treins, C., Warne, P.H., Magnuson, M.A., Pende, M., and Downward, J. (2009). Rictor is a novel target of p70 S6 kinase-1. Oncogene *29*, 1003-16.

Tremblay, F., Brule, S., Hee Um, S., Li, Y., Masuda, K., Roden, M., Sun, X.J., Krebs, M., Polakiewicz, R.D., Thomas, G., and Marette, A. (2007). Identification of IRS-1 Ser-1101 as a target of S6K1 in nutrient- and obesity-induced insulin resistance. Proceedings of the National Academy of Sciences USA *104*, 14056-14061.

Tzatsos, A., and Kandror, K.V. (2006). Nutrients suppress phosphatidylinositol 3-kinase/Akt signaling via raptor-dependent mTOR-mediated insulin receptor substrate 1 phosphorylation. Moleular and Cellular Biology *26*, 63-76.

Ullah, M.S., Davies, A.J., and Halestrap, A.P. (2006). The plasma membrane lactate transporter MCT4, but not MCT1, is up-regulated by hypoxia through a HIF-1alpha-dependent mechanism. The Journal of Biological Chemistry *281*, 9030-9037.

Urano, J., Sato, T., Matsuo, T., Otsubo, Y., Yamamoto, M., and Tamanoi, F. (2007). Point mutations in TOR confer Rheb-independent growth in fission yeast and nutrient-independent mammalian TOR signaling in mammalian cells. Proceedings of the National Academy of Sciences USA *104*, 3514-3519.

van Veelen, W., Korsse, S.E., van de Laar, L., and Peppelenbosch, M.P. (2011). The long and winding road to rational treatment of cancer associated with LKB1/AMPK/TSC/mTORC1 signaling. Oncogene *30*, 2289-2303.

Voigt, W. (2005). Sulforhodamine B assay and chemosensitivity. Methods in Molecular Medicine *110*, 39-48.

Wang, G.-L., Fu, Y.-C., Xu, W.-C., Feng, Y.-Q., Fang, S.-R., and Zhou, X.-H. (2009). Resveratrol inhibits the expression of SREBP1 in cell model of steatosis via Sirt1-FOXO1 signaling pathway. Biochemical and Biophysical Research Communications *380*, 644-649.

Wang, J., Yu, L., Schmidt, R.E., Su, C., Huang, X., Gould, K., and Cao, G. (2005). Characterization of HSCD5, a novel human stearoyl-CoA desaturase unique to primates. Biochemical and Biophysical Research Communications *332*, 735-742.

Wang, L., Harris, T.E., Roth, R.A., and Lawrence, J.C. (2007). PRAS40 regulates mTORC1 kinase activity by functioning as a direct inhibitor of substrate binding. The Journal of Biological Chemistry *282*, 20036-20044.

Wang, R., Kong, X., Cui, A., Liu, X., Xiang, R., Yang, Y., Guan, Y., Fang, F., and Chang, Y. (2010). Sterol-regulatory-element-binding protein 1c mediates the effect of insulin on the expression of Cidea in mouse hepatocytes. Biochem Journal *430*, 245-254.

Wang, X., Sato, R., Brown, M.S., Hua, X., and Goldstein, J.L. (1994). SREBP-1, a membrane-bound transcription factor released by sterol-regulated proteolysis. Cell *77*, 53-62.

Warburg, O. (1956). On the origin of cancer cells. Science *123*, 309-314.

Warnecke, C., Weidemann, A., Volke, M., Schietke, R., Wu, X., Knaup, K.X., Hackenbeck, T., Bernhardt, W., Willam, C., Eckardt, K.-U., and Wiesener, M.S. (2008). The specific contribution of hypoxia-inducible factor-2α to hypoxic gene expression in vitro is limited and modulated by cell type-specific and exogenous factors. Experimental Cell Research *314*, 2016-2027.

Wee, S., Wiederschain, D., Maira, S.M., Loo, A., Miller, C., deBeaumont, R., Stegmeier, F., Yao, Y.M., and Lengauer, C. (2008). PTEN-deficient cancers depend on PIK3CB. Proceedings of the National Academy of Sciences USA *105*, 13057-13062.

Whitmer, J.T., Idell-Wenger, J.A., Rovetto, M.J., and Neely, J.R. (1978). Control of fatty acid metabolism in ischemic and hypoxic hearts. The Journal of Biological Chemistry *253*, 4305-4309.

Wiederschain, D., Wee, S., Chen, L., Loo, A., Yang, G., Huang, A., Chen, Y., Caponigro, G., Yao, Y.M., Lengauer, C., Sellers, W.R., and Benson, J.D. (2009). Single-vector inducible lentiviral RNAi system for oncology target validation. Cell Cycle *8*, 498-504.

Williams, M.R., Arthur, J.S., Balendran, A., van der Kaay, J., Poli, V., Cohen, P., and Alessi, D.R. (2000). The role of 3-phosphoinositide-dependent protein kinase 1 in activating AGC kinases defined in embryonic stem cells. Current Biology *10*, 439-448.

Wolfrum, C., Asilmaz, E., Luca, E., Friedman, J.M., and Stoffel, M. (2004). Foxa2 regulates lipid metabolism and ketogenesis in the liver during fasting and in diabetes. Nature *432*, 1027-1032.

Wolfrum, C., Borrmann, C.M., Borchers, T., and Spener, F. (2001). Fatty acids and hypolipidemic drugs regulate peroxisome proliferator-activated receptors alpha - and gamma-mediated gene expression via liver fatty acid binding protein: a signaling path to the nucleus. Proceedings of the National Academy of Sciences USA *98*, 2323-2328.

Woodgett, J.R. (2005). Recent advances in the protein kinase B signaling pathway. Current Opinion in Cell Biology *17*, 150-157.

Worgall, T.S., Sturley, S.L., Seo, T., Osborne, T.F., and Deckelbaum, R.J. (1998). Polyunsaturated fatty acids decrease expression of promoters with sterol regulatory elements by decreasing levels of mature sterol regulatory element-binding protein. The Journal of Biological Chemistry *273*, 25537-25540.

Wullschleger, S., Loewith, R., and Hall, M.N. (2006). TOR signaling in growth and metabolism. Cell *124*, 471-484.

Wykoff, C.C., Beasley, N.J., Watson, P.H., Turner, K.J., Pastorek, J., Sibtain, A., Wilson, G.D., Turley, H., Talks, K.L., Maxwell, P.H., Pugh, C.W., Ratcliffe, P.J., and Harris, A.L. (2000). Hypoxia-inducible expression of tumor-associated carbonic anhydrases. Cancer Research *60*, 7075-7083.

Yahagi, N., Shimano, H., Hasegawa, K., Ohashi, K., Matsuzaka, T., Najima, Y., Sekiya, M., Tomita, S., Okazaki, H., Tamura, Y., Iizuka, Y., Nagai, R., Ishibashi, S., Kadowaki, T., Makuuchi, M., Ohnishi, S., Osuga, J., and Yamada, N. (2005). Co-ordinate activation of lipogenic enzymes in hepatocellular carcinoma. European Journal of Cancer *41*, 1316-1322.

Yang, J., Goldstein, J.L., Hammer, R.E., Moon, Y.A., Brown, M.S., and Horton, J.D. (2001). Decreased lipid synthesis in livers of mice with disrupted Site-1 protease gene. Proceedings of the National Academy of Sciences USA *98*, 13607-13612.

Yang, T., Espenshade, P.J., Wright, M.E., Yabe, D., Gong, Y., Aebersold, R., Goldstein, J.L., and Brown, M.S. (2002). Crucial step in cholesterol homeostasis: sterols promote binding of SCAP to INSIG-1, a membrane protein that facilitates retention of SREBPs in ER. Cell *110*, 489-500.

Yang, Y.A., Morin, P.J., Han, W.F., Chen, T., Bornman, D.M., Gabrielson, E.W., and Pizer, E.S. (2003). Regulation of fatty acid synthase expression in breast cancer by sterol regulatory element binding protein-1c. Experimental Cell Research *282*, 132-137.

Ye, J., Rawson, R.B., Komuro, R., Chen, X., Davé, U.P., Prywes, R., Brown, M.S., and Goldstein, J.L. (2000). ER stress induces cleavage of membrane-bound ATF6 by the same proteases that process SREBPs. Molecular Cell *6*, 1355-1364.

Yecies, J.L., Zhang, H.H., Menon, S., Liu, S., Yecies, D., Lipovsky, A.I., Gorgun, C., Kwiatkowski, D.J., Hotamisligil, G.S., Lee, C.-H., and Manning, B.D. (2011). Akt Stimulates Hepatic SREBP1c and Lipogenesis through Parallel mTORC1-Dependent and Independent Pathways. Cell Metabolism *14*, 21-32.

Yellaturu, C.R., Deng, X., Cagen, L.M., Wilcox, H.G., Mansbach, C.M., Siddiqi, S.A., Park, E.A., Raghow, R., and Elam, M.B. (2009). Insulin enhances post-translational processing of nascent SREBP-1c by promoting its phosphorylation and association with COPII vesicles. The Journal of Biological Chemistry *284*, 7518-7532.

Yokoyama, C., Wang, X., Briggs, M.R., Admon, A., Wu, J., Hua, X., Goldstein, J.L., and Brown, M.S. (1993). SREBP-1, a basic-helix-loop-helix-leucine zipper protein that controls transcription of the low density lipoprotein receptor gene. Cell *75*, 187-197.

Yoon, S., Lee, M.-Y., Park, S.W., Moon, J.-S., Koh, Y.-K., Ahn, Y.-H., Park, B.-W., and Kim, K.-S. (2007). Up-regulation of Acetyl-CoA Carboxylase and Fatty Acid Synthase by Human Epidermal Growth Factor Receptor 2 at the Translational Level in Breast Cancer Cells. The Journal of Biological Chemistry *282*, 26122-26131.

Yoshii, Y., Furukawa, T., Yoshii, H., Mori, T., Kiyono, Y., Waki, A., Kobayashi, M., Tsujikawa, T., Kudo, T., Okazawa, H., Yonekura, Y., and Fujibayashi, Y. (2009). Cytosolic acetyl-CoA synthetase affected tumor cell survival under hypoxia: the possible function in tumor acetyl-CoA/acetate metabolism. Cancer Science *100*, 821-827.

Yoshimoto, M., Waki, A., Yonekura, Y., Sadato, N., Murata, T., Omata, N., Takahashi, N., Welch, M.J., and Fujibayashi, Y. (2001). Characterization of acetate metabolism in tumor cells in relation to cell proliferation: acetate metabolism in tumor cells. Nuclear Medicine and Biology *28*, 117-122.

Yu, J., Wjasow, C., and Backer, J.M. (1998). Regulation of the p85/p110alpha phosphatidylinositol 3'-kinase. Distinct roles for the n-terminal and c-terminal SH2 domains. The Journal of Biological Chemistry *273*, 30199-30203.

Yuan, T.L., and Cantley, L.C. (2008). PI3K pathway alterations in cancer: variations on a theme. Oncogene *27*, 5497-5510.

Zeng, L., Lu, M., Mori, K., Luo, S., Lee, A.S., Zhu, Y., and Shyy, J.Y.-J. (2004). ATF6 modulates SREBP2-mediated lipogenesis. The EMBO Journal *23*, 950-958.

Zhang, C., Shin, D.-J., and Osborne, T.F. (2005). A simple promoter containing two Sp1 sites controls the expression of sterol-regulatory-element-binding protein 1a (SREBP-1a). Biochemical Journal *386*, 161-8.

Zhang, H., Gao, P., Fukuda, R., Kumar, G., Krishnamachary, B., Zeller, K.I., Dang, C.V., and Semenza, G.L. (2007). HIF-1 inhibits mitochondrial biogenesis and cellular respiration in VHL-deficient renal cell carcinoma by repression of C-MYC activity. Cancer Cell *11*, 407-420.

Zhang, H., Lipovsky, A., Dibble, C., Sahin, M., and Manning, B. (2006a). S6K1 Regulates GSK3 under Conditions of mTOR-Dependent Feedback Inhibition of Akt. Molecular Cell *24*, 185-197.

Zhang, L., Ge, L., Parimoo, S., Stenn, K., and Prouty, S.M. (1999). Human stearoyl-CoA desaturase: alternative transcripts generated from a single gene by usage of tandem polyadenylation sites. Biochem Journal *340 (Pt 1)*, 255-264.

Zhang, W., Patil, S., Chauhan, B., Guo, S., Powell, D.R., Le, J., Klotsas, A., Matika, R., Xiao, X., Franks, R., Heidenreich, K.A., Sajan, M.P., Farese, R.V., Stolz, D.B., Tso, P., Koo, S.-H., Montminy, M., and Unterman, T.G. (2006b). FoxO1 regulates multiple metabolic pathways in the liver: effects on gluconeogenic, glycolytic, and lipogenic gene expression. The Journal of Biological Chemistry *281*, 10105-10117.

Zufferey, R., Nagy, D., Mandel, R.J., Naldini, L., and Trono, D. (1997). Multiply attenuated lentiviral vector achieves efficient gene delivery in vivo. Nature Biotechnology *15*, 871-875.